DOCTORAL THESIS

Novel method and instruments for the techno-economic sizing of borehole heat exchangers

Nordin Aranzabal Barrio

VNIVERSITAT DE VALÈNCIA

DOCTOR OF PHILOSOPHY IN ELECTRONIC ENGINEERING

DOCTORAL THESIS

Novel method and instruments for the optimal techno-economic sizing of borehole heat exchangers

Author:

Nordin Aranzabal Barrio

Supervisors:

Dr. Julio Martos Torres

Dr. Jesús Soret Medel

March 2020

VNIVERSITAT DE VALÈNCIA

DOCTOR OF PHILOSOPHY IN ELECTRONIC ENGINEERING

DOCTORAL THESIS

Novel method and instruments for the optimal techno-economic sizing of borehole heat exchangers

---

Author:

Nordin Aranzabal Barrio

Supervisors:

Dr. Julio Martos Torres

Dr. Jesús Soret Medel

Universitat de València (UV)

Department of Electronic Engineering

46100 Burjassot, Spain – March 2020

DR. JULIO MARTOS TORRES, Doctor en Enginyeria Electrònica, Professor Titular al Departament d'Enginyeria Electrònica de l'Escola Tècnica Superior D'Enginyeria de la Universitat de València.

DR. JESUS SORET MEDEL, Doctor en Enginyeria Electrónica, Professor Titular al Departament d'Enginyeria Electrònica de l'Escola Tècnica Superior D'Enginyeria de la Universitat de València.

FAN CONSTAR QUE:

NORDIN ARANZABAL BARRIO, Bsc i MSc in Enginyeria Electrònica ha realitzat sota la seva direcció el treball *Novel method and instruments for the optimal techno-economic sizing of borehole heat exchangers*, que es presenta en aquesta memòria per optar al grau de Doctor per la Universitat de València.

I per tal què així conste a efectes oportuns, i donant el vistiplau per a la presentació d'aquest treball davant el Tribunal de tesi que corresponga, signem el present certificat a València el 20 de Juliol 2020.

Julio Martos Torres

Jesús Soret Medel

TESI DOCTORAL:

Novel method and instruments for the optimal techno-economic sizing of borehole heat exchangers

AUTOR:

Nordin Aranzabal Barrio

DIRECTORS:

Dr. Julio Martos Torres
Dr. Jesús Soret Medel

El tribunal nombrat per jutjar la Tesi Doctoral citada anteriorment, compost per:

President: _____

Vocal: _____

Secretari: _____

Acorda atorgar-li la qualificació de _____

I per a què així conste a efectes oportuns, signem el present certificat.

A Burjassot el ____ de _____ de 2020

NOTE TO THE READER

According to the University of Valencia Doctorate Regulation[1] this PhD dissertation is presented as a compendium of at least three publications in international journals containing the results of the conducted work. Furthermore, in accordance with the aforementioned regulation and with the aim to foster the language of the University of Valencia in research and education activity, this PhD dissertation starts with two extended abstracts in the official languages of Valencian Community, Spanish and Valencian. This thesis really begins at page XXVII with a short abstract in English followed by the research context, motivation, objectives, theoretical fundamentals, methodology, results and conclusion.

[1]Reglament sobre depòsit, avaluació i defensa de la tesi doctoral aprovat pel Consell de Govern de 28 de Juny de 2016. ACGUV 172/2016.
Pla d'increment de la docència en valencià (ACGUV 129/2012) aprovat i modificat pel Consell de Govern de 22 de desembre de 2016. ACGUV 308/2016.

Resumen

El test de respuesta térmica (TRT) es ampliamente utilizado como método estándar para caracterizar las propiedades térmicas del terreno adyacente a un intercambiador de calor enterrado (BHE). Los métodos tradicionales para interpretar los resultados aplican soluciones analíticas o numéricas asumiendo que el terreno es infinito, homogéneo e isotrópico. Sin embargo, en realidad el subsuelo presenta generalmente una estructura estratificada y heterogénea, y por lo tanto las propiedades térmicas pueden variar sustancialmente con la profundidad. En este sentido y con la intención de resolver las limitaciones del TRT estándar, la presente tesis doctoral se centra en el desarrollo de métodos e instrumentos para cuantificar las propiedades de transferencia de calor de las capas geológicas alrededor de un BHE. Información que resulta imprescindible para alcanzar la máxima eficiencia energética y el dimensionado técnico-económico óptimo de un BHE.

En particular, se propone un nuevo método de TRT, llamado *observer pipe TRT* (OP-TRT), basado en una medición de temperatura adicional a lo largo de una tubería auxiliar. En las últimas décadas, varios investigadores han desarrollado TRT distribuidos (DTRT) en los cuales se realizan mediciones de temperatura a lo largo del tubo-U en el que se inyecta calor. No obstante, a partir de las investigaciones llevadas a cabo en esta tesis, el tubo observador ha demostrado amplificar los efectos térmicos producidos debido a capas geológicas con propiedades termo-físicas diferentes, requiriéndose así sensores menos precisos para obtener resultados más detallados. En base a este logro, se ha desarrollado un modelo numérico de simulación inversa para parametrizar la conductividad térmica de las capas geológicas a partir de las mediciones a lo largo del tubo observador. Básicamente, el modelo ajusta la conductividad térmica de las capas geológicas hasta que los resultados de la simulación coinciden con el perfil de temperatura experimental a lo largo del tubo observador. El modelo ha sido desarrollado con un algoritmo de estimación de parámetros para un ajuste automático y obtención de resultados más precisos. Otra ventaja es que este método solo requiere dos perfiles de temperatura: (1) subsuelo en reposo (antes del TRT) y (2) al final del TRT (antes de detener la inyección de calor).

Con la intención de continuar investigando el método propuesto a partir de datos de mayor calidad, se ha desarrollado un instrumento específico (Geowire) para medir de forma automática y con mayor precisión los perfiles de profundidad-temperatura requeridos. El diseño del Geowire también ha sido orientado para cubrir otros requisitos, como compatibilidad con equipos de TRT y operación intuitiva. Además, se ha desarrollado una versión mejorada de una sonda de temperatura (Geoball) que es

arrastrada por el fluido que circula en las tuberías a la vez que calcula su posición, con la ventaja de que puede ser utilizada en tuberías con disposición vertical y horizontal. Después de las pruebas de validación en el laboratorio, las características fundamentales de ambos instrumentos han sido evaluadas en comparación con otros instrumentos novedosos y estándar para mediciones de temperatura distribuidas durante un experimento en un BHE de pruebas. La ventaja principal de los instrumentos propuestos sobre la popular fibra óptica es que miden la temperatura instantáneamente (para intervalos temporales precisos). Asimismo, no necesitan de una calibración dinámica para obtener resultados precisos mientras que proporcionan una mayor resolución espacial y de temperatura: Geowire (0.5 mm, 0.06 K) y Geoball (10 mm, 0.05 K). Además, son más fáciles de integrar en pozos existentes y son una solución potencialmente más rentable para medir la temperatura distribuida.

Finalmente, se demuestran los beneficios del método e instrumentos propuestos durante un DTRT en comparación con la fibra óptica y con un programa basado en el modelo de línea infinita para estimar la conductividad térmica distribuida. Los resultados del modelo propuesto revelaron una zona altamente conductiva al usar los datos del Geowire, mientras que esta zona no fue detectada al procesar los datos de fibra óptica.

Palabras clave: Bomba de calor geotérmica; Intercambiador de calor enterrado; TRT tubo observador; Subsuelo multicapa; Conductividad térmica; Simulación numérica; Eficiencia energética; Optimización técnico-económica.

1. Contexto de investigación y motivación

Los sistemas de bombas de calor geotérmica (GSHP) se expanden gradualmente como una alternativa prometedora para ahorrar energía y reducir las emisiones de gases de efecto invernadero. Los sistemas GSHP intercambian calor con el subsuelo con el objetivo de proporcionar agua caliente o climatización (calefacción o refrigeración) en aplicaciones domésticas, urbanas o agrícolas. Estos sistemas han demostrado lograr una mayor eficiencia energética que los sistemas de aire acondicionado. Sin embargo, el capital de inversión inicial es normalmente mayor y depende principalmente de la longitud, el tamaño y el número de intercambiadores de calor enterrados (BHE) necesarios.

El test de respuesta térmica (TRT) es el método estándar para caracterizar las propiedades térmicas del subsuelo y los BHE, información esencial para el dimensionado técnico-económico óptimo de los sistemas GSHP. Generalmente, el TRT se lleva a cabo en un circuito cerrado (tubo en U) donde el fluido portador de calor desciende y asciende a lo largo de la perforación del BHE. Durante el test, el fluido se

bombea a una velocidad relativamente estable mientras que se inyecta calor a una potencia constante utilizando un elemento eléctrico. Asimismo, se monitoriza y registra de manera continua la potencia calorífica inyectada, el caudal del fluido, las temperaturas de entrada y salida al BHE y la temperatura exterior. A partir de estos parámetros, varias soluciones analíticas y semi-numéricas han sido propuestas durante las últimas décadas para estimar las propiedades de transferencia de calor a lo largo del intercambiador y el terreno adyacente. Estas soluciones consideran el subsuelo como un medio homogéneo, isotrópico e infinito y, por lo tanto, solo determinan parámetros globales y efectivos, como la conductividad térmica efectiva y la resistencia térmica efectiva del intercambiador.

Sin embargo, en realidad, la composición geológica del subsuelo es típicamente heterogénea, normalmente dividida en capas formadas por diferentes materiales como tipos de tierra, tipos de roca y/o agua subterránea. Además, el subsuelo también puede estar dominado por fracturas o cavidades. Esto significa que es improbable que el calor se transfiera de manera uniforme a través de las capas geológicas del subsuelo situado alrededor de un pozo. Es por ello por lo que conocer la tasa de transferencia de calor de estas capas podría ayudar a evitar el sobredimensionamiento de instalaciones, así como a reducir la inversión de capital innecesariamente mayor que esta práctica conlleva: costes adicionales derivados de una mayor demanda de presión, una mayor demanda de bombeo, caídas de presión adicionales y todo el material adicional necesario para construir un BHE más profundo (mano de obra, perforación, tuberías, material de relleno, etc.). Por ejemplo, en caso de alcanzar una zona con propiedades de transferencia de calor poco favorables, se podría limitar la longitud de la perforación y construir un mayor número de pozos menos profundos en vez de menos pozos más largos. Es decir, se trata de información de gran interés que no es posible obtener a partir de un TRT convencional, la cual permitiría detectar las capas más favorables para intercambiar calor y así poder establecer la longitud óptima de un BHE para lograr el máximo rendimiento de transferencia de calor al mínimo coste.

A partir de esta problemática sin resolver surgió la hipótesis que lanzó el enfoque de esta tesis. ¿Es posible desarrollar métodos e instrumentos específicos que permitan parametrizar de forma detallada la tasa de transferencia de calor de las capas geológicas que cruzan un BHE?

2. Objetivos

El objetivo general de la presente tesis doctoral consiste en la exploración de métodos e instrumentos para evaluar la respuesta térmica de las diferentes capas geológicas que rodean a un intercambiador de calor enterrado. Así, con el propósito de

alcanzar este objetivo general, se proponen e investigan los siguientes objetivos específicos:

I. Desarrollo de un método de simulación inversa para calcular la conductividad térmica del subsuelo que rodea a un BHE en función de la profundidad a partir de mediciones de temperatura adicionales, en un tubo auxiliar a lo largo de toda la perforación, durante un TRT. Elaboración de un experimento para evaluar el método en un BHE experimental.

II. Desarrollo de un instrumento específico para medir los perfiles de temperatura requeridos para aplicar el método. Deben investigarse las características apropiadas del instrumento, tales como: compatibilidad con equipos de TRT estándar; alta resolución espacial, temporal y de temperatura; perturbación térmica mínima en el BHE; respuesta térmica de la sonda lo suficientemente rápida para su modo de funcionamiento; un sistema embebido que incorpore el conjunto apropiado de tecnologías de la información y la comunicación; registro automático de datos para intervalos de tiempo y profundidad predefinidos; una operación fácil y conveniente; interfaz gráfica amigable e intuitiva; capacidades para almacenar datos; posibilidades de control remoto (interfaz gráfica y descarga de datos); visualización de datos en tiempo real; recursos suficientes para integrar un método que permita estimar las propiedades térmicas en función de la profundidad. Elaboración de pruebas para validar las características del instrumento, primero en el laboratorio y luego en un BHE experimental.

III. Desarrollo de una versión mejorada de la sonda de temperatura-posición propuesta en Martos et al. (2011). Deben investigarse las características apropiadas del instrumento, tales como: compatibilidad con equipos de TRT estándar; menor tamaño; respuesta térmica más rápida; menor peso; tiempos de operación más largos; registro automático de datos para intervalos temporales y espaciales predefinidos; comunicaciones y carga de la batería inalámbricas; mediciones de temperatura a lo largo de toda la red de tuberías (flujo descendente y ascendente); capacidades para circular en tuberías con disposición vertical y horizontal. Elaboración de pruebas para evaluar el instrumento en el laboratorio.

IV. Desarrollo de una metodología experimental que permita analizar y comparar los instrumentos propuestos con instrumentos novedosos y estándar para mediciones de temperatura distribuida en un BHE de pruebas aislado de condiciones externas.

V. Desarrollo de una metodología experimental para analizar y comparar el método e instrumentos propuestos con otros métodos e instrumentos durante

un TRT en un BHE experimental.

3. Metodología

La presente tesis doctoral se basa en un compendio de publicaciones científicas las cuales han superado una revisión por pares. El cuerpo de la tesis incluye un total de cinco artículos cada uno de ellos describiendo la investigación llevada a cabo para alcanzar cada uno de los objetivos específicos planteados en la sección anterior. En base a este formato de tesis la metodología se divide en cinco apartados.

Artículo 1. Extraction of thermal characteristics of surrounding geological layers of a geothermal heat exchanger by 3D numerical simulations

En este primer artículo se propone un nuevo método para calcular la conductividad térmica de las capas geológicas que atraviesan un BHE. El método sugerido, denominado *observer pipe TRT* (OP-TRT), complementa al TRT estándar proporcionando mediciones de temperatura adicionales a lo largo de una tubería auxiliar introducida en paralelo y equidistante a las tuberías del TRT. Asimismo, se propone un procedimiento de simulación inversa para estimar la conductividad en función de la profundidad a partir de los datos medidos durante la implementación de un OP-TRT.

Este estudio cubre el desarrollo e implementación de un experimento donde se evalúa el método propuesto en un BHE situado en el campus de la Universidad Politécnica de Valencia. El BHE tiene una profundidad de 40 m y el subsuelo que lo rodea está compuesto por seis capas geológicas diferentes incluyendo presencia de agua por debajo de los cuatro metros. Después de la perforación e inserción de las tuberías geotérmicas, el pozo se rellena con una mezcla de cemento y bentonita. En esta instalación, se realiza un TRT en un tubo-U en el cual además de medir los parámetros típicos (e.g. caudal, potencia, temperatura de entrada y salida, etc.) también se mide la evolución de temperatura en la tubería auxiliar, denominada tubo observador. En este caso, la temperatura distribuida a lo largo del interior del tubo observador se obtiene desplazando una sonda cableada manualmente a intervalos de distancia conocidos. La sonda mide la temperatura con una resolución de 0.06 K y una precisión de ±0.5 K y es calibrada en el laboratorio con un termómetro de precisión.

Después de llevar a cabo el OP-TRT, se desarrolla un modelo 3D de elementos finitos (FEM) utilizando COMSOL Multiphysics® con la misma geometría y respuesta térmica que el BHE experimental. El modelo se implementa utilizando los módulos de transferencia de calor en solidos (HT) y flujo no isotérmico en tuberías (NIPFL). Además, se implementa un plano de simetría definido por los dos extremos del tubo-U

reduciendo así el volumen del modelo a la mitad. Asimismo, se ejecuta un estudio para determinar el mallado óptimo persiguiendo un compromiso entre tiempo de simulación y precisión de los resultados. Antes de comenzar con el algoritmo de simulación inversa el modelo se calibra para que la respuesta de temperatura en la entrada y salida de las tuberías del TRT coincida con los resultados experimentales. Para ello, el modelo se configura con los parámetros medidos durante el TRT, como la potencia dinámica, el caudal dinámico, la temperatura ambiente dinámica del aire y la temperatura inicial del subsuelo. A los dominios del subsuelo y el pozo se asignan los valores efectivos de conductividad y resistencia térmica calculados a partir del TRT standard. Al dominio del pozo se asignan las propiedades térmicas de los materiales utilizados: relleno, tuberías, fluido, etc. Y al dominio del subsuelo la densidad y capacidad térmica de los tipos de tierra detectados durante la perforación. Después de la calibración del modelo, el subsuelo se divide en capas a lo largo del eje vertical separadas a partir de las muestras de temperatura espaciales medidas en el tubo observador. Posteriormente se implementa el algoritmo iterativo, (1) se lanza una simulación, (2) se compara el perfil de temperatura en el tubo observador al final del TRT con los resultados experimentales y (3) se ajusta la conductividad térmica de cada una de las capas. Este proceso se repite hasta que los resultados de simulación coinciden con los resultados experimentales teniendo en cuenta un margen de error establecido.

Artículo 2. Novel instrument for temperature measurements in borehole heat exchangers

Este segundo artículo cubre el diseño, construcción y verificación de un instrumento específico, llamado Geowire, para medir de forma automática y con mayor precisión los perfiles de profundidad-temperatura requeridos para implementar el método propuesto. Asimismo, el instrumento cumple con las especificaciones de diseño presentadas en el segundo punto de los objetivos. El Geowire consiste en un enrollador de cable automático que desplaza un sensor de temperatura a distancias previamente establecidas. Básicamente, el cable del sensor se enrolla en un carrete, un servomotor gira el carrete y un encoder mide la longitud del cable liberado para calcular la posición del sensor en las tuberías.

En el artículo se presentan los aspectos de diseño que van desde la mecánica, hardware, software, hasta el sistema operativo y la interfaz gráfica de usuario. Posteriormente, se proponen una serie de experimentos de laboratorio para evaluar el funcionamiento y características del instrumento:

- Repetitividad y fiabilidad de las medidas usando como referencia un termómetro de alta recisión (precisión ±0.03 K; resolución ±0.01).

- Mediciones para determinar el tiempo de respuesta del sensor utilizando un termómetro de alta precisión (precisión ±0.03 K; resolución ±0.01) y un baño térmico (precisión ±0.01 °C, estabilidad ±0.01 °C).
- Pruebas para determinar la repetitividad y fiabilidad de los desplazamientos espaciales.
- Calculo del tiempo mínimo de reposo para lograr un equilibrio térmico después de desplazar la sonda a una nueva posición.
- Pruebas para validar la solidez y fluidez de la aplicación del usuario (alarmas, gráficas en tiempo real, control remoto, seguridad y acceso simultaneo de múltiples usuarios).

Una vez validado el instrumento en el laboratorio se prepara un experimento en un BHE de pruebas (aislado de condiciones externas) situado en la universidad de Karlsruhe, Alemania. El pozo tiene una profundidad de 30 m y un diámetro de 450 mm. Al introducir el tubo-U dentro del pozo se colocan sensores comerciales de tipo pt100 a lo largo de la tubería para usarlos como referencia en la validación del Geowire. Asimismo, el pozo se llena con agua y se instala un cable calefactable en la mitad superior. Finalmente, se llevan a cabo dos pruebas, una midiendo la temperatura en reposo y otra después de calentar el pozo.

Artículo 3. Design and test of an autonomous wireless probe to measure temperature inside pipes

Este artículo presenta el diseño, construcción y verificación de una sonda de temperatura, llamada Geoball, la cual es arrastrada por el fluido que circula en las tuberías a la vez que calcula su posición. Se trata de una versión mejorada de la versión propuesta en Martos et al. (2011) cuyo diseño cumple con las características presentadas en el tercer punto de los objetivos.

En el artículo se presentan los aspectos de diseño relacionados con la parte mecánica, hardware, firmware e interfaz gráfica de usuario. Asimismo, se preparan las pruebas de laboratorio para validar el funcionamiento y características principales de la sonda:

- Mediciones para determinar el rango, precisión, tiempo de muestreo y resolución de temperatura.
- Fiabilidad de las comunicaciones inalámbricas.
- Capacidad para recolectar energía de manera inalámbrica.
- Duración de la batería.

- Capacidad para almacenar y representar de datos.

Artículo 4. Comparison of the developed instruments (Geowire and Geoball) with new and standard in-borehole temperature measurement instruments

Esta cuarta publicación acorde al cuarto objetivo describe un experimento con la intención de comparar las cualidades cuantitativas y cualitativas de los instrumentos desarrollados en esta tesis doctoral con instrumentos comerciales (novedosos y estándar) para mediciones de temperatura en intercambiadores enterrados, como el GEOsniff®, equipos de fibra óptica y cadenas de sensores Pt100.

En primer lugar, se realizan experimentos de laboratorio para comparar las características principales de cada equipo (rango de temperatura, resolución de temperatura, tiempo de muestreo, respuesta térmica, resolución espacial, etc.). En segundo lugar, se implementa un experimento de campo en un BHE de pruebas con una profundidad de 30 m y un diámetro de 450 mm situado en la universidad de Karlsruhe, Alemania. En el pozo se introduce una carcasa cilíndrica de 450 x 19,5 mm y otra de 180x10,7 mm, las cuales se llenan con agua para crear una barrera aislante entre el pozo y los posibles efectos térmicos del subsuelo adyacente. Posteriormente, se introduce un tubo-U hasta 21.5 m de profundidad para poder circular el Geoball y GEOsniff®, ya que se precisa de un circuito cerrado para su operación. Durante la inserción del tubo-U se adhieren cables de fibra óptica y una cadena de sensor Pt100 a lo largo de la superficie exterior del tubo. Además, se instala un cable calefactable a lo largo de la mitad superior del pozo con la finalidad de crear una situación térmica diferente a la de reposo. Posteriormente, se evalúan las características de los instrumentos ante dos situaciones térmicas diferentes. Por último, se desarrolla un modelo de elementos finitos 3D con la misma geometría y comportamiento térmico del BHE para evaluar la fiabilidad de los datos obtenidos con cada instrumento.

Artículo 5. Novel instruments and methods to estimate depth-specific thermal properties in borehole heat exchangers

Este quinto artículo describe un experimento en el cual se evalúan el método e instrumentos propuestos durante un TRT distribuido (DTRT) en comparación con termómetros de fibra óptica y un programa basado en el modelo de línea infinita de Kelvin (ILS) para estimar la conductividad distribuida. El estudio se lleva a cabo para alcanzar el quinto objetivo.

En el experimento presentado en el Capítulo 2 la conductividad térmica a lo largo de las capas geológicas se ajusta manualmente tras lanzar una simulación y este proceso

se repite hasta que los resultados del modelo coinciden con los resultados experimentales. No obstante, la ejecución de una sola simulación puede tardar del orden de días, por lo que el ajuste final puede resultar en una tarea excesivamente larga. Por esta razón, se añade un método de optimización por mínimos cuadrados (Nelder-Mead) para calcular de manera automática la conductividad lanzando una sola simulación. De esta manera se pretende reducir el tiempo de simulación y aumentar la precisión de los resultados.

En este caso se utiliza un BHE de 50 m de profundidad localizado en Vallentuna, Suecia. La estratificación del subsuelo adyacente al intercambiador enterrado está compuesta por una capa de arcilla hasta una profundidad de 6 m. Luego sigue un lecho de roca de granito y pegmatita hasta el final del pozo, que se llena naturalmente con agua subterránea. En el pozo se inserta un único tubo-U y una tubería auxiliar hasta una profundidad de 48.5 m. El tubo se conecta a un equipo de TRT mientras que en la tubería auxiliar (tubo observador) se obtienen los perfiles de temperatura requeridos para implementar el método de análisis propuesto en esta tesis. Asimismo, se introducen cables de fibra óptica en el interior del tubo-U (tramo con flujo descendente) y dentro del tubo observador para contrastar los resultados con el Geowire y Geoball.

Por otro lado, los perfiles de temperatura obtenidos a partir de la fibra óptica en el tubo observador se utilizan para evaluar el método propuesto en comparación con el programa ILS para calcular la conductividad distribuida. También se calcula analíticamente la conductividad global del subsuelo a partir del método de análisis típico en un TRT (ILS) para contrastar este valor con el valor promedio de los datos de conductividad locales estimados a partir de los métodos anteriores. Por último, se evalúan los resultados obtenidos al utilizar el método propuesto en combinación con el instrumento diseñado específicamente (Geowire) y se estos se comparan con los resultados obtenidos al aplicar el método a partir de los datos de fibra óptica.

4. Conclusión

El método e instrumentos propuestos en este trabajo de doctorado han demostrado su utilidad para mejorar la optimización de los sistemas de bomba de calor geotérmica en términos de eficiencia energética, así como para reducir la inversión de capital. Además, esta tesis doctoral ofrece una visión general en cuanto a la estimación de las propiedades térmicas distribuidas del terreno adyacente a un pozo o un intercambiador de calor enterrado (BHE).

Se ha propuesto un nuevo método, denominado *observer pipe TRT* (OP-TRT), para calcular la conductividad térmica de las capas geológicas a lo largo de la profundidad de

un pozo. Este método se basa en una medición adicional que se puede implementar en combinación con el TRT estándar para mejorar sus resultados: Un perfil de temperatura a lo largo de una tubería auxiliar, denominada tubo observador, llena de agua e instalada en paralelo a los extremos del tubo-U utilizado para inyectar calor. Además, se ha desarrollado un procedimiento de simulación inversa para estimar la conductividad térmica en función de la profundidad a partir de los datos recopilados durante un OP-TRT. Con la intención de valorar el método propuesto, se ha llevado a cabo un primer experimento bajando una sonda de temperatura cableada manualmente dentro del tubo observador durante un TRT. Este experimento se presenta en el Capítulo 3, del cual se pueden extraen las siguientes conclusiones:

- El OP-TRT ha demostrado reflejar en una escala de temperatura mayor las fluctuaciones térmicas producidas debido a la presencia de capas con diferentes propiedades térmicas y, por lo tanto, requiriéndose sensores menos precisos para obtener resultados más detallados.
- El OP-TRT y el procedimiento de simulación inversa han sido evaluados como método potencialmente viable para medir las propiedades térmicas en función de la profundidad del subsuelo que rodea un BHE.
- Tras aplicar el procedimiento de simulación inversa a los datos recolectados, se ha detectado una zona altamente conductiva entre 24 y 26 m, probablemente dominada por flujos de agua subterráneos.

Después de los buenos resultados obtenidos a partir del OP-TRT y el método de simulación inversa, los esfuerzos de investigación asociados a esta tesis han sido orientados hacia el desarrollo de un instrumento específico, llamado Geowire, con la intención de medir de manera fiable los perfiles de temperatura a lo largo del tubo observador. Como se indica en el Capítulo 4, el funcionamiento del Geowire ha sido analizado primero en el laboratorio, y posteriormente en BHE de pruebas utilizando sensores Pt100 como referencia.

- Mediciones entre el Geowire y los sensores Pt100 comparables (error cuadrático medio de 0.042), validándose así su aplicabilidad.
- El Geowire ha demostrado ser un dispositivo apropiado para medir los perfiles de temperatura distribuida con alta resolución espacial, temporal y de temperatura (0.5 mm, 750 ms, 0.06 K).
- Otras características que han sido validadas positivamente: registro automático de datos a intervalos de tiempo predefinidos; incertidumbre en las mediciones muy poco significativa (±5 mm en 10 m, ± 0.06 K); respuesta térmica de la sonda aceptable, interfaz intuitivo; control remoto (interfaz gráfica y descarga de datos); alarmas para detectar anomalías durante su funcionamiento; y gran

capacidad para almacenar datos.

Además, se ha desarrollado una versión mejorada de la sonda autónoma (Martos et al., 2011), llamada Geoball, la cual ha sido evaluada en el laboratorio (Capítulo 5). De este estudio se pueden extraen las siguientes conclusiones:

- Mejoras adicionales con respecto a la primera versión, como menor tamaño, menor peso y mayor tiempo de operación.
- Adecuado para obtener mediciones espaciales y de temperatura dentro de tuberías geotérmicas a lo largo de todo el circuito cerrado (flujo ascendente y descendente).
- Adecuado para distribuciones de tuberías verticales y horizontales.

Posteriormente, los dos instrumentos desarrollados en esta tesis doctoral (Geowire y Geoball) han sido comparados con instrumentos comerciales novedosos y estándar para la medición de temperatura en un BHE, como el GEOsniff®, termómetros de fibra óptica y cadenas de sensores Pt100. Las características principales de estos instrumentos han sido evaluadas primero en el laboratorio, y luego en BHE de pruebas aislado de condiciones externas (Capítulo 6). En este estudio se ha demostrado la importancia de analizar las diferencias cuantitativas y cualitativas de cada instrumento, procedimiento de calibración y método de análisis antes de implementar un TRT distribuido. A partir del cual además se pueden extraen las siguientes conclusiones con relación a los instrumentos desarrollados:

- En el laboratorio los nuevos instrumentos han medido la temperatura con una respuesta térmica rápida y alta precisión: Geowire (<2.0 s, ± 0.06 K) y Geoball (<0.5 s, ± 0.04 K).
- Los nuevos instrumentos han medido la temperatura con altas resoluciones espaciales y de temperatura: Geowire (0.5 mm, 0.06 K) y Geoball (10 mm, 0.05 K).
- El Geowire y el Geoball miden la temperatura instantáneamente, sin que la precisión dependa de la resolución espacial, temporal y del tiempo de muestreo. Por ello, en comparación con la fibra óptica, estos instrumentos proporcionan resoluciones espaciales y precisiones más altas en entornos con respuestas térmicas transitorias, p. ej. durante un TRT distribuido (DTRT).
- No requieren de una calibración dinámica para obtener resultados precisos, son más fáciles de integrar en los BHE existentes y también son una solución más rentable.
- Se pueden evitar errores en la calibración de múltiples sensores, como puede ser

el caso al utilizar una cadena de sensores.

Finalmente, se ha preparado un experimento (Capítulo 7) con la intención de evaluar el método y los instrumentos en un BHE durante un OP-TRT. En dicho experimento, se han introducido termómetros de fibra óptica dentro del tramo con flujo descendente del tubo-U y dentro del tubo observador para evaluación del Geowire y Geoball. Además, el modelo de simulación inversa ha sido evaluado en comparación con un programa basado en el modelo de línea infinita de Kelvin (ILS) para estimar la conductividad térmica distribuida a partir de los datos recolectados en el tubo observador:

- Las mediciones de temperatura a lo largo del tubo observador han mostrado diferencias de temperatura amplificadas para capas geológicas con propiedades térmicas diferentes en comparación con las medidas tomadas en el tubo con flujo descendente del TRT.
- El Geoball y el Geowire han demostrado una vez más medir la temperatura con una resolución espacial, temporal y de temperatura mayor que el equipo de fibra óptica utilizado.
- El modelo de simulación inversa ha sido mejorado efectivamente al incluir un modulo de estimación de parámetros. Tanto la precisión de los resultados como el tiempo de simulación han sido mejorados significativamente mediante un proceso automático para ajustar el perfil de temperatura objetivo (tubo observador) lanzando una única simulación.
- Se han obtenido resultados comparables entre el valor promedio de las estimaciones locales efectivas calculadas por ambos métodos y la conductividad efectiva para todo el subsuelo calculada analíticamente a partir de las ecuaciones de línea infinita típicas de un TRT estándar: 1.27% por debajo para el programa basado en ILS y 0.28% por debajo para el modelo de simulación inversa.
- Las estimaciones locales de conductividad efectiva calculadas con el modelo de simulación inversa a partir de los datos del Geowire han mostrado la mayor dispersión con respecto a la conductividad efectiva global de un TRT estándar. Consiguiendo así detectar una zona de 5 m de largo con elevada conductividad al utilizar el instrumento y método propuestos.
- Una de las ventajas del modelo de simulación inversa radica en que solo requiere dos perfiles de temperatura como entrada: (1) subsuelo en reposo y (2) al final del TRT.

Resum

El test de resposta tèrmica (TRT) és àmpliament utilitzat com a mètode estàndard per la caracterització de les propietats tèrmiques del terreny adjacent a un intercanviador de calor soterrat (BHE). Els mètodes tradicionals per interpretar els resultats fan ús de solucions analítiques o numèriques assumint que el terreny és infinit, homogeni i isotròpic. No obstant això, en realitat el subsol presenta generalment una estructura estratificada i heterogènia, i per tant les propietats tèrmiques poden variar substancialment amb la profunditat. En aquest sentit i amb l'objectiu de resoldre les limitacions del TRT estàndard, la present tesi doctoral se centra en el desenvolupament de mètodes i instruments per a quantificar les propietats de transferència de calor de les capes geològiques al voltant d'un BHE. Informació que resulta imprescindible per assolir la màxima eficiència energètica i el dimensionat tècnic-econòmic òptim d'un BHE.

En particular, es proposa un nou mètode de TRT, anomenat *observer pipe TRT* (OP-TRT), basat en un amidament de temperatura addicional al llarg d'un tub auxiliar. En les últimes dècades, diversos investigadors han desenvolupat TRT distribuïts (DTRT) en els quals es realitzen amidaments de temperatura al llarg del tub-U en el que s'injecta la calor. No obstant, a partir de les investigacions dutes a terme en aquesta tesi, el tub observador ha demostrat amplificar els efectes tèrmics produïts per culpa de capes geològiques amb propietats termo-físiques diferents, requerint-se així sensors menys precisos per tal d'obtindre resultats més detallats. Basant-se en aquest resultat, s'ha desenvolupat un model numèric de simulació inversa per parametritzar la conductivitat tèrmica de les capes geològiques a partir dels amidaments al llarg del tub observador. Bàsicament, el model ajusta la conductivitat tèrmica de les capes geològiques fins que els resultats de la simulació coincideixen amb el perfil de temperatura experimental al llarg del tub observador. El model ha sigut desenvolupat amb un algoritme d'estimació de paràmetres per a un ajust automàtic i obtenció de resultats més precisos. Un altre avantatge és que aquest mètode només requereix dos perfils de temperatura: (1) subsol en repòs (abans del TRT) i (2) al finalitzar el TRT (abans d'aturar la injecció de calor).

Amb l'objectiu de continuar investigant el mètode proposat a partir de dades de major qualitat, s'ha desenvolupat un instrument específic (Geowire) per tal de mesurar de forma automàtica i amb major precisió els perfils de profunditat-temperatura requerits. El disseny de Geowire també ha estat orientat a cobrir altres requisits, com ara compatibilitat amb equips de TRT i operació intuïtiva. A més, s'ha desenvolupat una versió millorada d'una sonda de temperatura (Geoball) la qual és arrossegada pel fluid que circula en les canonades i a la vegada calcula la seua posició amb l'avantatge de què pot ser utilitzada en tubs amb disposició vertical i horitzontal. Després de les proves de

validació al laboratori, les característiques fonamentals d'ambdós instruments han sigut avaluades en comparació amb altres instruments recents i estàndard per tal de mesurar temperatures distribuïdes durant un experiment en un BHE de proves. L'avantatge principal dels instruments proposat sobre la popular fibra òptica és que mesuren la temperatura instantàniament (a intervals temporals precisos). Així mateix, no necessiten un calibratge dinàmic per a donar resultats precisos proporcionant una major resolució espacial i de temperatura: Geowire (0.5 mm, 0.06 K) i Geoball (10 mm, 0.05 K). A més, són més fàcils d'integrar en pous existents i són una solució potencialment més rendible per mesurar la temperatura distribuïda.

Finalment, es demostren els beneficis del mètode i instruments proposats durant un DTRT en comparació amb la fibra òptica i amb un programari basat en el model de línia infinita per estimar la conductivitat tèrmica distribuïda. Els resultats del model proposat revelaren una zona altament conductiva a l'emprar les dades de Geowire, mentre que aquesta zona no va ser detectada al processar les dades de la fibra òptica.

Paraules clau: Bomba de calor geotèrmica; Intercanviador de calor soterrat; TRT tub observador; Subsol multicapa; Conductivitat tèrmica; Simulació numèrica; Eficiència energètica; Optimització tècnic-econòmica.

1. Context d'investigació i motivació

Els sistemes de bombes de calor geotèrmica (GSHP) s'expandeixen gradualment com una alternativa prometedora per tal d'estalviar energia i reduir les emissions de gasos d'efecte hivernacle. Els sistemes GSHP intercanvien calor amb el subsol amb l'objectiu d'obtindre aigua calenta o climatització (calefacció o refrigeració) en aplicacions domèstiques, urbanes o agrícoles. Aquests sistemes han demostrat assolir una major eficiència energètica que els sistemes d'aire condicionat. No obstant això, el capital d'inversió inicial és normalment major i depén principalment de la longitud, el grandària i el nombre d'intercanviadors de calor soterrats (BHE) necessaris.

El test de resposta tèrmica (TRT) és el mètode estàndard per a caracteritzar les propietats tèrmiques del subsol i els BHE, informació que és essencial per al dimensionat tècnic-econòmic òptim dels sistemes GSHP. Generalment, el TRT es realitza mitjançant un circuit tancat (tub en U) on el fluid portador de calor circula en sentit descendent i ascendent al llarg de tota la perforació del BHE. Durant el test, el fluid es bombeja a una velocitat relativament estable mentre que s'injecta calor a una potència constant mitjançant un element elèctric. Així mateix, es monitoritza i registra de manera contínua la potència calorífica injectada, el cabal del fluid, les temperatures d'entrada i sortida al BHE i la temperatura exterior. A partir d'aquests paràmetres, diferents solucions

analítiques i semi-numèriques han sigut proposades durant les últimes dècades per a estimar les propietats de transferència de calor al llarg de l'intercanviador i el terreny adjacent. Aquestes solucions consideren el subsol com un medi homogeni, isotròpic infinit i, per tant, únicament determinen paràmetres globals i efectius, com ara la conductivitat tèrmica efectiva i la resistència tèrmica efectiva de l'intercanviador.

No obstant, en realitat, la composició geològica del subsol és típicament heterogènia, normalment dividida en capes formades per diferents materials com a tipus de terra, tipus de roca i/o aigua subterrània. A més, el subsol també pot estar dominat per fractures o cavitats. Això significa que és improbable que la calor es puga transferir de manera uniforme a través de les capes geològiques del subsol situat al voltant d'un pou. És per això que el fer de conéixer la capacitat de transferència de calor d'aquestes capes podria ajudar a evitar el sobredimensionament d'instal·lacions, així com a reduir la inversió de capital innecessàriament major que aquesta pràctica comporta: costos addicionals derivats d'una major demanda de pressió, una major demanda de bombeig, caigudes de pressió addicionals i tot el material addicional necessari per a construir un BHE més profund (mà d'obra, perforació, canonades, material de farcit, etc.). Per exemple, en cas d'arribar a una zona amb propietats de transferència de calor poc favorables, es podria limitar la longitud de la perforació i construir un major nombre de pous menys profunds en lloc de menys pous més llargs. És a dir, es tracta d'informació de gran interés que no és possible obtindre a partir d'un TRT convencional, la qual permetria detectar les capes més favorables per a intercanviar calor i així poder establir la longitud òptima d'un BHE amb l'objectiu d'aconseguir el màxim rendiment de transferència de calor al mínim cost.

A partir d'aquesta problemàtica sense resoldre va sorgir la hipòtesi que motivà l'enfocament d'aquesta tesi. És possible desenvolupar mètodes i instruments específics que permetran parametritzar de forma detallada la capacitat de transferència de calor de les capes geològiques que creuen un BHE?

2. Objectius

L'objectiu general de la present tesi doctoral és l'exploració de mètodes i instruments per a avaluar la resposta tèrmica de les diferents capes geològiques que envolten a un intercanviador de calor soterrat. Així, amb el propòsit d'assolir aquest objectiu general, es proposen i investiguen els següents objectius específics:

I. Desenvolupament d'un mètode de simulació inversa per a calcular la conductivitat tèrmica del subsol que rodeja a un BHE en funció de la profunditat a partir d'amidaments de temperatura addicionals, en un tub auxiliar al llarg de tota la perforació, durant un TRT. Elaboració d'un

experiment per tal d'avaluar el mètode en un BHE experimental.

II. Desenvolupament d'un instrument específic per a mesurar els perfils de temperatura requerits per tal d'aplicar el mètode. Es deu investigar les característiques apropiades de l'instrument, com ara: compatibilitat amb equips de TRT estàndard; alta resolució espacial, temporal i de temperatura; pertorbació tèrmica mínima en el BHE; resposta tèrmica de la sonda prou ràpida per la seua manera de funcionament; un sistema embegut que incorpore el conjunt apropiat de tecnologies de la informació i la comunicació; registre automàtic de dades per a períodes de temps i profunditat predefinits; una operativa fàcil i convenient; interfície gràfica amigable i intuïtiva; capacitats per a emmagatzemar dades; possibilitat de control remot (interfície gràfica i descàrrega de dades); visualització de dades en temps real; recursos suficients per a integrar un mètode que permeta estimar les propietats tèrmiques en funció de la profunditat. Elaboració de proves per a validar les característiques de l'instrument, primer al laboratori i posteriorment en un BHE experimental.

III. Desenvolupament d'una versió millorada de la sonda de temperatura-posició proposta en Martos et al. (2011). S'investigaran les característiques apropiades de l'instrument, com ara: compatibilitat amb equips de TRT estàndard; menor grandària; resposta tèrmica més ràpida; menor pes; temps d'operació més llargs; enregistrament automàtic de dades per a intervals temporals i espacials predefinits; comunicacions i càrrega de la bateria sense fils; mesurament de temperatura al llarg de tota la xarxa de canonades (flux descendent i ascendent); capacitats per a circular en canonades amb disposició vertical i horitzontal. Elaboració de proves per a avaluar l'instrument en el laboratori.

IV. Desenvolupament d'una metodologia experimental que permeta analitzar i comparar els instruments proposats amb instruments innovadors i estàndard per a amidaments de temperatura distribuïda en un BHE de proves aïllat de condicions externes.

V. Desenvolupament d'una metodologia experimental per tal d'analitzar i comparar el mètode i instruments proposats amb altres mètodes i instruments durant un TRT en un BHE experimental.

3. Metodologia

La present tesi doctoral es basa en un compendi de publicacions científiques les quals han superat una revisió per parells. El cos de la tesi inclou un total de cinc articles cada u d'ells descrivint la investigació duta a terme per a assolir cada u dels objectius específics plantejat en la secció anterior. Basant-se en aquest format de la informació o

de tesis, la metodologia es divideix en cinc apartats.

Article 1. Extraction of thermal characteristics of surrounding geological layers of a geothermal heat exchanger by 3D numerical simulations

En aquest primer article es proposa un nou mètode per al càlcul de la conductivitat tèrmica de les capes geològiques que travessa un BHE. El mètode suggerit, denominat *observer pipe TRT* (OP-TRT), complementa al TRT estàndard proporcionant dades de temperatura addicionals al llarg d'un tub auxiliar introduït en paral·lel i equidistant als tubs del TRT. Així mateix, es proposa un procediment de simulació inversa per a estimar la conductivitat en funció de la profunditat a partir de les dades mesurades durant la implementació d'un OP-TRT.

Aquest estudi cobreix el desenvolupament i implementació d'un experiment on s'avalua el mètode proposat en un BHE ubicat al campus de la Universitat Politècnica de València. El BHE té una profunditat de 40 m i el subsol que ho envolta està format per sis capes geològiques diferents incloent presència d'aigua per davall dels quatre metres. Després de la perforació i inserció dels tubs geotèrmics, el pou es va farcir amb una barreja de ciment i bentonita. En aquesta instal·lació, es realitza un TRT en un tub-U en el qual a més de registrar els paràmetres típics (. cabal, potencia, temperatura d'entrada i eixida, etc.) també es mesura l'evolució de la temperatura en el tub auxiliar, denominat tub observador. En aquest cas, la temperatura distribuïda al llarg de l'interior del tub observador s'obté desplaçant una sonda cablejada manualment a intervals de distància coneguts. La sonda mesura la temperatura amb una resolució de 0.06 K i una precisió de ±0.5 K, i és calibrada al laboratori amb un termòmetre de precisió.

Després de la perforació i inserció dels tubs geotèrmics, el pou es va farcir amb una barreja de ciment i bentonita. En aquesta instal·lació, es realitza un TRT en un tub-U en el qual a més de registrar els paràmetres típics (p. ex. cabal, potència, temperatura d'entrada i eixida, etc.) també es mesura l'evolució de la temperatura en el tub auxiliar, denominat tub observador. En aquest cas, la temperatura distribuïda al llarg de l'interior del tub observador s'obté desplaçant una sonda cablejada manualment a intervals de distància coneguts. La sonda mesura la temperatura amb una resolució de 0.06 K i una precisió de ±0.5 K, i és calibrada al laboratori amb un termòmetre de precisió.

Després de dur a terme l'OP-TRT, es desenvolupa un model 3D d'elements finits (FEM) utilitzant COMSOL Multiphysics® amb la mateixa geometria i resposta tèrmica que el BHE experimental. El model s'implementa, utilitzant els mòduls de transferència de calor en sòlids (HT) i fluix no isotèrmic en tubs (NIPFL). A més, s'implementa un pla de simetria definit pels dos extrems del tub-U reduint així el volum del model a la

mitat. Així mateix, s'executa un estudi per a determinar el mallat òptim, buscant un compromís entre temps de simulació i precisió dels resultats. Abans d'iniciar amb l'algoritme de simulació inversa, el model es calibra per a què la resposta de temperatura en l'entrada i eixida dels tubs del TRT coincideix amb els resultats experimentals. Per això, el model es configura amb els paràmetres mesurats durant el TRT, com ara la potència dinàmica, el cabal dinàmic, la temperatura ambient dinàmica de l'aire i la temperatura inicial del subsol. Als dominis del subsol i el pou s'assignen els valors efectius de conductivitat i resistència tèrmica calculats a partir del TRT estàndard. Al domini del pou s'assignen les propietats tèrmiques dels materials utilitzats: farcit, tubs, fluid, etc. I al domini del subsol, la densitat i capacitat tèrmica dels tipus de terra detectats durant la perforació. Després del calibratge del model, el subsol es divideix en capes al llarg de l'eix vertical, separades a partir de les mostres de temperatura espacials mesurades en el tub observador. Posteriorment s'implementa l'algoritme iteratiu, (1) es llança una simulació, (2) es compara el perfil de temperatura en el tub observador al final del TRT amb els resultats experimentals i (3) s'ajusta la conductivitat tèrmica de cada una de les capes. Aquest procés es repeteix fins que els resultats de simulació coincideixen amb els resultats experimentals tenint en compte un marge d'error establit.

Article 2. Novel instrument for temperature measurements in borehole heat exchangers

Aquest segon treball cobreix el disseny, construcció i verificació d'un instrument específic, anomenat Geowire, per a mesurar de forma automàtica i con major precisió els perfils de profunditat-temperatura requerits per a implementar el mètode proposat. Així mateix, l'instrument compleix amb les especificacions de disseny presentades en el segon punt dels objectius. Geowire consisteix en un enrotllador de cable automàtic que desplaça un sensor de temperatura a distàncies prèviament establides. Bàsicament, el cable del sensor s'enrotlla en un rodet, un servomotor gira el rodet i un encoder mesura la longitud del cable alliberat per tal calcular la posició del sensor en el tub.

En l'article es presenten els aspectes de disseny que van des de la mecànica, hardware, software, fins al sistema operatiu i la interfície gràfica d'usuari. Posteriorment, es proposen una sèrie d'experiments de laboratori per tal d'avaluar el funcionament i característiques de l'instrument:

- Repetitivitat i fiabilitat de les dades prenent com a referència un termòmetre d'alta recessió (precisió ±0.03 K; resolució ±0.01).
- Mesuraments per a determinar el temps de resposta del sensor utilitzant un termòmetre d'alta precisió (precisió ±0.03 K; resolució ±0.01) i un bany tèrmic (precisió ±0.01 °C, estabilitat ±0.01 °C).

- Proves per a determinar la repetitivitat i fiabilitat dels desplaçaments espacials.
- Càlcul de la temperatura mínima de repòs per a assolir un equilibri tèrmic després de desplaçar la sonda a una nova posició.
- Proves per a validar la solidesa i fluïdesa de l'aplicació d'usuari (alarmes, gràfiques en tempo real, control remot, seguretat i accés simultani de múltiples usuaris).

Una vegada validat l'instrument en laboratori, es prepara un experiment en un BHE de proves (aïllat de condicions externes) situat en la Universitat de Karlsruhe, Alemanya. El pou té una profunditat de 30 m i un diàmetre de 450 mm. A l'introduir el tub-U dins del pou es col·loquen sensors comercials de tipus pt100 al llarg del tub per a emprar-los com a referència en la validació de Geowire. Així mateix, el pou s'ompli amb aigua i s'instal·la un cable calefactor en la meitat superior. Finalment, es completen dues proves, una mesurant la temperatura en repòs i altra després d'escalfar el pou.

Article 3: Design and test of an autonomous wireless probe to measure temperature inside pipes

Aquest article presenta el disseny, construcció i verificació d'una sonda de temperatura, anomenada Geoball, la qual es arrossegada pel fluid que circula en els tubs, calculant simultàniament la seua posició. Es tracta d'una versió millorada de la versió proposada en Martos et al. (2011), complint el disseny amb les característiques presentades en el tercer punt dels objectius.

En l'article es presenten els aspectes de disseny relacionats amb la part mecànica, hardware, firmware i interfície gràfica d'usuari. Així mateix, es preparen les proves de laboratori per a validar el funcionament i característiques principals de la sonda:

- Mediciones para determinar el rango, precisión, tiempo de muestreo y resolución de temperatura.
- Mesuraments per a determinar el rang, precisió, temps de mostreig i resolució de temperatura.
- Fiabilitat de les comunicacions sense fils.
- Capacitat per captar energia sense fils.
- Duració de la bateria.
- Capacitat per a emmagatzemar i representar dades.

Article 4: Comparison of the developed instruments (Geowire and Geoball) with new and standard in-borehole temperature measurement instruments

Aquesta quarta publicació d'acord al quart objectiu descriu un experiment amb la intenció de comparar les qualitats quantitatives i qualitatives dels instruments desenvolupats en la present tesi doctoral amb els instruments comercials (més recents i estàndard) per a mesurament de temperatura en intercanviadors soterrats, com ara el GEOsniff®, equips de fibra òptica i enfilalls de sensors Pt100.

En primer terme, es realitzen experiments de laboratori per a comparar les característiques principals de cada equip (rang de temperatura, resolució de temperatura, temps de mostreig, resposta tèrmica, resolució espacial, etc.). En segon lloc, s'implementa un experiment de camp en un BHE de proves d'una profunditat de 30 m i un diàmetre de 450 mm, situat en la Universitat de Karlsruhe, Alemanya. En el pou s'introdueix una carcassa cilíndrica de 450 x 19.5 mm i altra de 180x10.7 mm, les quals s'omplin amb aigua per tal de crear una barrera aïllant entre el pou i els possibles efectes tèrmics del subsol que l'envolta. Posteriorment, s'introdueix un tub-U fins a 21.5 m de profunditat per a poder circular el Geoball i GEOsniff®, ja que es requereix un circuit tancat per a la seua operació. Durant la inserció del tub-U s'adhereixen cables de fibra òptica i un enfilall de sensors Pt100 al llarg de la superfície exterior del tub. A més, s'instal·la un cable calefactor al llarg de la meitat superior del pou amb la finalitat de crear una situació tèrmica diferent de la de repòs. Posteriorment, s'avaluen les característiques dels instruments enfront de dues situacions tèrmiques diferents. Per últim, es desenvolupa un model d'elements finits 3D amb la mateixa geometria i comportament tèrmic del BHE per a avaluar la fiabilitat de les dades obtinguts per cada instrument.

Article 5. Novel instruments and methods to estimate depth-specific thermal properties in borehole heat exchangers

Aquest cinqué article descriu un experiment en el qual s'avaluen el mètode i instruments proposats durant un TRT distribuït (DTRT) en comparació amb termòmetres de fibra òptica i un programa basat en el model de línia infinita de Kelvin (ILS) per a estimar la conductivitat distribuïda. L'estudi es du a terme per a assolir el cinqué objectiu.

En l'experiment presentat en el Capítol 2 la conductivitat tèrmica al llarg de les capes geològiques s'ajusta manualment després de llançar una simulació i aquest procés es repeteix fins que els resultats del model coincideixen amb els resultats experimentals. No obstant, l'execució d'una sola simulació pot tardar de l'orde de dies, pel que l'ajust

final pot resultar en una tasca excessivament llarga. Per aquesta raó, s'afegeix un mètode d'optimització per mínims quadrats (Nelder-Mead) per a calcular de manera automàtica la conductivitat llançant una única simulació. D'aquesta manera es pretén reduir el temps de simulació i augmentar la precisió dels resultats.

En aquest cas s'utilitza un BHE de 50 m de profunditat localitzat en Vallentuna, Suècia. L'estratificació del subsol que envolta a l'intercanviador soterrat està composta per una capa d'argila fins a una profunditat de 6 m. A continuació, segueix una zona de roca de granit i pegmatita fins al final del pou, que s'ompli naturalment amb aigua subterrània. En el pou se inserta un únic tub-U i altre tub auxiliar fins a una profunditat de 48.5 m. El tub es connecta a un equipo de TRT mentre que en el tub auxiliar (tub observador) s'obtenen els perfiles de temperatura requerides per a implementar el mètode d'anàlisis proposat en aquesta tesi. Així mateix, s'introdueixen cables de fibra òptica en l'interior del tub-U (tram amb fluix descendent) i dins del tub observador per a contrastar els resultats enfront de Geowire i Geoball.

Per altra banda, els perfils de temperatura obtinguts a partir de la fibra òptica en el tub observador s'utilitzen per a avaluar el mètode proposat en comparació amb el programa ILS per a calcular la conductivitat distribuïda. També es calcula analíticament la conductivitat global del subsol a partir del mètode d'anàlisis típic en un TRT (ILS) per contrastar aquest valor amb el valor mitjà de les dades de conductivitat locals estimats a partir dels mètodes anteriors. Per últim, s'avaluen els resultats obtinguts a l'utilitzar el mètode proposat en combinació amb l'instrument dissenyat específicament (Geowire) i aquests es comparen amb els resultats obtinguts a l'aplicar el mètode a partir de les dades de fibra òptica.

4. Conclusió

El mètode i instruments proposats en aquest treball de doctorat han demostrat la seua utilitat per a millorar l'optimització dels sistemes de bomba de calor geotèrmica en termes d'eficiència energètica, així com per a reduir la inversió de capital. A més, aquesta tesi doctoral ofereix una visió general quant a l'estimació de les propietats tèrmiques distribuïdes del terreny adjacent a un pou o un intercanviador de calor soterrat (BHE).

S'ha proposat un nuo mètode, denominat *observer pipe TRT* (OP-TRT), per a calcular la conductivitat tèrmica de les capes geològiques al llarg de la profunditat d'un pou. Aquest mètode es basa en una mesura addicional que es pot implementar en combinació amb el TRT estàndard per a millorar els seus resultats: Un perfil de temperatura al llarg d'un tub auxiliar, denominat tub observador, ple d'aigua i instal·lat

en paral·lel als extrems del tub-U utilitzat per a injectar calor. A més, s'ha desenvolupat un procediment de simulació inversa per a estimar la conductivitat tèrmica en funció de la profunditat a partir de les dades obtingudes durant un OP-TRT. Amb la intenció de valorar el mètode proposat, s'ha dut a terme un primer experiment baixant una sonda de temperatura cablejada manualment dins del tub observador durant un TRT. Aquest experiment es presenta en el Capítol 3, del qual es poden extraure les següents conclusions:

- El OP-TRT ha demostrat reflectir en una escala de temperatura major les fluctuacions tèrmiques produïdes a causa de la presència de capes amb diferents propietats tèrmiques i, per tant, requerint sensors menys precisos per a obtenir resultats més detallats.
- El OP-TRT i el procediment de simulació inversa han sigut avaluats com un mètode potencialment viable per a mesurar les propietats tèrmiques en funció de la profunditat del subsol que envolta un BHE.
- Després d'aplicar el procediment de simulació inversa a les dades mesurades, s'ha detectat una zona altament conductiva entre 24 i 26 m, probablement dominada per fluxos d'aigua subterrànies.

Després dels bons resultats obtinguts a partir del OP-TRT i el mètode de simulació inversa, els esforços d'investigació associats a aquesta tesi, s'han orientat cap al desenvolupament d'un instrument específic, anomenat Geowire, amb la intenció de mesurar de manera fiable els perfiles de temperatura al llarg del tub observador. Com s'indica en el Capítol 4, el funcionament del Geowire ha sigut analitzat primer en laboratori, i posteriorment en BHE de proves utilitzant sensors Pt100 com a referència.

- Mesures entre el Geowire i els sensors Pt100 comparables (error quadràtic medi de 0.042), validant-se així la seua aplicabilitat.
- Geowire ha demostrat ser un dispositiu apropiat per a mesurar els perfils de temperatura distribuïda amb alta resolució espacial, temporal i de temperatura (0.5 mm, 750 ms, 0.06 K).
- Altres característiques que han sigut validades positivament: registre automàtic de dades a intervals de tempos redefinits; incertesa en les mesures molt poc significatiu (±5 mm en 10 m, ± 0.06 K); resposta tèrmica de la sonda acceptable, interfície intuïtiva; control remot (interfície gràfica i descàrrega de dades); alarmes per a detectar anomalies durant el seu funcionament; i gran capacitat per a emmagatzemar dades.

A més, s'ha desenvolupat una versió millorada de la sonda autònoma (Martos et al., 2011), anomenada Geoball, la qual ha sigut avaluada en laboratori (Capítol 5). D'aquest

estudi es poden extraure les següents conclusions:

- Millores addicionals respecte de la primera versió, com ara menor grandària, menor pes i major temps d'operació.
- Adient per a obtenir dades espacials i de temperatura dins de tubs geotèrmics al llarg de tot el circuit tancat (flux ascendent i descendent).
- Adequat per a distribucions de tubs verticals i horitzontals.

Posteriorment, els dos instruments desenvolupats en aquesta tesi doctoral (Geowire i Geoball) han sigut comparats amb instruments comercials tant de nova introducció com estàndard per a l'adquisició de temperatura en un BHE, com GEOsniff®, termòmetres de fibra òptica i enfilalls de sensors Pt100. Les característiques principals d'aquests instruments han sigut avaluades primer en laboratori, i posteriorment en un BHE de proves aïllat de condiciones externes (Capítol 6). En aquest estudi s'ha demostrat la importància d'analitzar les diferències quantitatives i qualitatives de cada instrument, procediment de calibrat i mètode d'anàlisis abans d'implementar un TRT distribuït. A partir del qual, a més, es poden extreure les següents conclusions amb relació als instruments desenvolupats:

- En laboratori, els nous instruments han mesurat la temperatura amb una resposta tèrmica ràpida i d'alta precisió: Geowire (<2.0 s, ± 0.06 K) i Geoball (<0.5 s, ± 0.04 K).
- Els nous instruments han mesurat la temperatura amb altes resolucions espacials i de temperatura: Geowire (0.5 mm, 0.06 K) i Geoball (10 mm, 0.05 K).
- Geowire i Geoball amiden la temperatura instantàniament, sense que la precisió presente dependència de la resolució espacial, temporal ni del temps de mostreig. Per tot això, en comparació amb la fibra òptica, aquests instruments proporcionen resolucions espacials i precisions més altes en entorns amb respostes tèrmiques transitòries, p. ex. durant un TRT distribuït (DTRT).
- No requereixen un calibrat dinàmic per a assolir resultats precisos, són més fàcils d'integrar en els BHE existents i també són una solució més rendible.
- Es poden evitar errors en el calibrat de múltiples sensors, com pot ser el cas a l'utilitzar enfilalls de sensors.

Finalment, s'ha preparat un experiment (Capítol 7) amb l'objectiu d'avaluar el mètode i els instruments en un BHE durant un OP-TRT. En aquest experiment, s'han introduït termòmetres de fibra òptica dins del tram amb flux descendent del tub-U i dins del tub observador per a avaluació de Geowire Geoball. A més, el model de simulació inversa ha sigut avaluat en comparació amb un programa basat en el model de línia

infinita de Kelvin (ILS) per tal d'estimar la conductivitat tèrmica distribuïda a partir de les dades obtingudes al tub observador:

- Els amidaments de temperatura al llarg del tub observador han mostrat diferències de temperatura amplificades per a capes geològiques amb propietats tèrmiques diferents en comparació als amidaments fets al tub amb flux descendent del TRT.
- Geoball i Geowire han demostrat, de nou, mesurar la temperatura amb una resolució espacial, temporal de temperatura major que l'equip de fibra òptica utilitzat.
- El model de simulació inversa ha sigut millorat significativament a l'incloure un mòdul d'estimació de paràmetres. Tant la precisió dels resultats com el temps de simulació han presentat millores significatives a l'utilitzar un procés automàtic per a ajustar el perfil de temperatura objectiu (tub observador) realitzant-lo tot en una única simulació.
- S'han obtingut resultats comparables entre el valor mitjà de les estimacions locals efectives calculades per ambdós mètodes i la conductivitat efectiva para tot el subsol calculada analíticament a partir de les equacions de línia infinita típiques d'un TRT estàndard: 1.27% per davall per al programa basat en ILS i 0.28% per davall per al model de simulació inversa.
- Les estimacions locals de conductivitat efectiva calculades amb el model de simulació inversa, a partir de les dades de Geowire, han mostrat la major dispersió respecte a la conductivitat efectiva global d'un TRT estàndard. Aconseguint així detectar una zona de 5 m de llarg amb elevada conductivitat a l'utilitzar l'instrument i mètode proposats.
- Un dels avantatges del model de simulació inversa radica en què només requereix dos perfils de temperatura com entrada de dades: (1) subsol en repòs i (2) al final del TRT.

Title

Novel method and instruments for the optimal techno-economic sizing of borehole heat exchangers.

Abstract

The thermal response test (TRT) is widely used as a standard test to characterize the thermal properties of the ground near a borehole heat exchanger (BHE). Typical methods to interpret the results apply analytical or numerical solutions which assume that the ground is infinite, homogeneous and isotropic. However, in reality the underground is commonly stratified and heterogeneous, and therefore thermal properties may significantly vary with depth. In this sense and with the intention to overcome standard TRT limitations, this Ph.D. study is focused on developing methods and instruments for the evaluation of the heat transfer behavior of the geological layers surrounding a BHE. This information is key for the optimal energy efficiency and techno-economic sizing of BHE.

In particular, a novel TRT method, called observer pipe TRT (OP-TRT), is proposed based on an additional temperature measurement along an auxiliary pipe. In the last decades, some researchers developed the so-called distributed TRT (DTRT) by measuring the temperature along the length of the heated U-pipe. However, from the studies carried out in this Ph.D. work, the observer pipe demonstrated to amplify the thermal effects produced due to geological layers with different thermo-physical properties, hence requiring less accurate sensors for obtaining more detailed results. Based on this achievement, an inverse numerical solution was developed to parametrize thermal conductivity of geological layers from the measurements along the observer pipe. Basically, the model adjusts thermal conductivity of the geological layers until simulation results fit experimental temperature profile along the observer pipe. The model was developed with a parameter estimation solver for an automatic fitting and more accurate results. Another advantage is that this method only requires two temperature profiles: (1) undisturbed ground (before the TRT) and (2) at the end of the TRT (before stopping the heat injection).

In order to further investigate the proposed method by using higher quality data, a specific instrument (Geowire) was developed to automatically measure the required depth-temperature profiles with high accuracy. The design of the Geowire also covered

other features, such as compatibility with TRT equipment and intuitive operation. In addition, an enhanced version of a flowing probe (Geoball) was developed, suitable for both vertical and horizontal pipe arrangements. After laboratory validation tests, the key features of both instruments were evaluated in comparison with new and standard in-borehole instruments for temperature measurements in a test BHE. The main advantage of the proposed instruments over the widespread fiber optics is that they measure the temperature instantaneously (for precise time instants). Moreover, they do not require a dynamic calibration for accurate results while providing higher spatial and temperature resolutions: Geowire (0.5 mm, 0.06 K) and Geoball (10 mm, 0.05 K). Also, they are easier to integrate in existing boreholes and are a potentially more cost-effective solution to measure the distribute temperature.

Finally, the benefits of the proposed method and instruments are demonstrated throughout a DTRT in comparison with fiber optics and with a computer program based on the infinite line source model to estimate the distributed thermal conductivity. The results from the proposed model revealed a highly conductive zone when using data from the Geowire, whereas this was not the case when data from fiber optics were processed.

Keywords: Ground source heat pump (GSHP); Borehole heat exchanger (BHE); Observer pipe thermal response test (OP-TRT); Layered subsurface; Thermal conductivity; Numerical simulation; Energy efficiency; Techno-economic optimization.

Acknowledgments

Although my name is the only one appearing on the cover of this thesis, I did not make this journey alone. This thesis would not have been possible if it were not for the support and contributions of many individuals and organizations.

I would like to thank my Ph.D. supervisors, Julio and Jesús, for their unfailing support and guidance. Thanks for sharing your knowledge and passion for electronics as a professor during my degree, and this journey. Without all your thoughtful recommendations, constructive critiques and contributions, this work would not have been possible. I am truly grateful for your time, expertise and patience. This achievement is also yours!

Many thanks to the DSDC family for their warm friendship, lively lunches and the brilliant atmosphere that made this journey easier. José and Rai, thanks for your advice, mentoring and opportunities during my path through the university. Likewise, I would also like to thank the rest of my colleagues and also friends: Adri, Abraham, Rober, Albert and Pedro.

Also, I would like to express my gratitude to Álvaro Montero and Llucia Monreal for their support and contributions.

I am grateful to Robert Charlier for accepting me as a guest researcher in the University of Liege at the Applied Sciences faculty, ArGEnCo department. My sincere thanks to Georgia Radioti for showing and helping me around and for her contributions to this work. Thanks to Pierre Illing for his kind assistance in the laboratory, his support was essential in adapting and repairing the first version of the Geowire that got broken apart during the first field test. Likewise, special thanks to Gaël Dumont for the field trip to Brussels, and to Frédéric Nguyen, Simon Delvoie and the rest of the group members.

My profound gratitude goes to Philipp Blum, first for giving me the opportunity to be a guest researcher in the Karlsruhe Institute of Technology (KIT), Institute of Applied Geosciences (AGW). Second, for sharing your knowledge with passion and enthusiasm, your ceaseless support with resources and your constructive contributions. Also, to Steger Hagen, I really enjoyed sharing the office with you. Thanks for helping me around, lending me a bike, your kind advice and all your support and ideas in the laboratory and field tests. In addition, I would like to thank all the group members for the great atmosphere, specially to Susanne and Tobias.

I would like to express my warm gratitude to José Acuña. Thank you for hosting me

as a guest researcher at the Division of Applied Thermodynamics and Refrigeration (ETT), Royal Institute of Technology (KTH). Thanks for providing all the resources to finalize the instruments and to carry out the field tests. I am deeply grateful for your support, efforts and useful contributions. A big thanks to Benny Sjöberg for his help in the laboratory to prepare the valve circuit to test the Geoball. Special thanks to Milan for his help during the field test and Willem for his contributions. Also, I would like to thank the KTH family for the easy-going atmosphere and support, specially to Patricia, Monika, Mohammad, Alberto, Adrian, Bruno, Davide and David.

I would also like to thank all the members of my Ph.D. panel for accepting to evaluate this work and I would like to express my gratitude to the reviewers for the constructive comments, which improved the quality of the papers appended to this. thesis.

Throughout this journey, I had the great fortune to meet my now wife, Jennifer. My loving and heartfelt thanks for all the support, endless patience and encouragement through my work. Thanks for the date in the borehole field during a cold Saturday evening in Liege, and for bringing pizza to the field when I needed to finish the test before my trip back home on Monday. Thanks for your patience that day and for many others when I was busy with work.

Lastly, I would like to deeply thank my parents and brother for all their constant support and understanding all the way through.

Thanks a lot!

Table of contents

Table of figures

List of symbols and abbreviations

ASHP	Air source heat pump
BHE	Borehole heat exchanger
B2G	Borehole-to-ground
CFD	Computational fluid dynamics
cm	Centimeter
CO_2	Carbone dioxide
COP	Coefficient of performance
COP21	2015 United Nations climate change conference
COP25	2019 United Nations climate change conference
CPU	Central processing unit
C_p	Specific heat capacity of water at 20 ºC, 4.192 kJ/kg-K
DHE	Downhole heat exchanger
DTS	Distributed temperature sensing
DTRT	Distributed thermal response test
FEM	Finite element model
FLS	Finite line source
g	Gram
GHE	Ground heat exchanger
GSHP	Ground source heat pump
h	Hour
HDPE	high-density polyethylene
HVAC	Heating, ventilation and air conditioning
ICS	Infinite cylindrical source
IEC	International electrotechnical commission
ILS	Infinite line source
J	Joule
K	Kelvin degree

kg	Kilogram
l	Litter
m	Meter
$\dot{m}$	Mass flow rate, kg/s
min	Minute
mm	Millimeter
MWt	Megawatt thermal
NIMO-T	Non-wired immersible measuring object for temperature
NITF	Non-isothermal flow
OP-TRT	Observer pipe thermal response test
Pt1000	Platinum resistance thermometer
Q	Heat flow
q	Heat transfer rate (W/m)
R	Thermal resistance
R^2	Coefficient of determination
RMSE	Root mean square error
R_{bg}	Borehole-wall to ground thermal resistance
R_f	Thermal resistance of the material filling the borehole
R_{fb}	Fluid to borehole-wall thermal resistance
R_g	Ground thermal resistance
R_{pf}	Thermal resistance of the heat carrier fluid inside the pipe
R_{pw}	Thermal resistance of the pipe-wall
R_T	Total thermal resistance
RTD	Resistance temperature detector
s	Second
SI	System of Units
SPF	Seasonal performance factor
SSE	Sum of squares due to error
T_b	Temperature in the borehole-wall

T_C	Temperature of the cold reservoir
T_{df}	Temperature in the TRT down-flow pipe
T_{exp}	Experimental temperature
T_f	Temperature of the fluid in the pipe circuit
T_{fg}	Far ground temperature
T_H	Temperature of the hot reservoir
T_{in}	Inlet temperature of TRT
T_{sim}	Temperature from simulation
T_{obs}	Temperature in the observer pipe
T_{out}	Outlet temperature of TRT
TJ	Terajoule
TRT	Thermal response test
TSE	Thermal shunt effect
UNFCCC	United Nations Framework Convention on Climate Change
UTES	Underground thermal energy storage
W	Watt
y	Linear equation
1D	One Dimensional
2D	Two dimensional
3D	Three dimensional
λ	Thermal conductivity
λ_{eff}	Effective thermal conductivity
n	Depth-specific layer number
η	Ratio of the work done by the engine to the heat drawn out of the hot reservoir
$\propto$	Thermal diffusivity
ρ	Density
ºC	Celsius degree

Chapter 1

Introduction

This introductory chapter sets out the context and unresolved challenges of the research topic covered in this doctoral thesis. In addition, the initial objectives and the structure of this thesis are presented.

1.1. Research context and motivation

Ground Source Heat Pump (GSHP) systems are incrementally expanding as a promising alternative for saving energy and reducing greenhouse gas emissions. GSHP systems exchange heat with the subsurface for providing hot water or temperature conditioning (heating or cooling) in domestic, urban or agricultural applications. These systems have proven to achieve a higher energy efficiency than air conditioning systems. However, the initial capital investment is normally higher and depends mainly on the length, size and required number of borehole heat exchangers (BHE). For this reason, an accurate evaluation of thermo-physical properties of geological layers surrounding the BHE is essential for determining the most cost-effective size and improving economic viability of installations.

The thermal response test (TRT) is the standard method for characterizing thermal properties of the ground and BHE critical in the tecno-economic design of GSHP systems. The TRT is typically carried out in a closed-loop (U-pipe) where the heat carrier fluid circulates downwards and upwards in the BHE. During the test, the fluid is pumped at a relatively stable rate while a constant heat power is injected using an electric element. The TRT monitors and registers the transitory fluid flow rate, injected heat power, inlet-outlet temperatures of the BHE and ambient air temperature. From these parameters, a number of analytical and semi-numerical solutions have been proposed during the last decades to estimate the heat transfer rate in the borehole and near ground. These solutions consider the ground as a homogeneous, isotropic and infinite media, and therefore only determine bulk and effective parameters such as the effective thermal conductivity and borehole thermal resistance.

However in reality, subsurface geological composition is typically heterogeneous, normally divided in layers formed by different materials such as types of soil, types of rock and/or groundwater. The underground may also be dominated by fractures or

cavities. This means that heat is not likely to be transferred at the same rate throughout the different layers crossed by the perforation of a borehole. Understanding the thermal behavior of these layers may help to avoid over-sized BHE with an unnecessary higher capital investment including the extra cost derived from higher pressure demand, higher pumping demand, additional pressure drops and all the additional material needed to build a longer BHE (e.g. manpower, drilling, piping, grouting, etc.). For instance, in the event of reaching an area with unfavorable heat transfer properties, the length of the borehole could be limited and hence, build more shallow boreholes instead of fewer longer boreholes. In other words, this information of great interest that is currently missing in conventional TRT would allow the detection of the most favorable layers to exchange heat and thus establish the optimal length of a BHE to achieve the maximum energy performance at minimum cost.

From this unresolved problematic emerged the hypothesis that triggered the focus of this Ph.D. work. Could methods and specific instruments be developed for a detailed heat transfer rate parametrization of the different geological layers crossed by a BHE?

1.2. Research objective

The overall aim of the present doctoral thesis is the exploration of methods and instruments for evaluating the thermal response of the different geological layers surrounding a borehole heat exchanger. To achieve this general objective the following specific objectives are proposed and investigated throughout this Ph.D. study:

I. Development of an inverse simulation method to calculate the depth-specific thermal conductivity of the ground surrounding a BHE from additional depth-specific temperature measurements, in an auxiliary pipe along the entire borehole, during a TRT. Elaboration of an experiment to evaluate the method in a BHE test facility.

II. Development of a specific instrument for measuring the temperature profiles required to apply the method. The appropriate features of the instrument should be investigated, such as: compatibility with standard TRT equipment; high spatial, temporal, and temperature resolution; minimal thermal disturbance in the BHE; thermal response time of the probe fast enough for its application; an embedded system that incorporates the adequate set of information and communication technologies; automatic data recording at pre-defined time intervals; easy and convenient to operate; user-friendly and intuitive graphical interface; data storing capabilities; remote control possibilities (graphical interface and data download); real-time data

visualization; capabilities to embed a method to estimate the depth-specific thermal properties. Elaboration of tests to validate the instrument, first in the laboratory and later in an experimental BHE.

III. Development of an enhanced version of the flowing probe proposed in Martos et al. (2011). The appropriate features of the instrument should be investigated, such as: compatibility with standard TRT equipment; smaller size; faster thermal response time; less weight; longer operation time; automatic data recording at pre-defined time intervals; wireless data transmissions, and simultaneous charge of the battery; measurements of temperature along the entire pipe network (down- and up-flow); suitable for vertical and horizontal pipe distribution. Evaluation of the instrument in the laboratory.

IV. Development of an experimental methodology to analyze and compare the proposed instruments with new and standard in-borehole instruments in a test BHE isolated from external conditions.

V. Development of an experimental methodology to analyze and compare the proposed method and instruments with other method and instruments during a TRT in a real BHE facility.

1.3. Thesis structure

This doctoral thesis is organized in seven chapters covering the evolution of the implemented research work. The main body is composed as a collection of five peer-reviewed papers that address the research objectives listed in Section 1.2.

Chapter 1 introduces the overall context, motivation and objectives of this research topic together with a description of its structure.

Chapter 2 provides a summary and discussion of earlier work (literature review) on the principal subjects of study, e.g. GSHP systems, heat transfer in the borehole and ground, heat transfer modelling, in-situ methods to estimate thermal properties in BHE, etc. This introductory part basically sets out the context of this research topic and provides the background necessary to understand the remainder of this thesis.

Chapter 3 (paper I) introduces an inverse simulation method to calculate the depth-specific thermal conductivity. The method results are evaluated in an experimental BHE after the implementation of a TRT.

Chapter 4 (paper II) covers the development of an instrument called Geowire, to

automatically measure the temperature profiles required for the inverse simulation method suggested in the previous chapter. The precision and uncertainty of the spatial and temperature measurements are assessed in the laboratory. Also, the instrument is assessed in a test BHE and results are compared with the well-known Pt100-sensors.

Chapter 5 (conference paper) introduces a new design of the flowing probe reported in Martos et al. (2011). The probe, called Geoball, measures the temperature and its position along pipes while it is carried by the fluid. The correct operation of the probe is verified in the laboratory.

Chapter 6 (paper III) describes an experiment for comparing the quantitative and qualitative attributes of the two instruments developed during this Ph.D. work with new and standard in-borehole temperature measurement instruments. The performance of each instrument is analyzed in a BHE test site isolated from external conditions. Moreover, a numerical model is developed to reproduce the thermal behavior in the borehole with the intention of investigating the reliability of the measurements recorded by each instrument.

Chapter 7 (paper IV) introduces an experiment to validate an enhanced version of the proposed inverse simulation method. The input data used is from the specifically designed instrument (Geowire) in a BHE installation during a TRT. In addition, the two instruments developed in this Ph.D. work, Geowire and Geoball, are evaluated with the fiber optical thermometer used typically in distributed TRT. Likewise, the inverse simulation method is evaluated with another method to estimate the depth-dependent thermal conductivity.

Chapter 8 presents the overall and specific conclusions drawn from this doctoral thesis. In addition, this part identifies possible lines for future research in order to continue the research work presented in this thesis. Finally, the scientific publications related to the Ph.D. study are also listed.

Each of the chapters based on a research paper can stand alone as an individual piece of research work, and thus can be read independently in whatever order. However, it is recommended to read them in the suggested chronological order of submission or publication in the corresponding journals as this is the most logical order for acquiring a better understanding of the connection among the different research papers.

1.4. Thesis framework

The present doctoral thesis summarizes the research efforts of its author, during the period 2013-2020, as a member of the Digital Systems Design Group (DSDC) in the Electronic Engineering Department at Universidad de Valencia.

In particular, this doctoral study has been carried out within the framework of the European Institute of Innovation and Technology Climate-Knowledge and Innovation Community, a body of the European Union inside the Ph.D. Program of Transforming the Built Environment Platform.

The author has carried out a relevant amount state-of-the-art developments including: electronic schematics and layouts, low-power oriented electronics, firmware for field-programmable gate array (FPGA) and microcontrollers, wireless communications, embedded operating systems, graphical user interface and database applications, instrumentation and calibration, mechanical designs, laboratory and field experiments as well as multi-physics based numerical simulations.

Moreover, during this time the author has performed more than seven months of research mobilities in three relevant universities around Europe:

- University of Liege, Applied Sciences faculty, ArGEnCo department, Liege, Belgium.
- Karlsruhe Institute of Technology (KIT), Institute of Applied Geosciences (AGW), Karlsruhe, Germany.
- Royal Institute of Technology (KTH), Division of Applied Thermodynamics and Refrigeration (ETT), Stockholm, Sweden.

Throughout these research experiences the author has presented and discussed the status of the research work, as well as prepared working plans to carry out some of the experiments that have derived in the publications appended to this thesis.

Chapter 2

Theoretical fundamentals

This chapter introduces the theoretical background and literature review for providing the basis on which this Ph.D. study has been developed.

2.1. Importance of renewable energies

The expected long-term exhaustion of fossil fuel reservoirs, together with successive crisis and raising of prices, have triggered and accelerated the search for alternative sources of energy. In addition to this concern, the uninterrupted and incrementing process of burning fossil fuels leads to serious repercussions for environment, as air pollution and global warming due to CO_2 (greenhouse gas) emissions into the atmosphere (Colmenar-Santos et al., 2016; Sarbu & Sebarchievici, 2014). To deal with these issues, in 1997 the Kyoto protocol to the United Nations framework convention on climate change (UNFCCC) was proposed and signed by 192 parties, accepting that global warming is real and derived from human produced CO_2 emissions. The objective to fight climate change was strongly influenced by the Kyoto protocol – reducing greenhouse gas concentration in the atmosphere to levels which do not influence the Earth's natural climate evolution. Scenarios studied by Gupta et al. (2007) suggest that Annex I Parties would need to be 25% to 40% below 1990 levels by 2020, and 80% to 95% below 1990 levels by 2050. In the United Nations climate change conference (COP21) held in Paris, France, from 30 November to 12 December 2015 the Paris Agreement was negotiated: a global agreement on mitigating climate change setting the goal of limiting the global warming to 1.5 ºC in comparison with the levels before the industrial revolution. In the final draft of the climate deal accepted in Paris, according to some scientists (Sutter et al., 2015), the goal will require the transition from fossil fuels to renewable energies (zero emissions) sometime between 2030 and 2050. The most recent update was the COP25 help in Madrid, Spain, from the 2 to 13 December 2019. The results of this conference were disappointing at a time when climate and concrete measures are considered urgent (Dennis & Harlan, 2019). Carbon emissions set a new record in 2019 and once more scientists warned that the time is running out to address the true scale of the crisis.

2.2. Geothermal energy

The potential of geothermal energy as environmentally friendly, cost-effective and a reliable source of energy is huge and can significantly contribute to stop the dependence on fossil fuels as well as to reduce CO_2 emissions. For this reason, it is one of the renewable sources of energy that has been developed extensively during the last years (Shortall et al., 2015). Studies carried out in 2015 pointed out energy savings quantified in 52.8 million tons of equivalent oil annually, which prevented 149.1 million tons of CO_2 from being released to the atmosphere (Lund & Boyd, 2016).

Geothermal energy is heat energy generated and stored in the Earth's crust from the original formation of the planet and from the decay of radioactive elements (Turcotte & Schubert, 2002). It is classified as renewable source of energy due to the fact that heat in geothermal reservoirs is replenished naturally from earth processes.

Generally, in areas without specific geothermal anomalies, temperatures along the vertical axis of the Earth's subsurface are distributed as follows. From surface until a depth of 10 m, underground temperatures are drastically affected by outdoor seasonal conditions. Below 10 m and until 100 m, underground temperature is affected by heat transferred from Earth's core and environmental temperature. However, temperatures within such a depth remain relatively constant and usually equal to the annual average outdoor temperature. For a depth below 100 m, underground thermal gradient presents a linear relation for which the temperature increases 2.5-3 ºC per each section of 100 m depth (Fridleifsson et al., 2008).

Humanity has harnessed the thermal energy accumulated in the subsoil since ancient times (Stober & Bucher, 2013) for instance in the Paleolithic era it was used for bathing and in Roman era as space heating. However, the utilization of thermal resources as source of energy did not progress significantly until the middle of the 19th century due to the fast development of thermodynamics. At present, geothermal energy is classified in two main categories in terms of the application:

- Shallow or low-enthalpy geothermal energy: depth <400 m and temperatures between 20 and 70 ºC.
- Deep or high-enthalpy geothermal energy: depth >400 m and temperatures between 70 and 400 ºC.

Deep geothermal energy is mainly used for generating electricity in power plants by the steam coming from underground aquifers. Unfortunately, the locations that allow exploitation of high-enthalpy geothermal energy are limited due to its requirement to

fulfill specific conditions, such as geological formation and the presence of magmatic heat source. An effective utilization of this energy is bounded to regions near the tectonic fault lines within the Earth's surface or highly volcanic areas, as Philippines, Indonesia, EEUU, Mexico or Italy.

On the other hand, low-enthalpy geothermal energy is utilizable at practically any part on the Earth's surface. Moreover, the development of new technologies has made it suitable for many applications in agricultural, domestic and urban sectors. Shallow geothermal energy is classified mainly in two categories (Sanner, 2001): underground thermal energy storage (UTES) systems and ground source heat pump (GSHP) systems.

In a UTES system, heat, cold or a combination of both are stored underground. Heat from solar radiation, geothermal energy or waste heat are kept in reservoirs underground for a later use. Cold air can be used to cool down the underground during winter and then used again in summer, or solar heat can be accumulated during summer for de-icing of road surfaces in winter.

Additionally, a GSHP system is a technology used for exchanging heat with the underground for heating or cooling buildings (residential or larger infrastructures) or hot water production. Outdoor air temperature oscillates depending on the changing seasonal weather, but shallow ground remains at a near constant temperature due to the Earth's high thermal inertia and insulation properties. Underground temperature is more favorable for exchanging heat in comparison to outside air temperature regardless whether it is winter or summer (Fig. 1). Therefore, GSHP systems have proven to achieve higher energy efficiency than conventional air source heat pump (ASHP) systems (Florides & Kalogirou, 2007). The concept of energy efficiency in a heat pump system is described in more detail in the next section.

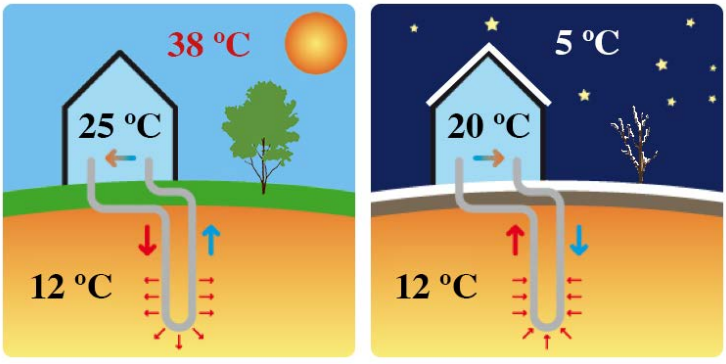

Fig. 1. GSHP system for heating in winter and for cooling in summer.

Currently, geothermal heat pumps are the most extensively-developed technology for extracting thermal energy, covering worldwide 70.9% of the installed capacity (MWt) and 55.2% of the annual energy use (TJ/year) (Lund & Boyd, 2016). Despite the increment in the number of applications involving GSHP systems in the last years, it is still a relatively new technology, and the margin for energy performance optimization and improving economic viability of installations is wide. Since this technology is the focus of this Ph.D. study, it is covered in more detail in the following section.

2.3. GSHP systems

Generally, a GSHP system is composed by the concatenation of three main elements: a ground heat exchanger (GHE), a compression heat pump and a heat distribution system. Fig. 2 illustrates the basic configuration of these main components and its principle of operation.

The GHE consists of a network of pipes buried in the ground along which a heat carrier fluid is pumped to exchange thermal energy with the ground. The underground acts as heat source for heating (in winter) and as a heat sink for cooling (in summer). The heat pump is a device that transfers heat energy from a lower-grade temperature to a higher-grade temperature by using a small amount of external energy (e.g. run a compressor). It is divided in three main parts: the evaporator, the compressor and the condenser. The thermodynamic principle of a heat pump consists of the fact that a gas increases its temperature and boiling point when compressed to a smaller volume. A heat pump can be reversible by a 3-way valve and operate in either direction to provide heating or cooling to buildings or other applications.

In heating mode, a liquified refrigerant solution enters the evaporator through an expansion valve where its volume is increased by lowering its temperature. In the evaporator, the refrigerant absorbs heat from the ground until it begins to boil and turns into gas. This gas is then fed into the compressor to increase its pressure making the gas temperature rise. The hot refrigerant gas then flows into the condenser where the heat is transferred to the heat distribution system. After the heat is transferred to the heat distribution system, the refrigerant gas reverts into liquid. Then, this liquid returns back to the evaporator through an expansion valve, reducing its pressure and temperature, ready to start the cycle all over again. In cooling mode, the cycle is similar but the outdoor coil is the condenser while the indoor coil is the evaporator. Heat from the building is injected to the ground and the building is effectively cooled by the expansion of the refrigerant.

Regarding the heat distribution system heating, ventilation and air conditioning (HVAC) is the most common technology to provide a comfortable temperature for buildings. Alternately, thermal energy from the ground can be transferred to water, which can be used to heat buildings via radiators or underfloor heating. The heated water can also be utilized directly for domestic hot water consumption.

Although, some elements of a GSHP system use external energy (electric power) to operate, such as the compressor, circulating fluid pumps and other auxiliary elements, the thermal energy generated by a GSHP system is typically 2-5 times higher than the consumed electric energy, therefore making them considerably energy efficient (Atam & Helsen, 2016; Bayer et al., 2014).

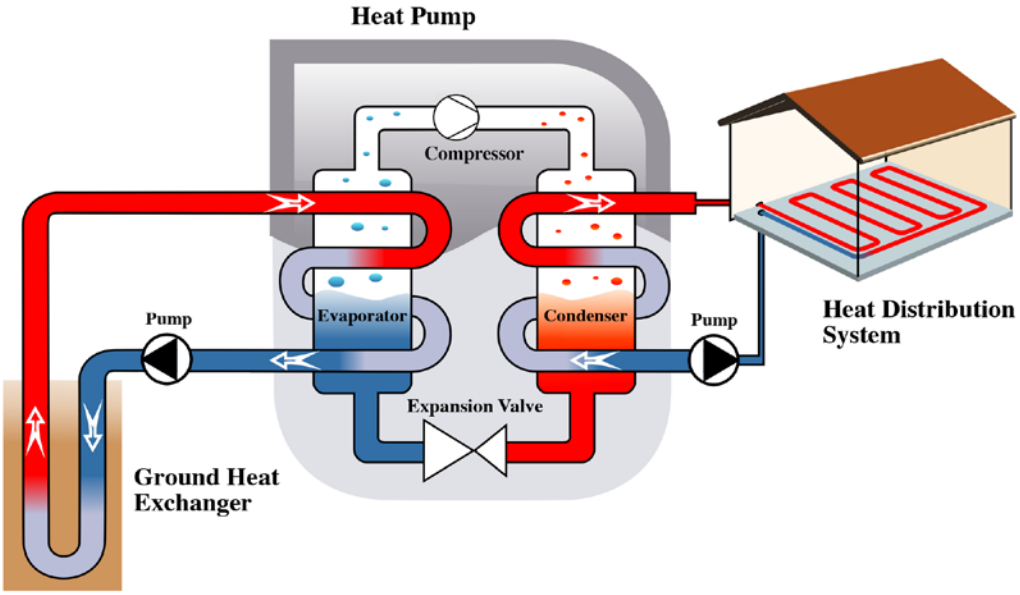

Fig. 2. *Diagram showing the principle of operation of a ground-source heat pump system.*

The energy efficiency units of a GSHP is represented by the coefficient of performance (COP) which is the ratio between the outlet energy (useful heat) divided by the inlet energy (external power).

$$COP = \frac{outlet\ energy\ (useful\ heat)}{inlet\ energy\ (external\ power)}$$

Higher COP values represent a lower amount of external inlet energy in comparison to the useful generated heat. COP depends on the energy efficiency of the heat pump itself (external electricity demand, refrigerant properties, compressor losses, etc.), the

GHE capacity to exchange heat and the temperature difference between the ground and the desired outlet temperature (e.g. building comfort temperature). The COP values can describe the system performance for pre-defined range of temperature (e.g. from -5 ºC until 30 ºC), or given the average annual COP of an installation, also known as seasonal performance factor (SPF).

Carnot's theorem states that "the efficiency of all reversible engines operating between the same two heat reservoirs is the same, and no irreversible engine operating between these reservoirs can have a greater efficiency than this", proving that the maximum energy efficiency of a reversible engine is given by the equation (1).

$$\eta_{max} = 1 - \frac{T_C}{T_H} \qquad (1)$$

Where T_C is the absolute temperature of the cold reservoir, T_H is the absolute temperature of the hot reservoir, and the energy efficiency, η, is the ratio of the work done by the engine to the heat drawn out of the hot reservoir. Clearly, the energy efficiency is limited by the temperature difference of the reservoirs between which heat is exchanged.

For a heat pump in a cooling mode Carnot's theorem states that the maximum COP is given by a cooling system that operates accordingly to a reversible cycle, such as that of Carnot. This maximum value is given by the expression (2).

$$COP_R = \frac{|Q_C|}{|Q_H| - |Q_C|} \leq COP_{max} = \frac{T_C}{T_H - T_C} \qquad (2)$$

If the same concept is applied to a heat pump in a heating mode, the maximum energy efficiency is given by the expression (3).

$$COP_R = \frac{|Q_C|}{|Q_H| - |Q_C|} \leq COP_{max} = \frac{T_C}{T_H - T_C} \qquad (3)$$

In both cases, the energy efficiency increases when the temperature difference between the cold and hot reservoirs becomes lower. Therefore, it will be possible to reduce the energy consumption if the heating engine is able to operate between reservoirs with stable and low temperature differences between each other.

Nonetheless, apart from the heat pump energy efficiency, the overall performance of a GSHP also depends on various other factors such as the heat distribution system efficiency, length of GHE, ground conditions and installation quality (Lund et al., 2004). For instance, thermal properties of subsurface play an important role in GHE performance, and previous evaluation is necessary to reach the maximum energy efficiency at minimum cost. The underground is commonly composed by layers with different thermal properties (e.g. soil, rock, groundwater or a mixture) and some layers

are more favorable to exchange heat, which can considerably affect GHE energy efficiency. The heat extraction and injection should be seasonally balanced to avoid local heating of the ground in long-term applications. Moreover, the borehole is normally filled with a grouting material or groundwater, which has a direct impact on the thermal resistance of a GHE. Hence, all aforementioned factors together with the required energy demand of the target application need to be considered for the techno-economic and energy-efficient design of a GSHP system.

2.3.1. GHE classification

GSHP systems are generally classified into two main groups (Fig. 3.) depending on the ground-source heat exchanger configuration: open-loop systems or closed-loop systems.

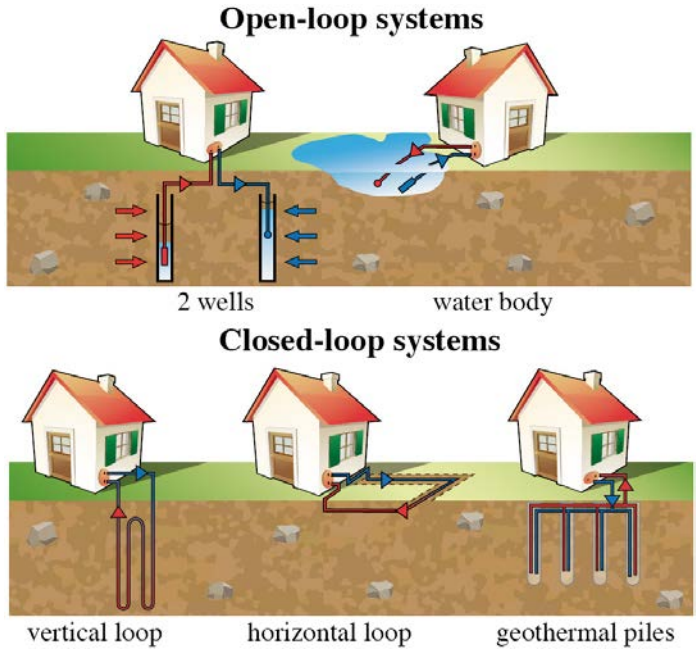

Fig. 3. *Open-loop and closed-loop pipe systems classification.*

Open-loop systems: Groundwater (underground aquifers or superficial groundwater) is used as heat carried medium, which is directly transported to the heat pump evaporator. The pipe loop system remains open and there is no barrier between the heat pump and groundwater.

Closed-loop systems: A fluid is pumped through a closed-loop pipe circuit coupled

with the ground for exchanging heat with the heat pump. The GHE and the heat pump are independent, closed circuits. Heat is exchanged by conduction in the link between the ground loop and the heat pump evaporator. Closed-loop heat exchanger collectors are distributed typically along the underground following a vertical loop, a horizontal loop or in geothermal piles.

GHE systems cannot always be categorized in one of the mentioned groups outlined above. If there is no real barrier but a certain differentiation between the heat carried fluid and groundwater, they are attributed to a third category. Examples of this exception are water tunnels, water mines or standing column wells. Originally, in the 1940's, GHE pipes made of iron or cooper were a feasible solution to build installations at a moderate cost. However, with the industrial revolution, iron pipes were replaced by plastic. Nowadays, geothermal pipes are generally made of high-density polyethylene (HDPE).

To choose the more suitable system for a particular application, several issues need to be considered: available land area on the surface (horizontal systems require larger extension of land than vertical systems), subsurface geological and hydrogeological composition (open-loop systems demand a minimum level of permeability), heating and cooling energy demand of the application, expected long-term ground thermal evolution due to injected/extracted heat, the presence of potential energy sources as mines and capital costs related to the system management as well as construction works and maintenance.

Open-loop systems

In an open-loop system, groundwater or surface water is directly transported to the heat pump to exchange heat. In most cases, the heat pump is connected with extraction wells, extraction and injection wells or surface water systems (e.g. lakes). Wells represent the main technical part of applications, where typically two wells are used, one to extract water and the other to pump water back to the aquifer where it originated. Groundwater circulates freely through solid ground, acting as both a medium to exchange heat and as a heat source/sink. Subsurface geology with a high permeability is a must, to enable regeneration of groundwater with a negligible decline. As an alternative to wells, aquifer layers are often used as direct heat source/sink.

Open systems offer the possibility to exploit a powerful heat source at relatively low cost (lower drilling requirements than closed systems). As the heat carried medium is directly in contact with the ground, under ideal conditions open-loop systems achieve a superior thermodynamic performance as opposed to closed-loop applications. However,

they are limited to regions with appropriate aquifers and geological compositions with elevated permeability. Subsurface chemistry needs to be investigated (e.g. low iron content is favorable) to avoid problems with scaling, corrosion and clogging. Clean water and surface water legislation needs to be considered before building an installation and pipe materials need to be strictly selected to avoid contamination of the environment. Normally, energy consumption of pumping is high and when oversizing or not implementing an optimal operation control electricity costs may be excessive.

Closed-loop systems

In a closed-loop system, a network of pipes is coupled with the subsurface where a fluid is circulated to exchange heat (no direct contact between circulating fluid and groundwater). Depending on the pipe loop distribution and coupling media, the closed-loop collectors are classified in four main groups (Fig. 4): (a) horizontal loop, (b) slinky loop, (c) pond loop and (d) vertical loop.

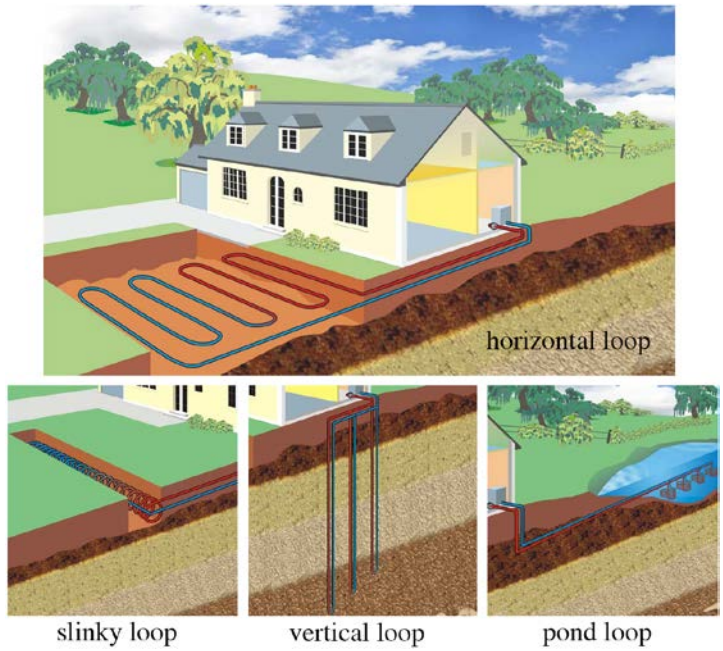

Fig. 4. *Closed-loop pipe system classification.*

a) Horizontal loop: Among the closed-loop arrangements the horizontal loop is the easiest to install. It is typically installed in ditches with a depth up to 10 m, hence thermal recharge is provided mainly by the solar radiation to the Earth's crust. It is crucial not to cover the ground surface above the piping loop to avoid reducing the amount of heat

received from the sun. Pipe loop connections can be arranged in series or parallel, in a single pipe trench or in multiple layer trench. The density of the pipe distribution pattern and the diameter of the pipes may vary depending on the available land area and heat transfer requirements. Horizontal loop systems can be buried beneath the landscaping, lawns or parking lots.

Trenching costs are typically lower than borehole drilling costs, however with latest technological developments this difference is becoming less significant. The main drawback of this system is the requirement of a large land area; thermal fluctuations of the ground depending on seasonal weather; rainfall and burial depth; foreseen soil dryness needs to be properly considered when designing the length of pipe collectors; pipe loops may be damaged during backfilling process; longer pipe length requirements compared to vertical exchangers; antifreeze fluid viscosity increases pumping energy consumption reducing overall system energy efficiency.

b) Slinky loop: An alternative to the horizontal loop mentioned above that requires less land area for same energy demand applications. It consists of a pipe assembly with spiral shape that is installed in horizontal or vertical trenches. In a horizontal slinky configuration, trenches of 1 to 2 m wide are commonly aligned with a gap of 3 to 4 m. For a vertical slinky loop, the pipe assembly is installed along the vertical axis of a trench with around 16 cm of diameter. In situations where the cost of trenching outstands over other components of the installation, implementing a slinky loop may result in a more cost-effective solution. It presents the following drawbacks: longer pipe assembly requirements than other ground couple systems; large land area requirement than vertical systems; energy consumption of pumping is higher; trench backfilling process is delicate, implying the risk to damage the pipe loop.

c) Pond loop: If a lake or a pond with a sufficient size is available, vertical collectors with a spiral shape can be installed under the water. The submerged piping arrangement is generally attached to anchors made of concrete. These anchors hold the collectors still above 25 to 50 cm of the pond floor, allowing them to take advantage of the more favorable convective water flow around the heat transfer surface. In addition, to preserve a suitable thermal mass during extended drought or in conditions with a low-level of water, it is recommended to place the heat transfer collectors at least 2 to 3 m below the top surface or deeper if possible. The use of rivers is typically discouraged as they are likely subjected to drought or flooding that can damage the installation.

The adequate size of collectors needs to be evaluated depending on heating or cooling requirements as the surface area, depth or weather conditions play an essential role. Some companies have favored the use of pond loops with the added value of

improving the esthetics of their facilities. The main advantage of a pond loop is a shorter pipe length requirement compared with the other closed-loop systems. If a pond or lake is available this generally presents as a more cost-effective solution. However, one disadvantage of this system is that a pond loop demands a large volume of water which may limit the use of the pond or lake for another activity.

d) Vertical loop: Also called a downhole heat exchanger (DHE) or a borehole heat exchanger (BHE). The closed-loop pipe circuits are installed in vertical or tilted boreholes. Borehole depth ranges typically between 30 to 160 m and a diameter between 0.06 to 0.21 m for most of the systems in Europe. However, deeper boreholes have been drilled recently with lengths ranging between 180 to 400 m. Borehole fields can harbor one borehole or multiple boreholes in systematic or arbitrary patterns. Vertical BHE are generally connected in parallel, but connections in series or with different inlet conditions are also an alternative.

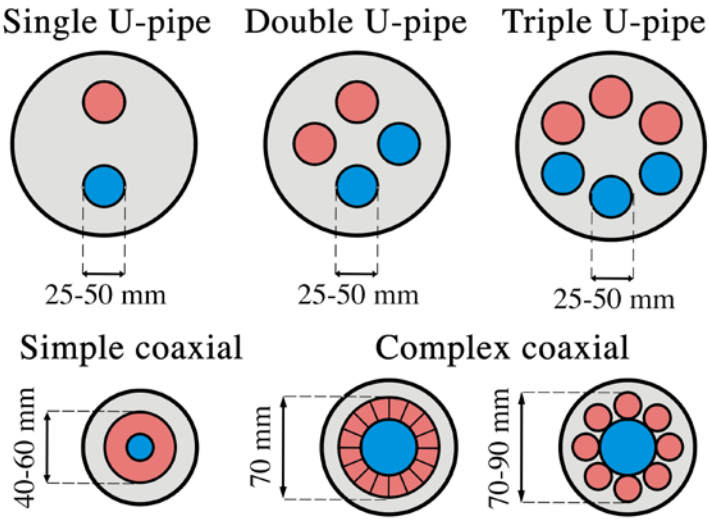

Fig. 5. *Different borehole heat exchanger pipes configurations.*

A BHE is classified mainly in two groups depending on the pipe geometry (Fig. 5): U-pipe or coaxial pipe. Single, double or triple U-pipe exchangers with diameters ranging from 25 to 50 mm and a wall thickness between 2.0 to 3.7 mm are the most extended solutions. Several studies demonstrated that double or triple U-pipe BHE produce better thermal efficiency than single U-pipe boreholes (Aydin & Sisman, 2015; Fang et al., 2017). Nevertheless, for some applications, depending on the capital cost and energy demand it may be a better alternative to build an exchanger based on a single U-pipe layout (Shu et al., 2006). On the other hand, typically coaxial pipe exchangers are also classified into two categories: simple and complex. For boreholes with

diameters ranging between 40 to 60 mm usually a simple coaxial layout is the most common practice, whether a complex coaxial layout is mostly preferred for boreholes with a diameter above 60 mm.

In a standard BHE, the gap remaining between the pipes and the borehole wall is usually filled with a grouting material consisting of a combination of singular materials such as bentonite, graphite, coarse sand or quartz. Particular mixtures, such as so-called thermally enhanced grouts have been developed to improve the heat thermal conduction of pure materials between the pipes and near ground (Borinaga-Treviño et al., 2013; Erol & François, 2014). The grouting material provides a heat transfer medium between the borehole wall and the pipes as well as acting as safeguard against underground water flows and contaminants. However, exceptions occur for example in Northern Europe, where it is common to let the borehole naturally fill with groundwater.

A BHE requires less land surface area (smaller impact on the landscape), shorter pipe collectors and less pumping energy than most of the closed-loop systems. Also, the efficiency to exchange energy is higher than other closed-loop systems as the ground in contact with the pipe loop is normally not subject to seasonal weather. On the other hand, it presents a few drawbacks in comparison with other closed-loop systems. For instance, an inadequate estimation of the spacing between boreholes may gradually heat the subsurface in long-term applications, producing a negative impact in the performance of the exchanger. It also requires specific drilling equipment which increases the cost compared to those for horizontal pipe collectors. Despite this, the advantages for vertical pipe arrangements outweigh the disadvantages and in recent years they have become a more popular solution than horizontal pipe arrangements. Moreover, the technological progress in plastic industry and drilling machinery have successfully increased the economic attractiveness of vertical exchangers.

As the vertical GHE configuration is the most commonly used solution, the experiments and developments of this Ph.D. work are mainly focused on it. In the following sections vertical GHE is addressed as BHE.

2.3.2. Optimal size of the GHE

Thermal response of the borehole field plays a critical role in the energy performance, capital cost and reliability of a GSHP system. During the design phase of the GHE, an under-sized borehole field may compromise the energy performance leading to an insufficient capacity to exchange heat. In such event, the entering fluid temperature to the heap pump will be less favorable, colder in heating mode and/or warmer in cooling mode, resulting in lower COP values and additional power

consumption. On the contrary, an over-sized GHE may result in unnecessary higher capital cost, such as those originating from higher pumping energy, higher pressure requirements, thicker geothermal pipes, added pressure losses, further resources for drilling (e.g. energy, time) as well as additional materials employed in a larger GHE.

From a practical life-cycle environmental perspective, an inadequately sized borehole field may result in an inefficient GSHP system with a higher capital investment. Therefore, throughout the design phase an in-situ evaluation of subsurface thermo-physical properties for the selected GHE configuration is necessary to determine the size of the borehole field that can achieve the maximum energy performance for the minimum capital cost. A precise estimation on the thermal behavior of the exchanger for the overall life of the GSHP system (>50 years) will allow designers to build all-out performance installations at an affordable capital cost. This life span is estimated for PE ground loops and by taking into account maintenance operations in the heat pump as the working life of its inside components is of around 20 to 25 years.

2.4. Heat transfer in the borehole

Throughout the operation of a GSHP system, inside the borehole domain, heat is transferred by both convective and diffusive mechanisms. Convective effects are identified along the fluid enclosed in the pipe-walls, while heat is transferred by conduction through the pipe-wall and borehole filling material. Convection also occurs between the outside part of the pipe-wall and the borehole-wall when the borehole is filled with groundwater. During the past decades, several investigations concerning the heat transfer phenomena along the length of the borehole were reported (Ghoreishi-Madiseh et al., 2019; Lamarche et al., 2010; Zeng et al., 2003a; Zhao et al., 2016).

Thermal conductivity λ *(W/m-K)* and thermal resistance *R (m-K/W)* are key parameters in the heat transfer performance of a BHE. Practitioners have dedicated a significant effort to estimate these parameters from in-situ tests to models that could predict the heat transfer rates along the borehole and the subsurface near the borehole. Thermal conductivity, which is primarily evaluated in terms of Fourier's law for heat conduction, determines the property of a material to transfer heat, whereas the thermal resistance reciprocal to thermal conductivity, describes the property of a material to resist a heat flow.

The total thermal resistance (R_T) along the horizontal axis of a BHE is typically defined as the addition of both fluid to borehole-wall thermal resistance (R_{fb}) and borehole-wall to ground thermal resistance (R_{bg}). The fluid to borehole-wall thermal

resistance represents the thermal resistance between the borehole-wall and the center of the pipe circulating the fluid, while the borehole-wall to ground thermal resistance parametrizes the resistance of the geological stratigraphy surrounding the borehole-wall.

$$R_T = R_{fb} + R_{bg} \qquad (4)$$

The fluid to borehole-wall thermal resistance (R_{fb}) is composed by the thermal resistance of the material filling the borehole (R_f), the thermal resistance of the pipe-wall (R_{pw}) and the thermal resistance of the heat carrier fluid inside the pipe (R_{pf}). The fluid to borehole-wall thermal resistance is defined as the addition of these three resistances:

$$R_{fb} = R_f + R_{pw} + R_{pf} \qquad (5)$$

Fig. 6 depicts the concept of thermal resistance in the borehole and near ground.

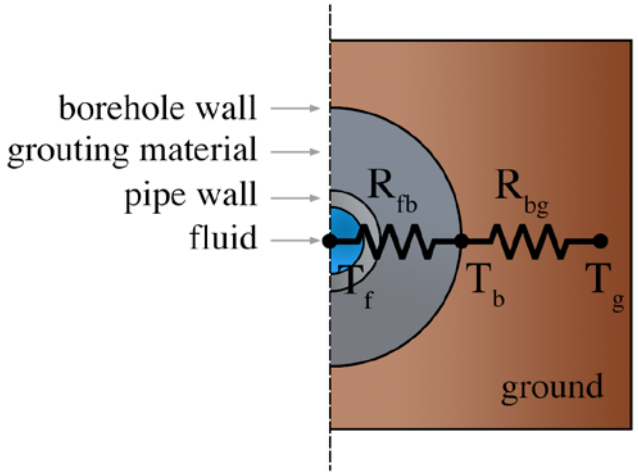

Fig. 6. *Concept of thermal resistance in a borehole heat exchanger.*

The temperature difference between the fluid in the pipe circuit (T_f) and the borehole-wall (T_b) is associated with the fluid to borehole-wall thermal resistance (R_{fb}) as well as the specific heat transfer rate q *(W/m)*. Thus, assuming a steady state, the heat transfer rate along the horizontal section of the borehole is estimated by the following equation:

$$q = \frac{T_f - T_b}{R_{fb}} \qquad (6)$$

From (6), the heat transfer rate is assumed to be proportional to the temperature difference between the heat carried fluid in the collector and the borehole-wall. The thermal resistance of the fluid to borehole-wall (R_{fb}) will vary depending on the size and disposition of the pipes inside of the borehole diameter as well as the thermal properties of the fluid, pipe and filling material. A small fluid to borehole-wall (R_{fb}) thermal resistance is preferred to improve heat transfer rate in the domain of the borehole.

In order to calculate the effective fluid to borehole-wall thermal resistance (R_{fb}*) it is necessary to account for the heat transfer processes between the neighboring U-pipe legs (Javed & Spitler, 2017). The heat flow between the transverse section of the down-flow and up-flow pipes is called thermal shunt effect (TSE). For high flow rates or short boreholes, the TSE is typically neglected as long as the effective temperature along the borehole length does not differ excessively over the simple mean temperature. The effect is aggravated for higher flow rates, longer borehole lengths, larger pipe diameters or pipe-to-pipe spacing, becoming relevant when the effective fluid to borehole-wall thermal resistance is higher than the fluid to borehole-wall thermal resistance (Sandler, et al., 2017).

2.5. Heat transfer in the ground

Thermal conductivity, thermal diffusivity and subsurface initial temperature are key parameters to estimate the heat transfer rate from the borehole-wall to the ground. Thermal diffusivity $\propto$ *(m^2/s)* defines how fast or easily heat can penetrate through a material from the hot side to the cold side. It measures the ability of a material to conduct thermal energy relative to its ability to store thermal energy. Thermal diffusivity is evaluated as the thermal conductivity (λ) divided by the density ρ *(kg/m^3)* and the specific heat capacity C_p *(J/(kg*K))* at constant pressure.

$$\propto = \frac{\lambda}{\rho \, . C_p} \qquad (7)$$

The thermal conductivity of the ground defines the capacity of the geological material to transfer heat from the borehole-walls to the surroundings or the other way around. The specific heat capacity (per unit mass) describes the ability of a material to retain internal heat energy while undergoing a given temperature transition. For a higher thermal conductivity of a material, greater the thermal diffusivity will be and lower the thermal capacity. Together, $\rho \, . C_p$ is considered as the volumetric heat capacity in the system of units (SI) derived units of *J/(m^3·K)*.

Heat transfer in the ground is typically dominated by both conductive and convective effects. Subsurface geological stratigraphy is typically heterogeneous and underground aquifers are common. While thermal conductivity of groundwater is low, the heat transfer rate between the borehole-wall and the surrounding ground is enhanced by natural convective effects. Depending on the geological materials such as sand, gravel or fractures in bedrocks, groundwater movements can have a relevant influence in the thermal behavior and of the exchanger and overall energy performance of the borehole field.

The parameters considered to evaluate ground thermal properties are not always the same. For instance, ground thermal conductivity and thermal resistance between the heat carrier fluid and the borehole-wall are usually evaluated in Europe, whereas ground and grouting material thermal conductivity are more commonly assessed in America.

2.6. Modelling heat transfer in the ground

Predicting the heat transfer process of the subsurface surrounding the borehole by evaluating all the feasible thermo-physical singularities increases the complexity of the model. Additionally, many factors such as geological heterogeneities, groundwater flow, seasonal weather conditions and human induced activities, are in most cases rather difficult to estimate in advance. Hence, most of the models are elaborated to embrace a compromise between the exactitude and complexity of the results based on the following assumptions:

- Convective effects are neglected, and only conduction is considered as heat transfer mechanism between the borehole-wall and the near ground.
- The subsurface is treated as a homogeneous and isotropic medium.
- The initial subsurface temperature is known and set equal to the undisturbed subsurface temperature.
- The top surface and far outer boundaries are considered to be equal and in equilibrium and also set to the undisturbed temperature.

The transitory thermal response, imposed by thermal loads in a BHE, can be determined by the superposition of heat transfer expressions derived from the heat conduction equation as from the ground temperature profile in equilibrium. Over many years, non-dimensional mathematical models assessing the heat transfer of the ground near the borehole, such as the infinite line source (ILS) (Ingersoll & Plass, 1948) or infinite cylindrical source (ICS) (Carslaw & Jaeger, 1959) were used in engineering applications by providing reliable results. These two classical methods provide solutions

to the transitory thermal response problem in the ground, assuming the heat transfer outside of the borehole to be a line or cylinder of infinite length. The long-term response of the ground is determined with significant accuracy. However, given that these solutions not only ignore the end of the ground domain but also the thermal properties inside the borehole as well as the geometry of the heat sources, some discrepancies occur for short-term assessments (Philippe et al., 2009).

Important progress was made by Eskilson (1987) who addressed some of the previous assumptions. He developed a semi-numerical transient solution accounting for the finite length of the borehole. In this approach, a numerical method on a radial-axial coordinate system is used to determine the non-dimensional thermal response factors at the boundary of the borehole. These factors are commonly known as g-functions. The g-functions are reported to be acceptable for operation times longer than 200 hours (Yavuzturk, 1999). Another major achievement was also accomplished by enhancing the model to predict the thermal response of interacting boreholes (Eskilson & Claesson, 1988). However, the downside of the g-functions is the need for them to be computed numerically, which is a time-consuming and cumbersome task. For practical applications, the g-functions are pre-compiled and stored in a massive database for different BHE geometries and configurations.

Later, several researches have attempted to further develop the finite line source (FLS) approach based on the g-functions to address the issues related with the lack of configurability. Zeng et al. (2002) presented an analytical solution of the g-functions incorporating a constant temperature along the borehole-wall. Lamarche & Beauchamp (2007) proposed and evaluated another analytical expression to compute the g-functions using the integral mean temperature alongside the borehole length. The authors concluded to achieve more accurate results using the integral mean temperature along the borehole rather than using the temperature along the borehole-wall. A few years later, the aforementioned analytical expressions were simplified while still obtaining comparable results in a contribution elaborated by Bandos et al. (2009) . Similarly, other researchers also developed analytical models with the intention to improve the long-term thermal response of the GSHP (Teza et al., 2012; Zeng et al., 2003b).

In order to evaluate the accuracy of each model, Philippe et al. (2009) conducted a comparative study involving the ILS, FLS and ICS models, with the objective of finding the operation times offering the best results under typical conditions. For small periods (<34 h), the ICS presented the best adjustment. The ISL showed smaller errors for time periods between 34 h and 19 months, while the FLS was most adequate for analysis periods larger than 19 months.

Throughout the last two decades, some other researchers developed analytical and semi-analytical calculations to evaluate the short-term thermal response of GSHP systems (Bandyopadhyay et al., 2008; Gehlin, 2002; Gustafsson & Westerlund, 2011; Jahangir et al., 2018; Yavuzturk & Spitler, 1999; Young, 2004). One of the most relevant investigations was carried out by Javed (2012), who proposed an analytical solution to model the radial heat transfer problem. The equations are derived from a thermal network used to represent Laplace transform equation. Since this approach accounts for the thermal properties of all borehole elements such as the duration of the test, fluid, pipe, ground and grouting material, it is valid for short-time scales. The dynamic thermal response of a BHE was predicted accurately with a more reliable results than earlier analytical solutions. Afterwards, the FLS solution was included in the model to produce transient responses in a simple or multiple BHE from minutes to decades (Claesson & Javed, 2011). Recently, Ghoreishi-Madiseh et al. (2019) proposed a robust analytical model with a user friendly tool to also predict the dynamic thermal transfer in a single or multiple BHE both in short and long-term with high accuracy.

Another solution to numerically describe a BHE is the thermal network approach, where the borehole and the near ground are represented by a series of temperature nodes connected to thermal resistances and/or capacitances. The fundamentals of this approach derived from the standard steady-state delta network (Eskilson & Claesson, 1988), in which one temperature node is located at the center of each of the U-pipe legs and another in the borehole-wall. Since then, the basic steady-state delta network has been positively enhanced, typically by expanding the network with more nodes or by adapting the network to different borehole or pipes geometries (Bauer et al., 2011a; Bauer et al., 2011b; Lamarche et al., 2010; Pasquier & Marcotte, 2012). It is possible to obtain a considerable level of accuracy by increasing the thermal network complexity to correctly describe the interaction between the borehole and the subsurface. However, it implies a further number of differential equations which can lead to higher simulation times. With the intention to find a compromise between model complexity and accuracy (Ruiz-Calvo, 2015; Ruiz-Calvo et al., 2015) introduced the borehole-to-ground (B2G) model, one of the most relevant contributions to this area. They accomplished to develop a thermal network model (Fig. 7), with the minimum number of nodes to simulate the short-term transient thermal behavior with high accuracy. Later, the B2G model was enhanced based on a decoupling technique, including both the short-term and the long-term responses together in the same model to achieve faster and more precise results in both sides (Ruiz-Calvo et al., 2016). They used the g-functions for the calculation of the long-term response.

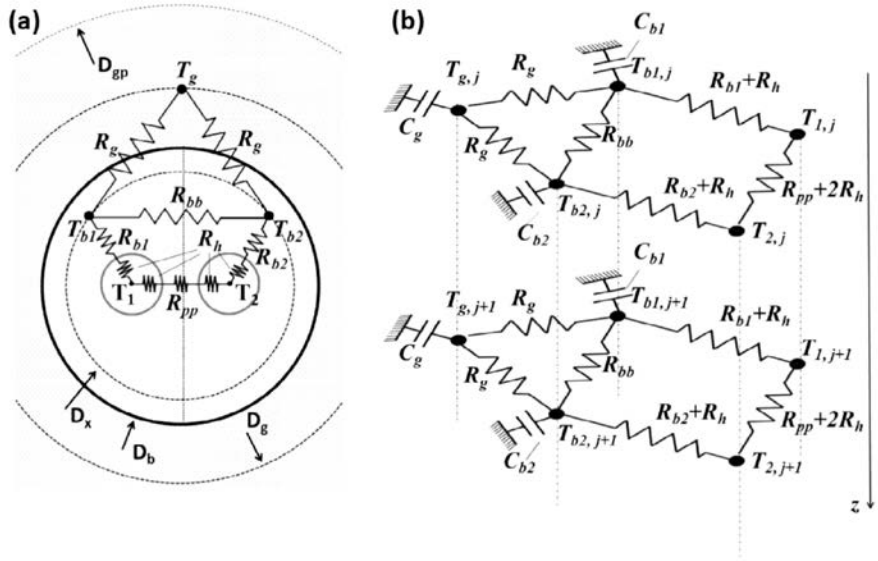

Fig. 7. *Thermal network of the borehole-to-ground model: (a) 2D model and (b) 3D model. (Ruiz-Calvo et al., 2015).*

Although groundwater movement has not been studied as much as heat conduction problems, it is important to be aware that it may have a significant impact on the heat transfer performance of a BHE. While in most of the approaches convective effects have been neglected in exchange for a reduction in the complexity, several other studies have been focused on demonstrating their relevance (Raymond et al., 2011; Wang et al., 2009; Zhang et al., 2012). From the point of view of particular energy demand application, accounting for groundwater axial effects may be crucial to reduce the length and number of boreholes. For example, Marcotte et al., (2010) carried out a design exercise in which the estimated length of the BHE could be shortened by at least 15% when axial flows were considered. Likewise, some other investigations have concluded that water movements improve heat exchange between the aquifer and the borehole (Chiasson & O'Connell, 2011; Fan et al., 2007; Wang et al., 2009). Hence, shorter or less boreholes are needed to achieve the same heat transfer performance.

Regarding the aforementioned third and fourth assumptions when modeling heat transfer of the ground: initial temperature for the subsurface domain and boundaries equal and also set to the undisturbed temperature. In Eskilson (1987) is reported a negligible deviation of 0.01 K when calculating the effective temperature from the average of the annual ambient temperature by assuming that the temperature of the top boundary decreases according to a prescribed thermal gradient throughout the length of the borehole. In this case, the thermal gradient of the subsoil was estimated by the

paleoclimatic variations of the land in the proximities of the borehole over 25 years. In Rivera et al., (2016) is indicated that considering a constant value for the ambient temperature may have a significant negative effect in short BHE. It was concluded that the influence of the transient ambient air temperature is negligible and could be represented as a constant value for boreholes deeper than 50 m. In such a case, temperature deviations smaller than 5% are observed for the average borehole-wall temperature.

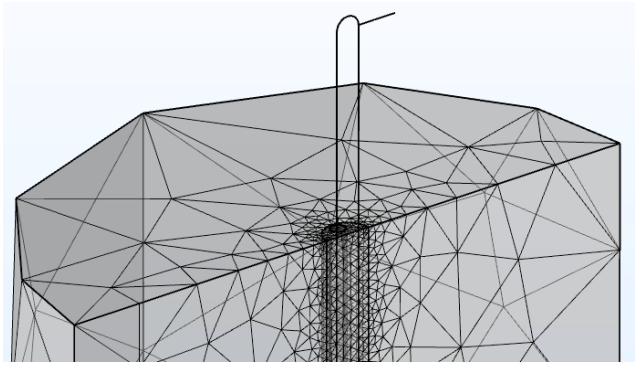

Fig. 8. *Upper part of a 3D model of a borehole heat exchanger composed by tetrahedral elements with a symmetry plane onto the XZ plane.*

As the computational technology is further developed, more complex models to simulate the transient heat transport phenomena of BHE with more ambitious precision expectations have attracted the interest of designers. For instance, several studies have reported developments of fully discretized finite element models (FEM) with extremely detailed three-dimensional (3D) geometrical mesh (Lamarche et al., 2010; Naldi & Zanchini, 2019; Signorelli et al., 2007). To reduce computational cost and simulation time, some of the models were restricted to describe the heat response in a two-dimensional (2D) representation (Austin et al., 1999; Yavuzturk et al., 1999). However, even if 2D models require less computing effort, their geometry is partial and result precision is limited. Only 3D models can account for the vertical heat transport, TSE between the down-flow and up-flow pipes, different geological layers, correct boundary conditions, undisturbed temperature and seasonal weather conditions (Cui et al., 2018). In some cases, if the pipes configuration is suitable, it is possible to reduce 3D model volume geometry by half using a symmetry plane along the length of the borehole (Fig. 8). An example of this technique is introduced in Aranzabal et al. (2016) where model computational load is significantly reduced while still obtaining comparable results. Florides et al. (2012) designed and validated another alternative to reduce the complexity of a FEM model by combining a 3D conduction in soil approach with a one-dimensional (1D) modeling of the heat carrier fluid.

The number of FEM developments incorporating a computational fluid dynamics (CFD) module have also increased. One of the most noteworthy advantages of such CFD simulations is that they are suitable to conduct both parametric or optimization (inverse model) approaches for improving precision of the results. Lenhard et al. (2012) assessed the performance of various scenarios and parameters (e.g. heat carrier, power, thermal conductivity, etc.) through a parametric numerical simulation. Chen et al. (2016) validated a 3D numerical model with experimental data and carried out a larger analysis to investigate the factors influencing the BHE thermal response such as operating conditions, grout and ground materials, inlet temperatures and the influence of convective effects. Nevertheless, it should be recalled that even in modern computers with powerful processors and parallel computing capabilities, FEM and/or CFD model compilations are still time-consuming due to the extreme number of tiny elements and/or variables.

While models present the ability to forecast heat transfer evolution in the borehole and near ground, in-situ measurements of thermo-physical particularities are necessary to validate or guide models through the most realistic approximation. For a specific engineering application, input parameters such as BHE geometry, inlet and outlet temperature evolution, injected/extracted heat power, fluid flow, initial temperatures (borehole, ground) and ambient air temperature will determine the accuracy of the model results.

2.7. In-situ methods to determine ground thermal properties

Ground thermal properties are critical parameters in the design of BHE, however, up to now they are still difficult to quantify with enough exactitude and confidence (Luo et al., 2016; Witte & van Gelder, 2002). A huge effort has been carried out in the past decades to improve accuracy of the in-situ methods: using values from literature, elaborating laboratory tests on geological samples and implementing in-situ tests.

Approximations based on literature notes require minimal effort, but the dissimilarities (range) of the thermal parameters reported in most cases are quite large. This is due to the fact that local conditions have a huge impact. Also, parameters from literature are global values for a particular type of geological material which needs to be adapted to represent the whole subsurface domain (heterogeneities are neglected). Thus, a cautious practitioner facing a design will select the lower values plus a safety margin to ensure the proper operation of the system, resulting in a (probably not competitive) overpriced design.

An alternative to the use of literature parameters is to collect samples of geological materials, during the perforation phase of the borehole, to analyze them independently in the laboratory. It is possible to investigate several factors such as mineral composition, degree of saturation and porosity on the thermal properties. The disadvantage of this method relies on the fact that only individual samples are taken which still needs to be adapted to represent the entire subsurface domain. Only punctual zones are evaluated and heterogeneities occurring at a larger scale are not considered. Moreover, any disturbance of the samples during the sampling process, storage or transportation will affect the accuracy of the results. As a final point, both these methods (literature and laboratory measurements) do not deliver any information about the local influence of groundwater effects on the thermal properties of the site.

In-situ tests for estimating thermal properties of the subsurface surrounding a BHE have been extensively developed during the last decades. The in-situ tests are attractive as they provide detailed information of the thermal conductivity and heat capacity of a significant volume of ground. They also take into account the real pipe collector configuration by providing precise information of the actual borehole. Moreover, new in-situ methods such as the ones developed in this Ph.D. work can provide accurate information of the local thermal properties along the pipe loops. An in-situ test estimates thermal properties of the ground by including site geology, hydrology, pipe loop configuration and borehole characteristics (size and grouting material), therefore they make it easier to predict the economic viability of a project for a specific energy demand application. The drawback of in-situ tests mainly relies on the influence of outside temperature variations, the length of the testing installation (much longer than the required for laboratory tests) and the current intrinsic limitations of the analysis methods. Nowadays, the standard in-situ test is known as the thermal response test (TRT).

2.7.1. Laboratory measurements

Several laboratory procedures to measure the ground thermal properties have been reported throughout the last decades (Farouki, 1986; Low et al., 2015; Mitchel & Kao, 1978). These methods are divided typically into two main categories: steady-state or transient.

Steady state laboratory tests consist on applying one directional uniform heat flux to a specimen in a thermal equilibrium state and by measuring the thermal gradient across it. The thermal conductivity of the specimen is calculated directly by applying Fourier's law to the obtained temperature profile along its cross section. Alrtimi et al. (2014) developed an improved steady-state apparatus for measuring thermal conductivity of

soils with a margin of error up to the 5%. On the other hand, transient methods consist of applying a heat source to the specimen while monitoring the temperature evolution over time. The obtained transient data during the test is normally used to calculate the thermal conductivity by applying an analytical solution based on the heat diffusion equation.

It should be noted that transient state methods are simpler to implement, however, steady state results are more accurate. The thermal cell (steady state) and needle probe (transient) instruments are currently industry (standard) recommended methods (ASTM D5334-08, 2008; Bristow, Kluitenberg, & Horton, 1994; GSHPA, 2012). Commonly the needle probe has less significant sources of error, but evaluates a smaller ground sample than the thermal cell (Low et al., 2015). Among various steady state procedures, the guarded hot plate (GHP) is considered as the most reliable and accurate technique to estimate thermal conductivity (Xamán et al., 2009).

2.7.2. Thermal Response Test

The in-situ TRT was initially proposed by Choudhary (1976) and Mogensen (1983) as a method to estimate subsurface thermal properties in BHE systems. A few years later the method was further improved with a mobile equipment (wheeled cart) where the chiller was replaced by a heater (Austin, 1998; Gehlin, 1998). Since that time, the in-situ TRT has been widely used worldwide both in research and commercial applications as a standard method to determine the ground thermal properties and BHE thermal performance (R_b). The test consists of pumping a heat carried fluid inside a pilot closed-loop BHE (U-pipe or coaxial) while being heated at an almost constant rate using an electric element (Fig. 9). Heat extraction TRT tests have also been reported but are less common. The TRT begins under the assumption that the subsurface temperature is in equilibrium. Once the heat injection begins, the temperature evolution at the inlet and outlet of the BHE is monitored for a minimum duration of 48 h. After the heating period, the recovery phase is monitored as well for a minimum duration of 24 h. Throughout the test, a data-logger system is usually used to monitor the inlet/outlet and outside temperature (temperature probes); inlet/outlet pressure (pressure probes); fluid velocity (flow meters); and electrical and heat power (power meters). (Spitler & Gehlin, 2015) elaborated a thorough review regarding the latest TRT equipment developments, test procedures and analyses methods.

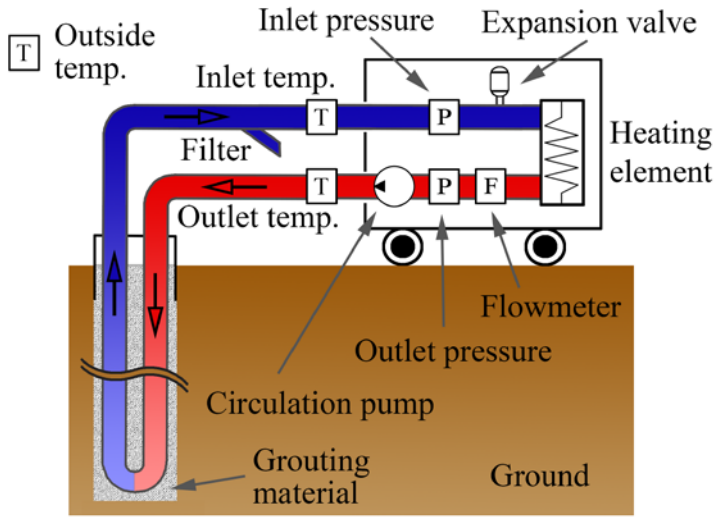

Fig. 9. Thermal response test set-up.

It should be noted the importance of insulating the parts of the pipes remaining outside of the borehole as well as the test rig, since the outside variable temperature can produce instabilities in the heat source. This adverse influence can be mitigated by improved insulation and by installing additional inlet/outlet temperature probes in the borehole itself (less influenced by atmospheric conditions). These measurements can then be used to calculate the instantaneous injected heat (q) in W by the convective heat transfer equation:

$$q = \dot{m} C_p (T_{out} - T_{in}) \qquad (8)$$

where $\dot{m}$ is the mass flow rate (kg/s), C_p is the specific heat capacity of water at 20 ºC (4.192 kJ/kg K) and T_{out} - T_{in} is the temperature difference between the inlet and outlet heated pipes of the borehole.

Furthermore, changes in viscosity of the heat carrier fluid due to temperature oscillations may lead to changes in the flow rate over the duration of an experiment. Hence, a continuous monitoring of the flow rate will lead to a more accurate data analysis interpretation.

From the obtained measurements, typically two main parameters are calculated: effective thermal conductivity (λ_{eff}) and borehole thermal resistance (R_b). These parameters can be inferred either by using analytical or numerical solutions (Section 2.7). The most popular analytical solutions are based on the Kelvin's ILS theory (Ingersoll & Plass, 1948), the ICS (Carslaw & Jaeger, 1959; Deerman & Kavanaugh, 1991) or the moving ILS (Stauffer et al., 2013). Moreover, several numerical models of varying complexities have been developed (BniLam et al. 2018; Ozudogru et al 2014;

Signorelli et al., 2007). Numerical models consider more complex geometries with more detailed events of the subsurface, such as groundwater flows, external conditions, layered subsurface heterogeneities, etc. In addition, they offer a more precise estimation for long-term applications (Zanchini et al., 2012). However, the validation and design process of a numerical model may become time consuming where mesh and simulation time steps need to be selected carefully.

The effective thermal conductivity and effective borehole thermal resistance are key parameters to determine the energy efficiency of a BHE installation. However, the term "effective" should be emphasized as the Earth's geology is typically heterogeneous and thermal conductivity is likely to vary with depth and in some cases even with direction. Moreover, heat transfer in the subsurface may not occur merely by conduction as it may be affected by groundwater flows (underground aquifers) or advection effects (Gehlin et al., 2003; Gustafsson, 2010). Therefore, the calculated thermal conductivity resulted from a TRT may inevitably not represent the actual values for the local regions spread along the length of the borehole. In addition, the borehole thermal resistance obtained with a TRT is an effective value between the mean fluid temperature and the borehole wall for the entire borehole length. In such case, to infer more realistic estimates of the local borehole resistance, analysis such as the 2-dimensional and TSE based approaches are required.

In order to overcome the limitations of standard TRT (effective values), the so-called distributed TRT (DTRT) are developed worldwide with different solutions to characterize the vertical distribution of thermo-physical properties of the ground surrounding a BHE.

2.7.3. Distributed thermal response test (state-of-the-art)

The DTRT complements standard TRT field measurements with temperature measurements along the length of the borehole. This additional information is fundamental to identify the location of the more favorable geological layers to exchange heat. Likewise, to determine the optimal size of ground collectors, and subsequently to improve economic viability of BHE installations.

Rohner et al., (2005) developed a small probe (235 mm x 23 mm) that sinks in the water filled U-pipes of a BHE up to a depth of 300 m (Fig. 10). The wireless probe integrates a data-logger electronic circuit to record pressure (depth) and temperature at preconfigured time intervals. The sensors and data-logger are embedded in a closed metal tube. The probe weighs 99.8 g and has a temperature resolution of ±0.003 °C. The device is inserted in one of the U-pipe legs and sinks to the bottom while recording pressure and temperature data. Once the probe reaches the bottom, it is flushed back to

the surface by using a small pump (Fig. 11). The measured data is then retrieved by connecting the probe to a computer. In this experiment, a data analysis method is provided based on a single temperature profile of the subsurface in thermal equilibrium and data of terrestrial heat flow near the test field. A patent for the device and method was released one year later (European Patent Office 1600749B1, 2006).

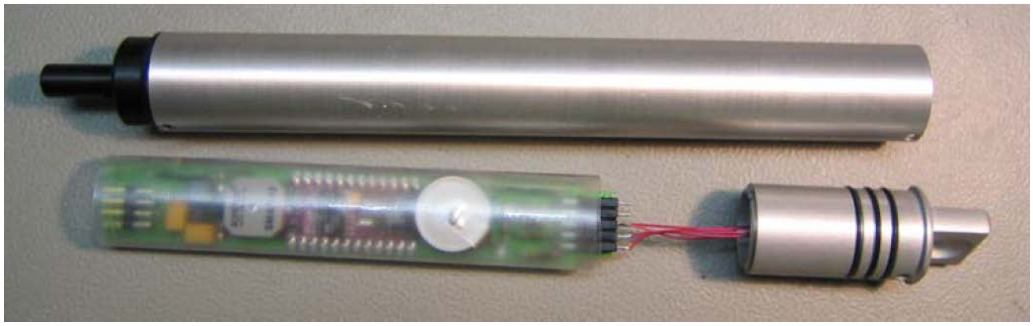

Fig. 10. *Data-logger submersible probe to measure pressure and temperature* (*Rohner et al., 2005*).

A few years later, Bayer et al. (2016) conducted an experiment with a commercial version of the aforementioned probe called NIMO-T (Non-wired Immersible Measuring Object for Temperature) and presented an analytical procedure to differentiate between the effects of urban heating and global warming.

Raymond et al. (2016) carried out an experiment using a similar commercial probe called RBRduet from RBR Ltd. (Fig. 12), and proposed an inverse numerical procedure (of conductive heat transfer) to extend the depth-specific thermal properties of a TRT to an adjacent borehole. The probe measures pressure (depth) and temperature, but since it is not wireless like the previous one, it needs to be hooked to a wire and lowered by hand inside of a vertical geothermal pipe filled with water. The submersible data-logger has a fast thermal response where the thermistor accuracy, resolution and time constant are $\pm 2 \times 10^{-3}$ °C, 5×10^{-5} °C, 2.5×10^{-1} °C, respectively. The pressure sensor can go up to a depth of 500 m and its accuracy and resolution for depth measurements are 2.5×10^{-1} m and 5×10^{-3} m, respectively. The model requires a single profile of the subsurface in thermal equilibrium of the target borehole. Then, with information of paleo-climatic changes and topography of the nearby field, as well as the results from a TRT in that area, the model can infer the depth-specific thermal properties of the target borehole. This is achieved without any further TRT and by lowering the probe once in the borehole.

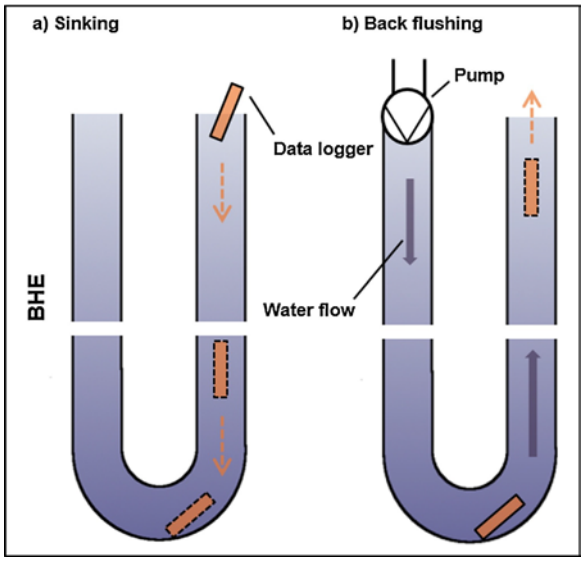

Fig. 11. *Working principle of the NIMO-T probe* (*Bayer et al., 2016*).

Fig. 12. *RBRduet data-logger probe.*

Martos et al. (2011) developed a small spherical probe that is carried by the thermal fluid inside geothermal pipes while measuring the temperature evolution of a specific volume of fluid (Fig. 13). The spherical probe has the same density as the fluid and is therefore transported by a constant flow while its position is calculated. The obtained temperature and depth samples are stored in a memory inside the probe. Once the probe is retrieved the data is wirelessly downloaded to a computer. It has a diameter of 25 mm, a temperature resolution smaller than 0.05 °C and an accuracy of ±0.05 °C. In this study, the probe is tested in real BHE installation during a TRT where the operability and performance of the sensor is assessed. The spherical-probe is inserted using a valve that does not stop the circulation of the fluid and it is recovered using a similar valve after completing a loop inside the U-pipe. The obtained temperature profiles through depth (downs-flow and up-flow) showed some correlations between the different geological layers and the local heat transfer rates. One of its advantages is that it can be circulated

in both vertical and horizontal pipe circuits. The drawback is that it is not suitable to measure the ground temperature in equilibrium (undisturbed ground) as when the probe is circulated (by moving the water inside the pipes) the stable temperature in the borehole is disturbed. However, other methods can be applied to measure the undisturbed ground profile, such as turning on the pump and using the outlet temperature probe at the U-pipe from the TRT to calculate this profile by knowing the fluid flow and pipe diameter.

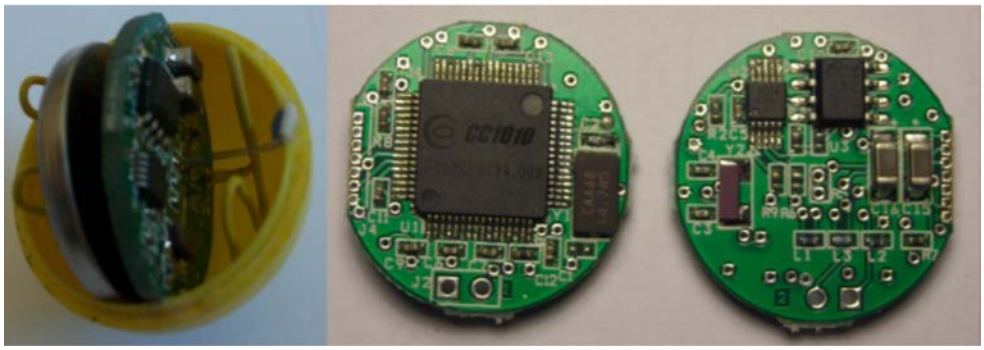

Fig. 13. *Autonomous sensor inside its ball-shaped enclosure (left) and layout of the electronic circuit (right)* (*Martos et al., 2011*).

Later, the company enOware developed a commercial version of a similar data-logger probe (temperature, pressure), called GEOsniff®. The probe also has the shape of a ball, but it is designed based on the NIMO-T working principle. It has higher density than the fluid allowing it to sink in the vertical pipes. Once the probe reaches the bottom, a pump is powered on to circulate the fluid and to expel the ball to a tank.

Yu et al. (2013) conducted a sensitivity analysis (Bland–Altman) of two TRT analysis methods, the ILS and ICS models, to determine the subsurface thermal properties. The experiment is implemented by embedding temperature sensors (Pt100 type) vertically in the ground along the BHE. The Bland–Altman analysis showed that the values of thermal conductivity calculated with the ILS model are slightly lower than the obtained ones with the ICS model. Moreover, (Raymond & Lamarche, 2014; Raymond et al., 2015) suggested a novel DTRT method involving reduced power consumption in comparison with standard TRT. In this case, instead of circulating and heating a fluid, a cable-assembly combining heating and non-heating sections is introduced in one of the U-pipe legs (Fig. 14). After ending the cable-based heat injection, the recovery phase of each section is monitored using temperature probes. Halfway along the length of each section a data-logger stores the probes measurements. The recorded data is then evaluated with an analytical approach based on a finite linear heat-source to discretize the punctual thermal conductivity at the depth of each probe (every 10 m). After the test is finalized, the cable assembly needs to be extracted to

retrieve and analyze the collected data. This can produce delays in case of a failure in one of the data-loggers or in the heating cable, as the recorded data is assessed after removing the cable assembly. Furthermore, it should be noted that it is easier to introduce calibration errors when carrying out tests involving multiple sensors. Also, long boreholes usually require an elevated number of sensors, therefore increasing the cost and complexity of the data-logger installation (e.g. high cable density).

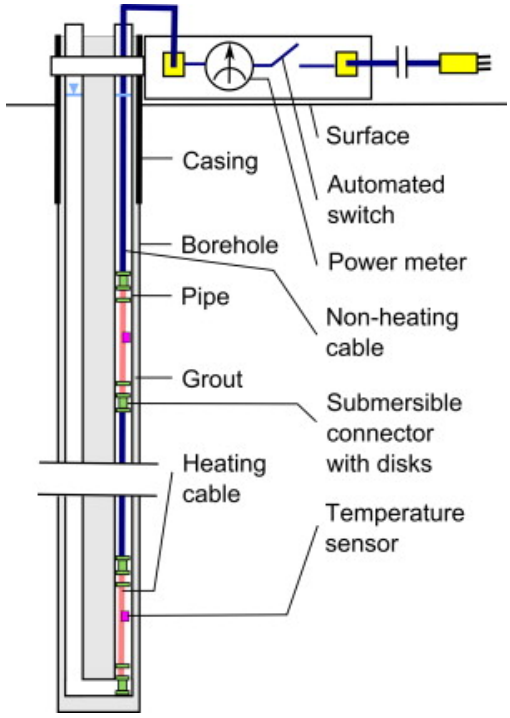

Fig. 14. *Apparatus to conduct thermal response test with heating cable sections (Raymond & Lamarche, 2014).*

(Fujii et al., 2006; Fujii et al., 2009) carried out a pioneer DTRT by installing fiber optical thermometers along the U-pipe (down-flow) in a BHE and also developed a computer program based on the ICS model (Ingersoll & Plass, 1948) to calculate the depth-specific thermal conductivity. The obtained results showed areas with vast temperature variations, possibly affected by the influence of hydrological conditions. Freifeld et al. (2008) deployed an in-situ methodology called distributed thermal perturbation sensor (DTPS) by installing a heater-resistance parallel to the fiber optics cable. In this research, an inverse numerical model was developed to estimate the depth-dependent thermal characteristics of the borehole by fitting measured temperature profiles with heat flow maps of the region. (Acuña, 2010; Acuña, 2013; Acuña & Palm, 2013; Beier et al., 2012) went one step further and improved DTRT measurements by

installing fiber optic thermometers inside the entire U-pipe loop (down-flow and up-flow). This enabled monitoring of the TRT thermal progression along the entire pipe loop. DTRT with fiber optics inside coaxial geothermal pipes were also carried out. In these studies, depth-specific thermal properties are inferred by assessing the temperature difference between the undisturbed subsurface and the fluid as a function of time (heat injection and recovery phase). A numerical algorithm implements the ILS equation (Ingersoll & Plass, 1948) and using a least-squares parameter estimation solver, a computer program calculates the depth-specific thermal conductivity and thermal resistance. Since the DTRT using fiber optics was first introduced, this technique has become increasingly more popular and has attracted the interest of many researchers and practitioners worldwide. As a result, new solutions to improve the obtained data quality as well as new data analysis methods were reported recently (Hakala et al. 2014; Luo et al., 2015; McDaniel et al., 2018; Monzó, 2018; Radioti, 2016; Soldo et al. 2016). Fig. 15 illustrates a DTRT (at the top level of the borehole) carried out during this Ph.D. work where the fiber optics cables (grey and red) are located inside the geothermal pipes using a valve to tighten the cable over a joint for preventing leakage.

Fig. 15. *Fiber optics installed inside geothermal pipes (Vallentuna, Sweden).*

Fiber optic thermometers measure continuous, high-resolution temperature profiles based on Raman-spectra distributed temperature sensing (DTS) technique (Hermans et al. 2014; Tyler et al., 2010) and complex algorithms (Hausner & Kobs, 2016; Hausner et al., 2011; van de Giesen et al., 2012). A DTS equipment calculates the temperature over cable sections and time intervals by injecting laser pulses that interact with the silica core of the optical fiber. However, despite the fact that accurate DTS equipment is rather expensive, it is also limited given a tradeoff among temperature

resolution, spatial resolution, range and speed of measurement. For instance, averaging the temperature for longer time or longer distance intervals improves measurements resolution. The side effect is that longer integration times may hide the actual heat transfer progression in environments with a fast-transient response (e.g. during a TRT). Likewise, a longer spatial resolution may attenuate the temperature differences occurring between two consecutive measuring points. For example, a temperature reading with a spatial resolution of 6 m, for a particular position, is calculated by taking into account the measured points 3 m after and before that position. Meaning that a 4 m long highly conductive zone might pass unnoticed. Moreover, an exhaustive calibration is also necessary to assure reliable measurements. If the DTS equipment is placed in an environment with varying temperatures, a continuous calibration is required as almost all the component parts of a DTS equipment are temperature sensitive (e.g. power supply, laser, detector amplifiers, etc.) (Hausner et al., 2011). This is the typical situation in a field experiment where an invariant temperature spot should be used as reference for DTS equipment calibration (e.g. isolated box with ice, portable thermal bath, etc.).

A thorough review on the historical and technical developments and the current status of distributed (DTRT) and enhanced (ETRT) thermal response tests (TRT) is reported in (Wilke et al. 2020).

The DTRT has demonstrated to be a valuable method to enhance the energy efficiency and reduce the capital cost of BHE installations. However, more developments are required until a method to overcome current limitations is developed and more affordable equipment reaches the market. It is this research gap which inspired the general objective of this Ph.D. study: advance the science behind DTRT methods.

Chapter 3

Proposal of an inverse simulation method to calculate the depth-specific thermal conductivity

> *This chapter covers the proposal of a method to estimate the thermal properties of the geological layers crossed by perforation in a borehole. As a preliminary assessment, the method is carried out from the experimentally recorded temperature profiles during a TRT in a real BHE facility. The appended paper includes a detailed description of the experiment, method and results.*

3.1. Paper I: Extraction of thermal characteristics of surrounding geological layers of a geothermal heat exchanger by 3D numerical simulations

Authors: Nordin Aranzabal, Julio Martos, Álvaro Montero, Llucia Monreal, Jesús Soret, José Torres and Raimundo Garcia-Olcina.

Published in: Applied Thermal Engineering, vol. 99, pp. 92–102 (2016).
DOI: 10.1016/j.applthermaleng.2015.12.109

Impact factor: 4.026

Quartile (category: "Engineering, Thermodynamics"): Q1 (2018)

Summary:

This first paper is focused on the proposal of a method to calculate the depth-specific thermal conductivity of the typically heterogenous subsurface surrounding a BHE. The suggested method, called observed pipe TRT (OP-TRT), complements the standard TRT by providing additional information of the ground thermal properties along the length of an auxiliary pipe. This information is of great interest during the design phase of a borehole or borehole field. It allows detection of the most favorable layers to exchange heat, and thus optimal length of the BHE to achieve the maximum heat transfer performance at the minimum capital cost.

This study covers the design and implementation of an experiment to assess the proposed method in an available BHE on the campus at the Universidad Politécnica de Valencia. The BHE is 40 m deep and the subsurface is known to be composed by six different layers of geological strata, with water presence below four meters. After the drilling and insertion of geothermal pipes, the borehole is filled with a mixture of concrete and bentonite. In this installation, a TRT of three days long is conducted in a single U-pipe while measuring the transient thermal evolution along the depth of an auxiliary pipe with a wired probe. The proposed method requires the input of the recorded temperature profiles throughout the auxiliary pipe, called observed pipe, to calculate the conductivity values.

The introduced method consists of an inverse simulation procedure to fit experimental data by adjusting the thermal conductivity of the different geological layers. For that, a 3D FEM is developed with the same geometry and thermal behavior of the experimental BHE. The model is initialized with the effective thermal conductivity and borehole thermal resistance calculated from the conventional TRT. Afterwards, an algorithm describing the required steps is proposed to estimate the conductivity. Basically, it consists of an iterative simulation process where the thermal conductivity of the different geological layers is adjusted until the recorded temperature profiles along the observed pipe fit with simulation results.

Finally, the calculated effective thermal conductivity from the standard TRT agrees with simulations results, demonstrating the applicability and reliability of the testing and data interpretation methods. Moreover, the measured inlet-outlet and observer pipe temperature profiles during the course of the TRT are significantly close to the obtained results from simulation. From the obtained results, a small highly conductive zone located between 24 and 26 meters is detected. This zone is likely to be dominated by groundwater movements.

Applied Thermal Engineering 99 (2016) 92–102

Contents lists available at ScienceDirect

Applied Thermal Engineering

journal homepage: www.elsevier.com/locate/apthermeng

Research Paper

Extraction of thermal characteristics of surrounding geological layers of a geothermal heat exchanger by 3D numerical simulations

N. Aranzabal [a,*], J. Martos [a], Á. Montero [b], L. Monreal [c], J. Soret [a], J. Torres [a], R. García-Olcina [a]

[a] Department of Electronic Engineering, Universidad de Valencia, Burjassot 46100, Spain
[b] Department of Applied Thermodynamics, Universidad Politécnica de Valencia, Valencia, 46022, Spain
[c] Department of Applied Math, Universidad Politécnica de Valencia, Valencia, 46022, Spain

HIGHLIGHTS

- An innovative analysis procedure, complementing the standard TRT analysis.
- A novel temperature profile is presented as an additional measurement during the TRT.
- Estimate thermal conductivity profile of geothermal layers crossed by perforation.
- Implemented by fitting 3D FEM simulation results with experimental data.
- Allowed the detection of a highly conductive layer in an experimental BHE installation.

ARTICLE INFO

Article history:
Received 4 September 2015
Accepted 22 December 2015
Available online 19 January 2016

Keywords:
Ground coupled heat pump
Numerical simulation
Thermal Response Test
Heat transfer
Technic-Economical optimization
Energy efficiency

ABSTRACT

Ground thermal conductivity and borehole thermal resistance are key parameters for the design of closed Ground-Source Heat Pump (GSHP) systems. The standard method to determine these parameters is the Thermal Response Test (TRT). This test analyses the ground thermal response to a constant heat power injection or extraction by measuring inlet and outlet temperatures of the fluid at the top of the borehole heat exchanger. These data are commonly evaluated by models considering the ground being homogeneous and isotropic. This approach estimates an effective ground thermal conductivity representing an average of the thermal conductivity of the different layers crossed by perforation. In order to obtain a thermal conductivity profile of the ground as a function of depth, two additional inputs are needed; first, a measurement of the borehole temperature profile and, second, an analysis procedure taking into account ground is not homogeneous. This work presents an analysis procedure, complementing the standard TRT analysis, estimating the thermal conductivity profile from a temperature profile along the borehole during the test. The analysis procedure is implemented by a 3D Finite Element Model (FEM) in which depth depending thermal conductivity of the subsoil is estimated by fitting simulation results with experimental data. The methodology is evaluated by the recorded temperature profiles throughout a TRT in a BHE (Borehole Heat Exchanger) monitored facility, which allowed the detection of a highly conductive layer at 25 meters depth.

1. Introduction

To reduce primary energy consumption and emissions of green house gases, more and more attentions are paid to GSHP as heating ventilation and cooling system (HVAC) to conditioning spaces into buildings and to provide hot water [1–5]. In general, a typical GSHP system mainly consists of a heat pump, a group of borehole heat exchangers and indoor units. Commonly, these are coupled with the ground as a heat source or sink for exchanging energy by the circulation of a heat carrier fluid in the tubes of BHEs [6,7]. The GSHP system takes advantage of subsoil high thermal inertia that remains at a constant temperature, that is more favourable than the outside, so higher energy efficiency can be obtained as compared to traditional air-conditioning systems [8].

The performance of GSHP systems is determined by ground stratigraphy in which thermal conductivity, ground water flow and initial temperature play an essential role [9,10]. Detailed and accurate information of thermal behaviour of subsoil layers crossed by perforation is a prerequisite for improving the ratio between the heat transfer optimization and cost of the installations [11], namely,

* Corresponding author. Tel.: 0034 646420398; fax: 0034 963 544 353.
E-mail address: nordin.aranzabal@uv.es (N. Aranzabal).

http://dx.doi.org/10.1016/j.applthermaleng.2015.12.109
1359-4311/

for determination of the maximum heat transfer using the minimum length of the GHE installations.

In order to estimate heat transfer at the vertical BHE, diverse numerical and analytical methods have been proposed from data obtained in field investigation studies [12,13]. Currently, the more extended method is the TRT based on Infinite Line Source Model (ILS) [14], which describes conductive heat transfer in a homogeneous medium with a constant temperature at infinite boundaries. The TRT consists in applying a constant power input to the soil by a fluid flow inside the pipes and monitoring changes of temperatures at inlet and outlet of the perforation. Mainly two parameters are obtained: effective thermal conductivity, λ_{eff}, and borehole thermal resistance, $\mathbf{R_b}$, by following theory proposed by Hellström et al. [15]. However, it is difficult to accomplish the optimum design of a GHE and some factors as significant temperature variations produced by weather conditions, pipe insulation, variations in the power source, heterogeneous distribution of subsurface properties… can affect the measuring output of TRT. Additionally, standard TRT measuring output can be considerably affected by the advection effect of groundwater flows and lead to an undesirable deviation of the λ_{eff} [16].

Some other studies [17–19] presented the importance of groundwater flow on improving the performance of BHE and argued that those effects should not be neglected. From the point of view of engineering applications, this enhanced effect is favourable for reducing the possible imbalance between heat injection and extraction from and to the ground, which is helpful for the long-term operation of GSHP systems. For a specific energy demand of a GSHP system, accounting for the axial effects can lower the required length and numbers of boreholes. Marcotte et al. [20] showed, for an example, a design problem that the calculated borehole length could be 15% shorter when axial effects are considered, which conclusively means a more cost-efficient system. Chiasson et al. [21], Wang et al. [22] and Fan et al. [23] evaluated the effects of groundwater flow on the heat transfer into the BHE. They concluded that groundwater flow enhances heat transfer between the BHE and the aquifer. In this case, shorter or less BHEs are needed for the same technical performance.

In the last decades various investigations have been conducted to reliably calculate TRTs influenced by groundwater flow. One possibility to calculate the influence of groundwater flow is a stepwise TRT evaluation based on the Kelvin line source theory [24]. Witte et al. [25] illustrated an increasing value with increasing evaluation time step size as an indicator for groundwater flow. Another possibility is the suggested analytical solution by Molina-Giraldo et al. [26] based on a Moving Finite Line Source model (MFLS) which takes into account both aspects: groundwater flow and axial effects overcoming the limitations of previous analytical models [27,28]. The analytical procedure is verified with a finite element model and is concluded that the performance of axial effects essentially depends on the groundwater velocity in the aquifer and the length of the borehole heat exchanger. Some other studies based on the recorded data during the TRT and finite element simulations analysed the importance of natural subsurface conditions, such as vertical geothermal gradients and thermal dispersion [29]. And later, a parameter estimation strategy to calculate information about the actual Darcy velocity based on MFLS was presented by Wagner et al. [30,31], which is sensitive to conduction and advection.

However, these concepts provide neither information about the exact location of the underground water flow nor information about the depth-depending thermal conductive parameters of heterogeneous ground profiles. For overcoming that, novel strategies are developed based on Distribution Temperature Sensing (DTS) system [32]. In DTS systems, optical fibre thermometer is placed along the inlet pipe of the installation, from which the vertical temperature distribution can be measured. Hence, thermal conductivity of the ground can be evaluated along depth [33]. Fujii et al. [34] performed a comparative study on conventional TRT and the enhanced TRT on DTS. The obtained effective thermal conductivity for both cases is very similar and furthermore, the enhanced TRT indicated the presence of a highly conductive region due to the presence of an aquifer. Wagner and Rohner et al. [35] showed how specific layers with groundwater flow (enhanced λ_{eff} values) can be estimated. Nevertheless, the cost of the required equipment for optical fibre thermometer is high and the process to guarantee the correct placement along the diameter of the pipes can be difficult.

In this research work, an innovative analysis procedure to obtain a detailed depth-depending thermal conductivity profile along vertical BHE subsoil surrounding is presented. The vertical thermal conductivity gradient is estimated from an additional temperature profile along an auxiliary pipe during an experimental TRT and by fitting a 3D finite element model with test results. Likewise, the measured additional temperature profile along an auxiliary pipe by a wired digital temperature probe overcomes the limitations of the methods discussed above.

This paper is divided as follows. Firstly, a BHE built at Universidad Politécnica de Valencia campus of 40 meters depth and composed by six different layers of geological strata is described and the obtained data throughout a TRT of 1 kW are presented. Secondly, the analysis procedure to estimate the thermal conductivity profile of the subsoil layers crossed by perforation based on a finite element model is described. Thirdly, the obtained results after applying the procedure to the recorded data from the performed 1 kW TRT are presented, which allow the detection of a highly conductive layer at 25 meters depth. Finally as conclusions, the obtained results and the hypothetical causes of the discovered thermal conductivity profile are discussed.

2. Experimental facility and data

On the Universidad Politécnica de Valencia campus is available a BHE of 40 m depth, 160 mm drill diameter and two geothermal independent pipes, ALB GEROtherm PE-100 of 40 mm diameter and 29 and 39 m long, respectively. The pipes are disposed with a turn of 90° between them, keeping uniform the distance between the pipes of the geothermal probes with separators of polyethylene distributed every meter depth. The borehole was drilled by rotopercussion technique with a metallic cylinder contention, which was not extracted during refilling phase. Samples of the subsoil stratigraphy were taken during the drilling to determine composition. In Fig. 1 is depicted the geological profile and a diagram of the pipes disposal inside drilling and in Fig. 2 is shown an image of the installation.

The obtained samples were mixed with water during its transportation and thus were not suitable for an accurate analyse of thermal characteristics of geological layers in laboratory tests. Consequently, only the dry material and a thermal conductivity that varies between 1.5 W/mK and 2.0 W/mK was analysed and was estimated from thermal data tables. Besides, from other geological studies performed in 2008 throughout a building construction near the facility, a stratigraphic profile that matched with the samples taken during the drilling was obtained. Specifically, it was conducted by a rotating drilling technique in which samples were obtained unchanged. In the analysis of this stratigraphic column, the presence of a groundwater level about 4 meters depth was detected and from samples and laboratory tests a content of moisture between 14% and 30% was measured.

The drilling filling is done with CEMEX 32.5 raff concrete and bentonite in a proportion of twelve parts of concrete and one of bentonite. This filling solution is suitable for typical Valencian soil, rich in moisture and water flows. The drilling was performed in May of 2010 and during the next months the temperature inside the pipes was monitored in order to determine when the soil recovered its

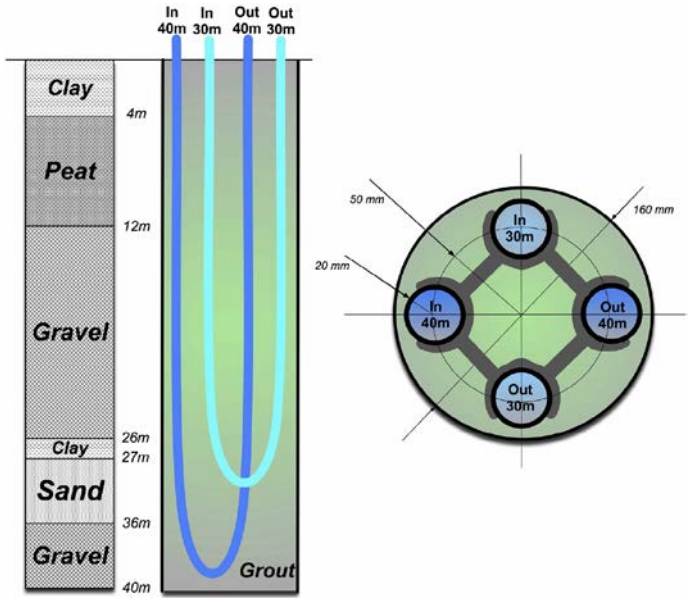

Fig. 1. Geological profile and distribution of geothermal probes inside the drilling.

temperature before the drilling. In Fig. 3, a graph with the inside temperature of the 39 m depth pipes is depicted from its insertion in the exchanger until the stabilization with the surrounding ground, a process that lasted about 6 months.

An equipment to perform heat injection TRT was provided to the installation, consisting of an electronic adjustable circulating pump, a heating resistor of 3×1 kW/220 V; a flowmeter; a 5 litre expansion tank; temperature probes at input and output of the exchanger, connected to an acquisition system through a 4 wire 4–20 mA loop of TC Direct adjusted in a range from 0 °C to 50 °C. The temperature sensors were calibrated through a thermal bath and an electronic precision thermometer, performing a two point lineal adjustment within the dynamic range from 0 °C to 50 °C chosen for the sensors.

Furthermore, an energy meter was employed for monitoring electric power source of the installation and a meteorological station for measuring surface environmental temperature and humidity. The full system was managed from a PC with a touch screen and Internet access that performed acquisition and register of the data during the TRT, through a program developed in Matlab.

On 9th March 2011 at 11:00 a 1 kW heat injection TRT was started, using the geothermal pipe of 29 meters length, and leaving the one of 39 meters filled with water in order to use it as an observer pipe and measure the temperature profiles during the TRT. A flow of 410 l/h of water without glycol was fixed, and the PC program was configured to acquire data with a 3 minute period. The test lasted 3 days, with an environmental average temperature of 10.6 °C, oscillating between the maximum of 18.1 °C and the minimum of 6.5 °C. Fig. 4 depicts the temporary evolution of environment temperature and temperature evolution at inlet (T_{in}) and outlet (T_{out}) of the TRT during 3 days. Temperature profiles at inlet and outlet show some fluctuations that correspond to the environment temperature variations during the test realization.

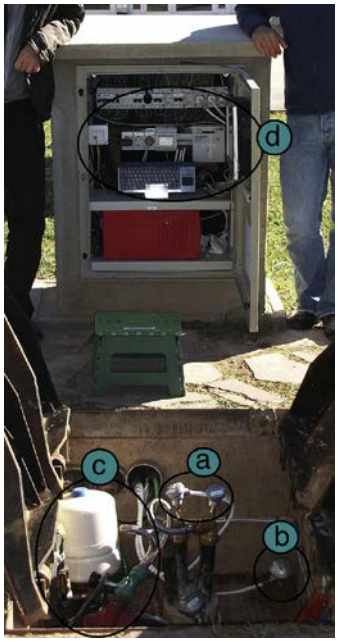

Fig. 2. Photography of the experimental installation at UPV Campus. (a) T_{in}, T_{out} temperatures probes; (b) Ground temperature probe; (c) Hydraulic subsystem; (d) Equipment of control and acquisition.

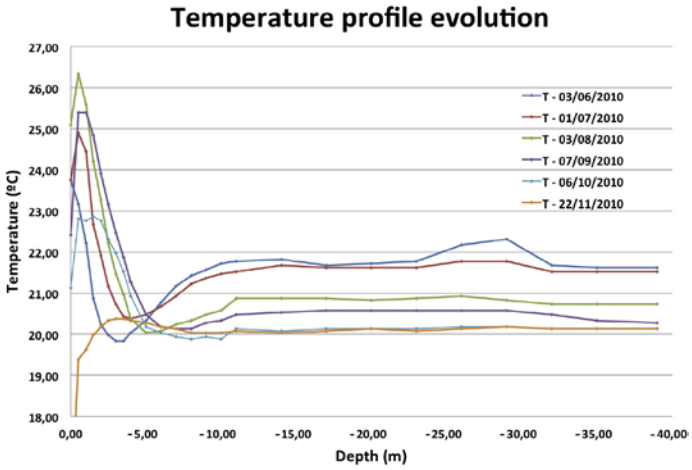

Fig. 3. Temperature evolution inside and along the 39 m depth pipe from the insertion date until thermal stabilization.

An approximation of the effective thermal conductivity parameter of the ground was calculated applying the ILS model of Kelvin [36] to the obtained experimental data during the TRT. Fig. 5 shows two straight sections that give higher conductivity estimation for the final test hours than for the first test hours, deviating from the ILS model prediction. The observed behaviour is typical scenario of areas with presence of moisture or water flows produced by the greater heat absorption of the layers affected by groundwater flows. In this case the turning point is placed at 10 hours from the beginning of the TRT and the last stretch based on TRT sizing gave a borehole resistance of 0.12 K/W and a conductivity of 2.41 W/m K.

Additionally, from the beginning of the TRT the temperature profile was obtained in one of the 39 meter length pipe, which was not used in this TRT for heat exchanging and named before as observer pipe. The measured data are depicted in Fig. 6. Each coloured marked line corresponds to a temperature profile along the observer pipe through time from 9th March (start of TRT) until 12th March (end of TRT). Furthermore, the five dashed black lines show the edges between geological strata determined by the obtained samples during the drilling.

To obtain the temperature data inside the observer pipe, a waterproof sensor was connected to an end of a 50 m length cable. This wired digital sensor only requires 2 wires for the connection and it transmits temperature data in digital format, reducing the errors that could be produced due to the cable length. The accuracy of the measurement is 0.5 °C in the range from –10 °C to 85 °C, and it has a maximum resolution of 12 bits; thus, a temperature resolution of 0.0625 °C is achieved.

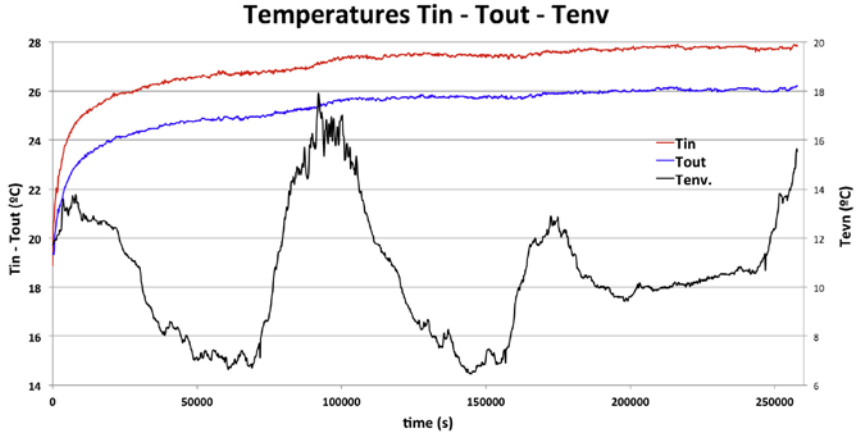

Fig. 4. Inlet, outlet and environment temperature evolution during the analysed TRT injection of 1 kW.

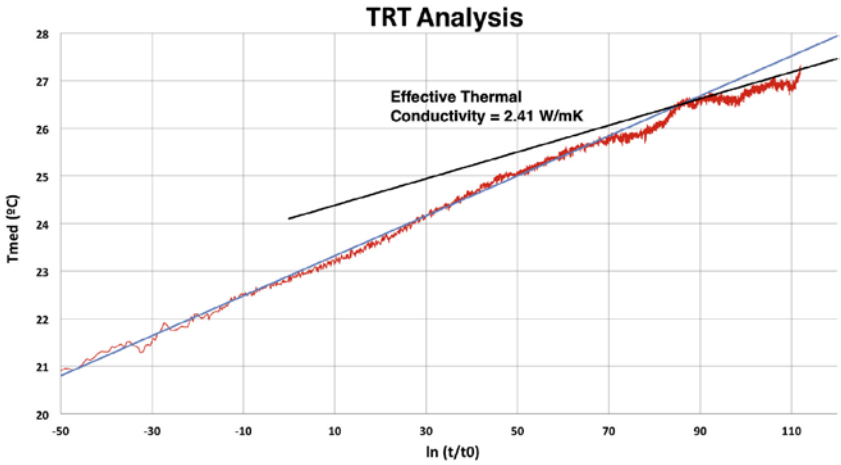

Fig. 5. Semilogarithmic representation of the average fluid temperature $T_{in} - T_{out}$ as a function of the variable x during a TRT injection of 1 kW and the calculated effective conductivity.

The process of obtaining a temperature profile consists in descending the sensor at prefixed depths of 0.5 meters in the first 4 meters of the drilling, and at 1 meter between the 5 meter and 28 meter depth then again at 0.5 meters between 28.5 and 30.5, ending the descent with 1 meter gaps. At each measuring point, the sensor was held in position for 5 seconds for thermal stabilization, before new temperature data was taken at the next depth. A temperature profile disturbance was created as the sensor was lowered but it was not taken into account due to its small size (<5 mm ø). This sensor was also calibrated with the same equipment used with the temperature sensors disposed along the rest of the installation.

After a careful drilling execution, insertion of geothermal probes and filling process, a borehole with the same thermal characteristics for the whole volume was built. Therefore, the measured

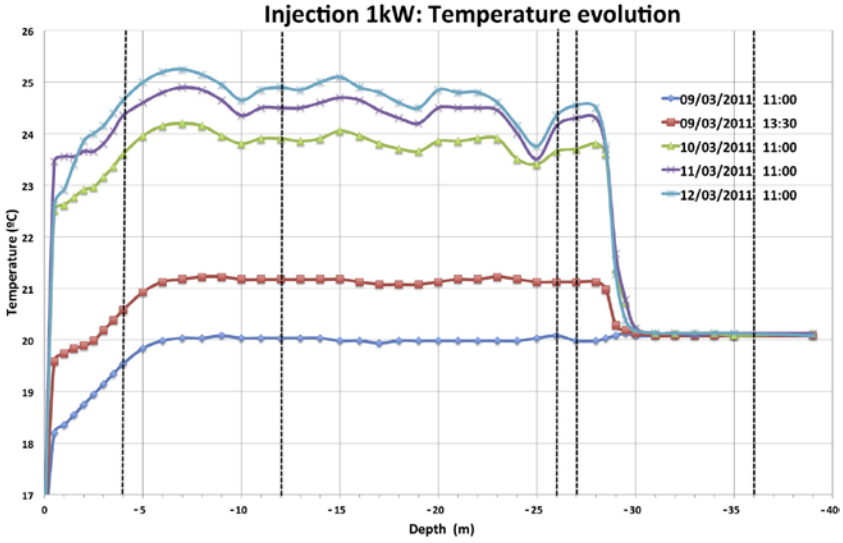

Fig. 6. Temperature profiles along the observer pipe during the analysed TRT injection of 1 kW. Coloured marked lines: five temperature profiles taken from 9th March to 12th March. Dashed lines: edges of geological layers determined during the drilling.

temperature variations inside the observer pipe will be due to the conductivity values of geological layers, and heat transfer between the borehole and the subsoil can be evaluated.

3. Procedure to estimate thermal conductivity

The aim of this research work is to estimate the thermal conductivity profile of the borehole surrounding layers crossed by perforation, from the registered data throughout the execution of a TRT. Due to the fact that TRT considers the medium homogenous and heat transmission in solids as a mechanism of diffusion, an infinite set of subsoil conductivity profiles ($\lambda_s(z)$) would generate the same set of data for the recorded T_{in} and T_{out} during the execution. Additional information is necessary in order to restrict the possible set of thermal conductivity profiles to only one. In this approach, the data that will impose the last restriction is taken as a series of vertical temperature profiles inside the filling of the exchanger, measured in determined time periods ($T_{op}(z,t)$). In addition, only heat transmission in solid will be considers as heat transfer mechanism.

If an exchanger is analysed by the model of thermal resistances and capacitances, across section of a BHE can be depicted by a delta network [37], such as the one in Fig. 7a.

This network can be simplified by an equivalent circuit formed only for 2 resistances and 2 capacitances, as is shown in Fig. 7b. If a careful BHE construction is performed, R_{bo} will be constant in all the domain of the grouting material and R_{og} will vary its value accordingly to the thermal characteristics of the geological layer for which is surrounded. Thus, the temperature ($T_{op}(z)$) will change in function of R_{og} resistance that is dependent on the conductivity of the subsoil.

In this approach, a 3D finite element model simulation is employed, in order to adjust a series of temperature profiles taken inside the borehole ($T_{op}(z,t)$). The procedure is initiated by assigning the effective thermal conductivity obtained from the TRT to both borehole and subsoil, and is performed a simulation of the TRT. Once the simulation is finished, the obtained temperature profiles are compared with those measured during the experimental TRT, and thermal conductivity of the subsoil is modified based on the following algorithm:

If $\max(\mathrm{abs}(T_{op\_simu}(z,t) - T_{op\_exp}(z,t))) > \varepsilon$
  If $(T_{op\_simu}(z,t) < T_{op\_exp}(z,t))$ **then** increase $\lambda_s(z)$
  If $(T_{op\_simu}(z,t) > T_{op\_exp}(z,t))$ **then** decrease $\lambda_s(z)$
  Start a new simulation
Else Simulations are completed

Namely, it will be conducted as many simulations and adjustments of thermal conductivity profiles $\lambda_s(z)$ as it will be necessary for reaching an error smaller than the desired value between the measured temperature profiles during the TRT and the obtained during the simulation. The resultant conductivity profile is taken as the one that represents the subsoil surroundings of the exchanger.

4. Application of the procedure to an experimental TRT

In this paragraph the previously elaborated procedure is applied to the recorded data from the experimental TRT of 1 kW heat injection described before. A 3D finite element model with the same geometry of the experimental BHE is developed using COMSOL Multiphysics ® version 4.4. Then, the model is adjusted to fit with the measured data in order to estimate the thermal conductivity profile of the borehole surrounding layers.

From all the modules available, the Heat Transfer in Solid (ht) and Non-Isothermal Pipe Flow (nipfl) have been used.

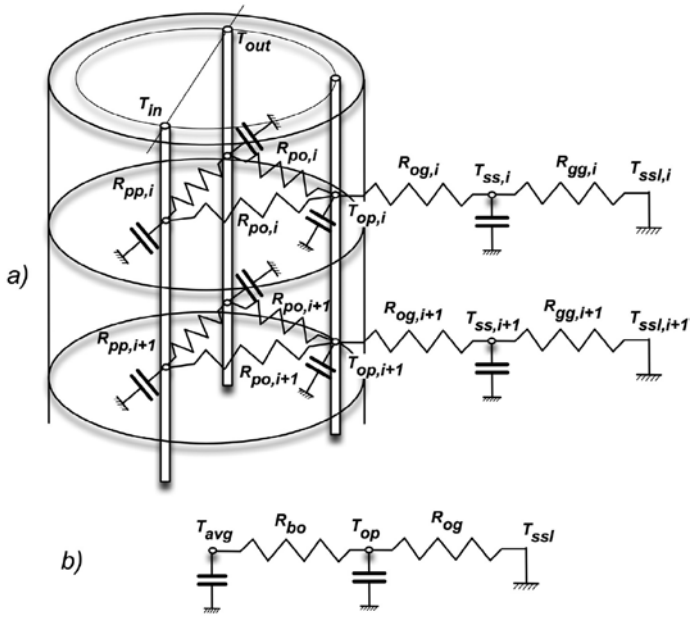

Fig. 7. (a) Resistances and capacitances model by delta network across a section of a BHE. (b) Previous model simplification by an equivalent circuit.

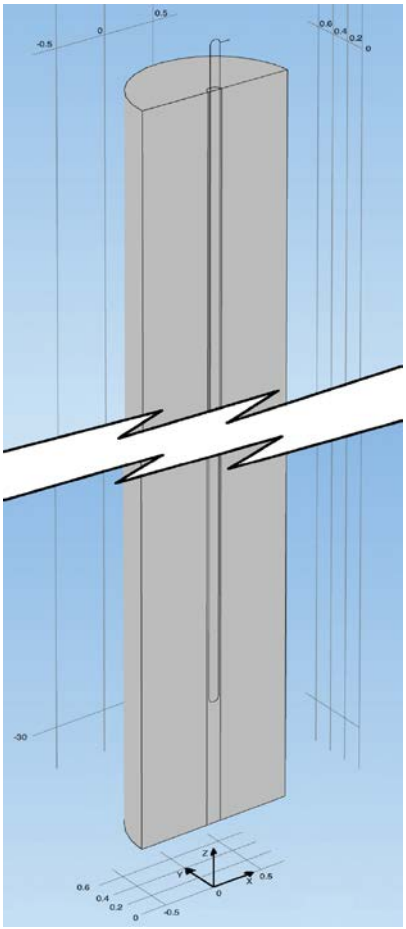

Fig. 8. 3D model of the experimental exchanger implemented in COMSOL Multiphysics 4.4.

The simulations have been completed under following conditions:

- Only heat transmission in solid has been considered into borehole and surroundings (convective effects has been neglected).
- Thermal parameters of borehole grouting materials have been considered constants, λ_b = constant, Cp = constant, ρ = constant.
- Thermal conductivity of surrounding has been defined as depth dependent, $\lambda_s(z)$, and has been adjusted in order to fit the temperature profile into observer pipe.

In order to simplify computer operations and to reduce the calculation time, a symmetry plane defined by the pipes that form the U of the exchanger has been considered, which has reduced the total volume of the model by half. In Fig. 8 is presented the resultant model after applying symmetry, in which is possible to appreciate the two contained domains as two concentric cylinders. The smaller cylinder of 0.08 m radius represents the perforation filled with the grouting material in which the U pipes are inserted, and the other cylinder of 0.75 m, the subsoil volume in which the heat is transferred. Looking for the optimal volume to simulate the borehole, two models were built with different subsoil radius, one of 0.75 m and another of 1 m. The obtained results for both models were very similar, with a maximum difference of 0.083 °C and a relative error of 0.03% in both measured points (T_{in} and T_{out}). After, another model of radius 0.6 m was built and compared with the model of 1 m radius obtaining an absolute error of 0.235 °C and a relative error of 0.9%. Thereby, the decision of employing a 0.75 m radius for subsoil volume was taken due to the model simplicity and behaviour similarities. Since symmetry onto XZ plane has been used, the final model is displayed, shaped as a 30 meter length semi-cylinder. In Table 1 the configuration data of the developed 3D model can be appreciated.

Table 1
Simulation parameters.

Parameter	Value
Borehole depth	30 m
Borehole radius	0.08 m
Outer radius of U-tube pipe	0.02 m
Inner radius of U-tube pipe	0.016 m
Centre to centre half distance	0.06 m
Pipe thermal conductivity	0.6 W/m K
Pipe's length	29 m
Ground radius	0.75 m
Ground depth	30 m

After establishing a finite geometry, both domains were defined with equal characteristics assigning the effective conductivity of 2.41 W/m K obtained during the last stretch of the realized experimental TRT.

Therefore, for the first simulation both domains were configured with a thermal conductivity of 2.41 W/m K, a density of 1800 kg/m^3 and a specific heat capacity of 2000 J/kg K. The simulation was set up using an injected power of 950 W and a caudal of 420 l/hour. The initial temperature value of the topsoil was established as the recorded average value of 16 °C throughout the days of the TRT implementation. Also, the layers of the ground were initialised with the obtained temperature values along the observer pipe before the beginning of the TRT.

Another important factor that directly affects to the simulation time and accuracy is the model meshing. Some simulation trials were run with different user-defined meshing configurations until the most suitable solution was found in the simplest model as less time was used in converging to a solution without lose accuracy in the results. Finally, a model meshing with a maximum size of element of 0.25 m, a minimum size of 0.03 m, a factor curvature of 0.3, a narrow regions resolution of 0.85 and a maximum growth of 1.35 elements was selected. With those parameters, 423,256 tetrahedral elements for model domains were obtained. Another model composed of 684,863 elements was built and simulated in order to check if the accuracy was improved but, after comparing both results, an absolute error of 0.005 °C and a relative error of 0.05% were obtained. A third model with 265,088 elements was built, obtaining an absolute error of 0.013 °C and a relative error of 0.05% compared to the model of 423,256, but with similar simulation time. In consequence the decision of employing a model with 423,256 elements was taken.

Temporal parameters of simulation were established as follow: total simulation time of 3.1 days, maximum step of 100 seconds and data registration every 20 minutes.

Then, the calculated effective thermal conductivity from TRT datasets were adjusted to both domains and the first simulation was conducted. In Fig. 9 the obtained T_{in} and T_{out} temperature profiles from simulation are presented in superposition with the recorded

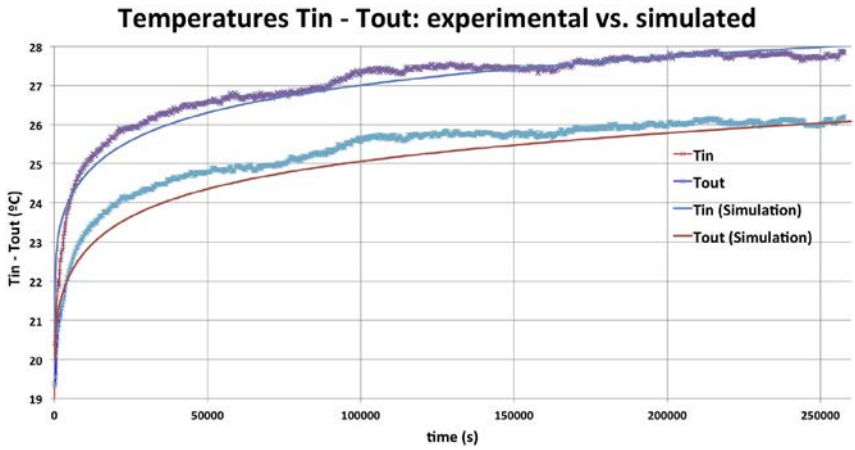

Fig. 9. Superposition of T_{in}–T_{out} temperature evolution during a TRT and the obtained ones in the initial simulation. Experimental data (thick lines) and temperature simulation (thin lines).

data during the experimental TRT. Additionally, in a similar manner, in Fig. 10 is depicted the superposition of simulated temperature profiles and the obtained ones along the observer pipe during the experimental TRT.

The next phase of the simulation was implemented by adjusting the conductivity values of the subsoil. Following the proposed analysis procedure, the model adjustment was continued with the iterative set of simulations. In this case, a maximum temperature value between samples of 0.3 °C was selected because the error in the sensor measurement range from 20 °C to 25 °C is bounded between 1.5% and 1.2%, which was considered acceptable in our approach. After a few iterations, it was possible to get an improvement in the adjustment between the experimental TRT data and simulation results, maintaining the correspondence both in the evolution of the temperatures T_{in} and T_{out} and in the observer pipe, as is presented in the graph of Fig. 11.

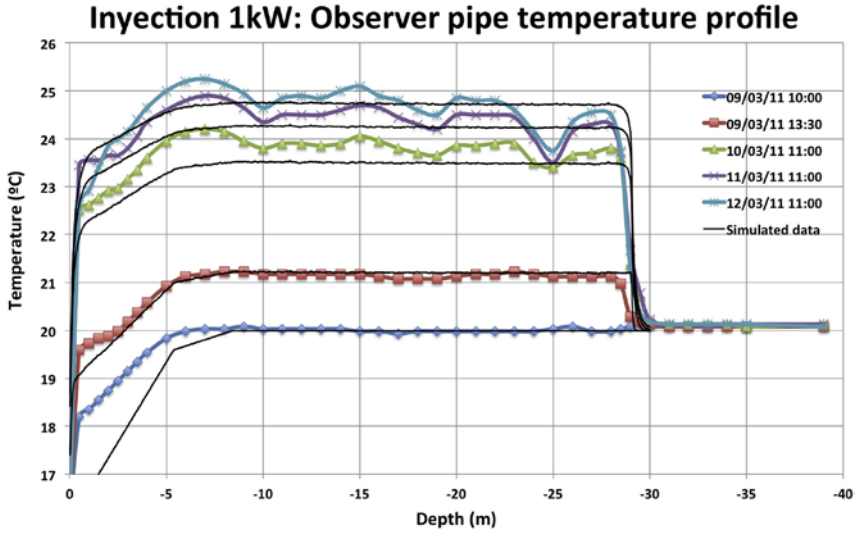

Fig. 10. Superposition of experimental data along the observer pipe and the obtained data from the initial simulation. Experimental data (coloured marked lines) and temperature simulation (black lines).

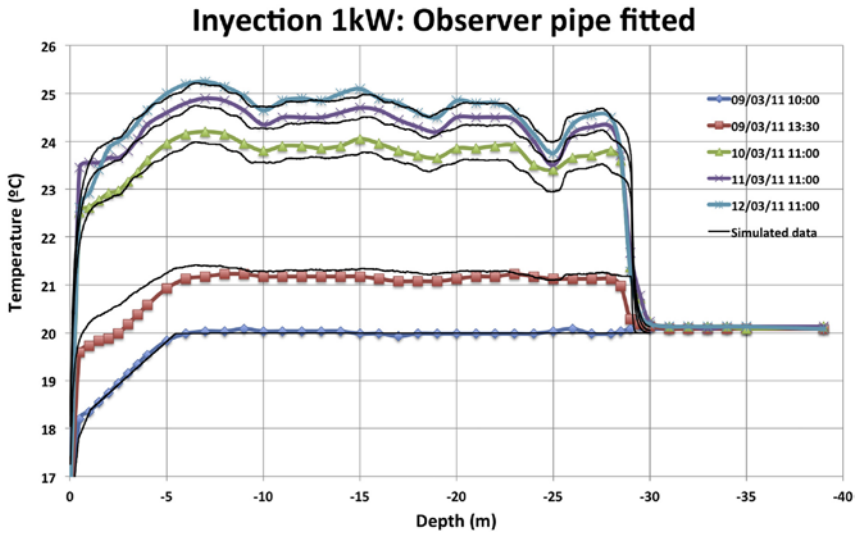

Fig. 11. Superposition of temperatures profiles evolution along the observer pipe during the TRT and the obtained results from final simulation. Experimental data (coloured marked lines) and temperature simulation (garnet lines).

Besides, in Fig. 12 is shown the resultant adjusted thermal conductivity distribution along the vertical subsoil layers from the last simulation (using the best achieved settings). It is noteworthy to observe the high conductivity layers located between the 24 and 26 meter depth.

Moreover, two heat injections, TRT of 2 kW and 3 kW, were conducted over the same installation, on 22nd November 2010 and on 15th December 2010, respectively. In those tests, the observer pipe temperature profiles were not registered with enough spatial and temporal resolution, so it was not possible to perform the same procedure described above for obtaining the subsoil conductivities profile. Although, aiming to test the developed 3D FEM with more experimental data and different heat sources, the recorded T_{in}–T_{out} temperature profiles for the TRT of 2 kW and 3 kW were compared with results from simulation. For that, two simulations were carried on over previously adjusted model, one with a power of 2 kW and other with a power of 3 kW. The comparison between obtained simulation values and the registered in the TRTs are depicted in Fig. 13, which presents a quite accurate adjustment.

5. Conclusions

One of the main findings of this research work is the estimated conductivity profile of geothermal layers crossed by perforation from the results of a 3D finite element model simulation. The presented novel temperature profile is an additional measurement that

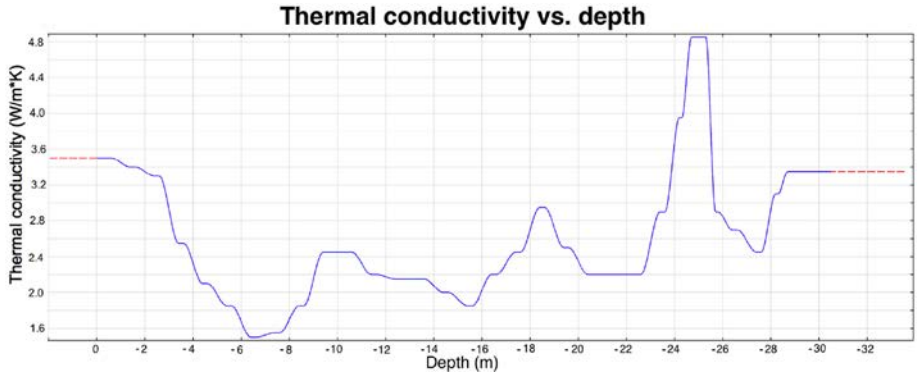

Fig. 12. Conductivity profile in the geological layers of the subsoil obtained from simulation.

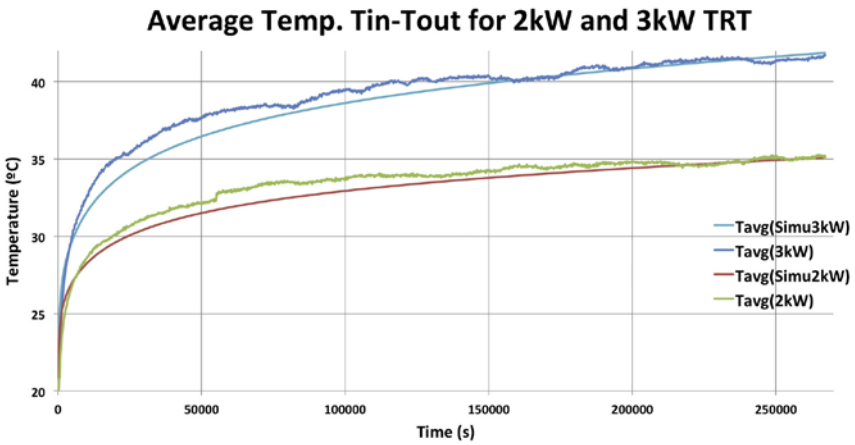

Fig. 13. Superposition between the obtained data in experimental TRT for 2 kW and 3 kW between the obtained results from model simulation.

can be implemented in combination with the conventional TRT enhancing the obtained results. This methodology does not require samples of ground stratigraphy and has been possible to obtain a thermal conductivity profile of the subsoil by the recorded data during the suggested enhanced TRT. Furthermore, the calculated effective thermal conductivity of 2.41 W/m K during the experimental TRT agreed with the obtained value from simulations, demonstrating the applicability and reliability of the testing and data interpretation methods. Also, the recorded U pipe inlet and outlet and observer pipe temperature profiles during the experimental TRT are very similar to the achieved results from simulation.

The obtained thermal conductivity profile presents an accurate adjustment of the temperatures along the observer pipe, except for a region located between 24 and 26 meters that may be caused by the groundwater advection effects. The development of a new model in which conduction and advection are taken into account will likely improve the obtained results. In such case, more detailed information of the axial effects can be interpreted, as for example, an estimation of the location and the velocity of underground water flows.

To sum up, the proposed enhanced TRT and the analysis procedure are validated as a useful method to identify the position of the groundwater flow in a borehole subsoil surroundings. The location of groundwater flow can help to improve heat transfer efficiency of BHE. Therefore, the obtained data could easily parameterize the length of the drilling for implementing a totally optimized heat exchanger in order to maximize the W/m relation of the thermal transfer. The findings of this study will provide valuable information for thermal conductivity measurements in field and will improve the performance analysis of BHE in layered subsurface.

Acknowledgements

This work has been supported by the EIT Climate-KIC, a body of the European Union inside the PhD Programme of TBE Platform.

Nomenclature

T_{in}	Water temperature inside inlet pipe
T_{out}	Water temperature inside outlet pipe
T_{avg}	Water average temperature between inlet and outlet pipes
T_{op}	Temperature inside observer pipe
$T_{op}(z)$	Observer pipe temperature related to depth
$T_{op}(z,t)$	Observer pipe temperature related to depth and time
$T_{op\_simu}(z,t)$	Simulated observer pipe temperature related to depth and time
$T_{op\_exp}(z,t)$	Experimental observer pipe temperature related to depth and time
T_{SS}	Near subsoil temperature
T_{ssl}	Far subsoil temperature
R_{pp}	Thermal resistance between pipes
R_{po}	Thermal resistance between pipes and observer pipe
R_{og}	Thermal resistance between observer pipe and near ground
R_{gg}	Thermal resistance between near ground and far ground
R_{bo}	Thermal resistance between borehole and observer pipe
λ_b	Borehole grouting material thermal conductivity
$\lambda_s(z)$	Borehole surroundings thermal conductivity profile
λ_{eff}	Effective thermal conductivity, the mean thermal conductivity of the surrounding subsurface
R_b	Heat transfer between pipes and borehole wall

References

[1] P. Bayer, D. Saner, S. Bolay, L. Rybach, P. Blum, Greenhouse gas emission savings of ground source heat pump systems in Europe: a review, Renew. Sustain. Energy Rev. 16 (2012) 1256–1267.
[2] A.M. Omer, Ground-source heat pump systems and applications, Renew. Sustain. Energy Rev. 12 (2008) 344–371.
[3] H. Yang, P. Cui, Z. Fang, Vertical-borehole ground-coupled heat pumps: a review of models and systems, Appl. Energy 87 (2010) 16–27.
[4] J.W. Lund, B. Sanner, L. Rybach, R. Curtis, G. Hellström, Geothermal (ground-source) heat pumps. A world overview, Geo-Heat Centre Quart. Bull. 25 (3) (2004) 1–10.
[5] J.F. Urchueguía, M. Zacarés, J.M. Corberán, A. Montero, J. Martos, H. Witte, Comparison between the energy performance of a ground coupled heat pump system and an air to water heat pump system for heating and cooling in typical conditions of the European Mediterranean coast, Energy Convers. Manag. 49 (2008) 2917–2923.
[6] J.A. Adaro, P.D. Galimberti, A.I. Lema, A. Fasulo, J.R. Barral, Geothermal contribution to greenhouse heating, Appl. Energy 64 (1999) 241–249.
[7] P.M. Congedo, G. Colangelo, G. Starace, CFD simulations of horizontal ground heat exchangers: a comparison among different configurations, Appl. Therm. Eng. 33–34 (2012) 24–32.

[8] G. Florides, S. Kalogirou, Ground heat exchangers-a review of systems, models and applications, Renew. Energy 32 (15) (2007) 2461–2478.
[9] M. Bernier, Closed-loop ground-coupled heat pump systems, ASHRAE J. 48 (9) (2006) 13–24.
[10] H.V. Nguyen, Y.L.E. Law, M. Alavy, P.R. Walsh, W.H. Leong, S.B. Dworkin, An analysis of the factors affecting hybrid ground-source heat pump installation potential in North America, Appl. Energy 125 (2014) 28–38.
[11] P. Blum, G. Campillo, T. Kölbel, Techno-economic and spatial analysis of vertical ground source heat pump systems in Germany, Energy 36 (5) (2011) 3002–3011.
[12] P. Eskilson, Thermal analysis of heat extraction boreholes (Ph.D. Thesis), University of Lund, Lund, Sweden, 1987.
[13] S. Hähnlein, N. Molina-Giraldo, P. Blum, P. Bayer, P. Grathwohl, Ausbreitung von kältefahnen im grundwasser bei erdwärmesonden. (Cold plumes in groundwater for ground source heat pump systems), Grundwasser 15 (2010) 123–133.
[14] J.D. Spitler, S.E.A. Gehlin, Thermal response testing for ground source heat pump systems – An historical review, Renew. Sustain. Energy Rev. 50 (2015) 1125–1137.
[15] G. Hellström, Ground heat storage, thermal analysis of duct storage systems, University of Lund, Lund, Sweden, 1991.
[16] H. Witte, G.J. Van Gelder, J.D. Spitler, In-situ measurements of ground thermal conductivity: the Dutch perspective, ASHRAE Trans. Res. 108 (1) (2002) 263–272.
[17] W. Zhang, H. Yang, L. Lu, Z. Fang, Investigation on heat transfer around buried coils of pile foundation heat exchangers for ground-coupled heat pump applications, Int. J. Heat Mass Transf. 55 (21e22) (2012) 6023–6031.
[18] J. Raymond, R. Therrien, L. Gosselin, R. Lefebvre, Numerical analysis of thermal response tests with a groundwater flow and heat transfer model, Renew. Energy 36 (2011) 315–324.
[19] H.J. Wang, C.Y. Qi, H.P. Du, J.H. Gu, Thermal performance of borehole heat exchanger under groundwater flow: a case study from Baoding, Energy Build. 41 (12) (2009) 1368–1373.
[20] D. Marcotte, P. Pasquier, F. Sheriff, M. Bernier, The importance of axial effects for borehole design of geothermal heat-pump systems, Renew. Energy 35 (4) (2010) 763–770.
[21] A.D. Chiasson, S.J. Rees, J.D. Spitler, A preliminary assessment of the effects of ground water flow on closed-loop ground-source heat pump systems, ASHRAE Trans. 106 (1) (2000) 380–393.
[22] H. Wang, C. Qi, H. Du, J. Gu, Thermal performance of borehole heat exchanger under groundwater flow: a case study from Baoding, Energy Build. 41 (12) (2009) 1368–1373.
[23] R. Fan, Y. Jiang, Y. Yao, D. Shiming, Z. Ma, A study on the performance of a geothermal heat exchanger under coupled heat conduction and ground-water advection, Energy 32 (11) (2007) 2199–2209.
[24] B. Sanner, G. Hellström, J. Spitler, S. Gehlin Thermal response test – current status and world wide application. In: World Geothermal Congress, Antalya, Turkey, 2005; pp. 1436–1445.
[25] H.J.L. Witte Geothermal response test with heat extraction and heat injection: examples of application in research and design of geothermal ground heat exchangers. In: Europäischer Workshop über Geothermische Response Tests, Lausanne, Switzerland, 2001.
[26] N. Molina-Giraldo, P. Bayer, P. Blum, Evaluating the influence of thermal dispersion on temperature plumes from geothermal systems using analytical solutions, Int. J. Therm. Sci. 50 (7) (2011) 1223–1231.
[27] M.G. Sutton, D.W. Nutter, R.J. Couvillion, A ground resistance for vertical borehole heat exchangers with groundwater flow, J. Energy Resour-ASME 125 (3) (2003) 183–189.
[28] N. Diao, Q. Li, Z. Fang, Heat transfer in ground heat exchangers with groundwater advection, Int. J. Therm. Sci. 43 (12) (2004) 1203–1211.
[29] V. Wagner, P. Bayer, M. Kübert, P. Blum, Numerical sensitivity study of thermal response tests, Renew. Energy 41 (2012) 245–253.
[30] V. Wagner, P. Blum, M. Kübert, P. Bayer, Analytical approach for groundwater-influenced thermal response tests of grouted borehole heat exchangers, Geothermics 46 (2013) 22–31.
[31] V. Wagner, P. Bayer, G. Bisch, M. Kübert, P. Blum, Hydraulic characterization of aquifers by thermal response testing: validation by large scale tank laboratory and field experiments, Water Resour. Res. 50 (2014) 1–15.
[32] H. Fujii, H. Okubo, R. Itoi, Thermal response tests using optical fiber thermometers, GRC Transactions 30 (2006) 545–551.
[33] J. Luo, J. Rohn, W. Xiang, M. Bayer, A. Priess, L. Wilkmann, et al., Experimental investigation of a borehole field by enhanced geothermal response test and numerical analysis of performance of the borehole heat exchangers, Energy 84 (2015) 473–484.
[34] H. Fujii, H. Okuboa, K. Nishia, R. Itoi, K. Ohyama, K. Shibata, An improved thermal response test for U-tube ground heat exchanger based on optical fiber thermometers, Geothermics 38 (2009) 399–406.
[35] R. Wagner, E. Rohner Improvements of thermal response tests for geothermal heat pumps. In: IEA Heat Pump Conference, Zürich, Switzerland, 2008.
[36] Á. Montero, J.F. Urchueguía, J. Martos, B. Badenes, Á. Picard Ground temperature profile while thermal response testing. European Geothermal Congress. Pisa, Italy, 3–7 June 2013.
[37] F. Ruiz-Calvo, M. De Rosa, J. Acuña, J.M. Corberán, C. Montagud, Experimental validation of a short-term Borehole-to-Ground (B2G) dynamic model, Appl. Energy 140 (2015) 210–223.

Chapter 4

Development of a specific instrument (Geowire) to measure the temperature profiles required for the inverse simulation method

> *In the previous chapter, the temperature profiles required for the proposed inverse simulation method were obtained manually by descending a wired probe. Thus, to improve the reliability and accuracy of the method, this chapter covers the development and validation of a specific in-borehole instrument. The precision and uncertainty of the spatial and temperature measurements are assessed in the laboratory. Also, the instrument is evaluated in a test BHE and results are validated with the well-known Pt100-sensors.*

4.1. Paper II: Novel instrument for temperature measurements in borehole heat exchangers

Authors: Nordin Aranzabal, Julio Martos, Hagen Steger, Philipp Blum and Jesús Soret.

Published in: IEEE Transactions on Instrumentation and Measurement, vol. 68 (4), 1062–1070 (2018).
DOI: https://doi.org/10.1109/TIM.2018.2860818

Impact factor: 3.067

Quartile (category: "Instruments & Instrumentation"): Q1 (2018)

Summary:

This second paper introduces an in-borehole instrument called Geowire, to automatically measure the temperature profiles required for the inverse simulation method suggested in the previous chapter. The design of the instrument is based on certain attributes to fulfil the requirements of the method and its applicability in BHE. The Geowire is developed to be compatible with standard TRT equipment while causing

minimal thermal disturbance to the borehole. Also, it is designed to provide a high spatial temporal and temperature resolution with negligible uncertainty in the measurements. The instrument is implemented to automatically measure a number of temperature profiles along an auxiliary pipe inserted in a borehole at pre-defined time intervals during a TRT. The acquisition settings can be controlled through a user-friendly interface with remote access control, secure access, alarms, database and real-time plots.

This paper covers the following:

- Instrument implementation ranging from the electro-mechanical, hardware and software developments to the operating system and user interface application.
- Laboratory validation of the instrument features, such as accuracy and uncertainty of temperature/spatial measurements, thermal response time as well as minimum waiting time to achieve a thermal equilibrium after moving the probe to a new position. Also, some tests are conducted to validate the robustness of the user application.
- Validation of the instrument in an experimental BHE at a test site in Karlsruhe, Germany. The Geowire is tested under two thermal situations in the borehole and the accuracy of the measurements is validated with Pt100-sensors.

Novel Instrument for Temperature Measurements in Borehole Heat Exchangers

Nordin Aranzabal, *Member*, *IEEE,* Julio Martos, Hagen Steger, Philipp Blum, Jesús Soret

***Abstract*—The thermal response test (TRT) is the standard method for characterizing the thermal properties of the ground and those of a borehole heat exchanger (BHE). During the TRT, the inlet and outlet temperatures of the BHE are monitored. However, this test typically considers the ground as a homogeneous, isotropic, and infinite media, and therefore, it only determines the bulk and effective parameters, such as effective thermal conductivity and thermal borehole resistance. Hence, the enhanced TRT protocols are necessary where the depth-dependent temperatures are measured to estimate depth-specific thermal properties. Thus, a novel instrument with a data logger to automatically obtain the temperature measurements along the BHE is introduced. This device is based on a Zynq-7000 all programmable system on a chip. It has a dual-core central processing unit and a field-programmable gate array on one chip, thus providing a versatile architecture that reduces cost and improves efficiency in comparison with other systems of similar characteristics. This paper describes the implemented hardware and software developments that range from user interface application to a free-distribution operating system based on an embedded Linux. The proposed instrument can be easily incorporated throughout a TRT, and the nonspecialized staff can remotely manage or visualize the results through a menu-driven interface. The device is tested in a specific BHE installation and validated with standard Pt100-temperature-sensors. The results are comparable and, therefore, demonstrate the applicability of this novel instrument called Geowire.**

***Index Terms*—Borehole heat exchanger (BHE), embedded operating system, field-programmable gate array (FPGA), ground source heat pump (GSHP), open source, system on a chip (SoC), temperature profile, thermal response test (TRT).**

I. Introduction

OVER the last decades, the demand for renewable sources of energy has been increasing worldwide due to the growing concerns over global warming. Among the technologies designed to reduce greenhouse emissions, ground source heat pump (GSHP) systems have become progressively more attractive due to high-energy efficiency in many applications, such as heating and cooling residential houses a larger infrastructures [1]–[4]. Most of these systems primarily consist of a closed-circuit installation formed by a shallow borehole heat exchanger (BHE), heat pump equipment at ground surface, and indoor units. Shallow or low-enthalpy geothermal systems can reach a maximum depth of 400 m and temperatures between 20 °C and 70 °C. The BHE is formed by a buried network of pipes into which a fluid is pumped so that the heat is exchanged with the ground [5], [6]. Vertical borehole configurations are a more widespread solution than the horizontal collectors because they are less influenced by the surface atmospheric conditions and require a smaller geographical area. The subsoil acts as a heat source for heating or a heat sink for cooling. In this manner, GSHP systems exchange heat with the earth's top layers that maintain a near constant temperature regardless of the outside seasonal weather conditions and obtain a higher efficiency in comparison with air source heat pump systems that depend on ambient air temperature [7]. Below 10 m and up to 100 m, the subsurface temperatures are influenced by both the external average temperature and the heat transmitted from the earth's core. However, temperatures between such depths remain practically constant, usually with a temperature comparable to the average value of the atmospheric temperature throughout the year. For depths extending below 100 m, the temperature evolves linearly with the increments of approximately 2.5 °C–3 °C per interval of 100 m [8].

For an optimal design of BHE, estimation of thermophysical properties of the subsurface near the installation is necessary [9]. The theoretical basis of the thermal response test (TRT) was originally developed by Choudhary [10] and Mogensen [11]. The TRT has become the standard method to determine thermal borehole resistance and effective thermal conductivity. In a standard TRT, a fluid is pumped through a constant heat source in a closed-loop pipe (U-shaped or coaxial) to measure the temporal evolution of the temperature at inlet and outlet of the BHE. Typically, the TRT is evaluated by applying the Kelvin's line-source theory [12]–[15]. The latter assumes an infinite, isotropic, and homogeneous medium, where heat is transferred merely by conduction [16]. In addition, other line-source models also exist, such as the moving infinite line-source model and the cylindrical source model [17]. Due to the model assumptions, the derived effective thermal conductivity is an average and integral value and does not reflect the heterogeneity of the subsurface. Furthermore, convective effects are not considered and the presence of natural groundwater flows can lead to erroneous estimations for long-term operations [18]–[20]. Accounting for axial effects in a specific energy demand,

This work was supported in part by the European Institute of Innovation and Technology Climate-Knowledge and Innovation Community, a body of the European Union inside the Ph.D. Program of Transforming the Built Environment Platform and in part by the Institute of Applied Geosciences, Karlsruhe Institute of Technology. The Associate Editor coordinating the review process was Subhas Mukhopadhyay. *(Corresponding author: Nordin Aranzabal.)*

N. Aranzabal, J. Martos, and J. Soret are with the Department of Electronic Engineering, Universitat de València, Burjassot 46100, Spain (e-mail: nordin.aranzabal@uv.es; julio.martos@uv.es; jesus.soret@uv.es).
H. Steger and P. Blum are with the Institute of Applied Geosciences (AGW), Karlsruhe Institute of Technology, 76131 Karlsruhe, Germany (e-mail: hagen.steger@kit.edu; philipp.blum@kit.edu).

GSHP application can reduce the required length and number of boreholes [21]. Marcotte *et al.* [22] demonstrated the importance of axial conduction effect using various designs and showed that the length of the BHE could be shortened by up to 15%.

Detailed information of subsurface thermal properties may produce shorter and more efficient BHE to subsequently improve economic viability, especially for large-scale applications [23]. For this reason, enhanced TRT using different methods has been developed by various researchers, as the number of GSHP systems increases worldwide. Fujii [24] and Acuña and Palm [25] integrated the fiber optical thermometers along the depth of BHE to determine the bulk thermal conductivity at specific depths. More enhanced TRT using fiber optics and new data analysis procedures have been achieved during the last years [17], [26]–[29]. Fiber optic equipment measures the temperature based on the Raman spectra-distributed temperature sensing (DTS) technique and sophisticated calibration algorithms [30], [31]. However, aside from the fact that optical equipment is expensive, it is also limited due to the tradeoff among time, distance, and temperature resolution. For instance, improved resolution of measurements can be attained if the temperature is averaged for higher distance intervals or sampling times. The downside is that this method can lead to a larger loss of information in dynamic environments. Rohner *et al.* [32] designed and patented [33] both a method and a device for measuring the temperature in U-shaped geothermal pipes. A data logger probe with temperature and pressure sensors sinks along one of the U-pipes to measure the depth-dependent temperature profiles. A single temperature profile is measured, while the method relies on previous information of terrestrial heat flow near the test field to estimate a thermal conductivity profile. Unfortunately, the applicability of the method is limited to areas with detailed heat flow maps that are not easy to find in many regions. Bayer *et al.* [34] used a commercial version of the previously mentioned sensor, called non-wired immersible measuring object for temperature, based on the same theoretical principles to propose an analytical model for differentiating between the effects of urban heating and global warming. Moreover, Raymond *et al.* [35] conducted another study with a similar data logger sensor (pressure and temperature) called RBRduet and presented an inverse numerical model to extend the TRT assessments to a nearby borehole. This probe is lowered manually using a wire line to measure the ground temperature in equilibrium. The model requires information of the paleoclimatic changes of the nearby land and the results from a TRT in that area to estimate other nearby boreholes subsurface thermal properties. This is done without additional TRT and solely by lowering the probe once. Meanwhile, Martos *et al.* [36] developed a temperature probe and data logger that flows with the thermal fluid along the U-pipe. A spherical wireless sensor dynamically measures the thermal evolution of a specific volume of fluid during heat injection with high temporal, spatial, and temperature resolution. However, this probe is restricted to applications with fluid flow and is not valid for measuring undisturbed ground profiles. The movement of the fluid inside the pipes disturbs the subsurface temperature in equilibrium and the temperature of the fluid traveling with the sensor tends to homogenize with that of the borehole surroundings. Furthermore, Raymond and Lamarche [37] proposed an innovative method, combining probes and heating cables, to estimate the thermal conductivity at specific depths. Temperatures were then measured during the recovery phase following the termination of heat injection. The main advantage of this method is a reduction in the power needed to perform a TRT. However, it does require interchanging sections of heating and non-heating cables, where the punctual thermal conductivity is calculated for each section (e.g., in [38], the thermal conductivity is discretized every 10 m). This factor can prove to pose a limitation for the detection of small conductive zones. In addition, the temperature is measured by sensors with data loggers at the mid-length of each heating cable section. After the test, the cable assembly has to be recovered to analyze the data. This factor can cause delays in the test in the event of a failure in the data logger or in the heating cables, as the obtained results are analyzed after recovering the cable assembly.

Aranzabal *et al.* [39] proposed a procedure for estimating the depth-dependent thermal conductivity, which requires accurate and reliable temperature profiles along an auxiliary pipe during the implementation of a standard TRT. Those data sets were used as input to inverse simulation models for adjusting thermal conductivity of the subsurface surrounding the BHE. For this method, appropriate equipment needs to include certain attributes. The appropriate equipment for this measurement must be viable for integration into the current TRT and have high spatial, temporal, and temperature resolution while causing minimal disturbance to heat transfer. Moreover, it should be easy and convenient to operate and include the capacity to configure and program acquisition parameters, store and download data, as well as provide secure remote access. All these characteristics and functions can be achieved with an instrument controlled through an embedded system that incorporates the adequate set of information and communication technologies.

The objective of this paper is, therefore, to introduce a novel data logger instrument called Geowire. This device fulfills the previous requirements and provides valuable information to determine the depth-specific thermal conductivity of subsurface stratigraphy. Geowire adjusts the position of a small sensor, with negligible perturbation, along geothermal pipes for the automatic acquisition of temperature profiles at preestablished sequences. The data are not averaged in space and time, and therefore, the temperature resolution is not affected as in the case of fiber optical thermometers when applying the DTS technique. Thus, this innovative device can obtain instantaneous temperature samples with a depth resolution of 0.5 mm and is able to detect even small highly conductive zones that could pass unnoticed with other methods. It can be easily incorporated and removed from the BHE installations, and a single calibration would assure accurate measurements during the useful life of the

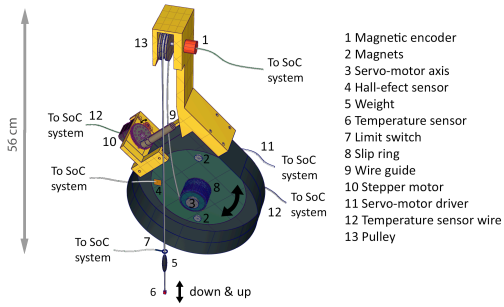

Fig. 1. Key parts of the temperature instrument Geowire (SoC).

instrument. In addition, personnel without any previous knowledge or experience can remotely configure automatic acquisition sequences as well as manage or visualize the data from an intuitive user interface. Hence, the device is presented as a potentially more cost-effective and easier to operate alternative to other existing temperature measurement instruments. Moreover, the Geowire provides information of great value for TRT with such detailed control over the sampling time and depth as well as a high-temperature resolution that has yet to be achieved by other devices yet.

This paper is structured as follows. First, the device is described covering the system architecture and the software implementation. Second, the conducted methodology in a BHE field installation to test the performance of the instrument is presented. Third, the obtained experimental results are exposed and discussed. Finally, as a conclusion, the significance and achievements of this paper are reported.

II. Instrument Implementation

The aim of the instrument is to determine the spatial and temporal thermal evolution along the depth of an auxiliary pipe during the TRT. This pipe, so-called observer pipe, remains in parallel to the U-pipe inside the BHE in order to obtain the data required to carry out the method elaborated in [39]. To do this, the Geowire is designed to automatically displace a small temperature sensor (negligible perturbation) down and up along the depth of geothermal pipes at preestablished acquisition sequences. In a U40 geothermal pipe, the lowering speed is configurable between 5 and 0.5 m/min. The cable of the sensor is rolled up using a reel, a servomotor rotates the reel, and an encoder measures the released cable length to calculate the position of the sensor inside the pipes. Fig. 1 depicts the different parts that compose the electromechanical body of the device, which can be easily adapted in BHE installations.

The device is managed from an embedded system to adjust the exact location of the sensor before measuring and storing the instantaneous temperature samples. The embedded system is the size of a credit card and runs a real-time operating system with secure remote access, database functionality, and user interface application, which allows the customization of the acquisition process (no additional computer is required). The instrument is implemented with a spatial minimum

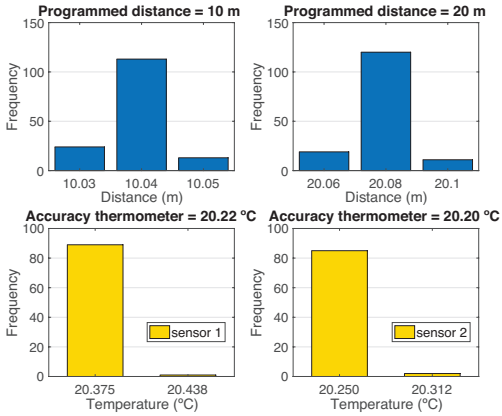

Fig. 2. Uncertainty analysis of the spatial and temperature measurements, represented in the top and bottom histograms, respectively.

resolution of 0.5 mm, a temperature maximum resolution of 0.06 °C, and an acquisition time of 750 ms.

Laboratory tests involving displacements of the sensor to measure stability and repeatability of the measurements demonstrated a maximum deviation of ±5 mm in 10 m. The obtained results when displacing the sensor 10 and 20 m are illustrated in the two histograms at the top of Fig. 2, from left to right, respectively. In addition, the stability and repeatability of the temperature measurements in an environment with a stable temperature are studied. A series of measurements are obtained inside a thermally isolated box with two noncalibrated sensors of the Geowire, the DS18B20 of Maxim Integrated, whereas the stability of the temperature inside the box is monitored with a high-accuracy thermometer of ±0.03 °C accuracy and ±0.01 °C resolution. Measurements of the sensors appealed to be significantly stable, one deviation out of 90 measurements for the sensor-1 and two out of 90 for the sensor-2, with an uncertainty of ±0.062 °C, as shown in the two histograms at the bottom of Fig. 2.

The thermal time constant (τ) of the sensor in still water is typically below 2 s. Hence, the time elapsed ($t1$), since the application of a step impulse, is calculated for the temperature difference between two consecutives measurements to be smaller than the temperature resolution of the sensor (0.06 °C). For a sampling time of 1 s, $t1$ is derived from the following equations:

$$T(t_1) = T_i - T_f\left(1 - e^{-t_1/\tau}\right) \quad (1)$$

$$T(t_2) = T_i - T_f\left(1 - e^{-t_2/\tau}\right) \quad (2)$$

$$t_2 = t_1 + 1 \quad (3)$$

$$T(t_2) - T(t_1) \le 0.06\,^{\circ}\mathrm{C} \quad (4)$$

where T_i is the initial temperature; T_f is the final step temperature; τ is the time required for the temperature to reach the 63.2% of the temperature step; and t_2 is t_1 plus 1 s.

By substituting (1)–(3) into (4), t1 is determined as follows:

$$t_1 = -\tau \ln\left(0.06 / \left(T_2\left(1 + e^{1/\tau}\right)\right)\right) \quad (5)$$

TABLE I
THERMAL RESPONSE TIME IN STILL WATER

t_l(s)	T_f(ºC) = 0.2	T_f(ºC) = 0.3	T_f(ºC) = 0.5
τ (s) = 2	**3.27**	**4.09**	**5.11**

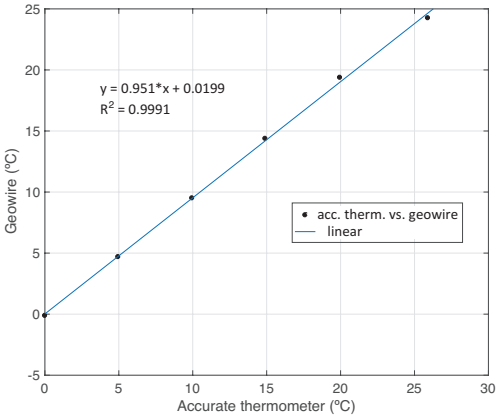

Fig. 3. Linear adjustment between the Geowire and a high-accuracy thermometer.

From (5), by assuming τ = 2, the calculated t_l for temperature increments of 0.2 °C, 0.3 °C, and 0.5 °C is presented in Table I. The maximum temperature difference between the inlet and outlet of a TRT is typically below 1 °C. Thus, the thermal steps between consecutive measuring locations inside the pipe are considered to be significantly smaller. In addition, depending on the sensor speed settings, the sensor requires 12–20 s to reach a new location, which is neglected in (5).

Fig. 3 depicts the representation of the temperature measurements of the Geowire versus a calibrated thermometer of ±0.01 °C accuracy by measuring at five points (0 °C, 5 °C, 10 °C, 15 °C, 20 °C, and 25 °C) in a thermal bath of ±0.01 °C stability. The latter results demonstrated a strong linearity of the sensor with an R^2 of 0.9991. In addition, the Geowire averages five samples of the temperature improving in 1 bit the quality of the measurements to achieve a resolution of 0.03 °C [40]. Hence, uncertainty of the temperature measurements is determined to be bounded between ±0.04 °C.

As far as the accuracy concerns, it should be noted that the absolute error in the measurements is not extremely important when calculating the thermal conductivity through the inverse simulation procedure. Since the Geowire only uses one sensor to measure the temperature inside the observer pipe, what it is important for the numerical model are the gradients relative to the spatial distribution as well as the temporal evolution of the temperature, more than the accuracy in the temperature.

A. System Architecture

The device processing system (PS) is based on the Xilinx Zynq-7000 all programmable system on a chip (AP SoC)

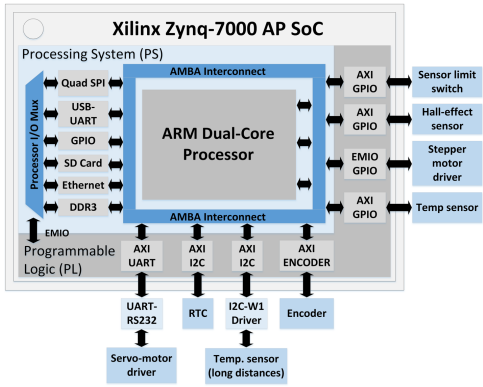

Fig. 4. Implemented architecture in Zynq-7000 AP SoC chip.

architecture that integrates an ARM 9 dual-core CPU and Xilinx 7 series field-programmable gate array (FPGA) on one chip. Zynq has two sections called PS and programmable logic (PL). The PS is a section for the dual-core CPU, and the PL is a section for the FPGA, a versatility architecture which reduces the cost and enhances the efficiency in comparison with other systems of analogous features [41]–[47].

The operating system is designed to run in the ARM processors, whereas the processes of the encoder and servomotor are implemented to run in parallel in the FPGA. FPGA concurrent processing capability assures reliable readings from the encoder and an accurate spatial positioning of the sensor inside the pipes.

In this case, an open-source Linux has been developed to manage the performance of the secondary elements that compose the device through a user interface application. Additional hardware is connected to the system using the peripheral module connectors to communicate with the following peripherals: motor driver, encoder, real-time clock, temperature sensors, temperature sensor driver, sensor limit switch, and stepper motor driver. Fig. 4 depicts the implemented architecture in the AP SoC chip and the link with the peripherals.

Two digital temperature sensors (DS18B20 of Maxim Integrated) are connected to the system, one to measure the ambient air temperature outside the borehole and the other the temperature inside pipes. The long length of the wire, at least the length of the borehole, needed to communicate with the sensor inside the pipes does not affect the accuracy of the measurements since the instantaneous temperature readings are converted to digital values in the sensor chip and transmitted to the SoC using one-wire communication protocol. Moreover, the latter communication protocol can reliably operate for cable lengths of up to 500 m.

B. Software design

The source code of a free-distribution embedded Linux operating system is configured and compiled to run over the

ARM processors. Linux is a robust operating system, which stands out among other platforms because it is assembled under the model of free and open-software development and distribution with a wide range of features [48]–[50].

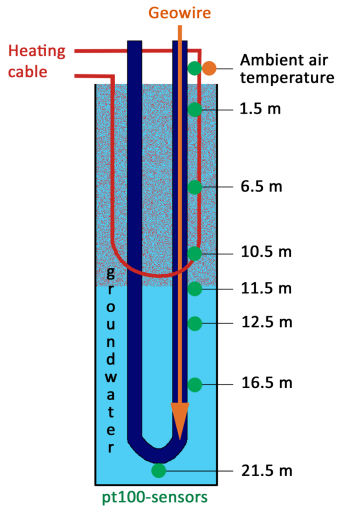

Fig. 6. Layout of the borehole in the experiment.

Moreover, in this development, the system hardware details are not hard coded in the kernel and the system is portable to other platforms.

The state-of-the-art feature of the software design relies on compiling the latest and most complete versions of Linux, Apache, MySQL, and PHP (LAMP) software bundle [51], [52] to run in this specific SoC architecture. The result of integrating a LAMP stack (see Fig. 5) produces a reliable and powerful database and webserver application (user interface) with comparable performance as a personal computer, but it is a more cost-effective solution (open-source software and more affordable hardware). Webserver robustness is verified by concurrent access of 20 users to different sections of the interface without affecting the system performance. Neither the speed nor the efficiency is affected in comparison with the access of a single user.

The menu-driven user interface is accessible locally or remotely from any device with Internet connection. The interface asks for the parameters of the acquisition sequence, such as spatial resolution for the different defined depths intervals, time interval between consecutive temperature profiles, and total time of measurement. Settings of established acquisitions profiles are saved in the memory and can be reloaded for future analysis. During the acquisition process, the real-time charts can be visualized, and once the measurement is completed, the recorded profiles can be loaded or downloaded.

The system analyzes and registers abnormal situations that are immediately sent to the administrator. As a security measure, the user has to log in before accessing the interface.

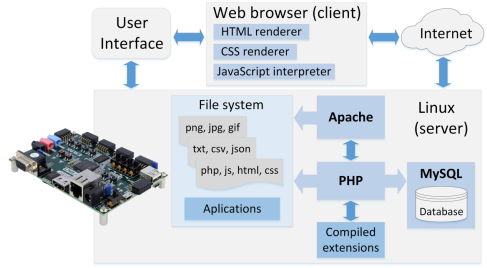

Fig. 5. Implemented LAMP stack client-server communication diagram.

III. Test Methodology

One borehole is used for the validation of the Geowire at a test site in Karlsruhe (Germany). The borehole has a diameter of 450 mm and a length of 30 m, where a single U-pipe of 25 mm × 3.5 mm is lowered until a depth of 21.5 m. During the insertion of the pipe, a pt100-sensors wireline is taped in direct contact with the outside surface of the pipes. Throughout this process, a heating cable is also installed to heat the upper half part of the borehole and create a gradient in the temperatures. The layout of the borehole is illustrated in Fig. 6.

The Pt100-sensors and the Geowire are calibrated in the laboratory with a thermal bath of ±0.01 °C stability and a calibrated thermometer of ±0.01 °C accuracy. After measuring the temperature at five points (0 °C, 5 °C, 10 °C, 15 °C, 20 °C, and 25 °C), a linear correction is applied to fit the Pt100-sensors and the Geowire measurements with the high-accuracy thermometer. The heating cable is connected to a power supply of 40 V, 125 A and adjusted to inject 35 W/m along the upper half of the borehole. The experiment consists of measuring the temperature with both devices during two thermal situations in the borehole: undisturbed temperature and temperature after heating the upper half part of the borehole for 3 h.

Before beginning with the test, the analytically estimated time to achieve a thermal equilibrium by the sensor, and to avoid possible perturbations due to turbulence produced by the displacement of the sensor, is calculated.

Before beginning the test, the analytically estimated thermal response time of the sensor (t_l) in Section II for a thermal step of 0.5 °C is validated experimentally. Likewise, it is verified that the possible thermal perturbations due to turbulences caused by the displacement of the sensor do not affect the sensor measurements. The instrument is configured to measure 10 samples of temperature with a sampling time of 1 s, every 0.5 m, and by displacing the sensor down and up continuously at a velocity of 2 m/min for 2 h. After analyzing the obtained data, a maximum interval of 5 s is determined as the time needed by the sensor to achieve a thermal equilibrium when moving to a new location. Hence, the Geowire is configured in the test to displace the temperature sensor with a

depth resolution of 0.5 m, a velocity of 2 m/min, and a waiting

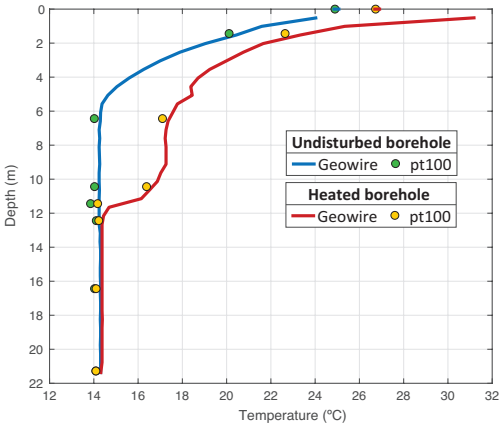

Fig. 7. Measured temperature profiles with both instruments (Geowire, pt100-sensors) for the two situations in the borehole (undisturbed and heated).

time of 5 s before measuring the temperature. After this time, five samples of the temperature are recorded with a sampling interval of 1 s, and the average value is stored in the database. Thus, the Geowire measures an entire profile along the depth of the borehole in less than 15 min. In addition, the data logger equipment of Pt100-sensors is established to obtain the temperature of each sensor every minute.

IV. Experimental Results and Discussion

Throughout the eight automatic data collection sessions carried out in the test installation, the operating system and the remote-control system run smoothly and faultfree, detecting no data corruption in the database.

Fig. 7 illustrates the temperatures obtained from both instruments for the two thermal conditions in the borehole (undisturbed and heated). Inside the borehole, temperatures from Pt100-sensors are 0.2 °C lower than those obtained by the Geowire, except for the sensor at 11.5 m, where the measurements are 0.37 °C lower. The Pt100-sensor at 11.5 m should agree with the other Pt100-sensors measuring the stable temperature of the undisturbed borehole. This small deviation may be attributed to an error in calibration. Apart from that outlier, the results from both instruments are comparable with a mean square error of 0.042 (see Fig. 8). Small differences might also occur due to the fact that the Geowire measures inside the pipe, while the Pt100-sensors take measurements from the outer part of the pipe wall. Meanwhile, regarding the ambient air temperature, the obtained values from the second sensor of the Geowire are approximately 0.1 °C higher than those from the Pt100-sensors.

The Geowire uses only one temperature sensor, thereby excluding the uncertainty produced by the calibration of multiple sensors along the borehole, as in the case of the Pt100-sensors. The data sets from the Geowire are obtained with a notably higher spatial and temperature resolution, as well as a level of control over the measuring points, not achieved by any other technique.

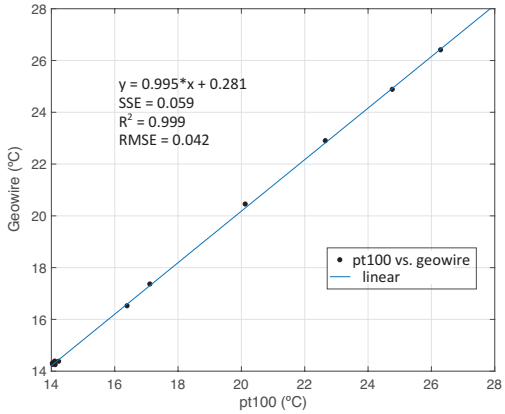

Fig. 8. Linear adjustment between the pt100-sensors and the Geowire.

The quality of the obtained temperature profiles provides the basis to determine depth-specific thermal conductivities on the TRT analysis proposed by Aranzabal *et al.* [39]. Implementations require both the underground temperature profile in equilibrium and a series of temperature profiles during the TRT. A 3-D numerical model is built to reproduce the geometry and thermal behavior of the TRT. Then, an inverse numerical algorithm estimates the depth-specific thermal conductivities by fitting the numerical results with the experimental measurements. Hence, the temperature measurements have to be abundant and accurate to reduce the errors in the computational simulations. Furthermore, the followings are required: 1) an instrument for temperature measurements integrated in a standard TRT; 2) a user-friendly and intuitive graphical interface; 3) the data storing capabilities; and 4) the possibility to remotely configure all the system features.

One key characteristic of the Geowire is that in the AP SoC, hardware resources for high-speed processing are still available. These can be used in the analysis of the data and in obtaining the real-time thermal properties of the subsoil. This is particularly the case if the procedure of Aranzabal *et al.* [39] is implemented over a model with smaller computational cost, such as the Borehole-to-Ground-based on thermal network approach and vertical discretization of the borehole [53]–[55].

Throughout the eight automatic data collection sessions carried out in the test installation, the operating system and the remote-control system run smoothly and fault free detecting no data corruption in the database.

Fig. 7 illustrates the temperatures obtained from both instruments for the two thermal conditions in the borehole (undisturbed and heated). Inside the borehole, temperatures from pt100-sensors are 0.2 ºC lower than those obtained by the Geowire, except for the sensor at 11.5 m, where

measurements are 0.37 ºC lower. The pt100-sensor at 11.5 m should agree with the other pt100-sensors measuring the stable temperature of the undisturbed borehole. This small deviation may be attributed to an error in calibration. Apart from that outlier, the results from both instruments are comparable with a mean square error (MSE) of 0.042 (Fig. 8). Small differences might also occur due to the fact that the Geowire measures inside the pipe, while the pt100-sensors take measurements from the outer part of the pipe wall. Meanwhile regarding the ambient air temperature, the obtained values from the second sensor of the Geowire are approximately 0.1 ºC higher than from the pt100-sensors.

The Geowire uses only one temperature sensor thereby excluding the uncertainty produced by the calibration of multiple sensors along the borehole, as in the case of the pt100-sensors. The datasets from the Geowire are obtained with a notably higher spatial and temperature resolution, as well as a level of control over the measuring points, not achieved by any other technique.

The quality of the obtained temperature profiles provide the basis to determine depth-specific thermal conductivities on the TRT analysis proposed by Aranzabal et al. [39]. Implementations requires both the underground temperature profile in equilibrium and a series of temperature profiles during the TRT. A 3D numerical model is built to reproduce the geometry and thermal behavior of the TRT. Then, an inverse numerical algorithm estimates the depth-specific thermal conductivities by fitting the numerical results with the experimental measurements. Hence, temperature measurements have to be abundant and accurate to reduce errors in the computational simulations. Furthermore, the following is required: (1) an instrument for temperature measurements integrated in a standard TRT; (2) a user-friendly and intuitive graphical interface; (3) data storing capabilities; and (4) the possibility to remotely configure all the system features.

One key characteristic of the Geowire is that in the AP SoC, hardware resources for high-speed processing are still available. These can be used in the analysis of the data, and in obtaining the real-time thermal properties of the subsoil. This is particularly the case if the procedure of Aranzabal et al. [39] is implemented over a model with smaller computational cost such as the Borehole-to-Ground (B2G) based on thermal network approach, and vertical discretization of the borehole [53]–[55].

V. Conclusion

New tools and methods for evaluating the subsurface thermal properties are necessary to improve the energy efficiency and economic viability of GSHP systems, particularly for large BHE installations [23]. Developing more affordable, accurate, and simpler methods in the sizing of BHE is the key for an efficient use of GSHP systems. The data logger instrument developed in this paper displaces a temperature sensor down and up along the depth of an auxiliary pipe during a TRT while storing the temperature together with its temporal and spatial locations.

The Geowire fulfills its design purpose, and the obtained profiles are suitable to implement the TRT analysis method based on the observer pipe for determining depth-specific thermal conductivities [39]. This method contributes the detection of more favorable geological layers for a heat exchange and, thus, aids in determining of the optimal size of the ground heat exchanger collector in order to maximize the W/m relation of the thermal transfer. The length of the perforation could be delimited when a weakly conductive layer is reached. With this knowledge, the amount of resources required to build a GSHP system can be reduced, such as those accounting to piping and drilling, rather than building a less efficient and deeper BHE.

The accuracy of the measurements obtained from the Geowire is demonstrated by the performed field test. Going beyond its basic functionality of obtaining temperature and depth with significant resolution, the Geowire exemplifies the further advantages, such as its compact size, user-friendly interface, remote access to full monitoring and control settings, alarming function for detecting anomalies during its operation, and extensive capacity to store data. In addition, the operating system and the database are developed based on the free distribution software to increase the diffusion and use of the instrument. Hence, license limitations are avoided, and the cost of a commercial version is also reduced.

Finally, this version of the Geowire is designed to introduce the sensor into an auxiliary pipe without fluid flow; however, it can be easily modified to displace the sensor in closed circuits with fluid flow. This facet enables the system to be enhanced to suit a wider range of applications.

References

[1] P. Bayer, D. Saner, S. Bolay, L. Rybach, and P. Blum, “Greenhouse gas emission savings of ground source heat pump systems in Europe: A review,” *Renew. Sustain. Energy Rev.*, vol. 16, no. 2, pp. 1256–1267, Feb. 2012.

[2] A. M. Omer, “Ground-source heat pumps systems and applications,” *Renew. Sustain. Energy Rev.*, vol. 12, no. 2, pp. 344–371, 2008.

[3] H. Yang, P. Cui, and Z. Fang, “Vertical-borehole ground-coupled heat pumps: A review of models and systems,” *Appl. Energy*, vol. 87, no. 1, pp. 16–27, 2010.

[4] J. Lund, B. Sanner, L. Rybach, R. Curtis, and G. Hellström, “Geothermal (ground-source) heat pumps, a world overview,” *Geo-Heat Cent. Q. Bull.*, vol. 25, no. 3, pp. 1–10, 2004. [Online]. Available: https://www.researchgate.net/publication/238065306_Geothermal_ground_source_heat_pumpsA_world_overview

[5] J. D. Spitler and S. E. A. Gehlin, “Thermal response testing for ground source heat pump systems—An historical review,” *Renew. Sustain. Energy Rev.*, vol. 50, pp. 1125–1137, Oct. 2015.

[6] S. Gehlin, “Thermal response test: Method development and evaluation,” Luleå Univ. Technol., Luleå, Sweden, Tech. Rep., 2002.

[7] G. Florides and S. Kalogirou, “Ground heat exchangers—A review of systems, models and applications,” *Renew. Energy*, vol. 32, no. 15, pp. 2461–2478, 2007.

[8] I. B. Fridleifsson, R. Bertani, E. Huenges, J. W. Lund, A. Ragnarsson, and L. Rybach, “The possible role and contribution of geothermal energy to the mitigation of climate change,” in *IPCC Scoping Meeting on Renewable Energy Sources, Proceedings*, O. Hohmeyer and T. Trittin, Eds. Luebeck, Germany, Jan. 2008, pp. 59–80. [Online]. Available: http://grsj.gr.jp/iga/igafiles/Fridleifsson_et_al_IPCC_Geothermal_paper_2008.pdf

[9] P. Cui, H. Yang, and Z. Fang, "Heat transfer analysis of ground heat exchangers with inclined boreholes," *Appl. Therm. Eng.*, vol. 26, nos. 11–12, pp. 1169–1175, 2006.

[10] A.-R. Choudhary, "An approach to determine the thermal conductivity and diffusivity of a rock *in situ*," Ph.D. dissertation, Fac. Graduate College Oklahoma State Univ., Stillwater, OK, USA, 1976. [Online]. Available: https://www.google.com/url?sa=t&rct=j&q=&esrc=s&source=web&cd=1&ved=2ahUKEwiR27_RxeXcAhXy4IUKHfzCBkcQFjAAegQIARAB&url=https%3A%2F%2Fshareok.org%2Fbitstream%2Fhandle%2F11244%2F32925%2FThesis-1976DC552a.pdf

[11] P. Mogensen, "Fluid to duct wall heat transfer in duct system heat storages," in *Proc. Int. Conf. Subsurface Heat Storage Theory Pract.*, no. 16, 1983, pp. 652–657.

[12] S. E. A. Gehlin and G. Hellström, "Influence on thermal response test by groundwater flow in vertical fractures in hard rock," *Renew. Energy*, vol. 28, no. 14, pp. 2221–2238, 2003.

[13] B. Sanner, G. Hellström, J. Spitler, and S. E. A. Gehlin, "Thermal response test—Current status and world-wide application," in *Proc. World Geotherm. Congr.*, 2005, pp. 24–29.

[14] S. Signorelli, S. Bassetti, D. Pahud, and T. Kohl, "Numerical evaluation of thermal response tests," *Geothermics*, vol. 36, no. 2, pp. 141–166, Apr. 2007.

[15] H. J. L. Witte, "TRT: How to get the right number," *Geo-Drilling Int.*, vol. 151, pp. 30–34, Apr. 2009.
[Online]. Available: http://www.groenholland.nl/download/Geodrilling_2009.pdf

[16] H. S. Carslaw and J. C. Jaeger, *Conduction of Heat in Solids*, vol. 108, 2nd ed. Oxford, U.K.: Oxford Univ., 1986.

[17] F. Stauffer, P. Bayer, P. Blum, N. Molina-Giraldo, and W. Kinzelbach, *Thermal Use of Shallow Groundwater*. Boca Raton, FL, USA: CRC Press, 2013.

[18] W. Zhang, H. Yang, L. Lu, and Z. Fang, "Investigation on heat transfer around buried coils of pile foundation heat exchangers for ground-coupled heat pump applications," *Int. J. Heat Mass Transf.*, vol. 55, nos. 21–22, pp. 6023–6031, 2012.

[19] J. Raymond, R. Therrien, L. Gosselin, and R. Lefebvre, "Numerical analysis of thermal response tests with a groundwater flow and heat transfer model," *Renew. Energy*, vol. 36, no. 1, pp. 315–324, 2011.

[20] H. Wang, C. Qi, H. Du, and J. Gu, "Thermal performance of borehole heat exchanger under groundwater flow: A case study from Baoding," *Energy Buildings*, vol. 41, no. 12, pp. 1368–1373, 2009.

[21] A. Chiasson and A. O'Connell, "New analytical solution for sizing vertical borehole ground heat exchangers in environments with significant groundwater flow: Parameter estimation from thermal response test data," *HVAC&R Res.*, vol. 17, no. 6, pp. 1000–1011, 2011.

[22] D. Marcotte, P. Pasquier, F. Sheriff, and M. Bernier, "The importance of axial effects for borehole design of geothermal heat-pump systems," *Renew. Energy*, vol. 35, no. 4, pp. 763–770, 2010.

[23] M. Reuß and M. Proell, "Quality control of borehole heat exchanger systems," in *Proc. Effstock Conf.*, 2009, pp. 1–8.

[24] H. Fujii, H. Okubo, K. Nishi, R. Itoi, K. Ohyama, and K. Shibata, "An improved thermal response test for U-tube ground heat exchanger based on optical fiber thermometers," *Geothermics*, vol. 38, no. 4, pp. 399–406, 2009.

[25] J. Acuña and B. Palm, "Distributed thermal response tests on pipe-in-pipe borehole heat exchangers," *Appl. Energy*, vol. 109, pp. 312–320, Sep. 2013.

[26] P. Hakala, A. Martinkauppi, I. Martinkauppi, N. Leppäharju, and K. Korhonen, "Evaluation of the distributed thermal response test (DTRT): Nupurinkartano as a case study," Geol. Survey Finland, Tech. Rep. 211, 2014. [Online]. Available: http://tupa.gtk.fi/julkaisu/tutkimusraportti/tr_211.pdf

[27] V.Soldo,L.Boban,andS.Borovic´,"Verticaldistributionofshallow ground thermal properties in different geological settings in Croatia," *Renew. Energy*, vol. 99, pp. 1202–1212, Dec. 2016.

[28] J. Luo *et al.*, "Experimental investigation of a borehole field by enhanced geothermal response test and numerical analysis of performance of the borehole heat exchangers," *Energy*, vol. 84, pp. 473–484, May 2015.

[29] G. Radioti, S. Delvoie, R. Charlier, G. Dumont, and F. Nguyen, "Heterogeneous bedrock investigation for a closed-loop geothermal system: A case study," *Geothermics*, vol. 62, pp. 79–92, Jul. 2016.

[30] M. B. Hausner, F. Suárez, K. Glander, N. van de Giesen, J. S. Selker, and S. W. Tyler, "Calibrating single-ended fiber-optic Raman spectra distributed temperature sensing data," *Sensors*, vol. 11, no. 11, pp. 10859–10879, 2011.

[31] N. van de Giesen *et al.*, "Double-ended calibration of fiber-optic Raman spectra distributed temperature sensing data," *Sensors*, vol. 12, no. 5, pp. 5471–5485, 2012.

[32] E. Rohner, L. Rybach, and U. Schärli, "A new, small, wireless instrument to determine ground thermal conductivity *in-situ* for borehole heat exchanger design," in *Proc. World Geotherm. Congr.*, 2005, pp. 1–4.

[33] U. Schärli, E. Rohner, and L. Rybach, "Method and device for measuring the temperature or another quantity in a U-shaped geothermal probe and flushing device therefor," U.S. Patent EP 160 0749 B1, Dec. 13, 2006.

[34] P. Bayer, J. A. Rivera, D. Schweizer, U. Schaärli, P. Blum, and L. Rybach, "Extracting past atmospheric warming and urban heating effects from borehole temperature profiles," *Geothermics*, vol. 64, pp. 289–299, Nov. 2016.

[35] J. Raymond, L. Lamarche, and M. Malo, "Extending thermal response test assessments with inverse numerical modeling of temperature profiles measured in ground heat exchangers," *Renew. Energy*, vol. 99, pp. 614–621, Dec. 2016.

[36] J. Martos, Á. Montero, J. Torres, J. Soret, G. Martínez, and R. García-Olcina, "Novel wireless sensor system for dynamic characterization of borehole heat exchangers," *Sensors*, vol. 11, no. 7, pp. 7082–7094, 2011.

[37] J. Raymond and L. Lamarche, "Development and numerical validation of a novel thermal response test with a low power source," *Geothermics*, vol. 51, pp. 434–444, Jul. 2014.

[38] J. Raymond, L. Lamarche, and M. Malo, "Field demonstration of a first thermal response test with a low power source," *Appl. Energy*, vol. 147, pp. 30–39, Jun. 2015.

[39] N. Aranzabal *et al.*, "Extraction of thermal characteristics of surrounding geological layers of a geothermal heat exchanger by 3D numerical simulations," *Appl. Therm. Eng.*, vol. 99, pp. 92–102, Apr. 2016.

[40] *Improving ADC Resolution by Oversampling and Averaging*. Accessed: Feb. 2018. [Online]. Available: https://www.silabs.com/documents/public/application-notes/an118.pdf

[41] K. S. Don and L. S. Eun, "An ARM cortex-M0 based FPGA platform in teaching computer architecture," *Int. J. Comput. Inf. Technol.*, vol. 4, no. 6, pp. 939–941, 2015.

[42] P. A. Schaumont, *A Practical Introduction to Hardware/Software Codesign*. Dhaka, Bangladesh: Univ. Asia–Pacific, 2013.

[43] Y. Zhang, K. K. Ma, and Q. Yao, "A software/hardware co-design methodology for embedded microprocessor core design," *IEEE Trans. Consum. Electron.*, vol. 45, no. 4, pp. 1241–1246, Nov. 1999.

[44] X.-Y. Xiang, I. Jangjaimon, M. Madani, and N.-F. Tzeng, "A reliable and cost-effective sand monitoring system on the field programmable gate array (FPGA)," *IEEE Trans. Instrum. Meas.*, vol. 62, no. 7, pp. 1870–1881, Jul. 2013.

[45] G. Betta, L. Ferrigno, and M. Laracca, "Cost-effective FPGA instrument for harmonic and interharmonic monitoring," *IEEE Trans. Instrum. Meas.*, vol. 62, no. 8, pp. 2161–2170, Aug. 2013.

[46] L. H. Crockett, R. A. Elliot, M. A. Enderwitz, and R. W. Stewart, *The Zynq Book: Embedded Processing With the Arm Cortex-A9 on the Xilinx Zynq-7000 All Programmable SoC*. New York, NY, USA: Academic, 2014.

[47] [N. Aranzabal *et al.*, "Design of digital advanced systems based on programmable system on chip," in *Field-Programmable Gate Array Technology*, G. Dekoulis, Ed. Vukovar, Croatia: InTech, 2017, pp. 124–157.

[48] P. Gandham and N. V. K. Ramesh, "Porting the Linux kernel to an ARM based development board," *Int. J. Eng. Res. Appl.*, vol. 2, no. 2, pp. 1614–1618, 2012.

[49] P. N. Sibi, V. Anjali, and S. Vishnu, "Wireless smart sensor nodes using embedded Linux kernel on ARM platform," *Int. J. Eng. Res. Technol.*, vol. 3, no. 7, pp. 832–834, Jul. 2014.

[50] A. A. P. Pohl, G. A. Michelon, S. M. Vidal, H. S. Filho, and K. V. O. Fonseca, "Remote RF and baseband video measurement laboratory based upon open-code software," *IEEE Trans. Instrum. Meas.*, vol. 57, no. 3, pp. 556–564, Mar. 2008.

[51] R. Mohanty, "LAMP: The prominent open source Web platform for query execution and resource optimization," *Int. J. Comput. Corporate Res.*, vol. 3, no. 3, pp. 1–17, 2013.

[52] J. Gerner, E. Naramore, M. Owens, and M. Warden, *Professional LAMP: Linux, Apache, MySQL and PHP5 Web Development*. Hoboken, NJ, USA: Wiley, 2006.

[53] F. Ruiz-Calvo, M. De Rosa, P. M. M. Cárcel, C. Montagud, and J. M. Corberan, "Coupling short-term (B2G model) and long-term (g-function) models for ground source heat exchanger simulation in TRNSYS. Application in a real installation," *Appl. Therm. Eng.*, vol. 102, pp. 720–732, Apr. 2016.

[54] F. Ruiz-Calvo, M. De Rosa, J. Acuña, J. M. Corberán, and C. Montagud, "Experimental validation of a short-term borehole-to-ground (B2G) dynamic model," *Appl. Energy*, vol. 140, pp. 210–223, Feb. 2015.

[55] M. De Rosa, F. Ruiz-Calvo, J. M. Corberán, C. Montagud, and L. A. Tagliafico, "A novel TRNSYS type for short-term borehole heat exchanger simulation: B2G model," *Energy Convers. Manage.*, vol. 100, pp. 347–357, Aug. 2015.

Nordin Aranzabal (M'12) received the B.S. in Electronic Telecommunications Engineering and M.S. in Electronics Engineering from the Universidad de Valencia, Spain.
He has been with the Electronic Engineering Department, Universidad de Valencia, since 2012. His research interests include wireless networks, real-time systems, embedded systems (FPGAs, PSoCs) and low power design. He is currently a Ph.D. student in the same department and has obtained an aid from the European Union Commission in charge of the European project "CLIMATE KIC 2013: Advance strategies, methods and algorithms for optimal economical-technical sizing of a geothermal heat exchanger". He also belongs to IEEE-UV Student Branch, being one of its founding members.

Julio Martos received the B.Sc. and Ph.D. degrees in Electronic Engineering from the University of Valencia, Spain, in 1997 and 2003, respectively. In 1997, he joined the Department of Electronic Engineering, where he developed his doctoral thesis, dealing with technologies for health and sport. His current research interests include energy efficiency in buildings, acquisition systems, wireless sensor networks with MEMS devices, energy harvesting and ultra-low power design.
Dr. Martos has participated, as a coordinator or researcher in some regional and national (Spanish) projects in collaboration with industrial partners from the energy, nuclear and health/sport sectors.
He is coauthor of more than 15 JCR refereed research papers and more than 30 international conference proceedings, among other technical papers.

Hagen Steger received the diploma degrees in Geology from the University of Karlsruhe, in 1998. From 1999 to 2005, he joined the Institute of Applied Geology (AGK) at the University of Karlsruhe, where he developed his doctoral thesis, dealing with electrokinetic remediation of volatile chlorinated hydrocarbon contaminated, low permeable soils.
Since 2006, he is a researcher at the Institute of Applied Geology (AGW) at the Karlsruhe Institute of Technology (KIT), Germany. His current research interests include the quality control and the backfill process of borehole heat exchangers, the development of monitoring systems of borehole heat exchanger, investigations about the thermal conductivity of rocks and grouting material and new technologies in the field of shallow geothermal systems.
Dr. Steger participated at the IEA-ECES-Annex 21, Thermal Response Test and 27, Quality Management in Design, Construction and Operation of Borehole Systems.

Philipp Blum is a Professor of Engineering Geology at the Karlsruhe Institute of Technology (KIT), Germany. In 1996 he graduated in Geology at the University of Heidelberg and in 1997 he joined the Cardiff University in Wales as part of the European Erasmus programme. In 2000 he received his M.Sc. degree in Applied Geology at the former University of Karlsruhe (now KIT). In 2003 he obtained his PhD in Earth Sciences at the University of Birmingham (UK).
From 2003 to 2005 he was working for an engineering and environmental consultancy. From 2006 to 2010 he was an assistant professor at the University of Tübingen (Germany), where in 2010 he received his habilitation (*venia legendi*) in Applied Geology.
Since 2010 he heads the engineering geology research group at the KIT. He published more than 100 scientific papers on hydrogeology, geothermal energy and engineering geology in porous and fractured rocks, and a book on the thermal use of shallow aquifers.

Jesús Soret received the B.Sc. and Ph.D. degrees in Electronic Engineering from the University of Valencia, Spain, in 1996 and 2000, respectively. Currently he is an associate professor and holds the position of head of the research group ''Communications and Digital System Design'' (DSDC). His current research interests include embedded computing to enable applications such as big data acquisition systems, energy monitoring and management, and wireless sensor networks. Soret has coordinated research and development in more than 15 projects, with the support of European Commission, and Spanish agencies, most of them in environmental and industrial applications. He is co-author of more than 15 JCR refereed research papers and more than 25 international conference proceedings, among other technical papers.

Chapter 5

Development of a wireless flowing probe for temperature measurements inside geothermal pipes

> *This chapter covers the development and laboratory evaluation of an autonomous probe for temperature measurements inside geothermal pipes.*

5.1. Conference paper: Design and test of an autonomous wireless probe to measure temperature inside pipes

Authors: Nordin Aranzabal, Julio Martos, Alvaro Montero, Jesús Soret, Raimundo Garcia-Olcina and José Torres.

Published in: ECOS2015, 28th International Conference on Efficiency, Cost, Optimization, Simulation and Environmental Impact of Energy Systems. Pau, France.
ISBN 978-2-9555539-0-9

Summary:

This peer reviewed conference paper introduces a miniaturized autonomous probe, called Geoball, for measuring the temperature inside the pipes. The probe is embedded in a sphere of 20 mm that has the same density as the fluid, and hence it is carried at fluid speed. The Geoball can be easily integrated in a TRT to complement its measurements, and it can be circulated in vertical and horizontal pipe collectors.

This paper covers the following:

- Instrument implementation ranging from the mechanical, hardware, firmware and user graphical interface application.
- Measurements to determine the range, precision, sampling time and temperature resolution.
- Laboratory validation of the probe operation and features, such as power

consumption and stability, reliability of wireless energy harvesting and communication, and data logging and representation.

1 PROCEEDINGS OF ECOS 2015 - ISBN: 978-2-9555539-0-9

Design and test of an autonomous wireless probe to measure temperature inside pipes

Nordin Aranzabal[1, *], Julio Martos[1], Alvaro Montero[2], Jesús Soret[1], Raimundo García-Olcina[1] and José Torres[1]

[1] Universidad de Valencia (UV), Department of Electronic Engineering, Burjassot, 46100, Spain
[2] Universidad Politécnica de Valencia (UPV), Institute of Energy Engineering, Valencia, 46022, Spain

[*]Corresponding author. E-mail address: nordin.aranzabal@uv.es

Abstract

The BHE length for a given output power depends on the thermal properties of the geological layers, such as moisture, heat transfer coefficients, etc. Measuring the temperature fluctuations inside the pipes of a heat exchanger is key for an accurate sizing of its length in turn reducing drilling costs and the payback of the installation.

A miniaturized autonomous wireless sensor, called Geoball, is designed to measure the temperature while it is carried by the fluid inside the pipes of a geothermal heat exchanger, with the intention of determining the heat transfer capacity of the geological layers surrounding the pipe collector. The developed probe is encapsulated in a sphere with a diameter of 20 mm which has the same density as the fluid, and thereby is carried at fluid speed. Its main features are:

- Temperature range: -10 a 50 ºC
- Temperature accuracy: ± 0.05 ºC
- Sampling period: 0.1 – 25 s
- Temperature resolution: <0.05 ºC
- Number of samples: up to 1000
- Wireless energy harvesting

The probe contains an ultra-low power microcontroller, a temperature element Pt1000 with a response time of 80 ms, a conditioning circuitry, a non-volatile memory and a radio-frequency identification (RFID) device for configuration, data download and energy harvesting, all carefully designed in a print circuit board (PCB) with a diameter of 16 mm. An ultracapacitor is charged by RFID to power a miniaturized data logger, which can acquire up to 1000 samples.

The objective of the Geoball is to complement the data collected during a conventional thermal response test (TRT) and for applying numerical analysis to determine the thermal characteristics of a layered subsurface and its influence in the borehole thermal behavior.

Keywords: Geothermal energy; Ground source heat pump (GSHP) systems; Numerical simulation; Thermal response test (TRT); Wireless sensors.

1. Introduction

To achieve the objectives of sustainability, environmental impact reduction and mitigation of climate change, the introduction of cleaner and more efficient energy technologies is essential. For instance, the use of ground source heat pumps (GSHP) or geothermal heat pumps (GHP) for a heating ventilation and cooling system (HVAC) to heat or cool buildings and to provide hot water, have a great potential to reduce greenhouse gas

(GHG) emissions, energy savings and energy efficiency improvements [1]. A GSHP system can reduce GHG emissions by 66% or more than conventional systems that use fossil fuels by saving up to 75% of electricity [2].

A great effort has been made to spread the GSHP technology around the world by publishing compilations and reviews which present the different models and constructive alternatives with their related advantages in energy saving and efficiency [2, 3, 4]. Some experimental facilities have been built with the aim of verifying the energy savings that can be obtained under conditions of normal use [5]. Thus, it has been shown that in temperate climates such as the Mediterranean coast, about 43% could be saved on heating and 35% on cooling. Moreover, studies of district heating and cooling systems, demonstrate estimable savings in energy consumption in front of individual systems [6].

A key factor in order to increase the dissemination of GHP systems, is to reduce the economic cost of a borehole heat exchanger (BHE) with accurate design and sizing of the pipe collectors. The thermal response test (TRT) was developed in Sweden and the USA in 1995 [7, 8] and is currently used as a standard method for sizing BHE [9]. These TRT, are based on the infinite line source (ILS) model of Kelvin. It measures the temperature evolution at the inlet and outlet points of the installation while a constant heating power is injected into or extracted out of the BHE. Some limitations of these methods are the sensitivity to small variations of injected or extracted heat and the assumption that the subsurface structure is homogeneous. Some studies suggest that in some cases, a significant uncertainty related to the analysis of thermal conductivity for a typical TRT is related with the uncertainty of the heat injection rate [10]. Moreover, the TRT is affected by other factors such as subsurface disturbance due to drilling and the ambient temperature. Therefore, different methods have been proposed to filter these effects [11]. To improve the calculus of thermal parameters obtained from the TRT, as subsurface thermal conductivity and borehole thermal resistance, several investigations have been carried out using both, analytical or numerical models [12, 13, 14, 15, 16, 17] and laboratory experiments.

The ILS model assumes that the subsurface structure is homogeneous but that is the exception and not the rule in real GHP installations. To determine the subsurface geological structure, moisture content and groundwater flow are key factors to optimize the energy transfer or drilling depth relationship. An improved methodology has been proposed involving a multi-level power injection, focused in revealing the effects of groundwater flow and other possible heat transport processes [18]. Moreover, several studies have explored alternative methods to the TRT, introducing new temperature measurement systems along the U-pipe using optical fiber temperature sensors or electronic autonomous sensor probes [18, 19, 20, 21, 22, 23, 24].

Furthermore, given the increased power of numerical computer-aided calculations and the introduction of very accurate and reliable simulation programs, numerous works have performed the modeling and simulation of heat transfer by applying finite element methods in 2D and 3D models in static or dynamic regimes [25, 26, 27, 28, 29]. Since the reduction of computational time is a factor of great interest, to calculate the thermal parameters of a layered subsurface some researchers proposed to model the BHE by a network of thermal resistance and capacities [30, 31, 32, 33]. This approach shows an excellent agreement between finite element models and capacity-resistance models, with a significant reduction

in computing time, while allowing both dynamic and static analysis. A proper use of these capacity-resistance models to represent real facilities, requires the measurement of the fluid temperature evolution along the pipes during a TRT. However, so far, only measuring methods using fiber optical thermometers or temperature sensors flowing into pipes [34] can obtain the required input data for using this capacity-resistance model. The main characteristics of the probe described in [34] are:

- Weight: 8 g
- Diameter: 25 mm
- Temperature range: 0–40 °C
- Temperature resolution: <0.05 °C
- Temperature accuracy: ±0.05 °C
- Sampling interval: 0.1–25 s
- Sampling capacity: 1000 samples
- Powered by a wireless rechargeable battery
- Configuration and data download by RF (ISM 868 MHz)

Therefore, it can only be used in pipes with a diameter larger than 25 mm and cannot be employed when the temperature is below 0 ºC. In addition, the useful life is limited by the battery capacity.

Another configuration of a heat exchanger used in GSHP, which is of great interest due to the reduction of costs involved, are those based on pipes embedded in diaphragm wall or energy piles [35]. For these installations, the conventional TRT offers no guarantee of applicability as its geometry is not compatible with the ILS model. Measuring the temperatures inside the pipes as inputs for 3D finite element models or capacity-resistance models, may allow to obtain the heat pump system design parameters more accurately. To achieve this goal, autonomous miniaturized sensors may be the most appropriate method to measure the evolution of the temperature inside the pipes while a TRT is completed.

In this paper, a new version of this wireless temperature probe that flows inside the pipes [34] for measuring the thermal fluid during a TRT is presented. It consists of a small sphere (20 mm of diameter), which contains a programmable temperature acquisition system with wireless radio-frequency identification (RFID) for communication and energy harvesting. It can be introduced inside the BHE pipes and flows with the thermal fluid along the whole pipe length while acquiring the fluid temperature. At the output, the sensor downloads all the measured temperature data by a wireless RFID connection to a laptop or tablet.

2. System description

The objective of the sensor is to capture the temperature evolution inside the pipes along a BHE. To do so, a miniature spherical probe configured to measure the temperature at specified time intervals is introduced by a special valve inside the BHE pipe collector. The system complements standard TRT equipment to obtain additional internal temperature data which allows the detection of the heat transfer effects produced by different geological layers, moisture and groundwater.

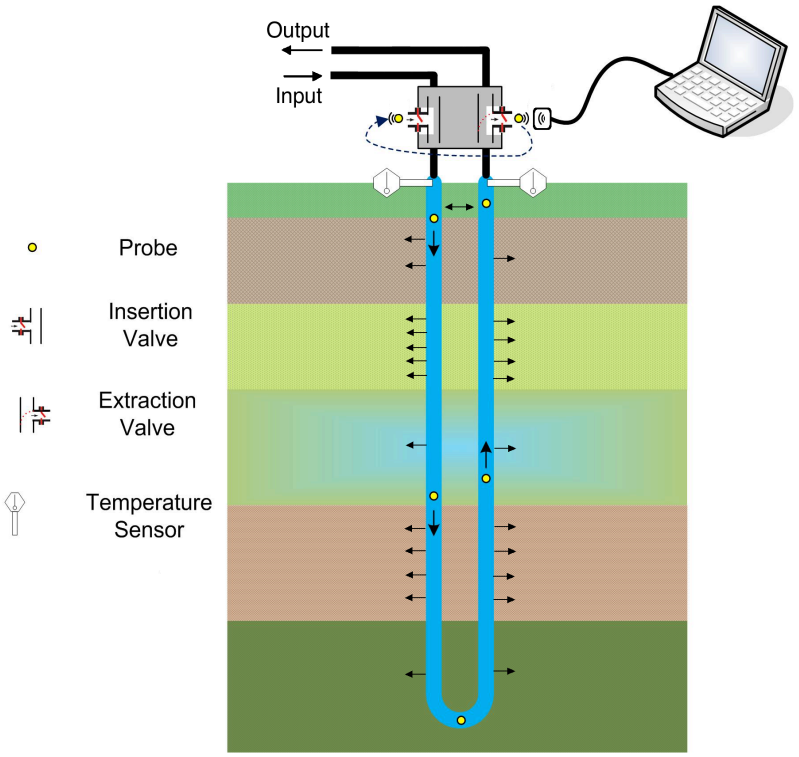

Fig. 1. Diagram of the wireless probe operation in a BHE.

Fig. 1 shows a diagram of the auxiliary elements for the system (insertion and extraction valves) and its operation process. The hydraulic and thermal power generation systems may be those of a TRT equipment. The Geoball, which has a 20 mm diameter and weighs 4 g, is carried by the flow at the same speed due to the fact that it has the same density as the fluid. Laboratory tests were performed to calculate the positioning error inside the pipe while the flow carried the probe, obtaining a value smaller than 2% [34].

The operation of the Geoball is carried out as follows: first, the laptop charges the power of the probe subsystem by radio frequency (RF) induction until the capacitor is full. Second, the sampling parameters, such as number of samples and period, are transferred to the Geoball by RFID and then it is inserted into the BHE fluid flow through the insertion valve. The probe starts the process of acquiring and storing fluid temperature automatically at programmed fixed intervals. Once a loop along the whole BHE pipe circuit is completed, the probe is extracted by an extraction valve. The temperature data is downloaded to the control system and the probe operation changes to a low-power mode.

Due to the small size of the Geoball, it is compatible with standard pipe collectors for BHE, which usually have a diameter of around 32 mm. This is an electronic device that measures (along the pipe loop) the thermal evolution of an elementary volume of fluid and how the probe exchanges heat with its surroundings. Fig. 2 presents an image of the Geoball,

both embedded in a sphere of 20 mm of diameter and the non-encapsulated circuit, compared with a one cent euro coin.

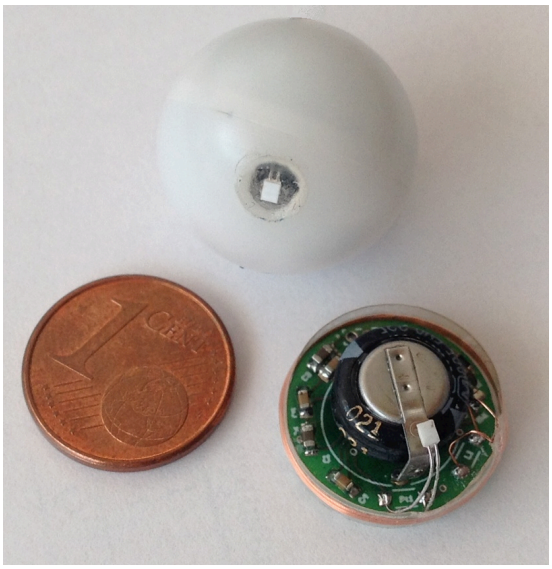

Fig. 2. Electronic circuit of the Geoball and an encapsulated probe.

The electronic circuits are mounted on a circular (16 mm diameter) double sided, printed circuit board (PCB) and includes: a 16-bit microcontroller with a 16-bit analog-to-digital converter (ADC) connected to a conditioning circuit to read a Pt1000 temperature sensor; a non-volatile RFID memory for wireless communications and energy harvesting; and an ultracapacitor to store the power needed for the operation of the probe (data acquisition and data logger).

The temperature sensor is a planar element Pt1000 class A according to DIN EN 60751, mounted on a ceramic substrate of 1.6 × 1.2 × 0.4 mm, with a response time of 80 ms on water. This type of sensor has some interesting characteristics, for example, it is inexpensive, it has an ultra-low power consumption during the measuring phase, and the measurements does not show a spatial, temporal and temperature dependency as it is the case for fiber optical thermometers. A Wheatstone bridge polarized in voltage is used to energize the Pt1000 temperature sensor to obtain a differential signal, which is amplified and digitized by the analogue circuitry of the ultra-low power microcontroller.

The characteristics of the autonomous sensor are:

- Temperature range: -10 – 50 °C
- Temperature resolution: <0.05 °C
- Temperature accuracy: ±0.05 °C
- Sampling interval: 0.1–25 s
- Sampling capacity: 1,000 samples
- Wireless energy harvesting

This new version presents improved characteristics regarding the weight, size, thermal response time, temperature range, power supply system, communication synchronization, and useful life, enabling a better usability and applicability in a wide type of buried heat exchangers.

A computer program has been developed using Labview® to configure, download, logging of data and graphical plotting. The graphical user interface (GUI) is illustrated in Fig. 3. The first step consists on setting the parameters for the acquisition process: flow, borehole depth, pipe diameter and spatial resolution. From this data, the period and number of samples to be acquired and transmitted to the probe by RF are calculated. This is done by issuing the start acquisition command, so the Geoball is ready to be inserted in the U-pipe by a special valve. Afterwards, the probe changes to "in acquisition" state, remaining in sleep mode until the preloaded waiting time is reached, then it changes to "acquisition" mode. Once the temperature acquisition is over, the Geoball saves the data in an internal memory, and the microcontroller switches to sleep mode again.

When all planed measurements are completed, the probe changes to "inactive" state, and the recorded data is marked as "completed". The PC can read the data by RF, write it into a file and plot it in a graphical interface.

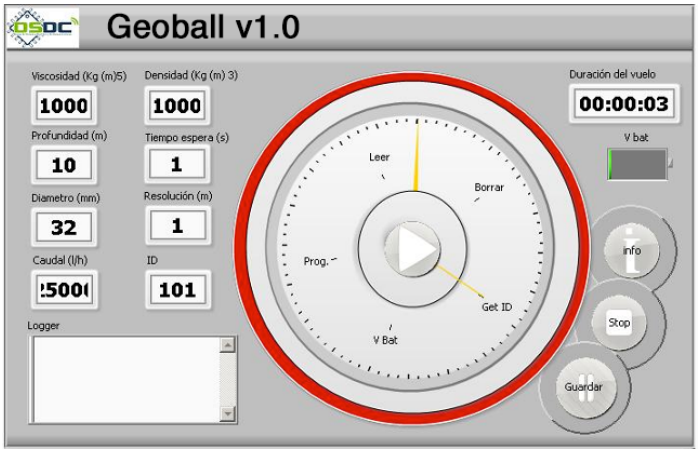

Fig. 3. Graphical user interface to configure the data acquisition, as well as for the data downloading, logging and visualization.

3. Laboratory test

A set of laboratory tests have been completed to verify the correct probe operation. First, a study was conducted concerning the voltage level and stability. In less than ten minutes in a RFID field, the ultracapacitor reached a voltage of 3.0 volts. In low power mode, the probes have maintained sufficient power during several hours, due to the extremely small current drained by the circuitry.

The tasks of the Geoball are coordinated using a clock signal, which wakes up the microcontroller when it is time to sample a new temperature value. The acquisition of a new

temperature measurement only requires 2 ms and drains a maximum of 2.04 mA of current. Throughout a laboratory test consisting of an acquisition of 600 temperature samples at a rate of one per second, the ultracapacitor only reduced its voltage in 300 mV, from 3 V to 2.7 V.

For correct and reliable use, each probe was individually calibrated by means of a thermal bath FRIGITERM 600038 from PSELECTA® and a high precision thermometer P755 from DOSTMANN electronic, to obtain the coefficients of the linear adjustment. The user interface stores each of the probe coefficients and processes the data to obtain values with the established resolution and accuracy. Fig. 4 presents one of the recorded temperature profiles for the room ambient temperature using the graphical user interface.

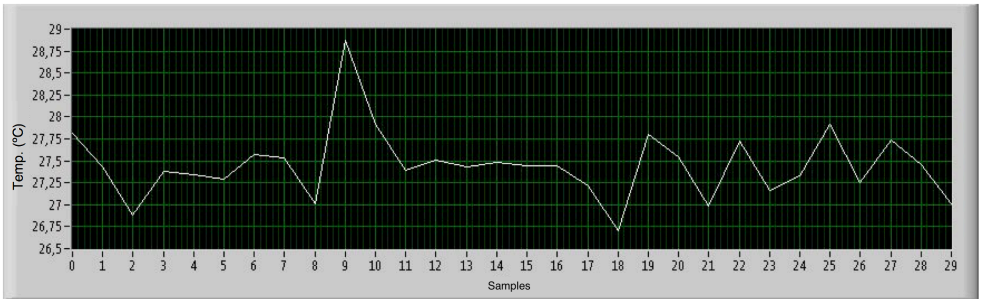

Fig. 4. *Graphical representation of a temperature profile recorded by the Geoball.*

4. Conclusions

The development of simpler and more economic methods in both, time and cost, regarding the sizing of a borehole heat exchanger (BHE) is key for the expansion of more efficient ground source heat pumps (GSHP) systems. Specially in the case of large BHE systems, new tools and methods are needed for calculating subsurface thermal properties to exploit the site conditions, such as moisture and groundwater flows. The probe and software presented in this work, due to its easy operation and simple integration with standard thermal response test (TRT) equipment, provides access to new data; offering the possibility of understanding the thermal properties of a heat exchanger surroundings, from inside the U-pipes, while performing the TRT.

Furthermore, the performance of the probe was validated, such as configurability, data logging and the circuitry for wireless energy harvesting and communication. The collected data from The Geoball allows to quantify thermal effects of the subsurface, such as groundwater flows, moisture, etc., usually not accessible in a conventional TRT. Additionally, this sensor technology uses a rechargeable battery, so its life is virtually infinite.

Finally, this measurement system opens the door for detailed quantitative assessment, not only for vertical BHE configuration, but it can also be extremely useful for the characterization of other configurations such as diaphragm walls or thermal piles, nowadays in expansion due to the reduction of the involved costs.

Acknowledgments

This work was supported by the "VLC/CAMPUS Valencia, International Campus of Excellence" under the program "Valoritza i Transfereix" of Universidad de Valencia 2011 and the PhD program of Climate-KIC Transforming the Built Environment Platform (TBE).

The sensor system presented in this work is protected by Spanish patent ES 2339735, 21 November 2008.

References

[1] Bayer P., Saner D., Bolay S., Rybach L., Blum P., Greenhouse gas emission savings of ground source heat pump systems in Europe: A review. Renewable and Sustainable Energy Reviews 2012; 16:1256-1267.

[2] Omer A.M., Ground-source heat pump systems and applications. Renewable and Sustainable Energy Reviews 2008; 12:344-371.

[3] Yang H., Cui P., Fang Z., Vertical-borehole ground-coupled heat pumps: A review of models and systems. Applied Energy 2010; 87:16-27.

[4] Lund J.W., Sanner B., Rybach L., Curtis R., Hellström G., Geothermal (ground-source) heat pumps. A World overview. Geo-Heat Centre GHC Bulletin Sept. 2004; 25(3):1-10.

[5] Urchueguía J.F., Zacarés M., Corberán J. M., Montero A., Martos J., Witte H., Comparison between the energy performance of a ground coupled heat pump system and an air to water heat pump system for heating and cooling in typical conditions of the European Mediterranean coast. Energy Conversion and Management 2008; 49:2917-2923.

[6] Nagota T., Shimoda Y., Mizumo M., Verification of the energy-savings effect of the district heating and cooling system – Simulation of an electrical-driven heat pump system. Energy and Buildings 2008; 40:732-741.

[7] Austin, W.A. Development of an *in situ* System for Measuring Ground Thermal Properties, MSc. Thesis, Oklahoma State University, Norman, OK, USA, 1998.

[8] Gehlin, S. Thermal Response Test–*In-situ* Measurements of Thermal Properties in Hard Rock. Licentiate Thesis, Lulea University of Technology, Lulea, Sweden, October 1998.

[9] Witte, H.; van Gelder, A.J.; Spitler, J.D. *In-situ* measurement of ground thermal conductivity: The dutch perspective. *ASHRAE Trans.* 2002; 108:263-272.

[10] Raymond, J.; Therrien, R.; Gosselin, L.; Lefebvre, R. A review of thermal response test analysis using pumping test concepts. Ground Water 2011; 49(6):932-945.

[11] Bandos T. V., Montero Á., Fernández de Córdoba P., Urchueguía J. F., Improving parameter estimates obtained from thermal response tests: Effect of ambient air temperature variations. Geothermics 2011; 40:136-143.

[12] Beier, R. Vertical temperature profile in ground heat exchanger during *in situ* test. Renewable Energy 2011, 36:1578-1587.

[13] Marcotte D., Pasquier P., On the estimation of thermal resistance in borehole thermal conductivity test. Renewable Energy 2008; 33:2407-2415.

[14] Raymond J., Therrien R., Gosselin L., Borehole temperature evolution during thermal response tests. Geothermics 2011; 40:69-78.

[15] Beier, R.; Smith, M.; Spitler, J. Reference data sets for vertical borehole ground heat exchanger models and thermal response test analysis. Geothermics 2011, 40:79-85.

[16] Bandos, T.; Montero, Á.; Fernández, E.; Santander, J.G.; Isidro, J.; Pérez, J.; Fernández de Córdoba, P.; Urchueguía, J. Finite line-source model for borehole heat exchangers: Effect of vertical temperature variations. Geothermics 2009, 30:263-270.

[17] Reuss, M.; Proell, M. Quality Control of Borehole Heat Exchanger Systems. In Proceedings of the Effstock'09 Conference, Stockholm, Sweden, 14–17 June 2009.

[18] Witte H., Van Gelder A. J., Geothermal response test using controlled multipower level heating and cooling pulses (MPL-HCP): quantifying ground water effects on heat transport around a borehole heat exchanger. Proceedings Ecostock 2006, Thenth International Conference on Thermal Energy Storage. New Jersey (USA) May 2006.

[19] Hurtig, E.; Ache, B.; Groβwig, S.; Hänsel, K. Fiber Optic Temperature Measurements: A New Approach to Determine the Dynamic Behavior of the Heat Exchanging Medium inside a Borehole Heat Exchanger. In Proceedings of the TERRASTOCK 2000, 8th International Conference on Thermal Energy Storage Stuttgart, Stuttgart, Germany, 28 August–1 September 2000.

[20] Rohner E., Rybach L., Schärli U., A New, Small, Wireless Instrument to Determine Ground Thermal Conductivity In-Situ for Borehole Heat Exchanger Design. Proceedings World Geothermal Congress 2005, Antalya, Turkey, April 2005.

[21] Fujii H., Okubo H., Nishi K., Itoi R., Ohyama K., Shibata K., An improved thermal response test for U-tube ground heat exchanger based on optical fiber thermometers. Geothermics 2009; 38:399-406.

[22] Fujii, H.; Okubo, H.; Itoi, R. Thermal response tests using optical fiber thermometers. Geotherm. Resour. Counc. Trans. 2006, 30:545-551.

[23] Acuña, J. Characterization and Temperature Measurement Techniques of Energy Wells for Heat Pumps. M.Sc. Thesis, KTH School of Industrial Engineering and Management Division of Applied Thermodynamic and Refrigeration, Stockholm, Sweden, 2008.

[24] Acuña, J.; Palm, B. A Novel Coaxial Borehole Heat Exchanger: Description and First Distributed Thermal Response Test Measurements. In Proceedings of the World Geothermal Congress, Bali, Indonesia, 25–30 April 2010.

[25] Beier R. A., Transient heat transfer in a U-tube borehole heat exchanger. Applied Thermal Energy 2014; 62:256-266.

[26] Bauer D., Heidemann W., Diersch H.-J. G., Transient 3D analysis of borehole heat exchanger modelling. Geothermics 2011; 40: 250-260.

[27] Corradi C., Schiavi L., Rainieri S., Pagliarini G., Numerical Simulation of the Thermal Response Test Within Comsol Multiphysics® Environment. Proceedings of the COMSOL Conference 2008 Hannover.

[28] Signorelli S., Bassetti S., Pahud D., Hohl T., Numerical evaluation of thermal response tests. Geothermics 2007; 36:141-166.

[29] Raymond J., Lamarche L., Simulation of thermal response tests in a layered subsurface. Applied Energy 2013; 109:293-301.

[30] de Carli M., Tonon M., Zarrella A., Zecchin R., A computational capacity resistance model (CaRM) for vertical ground-coupled heat exchangers. Renewable Energy 2010; 35:1537-1550.

[31] Bauer D., Heidemann W., Müller-Steinhagen H., Diersch H.-J. G., Thermal resistance and capacity models for borehole heat exchangers. International Journal of Energy Research 2011; 35:312-320.

[32] Nguyen A., Pasquier P., Marcotte D., Thermal resistance and capacity model for standing column Wells operating under a bleed control. Renewable energy 2015; 76:743-756.

[33] De Rosa M., Ruiz-Calvo F., Corberán J. M., Montagud C., Tagliaficio L. A., Borehole modelling: a comparison between a steady-state model and a novel dynamic model in a real ON/OFF GSHP operation. 32nd UIT (Italian Union of Thermo–fluid-dynamics) Heat Transfer Conference 23–25 June 2014, Pisa, Italy, Publisher: Journal of Physics: Conference Series 547 (2014) 012008, https://doi.org/10.1088/1742-6596/547/1/012008.

[34] Martos, J., Montero, Á., Torres, J., Soret, J., Martínez, G., García-Olcina, R., Novel wireless sensor system for dynamic characterization of borehole heat exchangers. Sensors 2011; 11:7082–7094.

[35] Xia C., Sun M., Zhang G., Xiao S., Zou Y., Experimental study on geothermal heat exchangers buried in diaphragm walls. Energy and Buildings 2012; 52:50-55.

Chapter 6

Comparison of the developed instruments (Geowire and Geoball) with new and standard in-borehole temperature measurement instruments

This chapter describes an experiment for comparing the quantitative and qualitative attributes of the two instruments developed during this Ph.D. work with new and standard in-borehole temperature measurement instruments. The performance of each of the instruments is analyzed in a BHE test site isolated from external conditions. Moreover, a numerical model is developed to reproduce the thermal behavior of the borehole, with the intention of investigating the reliability of the measurements recorded by each instrument.

6.1. Paper III: Temperature measurements along a vertical borehole heat exchanger: A method comparison

Authors: Nordin Aranzabal, Julio Martos, Hagen Steger, Philipp Blum and Jesús Soret.

Published in: Renewable Energy, 143, 1247–1258 (2019).
DOI: https://doi.org/10.1016/j.renene.2019.05.092

Impact factor: 6.274

Quartile (category: "Green & Sustainable Science & Technology"): Q1 (2019)

Summary:

This third paper compares the instruments developed in this Ph.D. work, Geowire (Chapter 4) and Geoball (Chapter 5), with new and standard commercial in-borehole temperature measurement instruments, such as the GEOsniff®, fiber optical thermometers and Pt100-sensors chain. It aims to offer an understanding of the most suitable temperature measuring method for each specific application by demonstrating the key advantages and disadvantages of each instrument. This study is intended as a guide for

choosing the most adequate in-borehole instrument while leading to a more reliable implementation of DTRT.

Firstly, it covers the description of the general characteristics and working principle of each instrument. Secondly, laboratory experiments are carried out to compare the key characteristics of each equipment (temperature range, temperature resolution, sampling time, thermal response time, spatial resolution, etc.). Thirdly, a field experiment is implemented in a test borehole with a depth of 30 m, which is isolated from external conditions. All instruments are located strategically along the geothermal pipes inserted in the borehole while the thermal response is evaluated under two thermal set-ups. Additionally, the development of a 3D FEM is presented with the same geometry as the experimental borehole. The model is configured to reproduce the thermal behavior of the borehole with the intention to evaluate the reliability of the datasets collected from each instrument.

The experimental results suggest that the new instruments have various advantages over the conventional instruments. For example, the new instruments are less expensive, more convenient and easier to operate.

Temperature measurements along a vertical borehole heat exchanger: A method comparison

Nordin Aranzabal[1, *], Julio Martos[1], Hagen Steger[2], Philipp Blum[2], Jesús Soret[1]

[1] Universidad de Valencia (UV), Department of Electronic Engineering, Burjassot, 46100, Spain
[2] Karlsruhe Institute of Technology (KIT), Institute of Applied Geosciences (AGW), 76131 Karlsruhe Germany

[*]Corresponding author. E-mail address: nordin.aranzabal@uv.es

Abstract

The standard thermal response tests (TRT) provide integral and effective thermal parameters of the ground in the vicinity of borehole heat exchangers (BHE). However, typical ground properties are heterogeneously distributed. As a result, advanced TRT such as distributed and enhanced TRT are growing in popularity as they provide more spatial information of the thermal properties. Thus, the objective of this study is to compare various instruments to measure the depth-dependent temperatures using standard Pt100-sensors, fiber optical thermometers and novel instruments such as Geowire, Geoball and GEOsniff®. The investigations are carried out in a 30 m length test borehole. The results showed an excellent agreement between both the Geowire and GEOsniff® in comparison with Pt100-sensors with a root mean squared error of 0.10 and 0.09 K, respectively. The results also suggest that the novel instruments have various advantages over the standard sensors and fiber optics. For example, with the novel instruments comparable, accurate, inexpensive, instantaneous and higher spatial resolution temperature measurements are obtained. Finally, the outcome of this study provides a guide for choosing the adequate temperature measurement along a BHE thus generally improving the evaluation of advanced TRT, while potentially increasing efficiency and economic viability of ground-source heat pump systems.

Keywords: Geothermal energy; Ground source heat pump (GSHP) systems; Borehole heat exchanger (BHE); Thermal response test (TRT); Temperature profile.

1. Introduction

In the past few decades, economical strategies to accomplish a reduction in primary energy consumption and mitigate greenhouse gases are increasing worldwide due to the imminent impact of climate change and global warming. Studies have shown that buildings depict the most important and cost-effective potential for saving energy and are accountable for about 80% of the energy demand for heating, while the energy demand for cooling is rising gradually every year [1]. Among renewable energy technologies, ground source heat pump (GSHP) systems are growing in popularity as they are proving to be energy-efficient in a range of applications, such as temperature conditioning in commercial and residential buildings and hot water production [2–4].

Low-enthalpy geothermal systems utilize GSHP systems to transfer the thermal energy stored in shallow ground to buildings for heating and from buildings to the ground for cooling [5]. The ground subsurface high thermal inertia makes it possible for the top layers

of the Earth to maintain a relatively constant temperature regardless of seasonal weather conditions. Thus, ground temperature is more favorable than the variable environmental air temperature for exchanging heat and GSHP systems are proven to achieve a higher energy efficiency than traditional air-conditioning systems [6]. In comparison to traditional air-conditioning systems, ground coupled heat pumps considerably reduce the use of electricity and therefore save associated carbon dioxide (CO_2) emissions in comparison with other conventional heating systems [7,8].

The general structure of a GSHP system that assists with the temperature conditioning of buildings is typically divided into two main elements: a borehole heat exchanger (BHE) installation and a heat pump system. A volume of fluid is circulated throughout a closed-loop distribution of pipes which are buried in vertical or horizontal ditches to exchange heat with the ground [9,10]. In both research and engineering, vertical BHE installations have attracted greater interest than horizontal BHE mainly due to the smaller land requirement [11].

In the design of BHE installations precise information of ground thermal parameters is necessary to calculate the most cost-effective size and distribution of BHE [12]. The in-situ thermal response test (TRT), initially proposed by Choudhary [13] and Mogensen [14] and fully developed with mobile equipment within the next decade [15,16], is a standard method for the evaluation of the subsurface thermal properties. In a TRT, a fluid is pumped throughout a closed-loop BHE while a nearly constant heat source is injected using an electrical element. The test starts from a subsoil temperature in equilibrium. For a minimum duration of 48 hours the introduced thermal perturbation is monitored at the inlet and outlet of the installation. From TRT results two parameters are usually determined: (1) effective thermal conductivity and (2) borehole thermal resistance. These are commonly estimated by analytical or numerical approaches [17–21] under the assumption of a homogeneous, isotropic and infinite medium. However, the typical ground stratigraphy is heterogeneous and these parameters are integral and average values. Furthermore, aquifers are abundant and previous models often neglect advective flow from groundwater resulting in erroneous estimations of effective thermal conductivity for long-term operations [22–25].

In order to overcome conventional TRT constraints, some researchers began to develop the so-called distributed TRT (DTRT) for an evaluation of depth-specific thermal properties [30–39]. This extra information is crucial to detect more favorable zones for heat exchange and therefore improves the efficiency while reducing piping, drilling and pumping costs. For instance, this knowledge of in-situ effective thermal conductivity determines the length of required BHEs. Some studies proved that the length of boreholes can be shortened when considering axial heat conduction effects and therefore increase efficiency and economic viability of BHE, particularly for high demand applications [26,27]. For this reason and with the intention to enhance TRT results, novel instruments and methodologies were developed and assessed over the past years. Fujii et al. [28,29] and Acuña [30,31] for example, conducted experiments by measuring temperature profiles along pipes with fiber optic thermometers to obtain an approximation of depth-specific effective thermal conductivities. In a similar manner, other researchers integrated fiber optics in BHE and proposed other methods for the evaluation of TRT [30–39].

Rohner et al. [41] developed a small probe with a data logger (time, temperature and pressure) which sinks to the bottom of geothermal U-tubes and proposed a method to estimate depth-specific thermal conductivity profiles. Pressure measurements are converted to depth and stored in the data logger together with the temperature and time. The probe stops when the bottom is reached and is flushed back to the surface with a pump for data reading. In order to calculate thermal conductivities from the data that is measured with the sensor, the method needs one temperature profile of the ground temperature in equilibrium and information of terrestrial heat flow near the test field.

Bayer et al. [42] conducted an experiment involving a commercial version of the latter sensor called NIMO-T (Non-wired Immersible Measuring Object for Temperature) and presented an analytical model to discriminate between the effects of global warming and urban heating. The model relies on information of past climatic and land use changes, as well as temperature logs obtained from the vertical pipes of BHE. Likewise, Raymond et al. [43] proposed an inverse numerical model to expand TRT results to adjacent boreholes using an analogous device with a data logger (temperature and pressure) called RBR*duet*^{3} (RBR Ltd.). In this study, the probe is lowered by hand using a wireline and after retrieving the data it is downloaded to a computer. The numerical model requires input of the results of a TRT in a near borehole, data of paleoclimatic variations of land proximities and a subsurface steady temperature profile of the borehole in order to estimate depth-specific thermal conductivity. Martos et al. [44] designed a small-spherical probe with a data logger that is transported by the thermal fluid in geothermal pipes and conducted a field experiment to measure the thermal evolution of the fluid along a U-shaped pipe throughout a TRT. This wireless device measures the thermal transition of a specific volume of fluid with high temperature, depth and time resolution. Moreover, Raymond et al. [45,46] provided a new method to discretize thermal conductivity along the depth of BHEs involving reduced energy consumption in comparison with a typical TRT. With this method a cable-assembly combining heating and non-heating sections is introduced in the borehole. After heating the cable, the recovery phase of each section is measured using temperature probes with a data logger midway along the height of each section. The recorded measurements are then evaluated with an analytical solution of a finite length linear heat-source to infer the thermal conductivity at the depth of each probe. Aranzabal et al. [47] elaborated an analysis procedure based on an inverse numerical model to estimate thermal conductivity along the depth of the borehole. For the input of the model, a series of depth-dependent temperature profiles throughout the course of a TRT are required. Following this, model results are fitted to experimental data by adjusting the thermal conductivity of defined depth-dependent layers along subsurface domain, in this case a new layer was defined every 2 m. Furthermore, to fulfill the requirements of the proposed method, Aranzabal et al. [48] introduced a novel data logger instrument for automatic measurements of depth-dependent temperature profiles along the borehole. Until now, these various types of temperature measurements have not been compared.

The objective of the present study is to carry out a quantitative and qualitative evaluation of standard and novel equipment for temperature measurements. The latter is crucial for the optimum design of vertical BHE for GSHP systems. Hence, it is intended to also reduce the capital costs of new installations and broaden the use of such systems. Nevertheless, some of the studied instruments are only reported in context with DTRT and the accuracy of the

obtained measurements has not been evaluated in a borehole under controlled conditions and using calibrated sensors as a reference.

This paper is structured as follows. Firstly, we used fiber optical thermometers, the wired equipment for automatic measurements of depth-dependent temperature profiles recently proposed by Aranzabal et al. [48] called "Geowire" and a commercial probe with a data logger (temperature and pressure) called "GEOsniff®". All three devices are compared with standard temperature sensors (Pt100). Secondly, an enhanced version of the probe initially introduced by Martos et al. [44] called "Geoball" is developed (smaller size, less weigth and extra features) and its thermal response is evaluated. Likewise, the uncertainty and thermal response time of the Geowire, Geoball and GEOsniff® is measured in the laboratory. Also, the reliability of the thermal response of the test borehole is also verified by a near-field numerical heat transport model.

2. Materials and methods

2.1. Novel instruments

In the present study three novel instruments are considered which are illustrated in Fig. 1.

One of the novel instruments used in this study is the Geowire [48]. An electro-mechanical device that automatically displaces a temperature sensor down and up along the depth of geothermal pipes at previously configured sequences. The sensor is connected to a wire the length of the borehole, which is rolled up on a reel (Fig. 1a). A servomotor rotates the reel and an encoder measures the length of the released wire. In this manner, the system adjusts the exact location of the small sensor (negligible perturbation) before measuring the temperature and storing its value. The displacement speed of the sensor in a U40 geothermal pipe can be adjusted between 0.5 and 5 m/min. The device provides two temperature sensors (DS18B20 of Maxim Integrated), one to measure the temperature inside the pipes and the other to measure the ambient air temperature. Digital transmissions are implemented using a one-wire communication protocol which operates reliably with wire distances of up to 500 m apart. Since instantaneous measurements of the temperature are digitalized in the sensor chip and transmitted to the processing system, a long deployment of wire does not compromise accuracy of measurements. On the other hand, non-specialized personnel can configure the acquisition process, visualize results or download data through a user-friendly graphical user interface (GUI) with remote access functionalities. The Geowire can be configured to measure automated profiles over the entire duration of a TRT. The instrument is compatible with standard TRT equipment without the need for additional modifications and is designed based upon a method of calculating the thermal properties of the subsurface with a high spatial resolution [47]. The main advantage of this method is that it only requires two temperature profiles to estimate a deph-dependent thermal conductivity profile. Despite that this version of the Geowire is designed to introduce the sensor in pipes without water flow, the previous version was designed to measure temperature inside heated pipes during a TRT, where the fluid could

cross through the enclosure of the device. Thus, the presented version of the Geowire could be modified accordingly.

Another instrument involved in this study is the Geoball, an electronic device that flows along pipes to measure the thermal evolution of a specific volume of fluid (Fig. 1b). The device used in this experiment is an improved version of the probe reported by Martos et al. [44]. The principle of its operation is the same, however it is smaller in size, weighs less and has longer operation times (Table 1). The electronic circuit is embedded in a polyoxymethylene (POM) sphere, while the sensing element is coupled to the surface of the sphere and stays in direct contact with the fluid. Thus, the measurement stabilizes fast over thermal gradients in the fluid to acquire instantaneous and accurate readings with a thermal response time less than 0.5 s. The temperature sensing element is a planar Pt1000 from Heraeus, A-class according to IEC 60751 and mounted on a ceramic substrate (size of 2.1 × 2.3 × 0.9 mm). The spherical probe has the same density as the fluid and is therefore carried by a constant flow while its position is determined. The temperature samples are stored in its internal memory together with its corresponding locations along the pipe. The small probe can be circulated in installations with vertical or horizontal pipe distribution, measuring the thermal evolution of fluid along the entire pipe network (down- and up-flow). In closed circuit applications, the ball can be stored in a bypass valve after each loop, where the data can be wirelessly transmitted and the battery simultaneously charged. It is also possible to use a manual bypass or an automated bypass without interrupting the heated fluid of a TRT. Thus, the insertion of the ball can be controlled to obtain continuous temperature datasets at pre-established time intervals. With an automated bypass system, the instrument can implement remote management and visualization functionalities. The instrument is compatible with standard TRT equipment and apart from the bypass valve, no additional modifications are required.

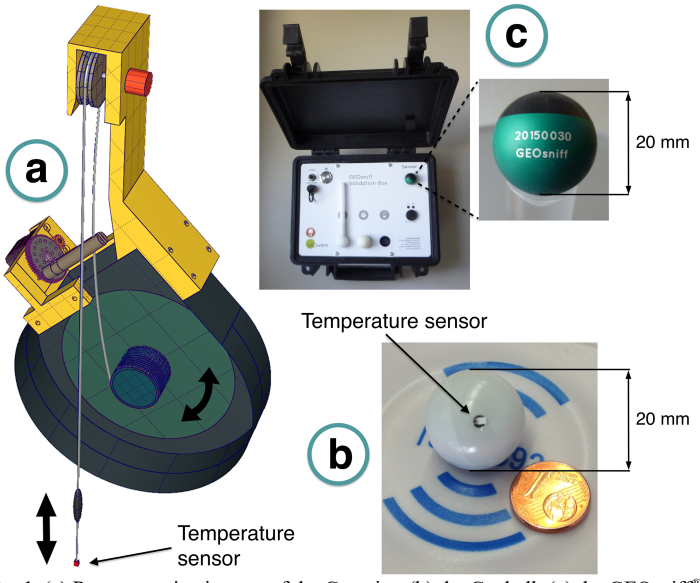

Fig. 1. (a) Representative images of the Geowire; (b) the Geoball; (c) the GEOsniff®.

Finally, the GEOsniff®, another depth-temperature sensor and data logger, also with the shape of a ball, developed by the German company enOware, is also included in the experiment (Fig. 1c). The design is similar to the Geoball, however this device calculates its position inside geothermal pipes by using a pressure sensor. The ball has a density higher than the water and sinks in vertical pipes, measuring the temperature until it reaches the bottom. Afterwards, a pump is turned on to circulate the water inside the pipes and expel the ball to a tank, where it is recovered. The temperature samples are stored in the device memory together with the pressure measurements and the user must convert the pressure data to depth equivalents. In this case the device required the installation of an additional closed-loop U-pipe (without a heat injection) inside the borehole in order to circulate the probe. Hence, the following materials are required in addition to standard TRT equipment: a tank filled with water, a bypass-valve, a pump and a U-pipe for monitoring purposes. An auto bypass-valve for online monitoring of the borehole whilst it is in operation can be also purchased. The latter is compatible with conventional TRT equipment and no additional materials are required which allows GEOsniff® to also circulate within the heated pipes of a TRT. Finally, the key characteristics of the three discussed novel instruments are summarized in Table 1.

Table 1. Key characteristics of the three studied instruments.

Instrument	**Geowire**	**Geoball**	**GEOsniff®**
Temperature range	-10 – 85 °C	-10 – 50 °C	-25 – 70 °C
Maximum temperature resolution	0.06 K	0.05 K	0.01 K
Sampling time	1 s	0.1 – 25 s	0.03 – 60 s
Diameter	5 mm	20 mm	20 mm
Density	3500 kg/m^3	1000 kg/m^3	1700 kg/m^3
Maximum spatial resolution	0.5 mm	10 mm	50 mm
Pressure resistance	tested until 40 bar	tested until 40 bar	45 bar
Energy supply and data transmission	wired and digital	wireless	wireless
Sampling capacity	no limitation (SD card)	1,000	3,200
Charging time	no required (wired power supply)	2 – 7 min	7 – 20 min
Pipe orientation	vertical	vertical and horizontal	vertical
Lowering speed (water, U40)	configurable (0.5 – 5 m/min)	same as the flow	15 m/min

2.2. Experimental test site and equipment

A test installation to reproduce a borehole heat exchanger was built for evaluating the different temperature measurement devices in a test site in Karlsruhe, Germany (Fig. 2, Table 3). The test borehole has a length of 30 m and a diameter of 450 mm, where two cases are introduced. The external case is 450 × 19.5 mm and covers the borehole. It is filled with water to isolate the thermal effects of surrounding subsurface. The internal case, which is also filled with water, is 180 × 10.7 mm where a single U-pipe of 25 × 3.5 mm is lowered to a depth of 21.5 m. The U-pipe is chosen because the ball-shaped instruments, GEOsniff®

and Geoball, need to be circulated inside a closed pipe loop. During the installation of the U-pipe, fiber optics and Pt100-sensor wirelines are taped to the outside surface of the U-pipe legs. Along the upper half of the borehole, a heating cable is installed to create a different thermal situation apart from the borehole in thermal equilibrium, i.e. undisturbed and heated borehole. Although, the ideal evaluation of the instruments appears to be in a real BHE or during a TRT, a test borehole isolated from external conditions is chosen as it provides a more reliable and controlled environment for the validation of the instruments. Moreover, a closed loop heat injection or extraction process is disregarded due to the dynamic thermal evolution in the borehole and the impossibility to measure with all instruments simultaneously inside the same pipe. Instead, the heated cable approach allowed to heat the borehole at a slow rate for measuring with all instruments in 20 min intervals.

Fiber optic thermometers obtain continuous, high-resolution temperature profiles along the length of the pipes using a Raman spectra distributed temperature sensing (DTS) technique and complex calibration algorithms [49,50]. In this case, the fiber optic cable model Helukabel (A-DSQ(ZN)B2Y 1x4 G50/125 + Cu), which has four fiber optic cables inside, is connected to the DTS equipment AP Sensing N4386A of four channels. In channel one, fiber optics are connected in a single-ended configuration and in channel two, a double-ended configuration. A single-ended configuration involves a DTS which measures temperatures along a single cable with only one connection to the instrument. A double-ended configuration of the fibers to the instrument makes observations from both directions on a looped cable, which has both ends connected to the DTS. Step losses can be corrected in a single-ended disposal by calibrating the cable sections on either side of the loss (e.g. Hausner & Kobs [51]). Double-ended deployments offer the potential to correct for non-uniform attenuation throughout the cable and are therefore preferred.

Pt100-sensors, Geowire, Geoball and GEOsniff® are calibrated linearly using five measurement points (0, 5, 10, 15, 20, and 25 °C) versus a thermometer of ± 0.01 K accuracy in a thermal bath stable to within ±0.01 °C. The calibration resulted in coefficient of determinations (R^2) ranging between 1 and 0.999.

A linear calibration of the Pt100-sensors, Geowire, Geoball and GEOsniff® is carried out by measuring at five points (0, 5, 10, 15, 20, and 25 °C) versus a thermometer of ± 0.01 °C accuracy in a thermal bath stable to within ±0.01 °C.

Table 2. Measured thermal time constant (τ) and uncertainty of the new instruments in the laboratory.

Instrument	Geowire	Geoball	GEOsniff®
Thermal time constant (τ)	< 2.0 s	< 0.5 s	< 5.8 s
Uncertainty (1000 samples)	± 0.062 K	± 0.042 K	± 0.044 K

The thermal time constant (IEC 60539-1) of the Geowire, Geoball and GEOsniff® is measured in the laboratory using a thermal bath of ±0.01 K stability. The instruments are programmed with a sampling time of 0.1 s to determine the time required for the probes to reach the 63.2% of a 20 K temperature step. The thermal step is created by transporting the probes from a thermally isolated box to the thermal bath. Also, the repeatability and stability of the temperature measurements in an environment with a stable temperature are studied. For this test, the different probes are programmed to measure the temperature every 0.5 s

and are inserted in a thermally isolated box while the stability of the temperature inside the box is monitored with a high-accuracy thermometer of ± 0.02 K accuracy and ± 0.01 K resolution. After 1000 measurements the three probes appealed to be significantly stable. The measured uncertainty and thermal time constant are presented in Table 2.

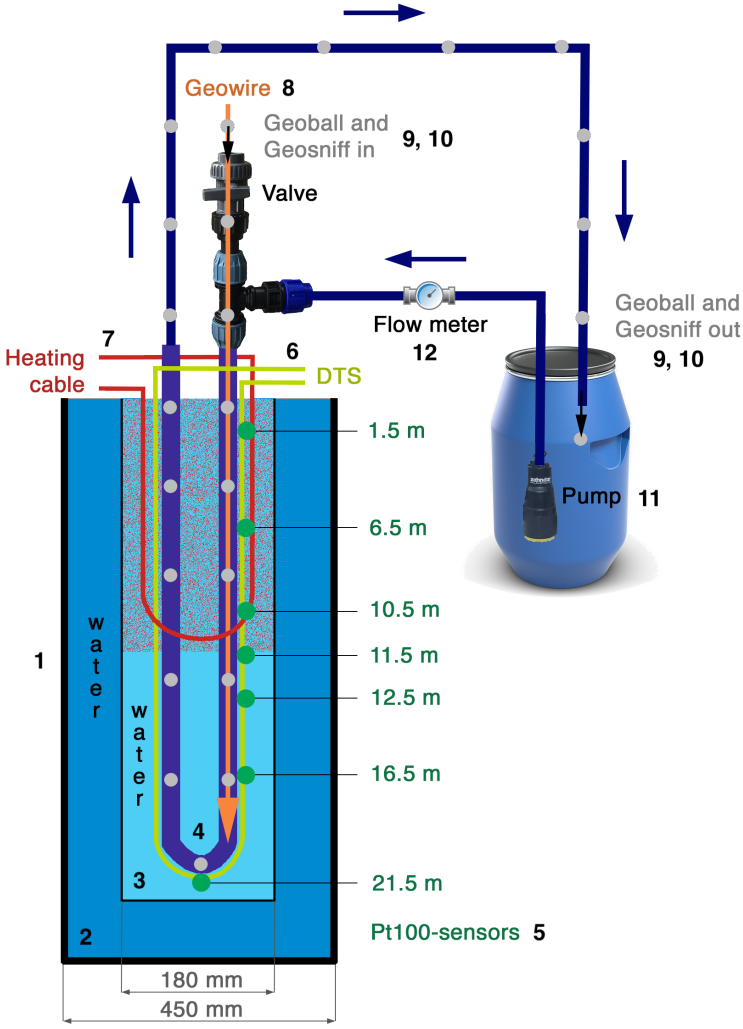

Fig. 2. Layout of the instruments and pipes in the test borehole. Reference and description of the enumerated components are presented in Table 3.

The acquisition and data logger equipment (Hewlett Packard 34970A) is configured to read and store the measurements from AA-class Pt100-sensors according to IEC 60751, in a four-wire mode. Furthermore, the heating cable is connected to a power supply of 40 V and 125 A for injecting 35 W/m throughout the upper half of the borehole. This cable is

chosen as it is suitable submerged conditions and it is appropriate to attain the same heat transfer as with a TRT. The obtained working conditions in the test installation are similar to the ones found in a real BHE in heat extraction mode with zones of different conduction capacities; the upper zone with high conductivity and the lower zone with less conductivity.

A pump by Zehnder (E-ZW 65A 850W, 9.5 m^3/h) is used for pumping the flowing sensor (Geoball) and pumping out the sinking sensor (GEOsniff®). In addition, the fluid flow rate is monitored using a flow meter (WG AG 131692/96, Wasser-Geräte GmbH).

The data logger equipment from the Pt100-sensors is configured to simultaneously measure the temperature of each sensor every minute. The Geowire is initially lowered to the bottom and then uplifted to the surface with a spatial resolution of 0.5 m and a lowering speed of 1.4 m/min. In a previous study with a pipe of the same diameter [48], the minimum waiting time to achieve a thermal equilibrium, as well as avoid possible perturbations produced by turbulences when moving the sensor to the next position, is calculated to be 5 s. Here, the sensor remains static for 5 s every 0.5 m. Afterwards, five samples of temperature are recorded with a sampling time of 1 s and the average value is stored in the database. By averaging as described in [48], the quality of the digital measurements is improved 1 bit to achieve a resolution of 0.03 K and an uncertainty bounded between ±0.04 K. Thus, the Geowire was able to record a complete temperature profile along the length of the pipe in 15 min. The GEOsniff® is configured to record the temperature with a sampling time of 0.5 s and a depth resolution of 0.05 m. The device took about 4 min to reach the bottom of the BHE. Lastly, the fiber optics equipment is adjusted to integrate the temperature along cable lengths of 0.5 m every 15 min. For the second set-up, based on the constant water flow, (measured at 0.67 l/s) the Geoball is programmed to obtain a temperature sample every 0.38 s storing a sample every 0.5 m. The Pt100-sensors and the fiber optics took measurements on the outside of the pipe wall, while the Geowire, Geoball and GEOsniff® measured inside the pipe (Fig. 2).

Table 3. Reference and description of the components involved in the experiment.

Layout components	Description, reference	Num. (Fig. 2)
Test borehole	30 m and a diameter of 450 mm	1
Outer case	450 × 19.5 mm. Filled with water	2
Inner case	180 × 10.7 mm. Filled with water	3
U-pipe	25 × 3.5 mm	4
Pt100-sensors wireline	taped to pipes, AA-class acquisition and data logger equipment (Hewlett Packard 34970A)	5
Fiber optics	taped to pipes, cable model Helukabel A-DSQ(ZN)B2Y 1x4 G50/125 + Cu, DTS equipment AP Sensing N4386A	6
Heating cable	35 W/m	7
Geowire	wired probe	8
Geoball	flowing probe	9
GEOsniff®	sinking probe	10
Pump	Zehnder (E-ZW 65A 850W, 9.5 m^3/h)	11
Flow meter	Wasser-Geräte GmbH (WG AG 131692/96)	12

2.3. Test method

The instruments are evaluated under two thermal set-ups in the experimental borehole: with undisturbed temperatures and then after heating the upper half part of the borehole (Fig. 2). At the same time, the test is divided into two measuring stages (Fig. 3) dependent on whether the instruments measured the temperature of a static fluid (Pt100-sensors, fiber optics, Geowire and GEOsniff®) or a specific volume of circulating fluid (Geoball). In the first measuring stage, Pt100-sensors, fiber optics, Geowire and GEOsniff® measured the temperature along one of the U-pipes, while the water inside the pipe remained still; in the second stage, the Geoball is circulated along the entire U-pipe loop by circulating water.

For the undisturbed borehole, the measurements from the Pt100-sensors, fiber optics, Geowire and GEOsniff® are simultaneously considered as the borehole is in thermal equilibrium. For the heated borehole, the upper half of the borehole is heated until the Pt100-sensors show the temperature increases at a slow rate (0.01 K/h). Each of the instruments then measure one temperature profile along the borehole in a total time of 20 min: from the start of test, the fiber optics and Geowire measured one profile in 15 min, Pt100-sensors at 8 min and GEOsniff® at 16 min. Temperature differences smaller than 0.01 K among the instruments were expected.

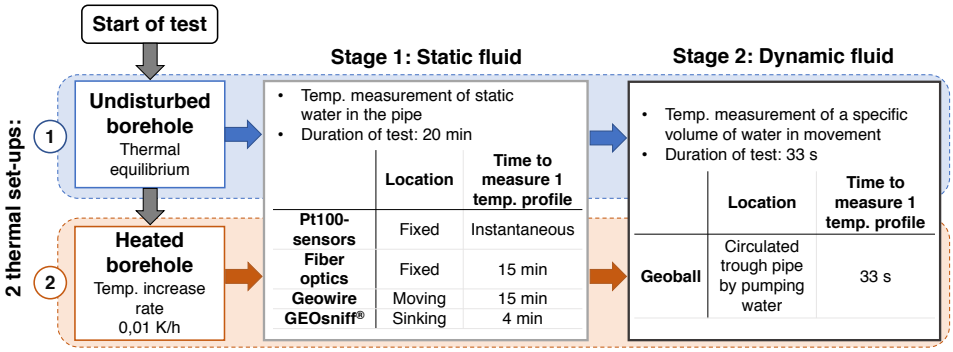

Fig. 3. Test procedure diagram.

With the intention to assess whether the observed differences among the sensors located at dissimilar positions are physically reasonable, as well as to evaluate the proper calibration of each of the Pt100-sensors and the thermal response of the BHE, an inverse numerical heat transfer model is developed (Fig. 4). COMSOL Multiphysics® is used to build a 3D finite element model with the same geometry and thermal behavior as the experimental BHE. From the available physics-based modules the following are added to the model component: laminar single-phase flow (SPF), heat transfer in fluids (HT), non-isothermal pipe flow (NIPFL) and non-isothermal flow (NITF). Water, copper and polyethylene (PE) materials from the COMSOL library are incorporated to the model component to assign thermo-physical parameters of the different domains. The domain representing the volume of water inside the outer case is assigned to water, the walls of the inner case are assigned to PE, and the inside domain is assigned to water. The U-pipe and heating cable inside the inner case are respectively assigned to PE and copper (Fig. 4).

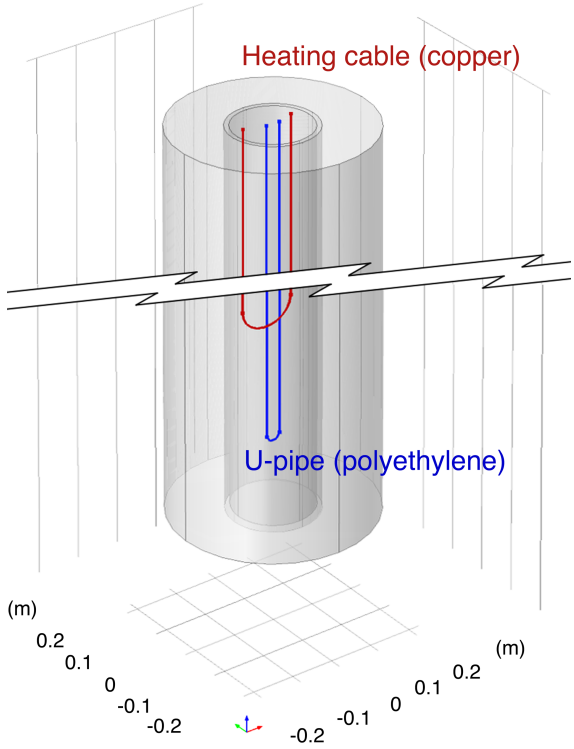

Fig. 4. 3D model representation of the experimental borehole heat exchanger.

The two domains of water are assigned to SPF, HT and NITF physical modules in order to reproduce convective and heat transfer effects in the fluid. From the HT module, a line heat source with a radius of 0.006 m and a heat source of 35 W/m is added and simulates the behavior of the heating cable. A heat transfer in a solid node is added inside the HT module and the inner case domain is assigned to this node. Likewise, the U-pipe is assigned to the NIPFL module and all the external boundary surfaces of the geometry are defined as thermal insulation.

The Geowire recorded more data points along the experimental BHE than the Pt100-sensors. Thus, the recorded undisturbed temperature profile from the Geowire is used to initialize the different domains.

The model meshing configuration is crucial to carry out reliable and time-effective simulations. When the number of tetrahedral elements is increased, convective and heat transfer effects are more pronounced and simulation results adjust more accurately with experimental results, however, the computational cost increases. In this case, three simulations are run to find the optimal meshing configuration. First, a user-defined mesh of 1,004,889 elements is used resulting a root mean squared error (RMSE) of 0.31 K in comparison with the measured temperature profile. Secondly, a simulation with 1,262,133 elements is carried out and an RMSE deviation of 0.25 K is calculated. Thirdly, the model

mesh with 1,422,533 elements is run and a similar RMSE of 0.25 K is calculated. Hence, the model mesh with 1,262,133 elements is considered to be optimal. Since the first simulation iterations of the temperature in the borehole remained constant below 12 m, the length of the model is shortened to reduce computational time. The geometrical model input parameters are summarized in Table 4. With this, a time dependent simulation is launched for a total of 7200 s with a maximum step of 10 s and to save computed data every 100 s. The time-stepping algorithm is configured with a relative tolerance of 0.01 and an absolute tolerance of $1e^{-3}$.

Table 4. Geometrical input parameters for the numerical model.

Parameter	Value (m)
Borehole depth	13.5
Borehole radius	0.225
PE-tube depth	12.5
PE-tube inner radius	0.0793
PE-tube outer radius	0.09
U-pipe length	12
U-pipe inner radius	0.0125
U-pipe outer radius	0.016
Heating cable length	10.75
Heating cable radius	0.006

3. Results and discussion

3.1. Experimental results

For the borehole in equilibrium, the Pt100-sensors, fiber optics, Geowire and GEOsniff® generally obtained constant values below a depth of 6 m (Fig. 5, left). Whereas with the heated borehole, temperature measurements were relatively stable below a depth of approximately 11 m and increased progressively above 11 m until the surface (Fig. 5, right). The Pt100-sensors were used as a reference and considered the most accurate measurement. To visualize and assess the reliability of recorded temperatures, Fig. 6 shows the measurements of each instrument at the depths of the Pt100-sensors versus the measurements from the Pt100-sensors from both the undisturbed and heated borehole.

The depth-temperature profiles obtained with fiber optics compared with the Pt100-sensors, show an RMSE difference of 0.378 K for the single-ended configuration and an RMSE of 0.397 K for the double-ended configuration (Fig. 6). When the Pt100-sensors measured stable values (Fig. 5, below 6 m for the borehole in equilibrium and below 11 m for the heated borehole), the temperature measurements for the double-ended configuration are about 1 K higher and for the single-ended configuration 2 K higher than those from the Pt100-sensors. The observed relatively constant temperature difference between the fiber optics measurements and Pt100-sensors along 6-22 m suggests that a dynamic field calibration of the DTS equipment is required. Since all component parts of the DTS equipment are temperature sensitive (e.g. amplifiers, detector, laser, power supplies), the changing ambient temperature is likely to have introduced the observed offset error [49].

Furthermore, the datasets from the fiber optics show some oscillations that may be related to the averaging of temperatures every 15 min and for cable sections of 0.5 m. In this case, slightly higher oscillations are detected for the double-ended configuration than for the single-ended. Additionally, the temperatures near the outer part of the borehole (above 5 m), are lower in comparison with the other devices. This is most likely due to the effect of the external conditions.

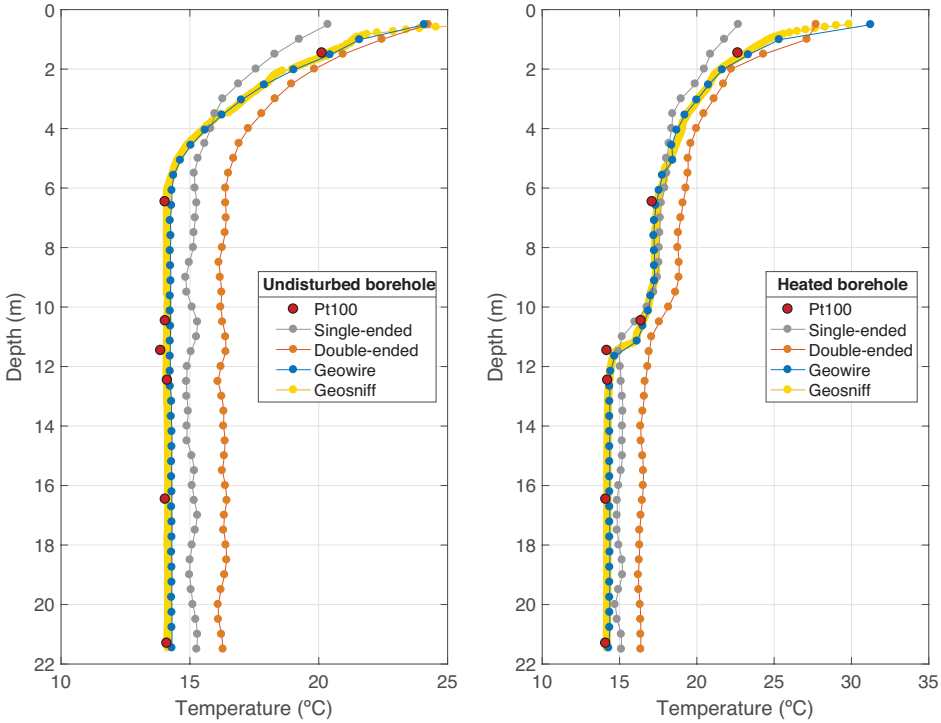

Fig. 5. Measured temperature profiles with the Pt100-sensors, Geowire and fiber optics (single-ended and double-ended) for the two thermal set-ups in the borehole (undisturbed and heated).

Temperature profiles from the Geowire and Pt100-sensors are comparable with a low RMSE difference of 0.094 K (Fig. 6) and negligible maximum deviations of 0.31 K at the same depths. Similarly, an excellent agreement is found between the GEOsniff® and Pt100-sensors with a very low RMSE difference of only 0.075 K (Fig. 6) and a maximum deviation of 0.39 K.

The Geoball is part of the second thermal set-up. Thus, it is not compared with the other instruments as it measures the temperature evolution of a fundamental volume of fluid in movement, in contrast to the other instruments which measure the temperature of a static fluid inside a pipe. Fig. 7 illustrates how the vertical thermal gradient is higher when the ball moves down versus when it moves up. This may occur due to the pump being stopped for a few minutes after a loop and before the probe is introduced into the pipe and pumped again. During this time, the water in the tank, as well as the section of the pipe at the surface,

may have heated with the higher outside temperature. Another observation is the decrement in the temperature of the entire profile every time the ball completes a loop along the U-pipe. Here, the fluid circulating in the closed-circuit exchanges heat with the borehole. The Geoball measured the thermal evolution along the whole length of the U-pipe in the BHE showing a fast response time over temperature. However, further research is required to compare the results.

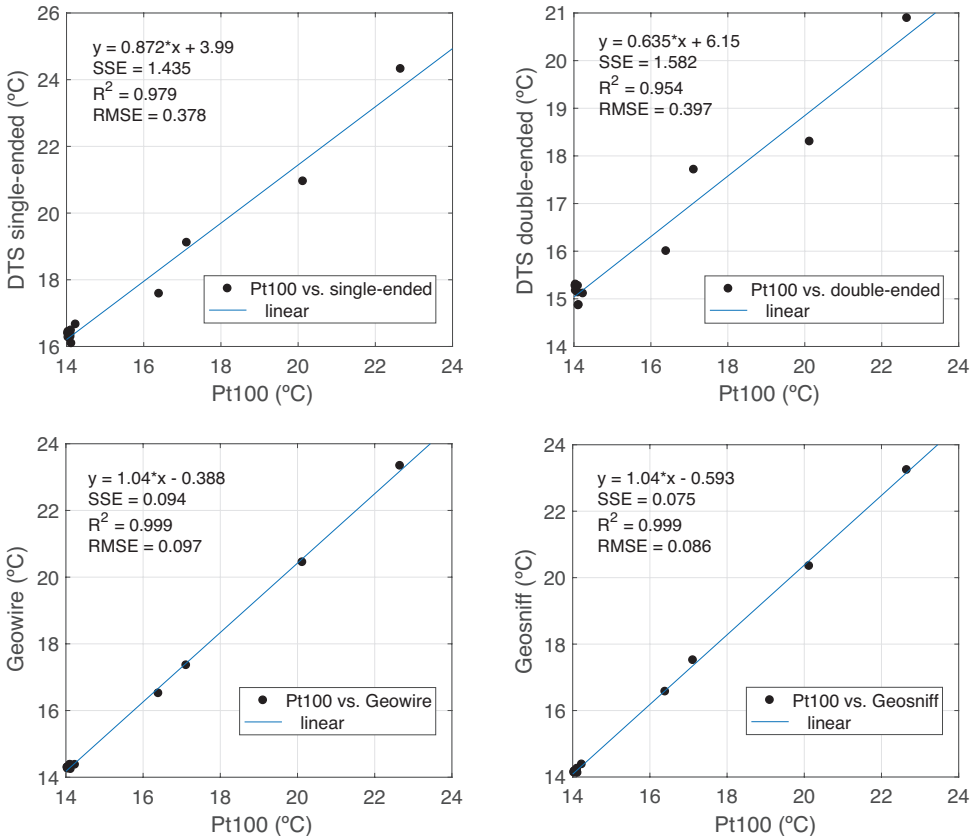

Fig. 6. Linear adjustment of the Pt100-sensors between the fiber optics (single-ended and double-ended), Geowire and GEOsniff®. Each plot includes the linear equation (y), the sum of squares due to error (SSE), the coefficient of determination (R^2) and the root mean squared error (RMSE).

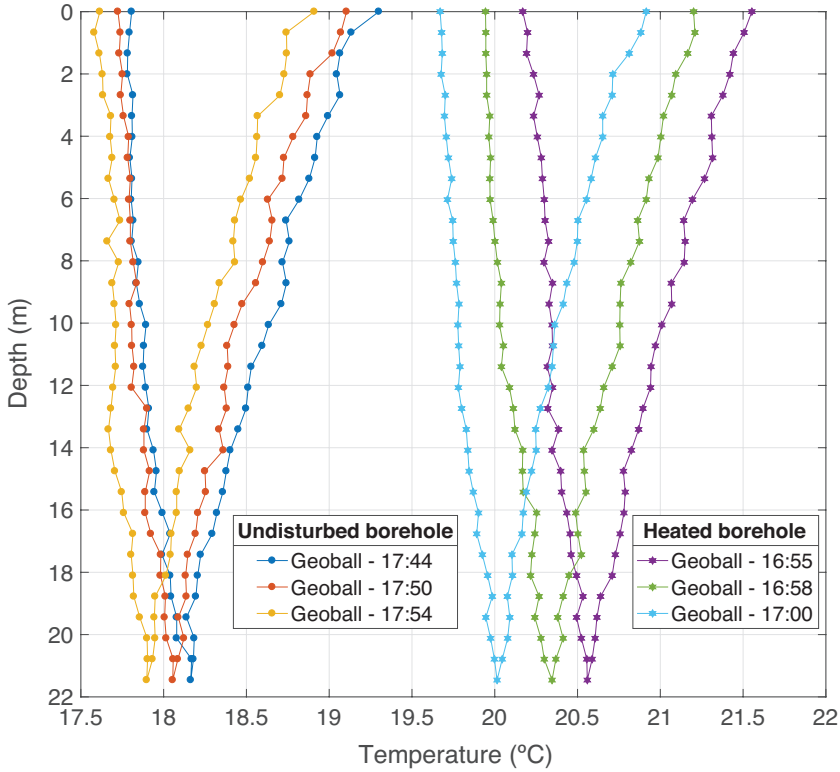

Fig. 7. Obtained depth-temperature profiles with the Geoball for the two thermal set-ups in the borehole (undisturbed and heated).

3.2. Numerical simulations

Due to the uncertainty resulting from the edge effects outside the borehole (top boundary), the first 1.25 m are ignored. After the model simulation, numerical and experimental depth-dependent temperature profiles inside the pipe are comparable with an RMSE deviation of 0.13 K (Fig. 8). According to the simulation results, there should be hardly any significant temperature difference between the outer and inner parts of the pipe.

Below 6 m in the undisturbed borehole (Fig. 5), the temperature is constant. However, the Pt100-sensor at 11.5 m shows a temperature decrement of 0.2 K in comparison with the other five Pt100-sensors below 6 m. Hence, the temperature difference found with the Pt100-sensor at 11.5 m might be caused by a calibration error. The measurements from the Geowire and GEOsniff® also support this assumption as they had the same readings as all other five Pt100-sensors. A higher temperature difference was only recorded for the Pt100-sensor at 11.5 m.

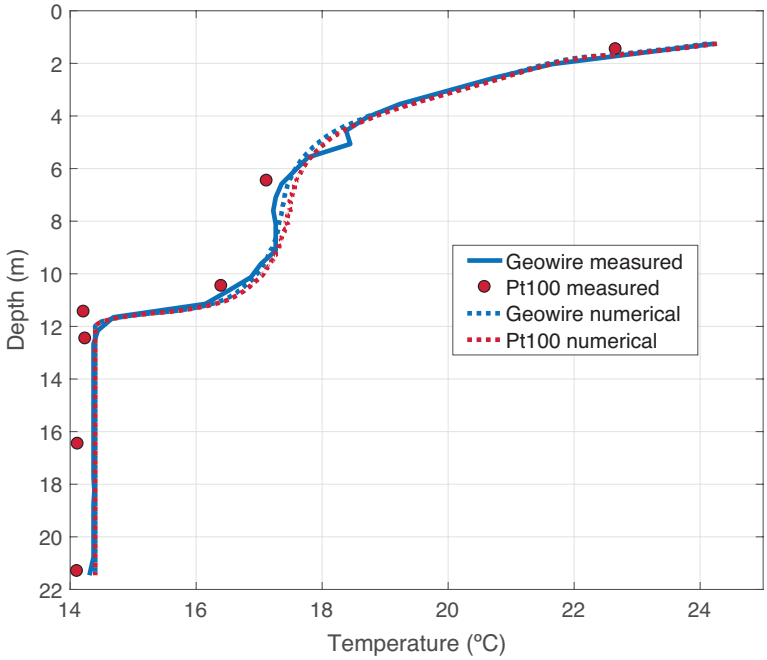

Fig. 8. Measured temperature profiles by the Pt100-sensors and Geowire in comparison with numerical modelling results (temperature in measured locations by the Geowire and temperature at Pt100-sensors locations).

3.3. Method comparison

According to IEC 60751, AA-class Pt100-sensors are very accurate (± [0.1 + 0.0017 |Temp.|]). However, long boreholes typically require a higher number of sensors. The latter directly affects the cost and complexity of the data logger installation (e.g. high cable density), which limits its current applications. In addition, the sensors are hard to recover after the measurement campaign.

In contrast, fiber optic thermometers are currently a very popular solution to measure the distributed temperature along the pipes of a BHE. Unfortunately, equipment to acquire consistent results is expensive, typically ranging between 20,000 and 50,000 € and limited with respect to the temperature resolution, spatial resolution, range and measurement speed. For example, longer integration times or spatial resolution increase measurement resolution. However, this also means loss of information in environments with fast thermal evolution. Moreover, the algorithms to calibrate and calculate measurements are complex [49,50]. When the fiber optics equipment is kept in an environment with a changing temperature, a single calibration is insufficient and a field dynamic calibration is urgently required. A possible solution might be to keep an isolated box with ice in the field to calibrate every measurement iteration of the fiber optics equipment. Installing fiber optic cables inside the down-flow of a U-pipe is relatively easy, whereas measuring the overall length of a U-pipe is more complex [29,34]. Another option is to install the fiber optic cables on the outer

surface of the pipes, as is done in this study. It is important to note that special attention should be taken to avoid cable displacements along the pipe diameter [52].

The three studied instruments (Geowire, Geoball and GEOsniff®) are an affordable alternative in evaluating subsurface temperatures in the near-field or inside a BHE. These novel instruments measure instantaneous samples of temperature, where the accuracy of the measurements is independent among spatial resolution, temporal resolution and sampling time. Thus, after applying a method to estimate the depth-specific thermal conductivity to the obtained results, these novel instruments are able to detect small, highly-conductive zones that might remain unnoticed with standard DTS equipment or a chain of Pt100-sensors.

Table 5 compares the studied instruments and indicates the difficulties of integrating them in a BHE or during a TRT. Apart from understanding the quantitative differences between the devices, it is also important to recognize the qualitative differences of each instrument in order to assess their applicability to specific tests and studies.

Table 5. Comparison of the studied instruments.

Instruments	Pt100-sensor-chain	Fiber optics	Geowire	Geoball	GEOsniff®
Integration in existing BHE installations	No	Yes, inside pipes but complex	Yes	Yes	Yes
Complex calibration	No	Yes	No	No	No
Trade-off between integration time, spatial and temperature resolution	No	Yes	No	No	No
Cost	Low	High	Moderate	Moderate	Moderate
Vertical borehole heat exchanger	Yes	Yes	Yes	Yes	Yes
Horizontal borehole heat exchanger	Yes	Yes	No	Yes	No
Spatial and temperature resolution	Low spatial resolution because wiring complexity, 0.05 K	For an advance equipment, 0.1 K integrating every 15 min along 2 m	Up to 0.5 mm, 0.06 K	Up to 10 mm, 0.05 K	Up to 50 mm, 0.01 K

4. Conclusion

To obtain vertically distributed effective thermal parameters of the ground in the vicinity of borehole heat exchangers (BHE), distributed temperature data monitoring the thermal evolution in a friendly, cost-effective and easily integrable way are required. Hence, in the current study the response and characteristics of novel and standard temperature measurements were assessed in the laboratory and in the field. From the laboratory tests, a fast thermal response time and a negligible uncertainty was measured for the tested devices: Geowire (< 2.0 s, ± 0.06 K), Geoball (< 0.5 s, ± 0.04 K) and GEOsniff® (< 5.8 s, ± 0.04 K). From the field using two thermal set-ups and conducting various temperature measurements with dissimilar devices, the following conclusions can be drawn:

- One out of seven Pt100-sensors showed a calibration error of 0.2 K.
- An excellent agreement was observed between both the Geowire and GEOsniff® in comparison with Pt100-sensors with an RMSE deviation of 0.10 K and 0.09 K, respectively.
- The fiber optics (for both single-ended and double-ended) showed a high linearity using the Pt100-sensors as a reference. However, a maximum offset of 2 K suggested that a single calibration of the fiber optics is insufficient in an environment with changing temperatures.
- Novel instruments such as Geowire, Geoball and GEOsniff® measured the temperature instantaneously, while the accuracy of the measurement is independent among spatial and temporal resolution and sampling time. In comparison to fiber optics, these instruments provide higher spatial resolutions and higher accuracies in environments with transient thermal responses like distributed thermal response tests (DTRT).
- The new instruments are easier to integrate in existing boreholes or borehole heat exchangers and are also inexpensive. Possible errors during the calibration of multiple sensors can also be avoided.

The quantitative and qualitative differences of the various temperature devices indicate that a careful assessment should be carried out, when choosing the instrument, calibration procedure and data analysis method prior to the implementation of a TRT or a temperature measurement in a borehole. Understanding the most suitable instrument for the specific need is crucial for accurate temperature measurements and a successful evaluation of a DTRT or other intended analysis. Hence, to avoid oversized ground source heat pump (GSHP) systems and unnecessary increased capital costs, novel temperature devices with higher accuracy and resolution are required for the determination of spatially distributed thermal properties.

Acknowledgments

The present work was partially supported financially by the European Institute of Innovation and Technology Climate-Knowledge and Innovation Community (EIT Climate-KIC).

List of symbols and abbreviations

A	Amp
BHE	Borehole heat exchanger
Cu	Copper
CO_2	Carbon dioxide
DTS	Distributed temperature sensing

DTRT	Distributed thermal response test
GSHP	Ground source heat pump
GUI	Graphical user interface
h	Hour
HT	Heat transfer in fluids
K	Kelvin degree
kg	Kilogram
l	Litter
IEC	International electrotechnical commission
m	Meter
mm	Millimeter
min	Minute
NITF	Non-isothermal flow
NIPFL	Non-isothermal pipe flow
PE	Polyethylene
POM	Polyoxymethylene
Pt100, Pt1000	Platinum resistance thermometer
RMSE	Root mean square error
s	Second
SD	Secure digital
SSE	Sum of squares due to error
SPF	Laminar single-phase flow
R^2	Coefficient of determination
TRT	Thermal response test
U40	Geothermal U-pipe with 40 mm of external diameter
V	Volt
W	Watt
y	Linear equation
τ	Thermal time constant
ºC	Celsius degree
€	Euro

References

[1] I. Sarbu, C. Sebarchievici, General review of ground-source heat pump systems for heating and cooling of buildings, Energy Build. 70 (2014) 441–454. https://doi.org/10.1016/j.enbuild.2013.11.068.

[2] P. Bayer, D. Saner, S. Bolay, L. Rybach, P. Blum, Greenhouse gas emission savings of ground source heat pump systems in Europe: A review, Renew. Sustain. Energy Rev. 16 (2012) 1256–1267. https://doi.org/10.1016/j.rser.2011.09.027.

[3] A. M. Omer, Ground-source heat pumps systems and applications, Renew. Sustain. Energy Rev. 12 (2008) 344–371. https://doi.org/10.1016/j.rser.2006.10.003.

[4] J.F. Urchueguía, M. Zacarés, J.M. Corberán, A. Montero, J. Martos, H. Witte, Comparison between the energy performance of a ground coupled water to water heat pump system and an air to water heat pump system for heating and cooling in typical conditions of the European Mediterranean coast, Energy Convers. Manag. 49 (2008) 2917–2923. https://doi.org/10.1016/j.enconman.2008.03.001.

[5] J. Lund, B. Sanner, L. Rybach, R. Curtis, G. Hellström, Geothermal (ground-source) heat pums A world review, Geo-Heat Cent. Q. Bull. (2004) 1–10.

[6] G. Florides, S. Kalogirou, Ground heat exchangers—A review of systems, models and applications, Renew. Energy. 32 (2007) 2461–2478. https://doi.org/10.1016/j.renene.2006.12.014.

[7] P. Blum, G. Campillo, W. Münch, T. Kölbel, CO_2 savings of ground source heat pump systems - A regional analysis, Renew. Energy. 35 (2010) 122–127. https://doi.org/10.1016/j.renene.2009.03.034.

[8] Y. Genchi, Y. Kikegawa, A. Inaba, CO_2 payback-time assessment of a regional-scale heating and cooling system using a ground source heat-pump in a high energy-consumption area in Tokyo, Appl. Energy. 71 (2002) 147–160. https://doi.org/10.1016/S0306-2619(02)00010-7.

[9] J. Spitler, S. Gehlin, Thermal response testing for ground source heat pump systems—An historical review, Renew. Sustain. Energy Rev. 50 (2015) 1125–1137. https://doi.org/10.1016/j.rser.2015.05.061.

[10] S. Gehlin, Thermal response test: method development and evaluation, Luleå University of Technology, 2002.

[11] H. Yang, P. Cui, Z. Fang, Vertical-borehole ground-coupled heat pumps: A review of models and systems, Appl. Energy. 87 (2010) 16–27. https://doi.org/10.1016/j.apenergy.2009.04.038.

[12] P. Cui, H. Yang, Z. Fang, Heat transfer analysis of ground heat exchangers with inclined boreholes, Appl. Therm. Eng. 26 (2006) 1169–1175. https://doi.org/10.1016/j.applthermaleng.2005.10.034.

[13] A.-R. Choudhary, An approach to determine the thermal conductivity and diffusivity of a rock in situ, Ph.D. Thesis, Oklahoma State University, 1976. https://www.google.com/url?sa=t&rct=j&q=&esrc=s&source=web&cd=1&ved=2ahUKEwiI4_i22OPgAhUD5uAKHbnmDF4QFjAAegQICRAC&url=https%3A%2F%2Fshareok.org%2Fbitstream%2Fhandle%2F11244%2F32925%2FThesis-1976D-

C552a.pdf%3Fsequence%3D1%26isAllowed%3Dy&usg=AOvVaw1FfdHNjJEWMqwokQwSAPAQ.

[14] P. Mogensen, Fluid to duct wall heat transfer in duct system heat storages, in: Proc. Int. Conf. Subsurf. Heat Storage Theory Pract., Swedish Council for Building Research, Stockholm, Sweden, 1983: pp. 652–657.

[15] W.A. Austin, Development of an in Situ System for Measuring Ground Thermal Properties, Oklahoma State University, 1998.

[16] S. Gehlin, Thermal response Test – In-situ Measurements of Thermal Properties in Hard Rock, Luleå University of Technology, 1998.

[17] H.S. Carslaw, J.C. Jaeger, Conduction of heat in solids, 2nd editio, 1986. https://doi.org/10.1115/1.3225900.

[18] B. Sanner, G. Hellström, J. Spitler, S. Gehlin, Thermal response test—current status and world-wide application, in: Proc. World Geotherm. Congr., 2005: pp. 24–29. LTU-DT-0239-SE.

[19] S. Signorelli, S. Bassetti, D. Pahud, T. Kohl, Numerical evaluation of thermal response tests, Geothermics. 36 (2007) 141–166. https://doi.org/10.1016/j.geothermics.2006.10.006.

[20] H.J.L. Witte, TRT: How to get the right number, GeoDrilling Int. 151 (n.d.) 30–34. http://www.groenholland.nl/download/Geodrilling_2009.pdf.

[21] F. Stauffer, P. Bayer, P. Blum, N. Molina-Giraldo, W. Kinzelbach, Thermal use of shallow groundwater, CRC Press, 2013. https://doi.org/10.1201/b16239.

[22] W. Zhang, H. Yang, L. Lu, Z. Fang, Investigation on heat transfer around buried coils of pile foundation heat exchangers for ground-coupled heat pump applications, Int. J. Heat Mass Transf. 55 (2012) 6023–6031. https://doi.org/10.1016/j.ijheatmasstransfer.2012.06.013.

[23] J. Raymond, R. Therrien, L. Gosselin, R. Lefebvre, Numerical analysis of thermal response tests with a groundwater flow and heat transfer model, Renew. Energy. 36 (2011) 315–324. https://doi.org/10.1016/j.renene.2010.06.044.

[24] H. Wang, C. Qi, H. Du, J. Gu, Thermal performance of borehole heat exchanger under groundwater flow: A case study from Baoding, Energy Build. 41 (2009) 1368–1373. https://doi.org/10.1016/j.enbuild.2009.08.001.

[25] A.D. Chiasson, A. O'Connell, New analytical solution for sizing vertical borehole ground heat exchangers in environments with significant groundwater flow: Parameter estimation from thermal response test data, HVAC&R Res. 17 (2011) 1000–1011. https://doi.org/10.1080/10789669.2011.609926.

[26] D. Marcotte, P. Pasquier, F. Sheriff, M. Bernier, The importance of axial effects for borehole design of geothermal heat-pump systems, Renew. Energy. 35 (2010) 763–770. https://doi.org/10.1016/j.renene.2009.09.015.

[27] M. Reuss, M. Proell, Quality control of borehole heat exchanger systems, in: Proc. Effstock'09 Conf., Stockholm, Sweden, 2009.

[28] H. Fujii, H. Okubo, R. Itoi, Thermal response tests using optical fiber thermometers, in: Geotherm. Resour. Counc. Trans., 2006: pp. 545–551.

[29] H. Fujii, H. Okubo, K. Nishi, R. Itoi, K. Ohyama, K. Shibata, An improved thermal

response test for U-tube ground heat exchanger based on optical fiber thermometers, Geothermics. 38 (2009) 399–406. https://doi.org/10.1016/j.geothermics.2009.06.002.

[30] J. Acuña, Improvements of U-pipe Borehole Heat Exchanger, KTH Royal Institute of Technology, 2010.

[31] J. Acuña, Distributed thermal response tests – New insights on U-pipe and Coaxial heat exchangers in groundwater-filled boreholes, 2013. http://kth.diva-portal.org/smash/record.jsf?pid=diva2%3A602905&dswid=-2080.

[32] M. Li, A.C.K. Lai, Parameter estimation of in-situ thermal response tests for borehole ground heat exchangers, Int. J. Heat Mass Transf. 55 (2012) 2615–2624. https://doi.org/10.1016/J.IJHEATMASSTRANSFER.2011.12.033.

[33] O. Ozgener, L. Ozgener, J.W. Tester, A practical approach to predict soil temperature variations for geothermal (ground) heat exchangers applications, Int. J. Heat Mass Transf. 62 (2013) 473–480. https://doi.org/10.1016/J.IJHEATMASSTRANSFER.2013.03.031.

[34] J. Acuña, B. Palm, Distributed thermal response tests on pipe-in-pipe borehole heat exchangers, Appl. Energy. 109 (2013) 312–320. https://doi.org/10.1016/j.apenergy.2013.01.024.

[35] P. Hakala, A. Martinkauppi, I. Martinkauppi, N. Leppäharju, K. Korhonen, Evaluation of the Distributed Thermal Response Test (DTRT): Nupurinkartano as a case study, GTK. (2014).

[36] V. Soldo, L. Boban, S. Borović, Vertical distribution of shallow ground thermal properties in different geological settings in Croatia, Renew. Energy. 99 (2016) 1202–1212. https://doi.org/10.1016/j.renene.2016.08.022.

[37] J. Luo, J. Rohn, W. Xiang, M. Bayer, A. Priess, L. Wilkmann, H. Steger, R. Zorn, Experimental investigation of a borehole field by enhanced geothermal response test and numerical analysis of performance of the borehole heat exchangers, Energy. 84 (2015) 473–484. https://doi.org/10.1016/j.energy.2015.03.013.

[38] G. Radioti, S. Delvoie, R. Charlier, G. Dumont, F. Nguyen, Heterogeneous bedrock investigation for a closed-loop geothermal system: A case study, Geothermics. 62 (2016) 79–92. https://doi.org/10.1016/j.geothermics.2016.03.001.

[39] M.A. Soto, P.K. Sahu, S. Faralli, G. Sacchi, F. Bolognini, F. Di Pascale, High performance and highly reliable Raman-based distributed temperature sensors based on correlation-coded OTDR and multimode graded-index fibers, in: SPIE 6619, Third Eur. Work. Opt. Fibre Sensors, Napoli, Italy, 2007.

[40] P. Monzó, Modelling and monitoring thermal response of the ground in borehole fields, KTH Royal Institute of Technology, 2018. http://kth.diva-portal.org/smash/record.jsf?pid=diva2%3A1178493&dswid=8886.

[41] E. Rohner, L. Rybach, U. Schärli, A new, small, wireless instrument to determine ground thermal conductivity in-situ for borehole heat exchanger design, in: Proc. World Geotherm. Congr., Antalya, Turkey, 2005: pp. 1–4.

[42] P. Bayer, J.A. Rivera, D. Schweizer, U. Schärli, P. Blum, L. Rybach, Extracting past atmospheric warming and urban heating effects from borehole temperature profiles,

Geothermics. 64 (2016) 289–299. https://doi.org/10.1016/j.geothermics.2016.06.011.

[43] J. Raymond, L. Lamarche, M. Malo, Extending thermal response test assessments with inverse numerical modeling of temperature profiles measured in ground heat exchangers, Renew. Energy. 99 (2016) 614–621. https://doi.org/10.1016/j.renene.2016.07.005.

[44] J. Martos, Á. Montero, J. Torres, J. Soret, G. Martínez, R. García-Olcina, Novel wireless sensor system for dynamic characterization of borehole heat exchangers, Sensors. 11 (2011) 7082–7094. https://doi.org/10.3390/s110707082.

[45] J. Raymond, L. Lamarche, Development and numerical validation of a novel thermal response test with a low power source, Geothermics. 51 (2014) 434–444. https://doi.org/10.1016/j.geothermics.2014.02.004.

[46] J. Raymond, L. Lamarche, M. Malo, Field demonstration of a first thermal response test with a low power source, Appl. Energy. 147 (2015) 30–39. https://doi.org/10.1016/j.apenergy.2015.01.117.

[47] N. Aranzabal, J. Martos, Á. Montero, L. Monreal, J. Soret, J. Torres, R. García-Olcina, Extraction of thermal characteristics of surrounding geological layers of a geothermal heat exchanger by 3D numerical simulations, Appl. Therm. Eng. 99 (2016) 92–102. https://doi.org/10.1016/j.applthermaleng.2015.12.109.

[48] N. Aranzabal, J. Martos, H. Steger, P. Blum, J. Soret, Novel Instrument for Temperature Measurements in Borehole Heat Exchangers, IEEE Trans. Instrum. Meas. PP (2018) 1–9. https://doi.org/10.1109/TIM.2018.2860818.

[49] M.B. Hausner, F. Suárez, K.E. Glander, N. van de Giesen, J.S. Selker, S.W. Tyler, Calibrating single-ended fiber-optic raman spectra distributed temperature sensing data, Sensors. 11 (2011) 10859–10879. https://doi.org/10.3390/s111110859.

[50] N. van de Giesen, S.C. Steele-Dunne, J. Jansen, O. Hoes, M.B. Hausner, S. Tyler, J. Selker, Double-ended calibration of fiber-optic raman spectra distributed temperature sensing data, Sensors (Switzerland). 12 (2012) 5471–5485. https://doi.org/10.3390/s120505471.

[51] M.B. Hausner, S. Kobs, Identifying and Correcting Step Losses in Single-Ended Fiber-Optic Distributed Temperature Sensing Data, J. Sensors. (2016) 10. https://doi.org/10.1155/2016/7073619.

[52] N. Aranzabal, G. Radioti, J. Martos, J. Soret, F. Nguyen, R. Charlier, Enhanced thermal response test using fiber optics for a double U-pipe borehole heat exchanger analysed by numerical modeling, in: Proc. 29th Int. Conf. Effic. Cost, Optimisation, Simul. Environ. Impact Energy Syst. June 19. - 23. 2016, Portorož, Slov., 2016.

Chapter 7

Evaluation of the developed instruments and method in a real installation during a thermal response test

> *The general purpose of this chapter is to validate an enhanced version of the proposed inverse simulation approach. Using as input, the data from the specifically designed instrument (Geowire) in a BHE installation during a TRT. In addition, the two instruments developed in this Ph.D. work, Geowire and Geoball, are evaluated with the fiber optical thermometer used typically in DTRT tests. Likewise, the inverse simulation method is evaluated with another method to estimate the depth-dependent thermal conductivity.*

7.1. Paper IV: Novel instruments and methods to estimate depth-specific thermal properties in borehole heat exchangers

Authors: Nordin Aranzabal, Julio Martos, Milan Stokuca, Willem Mazzoti Pallard, José Acuña, Jesús Soret and Philipp Blum.

Published in: Geothermics, vol. 86, 101813 (2020).
DOI: https://doi.org/10.1016/j.geothermics.2020.101813

Impact factor: 3.682

Quartile (category: "Geosciences, Multidisciplinary"): Q1 (2019)

Summary:

This fourth paper introduces improvements to the proposed inverse simulation method in Chapter 2. Also, the method is evaluated using the data from the specifically designed instrument (Geowire) as input to measure the required temperature profiles. The proposed approach in Chapter 2 is based on an iterative simulation process, where thermal conductivity of the defined geological layers needs to be adjusted manually until it fits with experimental measurements. One single simulation of the model may take on the order of days, which may result in a significantly time-consuming task, whereas it

might not provide a fully accurate adjustment. For this reason, the inverse simulation method is improved by adding an optimization module with a parameter estimation solver, to carry out an automatic adjustment of the thermal conductivity along the depth of the borehole. In this manner, the improved version of the numerical approach runs automatically by reducing the simulation time considerably as well as improving the accuracy of the results.

Additionally, two instruments developed throughout this Ph.D. work (Geoball and Geowire) are evaluated during the course of a TRT with the widespread fiber optical thermometers. A BHE of 50 m deep is used in a test site in Vallentuna, Sweden. The borehole subsurface stratification is characterized by clay until a depth of 6 m. A granite and pegmatite bedrock then follow until the end of borehole, which is naturally filled with groundwater. In the borehole a single U-pipe and an auxiliary pipe are inserted. The U-pipe is connected to a TRT equipment while the auxiliary pipe (observed pipe) is used to record the temperature profiles required for the inverse simulation procedure. Fiber optical cables are introduced inside the down-flow leg of the U-pipe and inside the observed pipe for the evaluation of the Geowire and Geoball. From the experiment results, the proposed instruments showed several advantages over the fiber optics. For example, they are more convenient to integrate in a TRT, easier to use and are potentially a more cost-effective solution. Another positive aspect is that they also measure the temperature instantaneously and with higher accuracy.

On the other hand, the inverse numerical simulation method is evaluated with a computer program using fiber optics data as input. The computer program is based on the ILS model to calculate the depth-dependent thermal conductivity. The average value of the local effective conductivity estimates calculated with both methods is significantly close to the global effective thermal conductivity from standard TRT: 1.27% below for the computer program and 0.28% below for the numerical procedure. Furthermore, the inverse numerical method is implemented using the data from the Geowire as input. In this case, the local effective conductivity estimates showed the highest dispersion with respect to the global effective conductivity of a standard TRT. A highly conductive zone of 5 m long is therefore detected using the novel method and instrument. The proposed method also demonstrated the advantage of estimating the conductivity with less input data than the computer program based on the ILS approach.

Novel instruments and methods to estimate depth-specific thermal properties in borehole heat exchangers

Nordin Aranzabal [1, *], Julio Martos [1], Milan Stokuca [c], Willem Mazzotti Pallard[2, 3], José Acuña [2, 3], Jesús Soret [1], Philipp Blum[4]

[1] Universidad de Valencia (UV), Department of Electronic Engineering, 46100 Burjassot, Spain
[2] Royal Institute of Technology (KTH), Department of Energy Technology, 10044 Stockholm, Sweden
[3] Bengt Dahlgren Geoenergi, Hammarby Allé 47, 12030 Stockholm, Sweden
[4] Karlsruhe Institute of Technology (KIT), Institute of Applied Geosciences (AGW), 76131 Karlsruhe, Germany

[*]Corresponding author. E-mail address: nordin.aranzabal@uv.es

Abstract

Standard thermal response tests (TRT) are typically carried out to evaluate subsurface thermal parameters for the design and performance evaluation of borehole heat exchangers (BHE). Typical interpretation methods apply analytical or numerical solutions, which assume that the ground is homogeneous, isotropic and infinite. However in reality, the underground is commonly stratified and heterogeneous, and therefore thermal properties might significantly vary with depth. Thus, novel instruments and methods are necessary to characterize thermo-physical properties along the BHE. In this study, two novel in-borehole temperature measurement instruments, Geoball and Geowire, are assessed during the performance of a distributed TRT (DTRT). The latter is evaluated in comparison to the widely used fiber optical thermometers. Our results suggest that both novel instruments have several advantages. For instance, both devices are able to instantaneously measure temperature with a higher spatial resolution. In addition, our study evaluates two methods to estimate depth-specific thermal conductivities: (1) a computer program based on infinite line source (ILS) approach and (2) a recently suggested inverse numerical procedure. For the latter less data is required, while demonstrating an accurate resolution to even detect thin conductive geological layers. Moreover, the average value of the depth-specific local effective estimates for both methods is significantly close to the effective subsurface conductivity of 3.20 W/m-K calculated based on standard TRT: 1.27% below for the computer program and 0.28% below for the numerical procedure.

Keywords: Ground source heat pump (GSHP); Borehole heat exchanger (BHE); Distributed thermal response test (DTRT); Layered subsurface; Thermal conductivity; Energy efficiency.

1. Introduction

Detailed information of subsurface thermo-physical properties is crucial to determine the right trade-off between cost-effectiveness and energy performance of borehole heat exchangers (BHE) [1,2]. Determining geological, hydrogeological and thermal conditions, such as thermal conductivity, groundwater effects and initial temperature, are fundamental for an optimal design (size, cost and energy efficiency) of ground source heat pump (GSHP) systems. Thermal conductivity is a key parameter of heat transfer rate of the BHE with the

subsurface (e.g. heat diffusion) [3,4], where heat transfer occurs at a lower rate for lower values of thermal conductivity. Nonetheless, this is only true if groundwater is not present, as axial advection-influenced conditions significantly increase heat transfer performance of the subsurface [5].

For instance, field samples can be analyzed in the laboratory to measure soil thermal conductivity [6]. However, laboratory tests of field samples only provide local information, i.e. only for particular zones without contemplating heterogeneities at a larger scale, and do not provide any information on local groundwater effects. In addition, laboratory experiments can be time consuming and expensive [7], and disruptions during sampling processes or transportation might negatively affect the results.

Nowadays, the standard method to calculate thermal properties of the subsurface is the thermal response test (TRT), originally suggested by Choudhary (1976) [8] and Mogensen (1983) [9]. The method was further refined with portable equipment in the next decade [10,11]. Since then, the in-situ TRT has been extensively used worldwide both in academic and commercial applications to calculate the optimal (cost and energy performance oriented) length and distribution of BHE [12]. The test is implemented in a pilot closed loop BHE and begins under the assumption of ground temperature in equilibrium. A fluid is circulated and heated at a constant rate for measuring the transient thermal progression at the inlet and outlet of the ground loop. Based on field measurements, two important parameters are calculated: effective ground thermal conductivity (λ) and effective borehole thermal resistance (R_b). These parameters are often inferred using analytical approaches such as the Kelvin line source [13,14], the cylindrical source [15] or the moving infinite line source [16]. Previous models assume a constant heat injection rate in a homogeneous, isotropic and infinite medium, where heat is merely transmitted by conduction [17]. Numerical models with parameter estimation-based solvers (e.g. inverse-modeling or history-matching problems) have also been developed addressing geometrical and temporal aspects generally ignored by analytical models [18–21]. Due to these assumptions and the conventional TRT constraints, the derived parameters represent an effective and integral value for the ground surrounding the BHE. However, the typical subsurface geological formation is heterogeneous in such that heat transfer occurs at different rates along the BHE [22,23]. Moreover, convective effects are neglected in TRT calculations and in this case can lead to erroneous approximations for long-term setups [16,20,24].

The conventional TRT is widely popular, however it does not always provide enough or accurate information to estimate the optimum size for the best trade-off between energy performance and cost of GSHP systems. Some studies reported the importance of considering depth-specific thermal properties of the subsurface, and demonstrated how the size and number of boreholes can be reduced for the same energy demand applications [25,26]. For example, the length of the BHE can be limited, when a poorly conductive layer is reached, reducing drilling/pipping cost without compromising the efficiency of GSHP system. A correct estimation of the depth-specific heat transfer rate between the BHE and the subsurface can avoid oversizing, and consequently results in more techno-economic and energy-efficient installations.

In the last decade, several tools and analysis methods have been developed to evaluate the depth-specific heat transfer ratio of BHE. These advances are triggered by the rapid

growth of GSHP applications, and the necessity in boosting their commercial attractiveness. A significant development is the distributed thermal response test (DTRT) to complement standard TRT field measurements with temperature profiles along the BHE. Rohner et al. [27] designed both a device for measuring the temperature along pipes, and a method to estimate the depth-dependent effective thermal conductivities. The device utilizes a small wireless probe with a weighted temperature and pressure data-logger that sinks in vertical pipes. The probe is flushed back to the surface by turning on a pump. However, this method requires precise heat flow maps of the ground in equilibrium, which are hard to find in many regions, as for instance, in some areas of Canada and the USA. Martos et al. [48] developed a wireless-probe with a spherical shape and data logger (temperature and position). The probe has same density as the fluid, thus, being carried at the flow rate inside the pipe loop (vertical or horizontal). The exact location along the pipes is then calculated with information of pipe geometry and the flow rate. In this study, the device is tested in a BHE installation during a TRT by measuring profiles that agreed with the geological conditions of the site. Later, the company enOware developed a commercial version of a similar data logger probe (temperature and pressure), called GEOsniff®. The probe also has the shape of a ball, but with higher density than the fluid allowing it to sink in the vertical pipes. Once the probe reaches the bottom, a pump is turned on to circulate the fluid and to expel the ball to a tank. Additionally, Raymond et al. [29] conducted a study using a commercial wired-probe with temperature and pressure sensors called RBRduet, and developed an inverse numerical model to extend the effective depth-dependent thermal properties of a TRT to a nearby borehole. An advantage of this method is that it can use regional heat flow maps (when are available) or a depth-specific temperature profile of an adjacent borehole.

Fujii et al. [30,31] carried out a pioneer field experiment integrating fiber optic thermometers along the depth of the down-flow U-pipe in a vertical BHE. The recorded datasets are used as input to a computer program that implements the cylindrical source function [32] to determine the effective depth-specific thermal conductivity. This method reflected zones likely affected by hydrological conditions (faster temperature variations) during the recovery of the temperature. Acuña & Palm [33–35] improved DTRT measurement procedure by installing fiber optics along the entire U-pipe. Fiber optical cables are inserted inside different borehole heat exchangers for measuring fluid thermal progression along the entire pipe circuit. In this study, effective depth-specific thermal conductivity and thermal resistance are determined by evaluating the temperature increment between the undisturbed ground and the heated/cooled fluid as a function of time. A numerical algorithm is processed based on the line source equation [32] and an optimization solver (least-squares parameter estimation) calculates depth-specific effective values of λ and R_b. Fiber optics have become a valuable tool for obtaining the distributed temperature along the length of BHE with more research activities reported in the recent years [36–40]. Raymond et al. [41,42] elaborated an approach to implement a distributed TRT by reducing the electrical energy consumption needed to heat the BHE in comparison with the standard TRT. A cable-assembly divided in heating and non-heating sections is installed in the borehole, with temperature sensors embedded at the middle length of each section. Temperature datasets are recorded throughout the heat recovery period. The heat injection rate, effective subsurface thermal conductivity and effective heat capacity are evaluated using a parameter sensitive analysis [43]. A possible set back in this experiment is that the thermal conductivity is discretized every 10 m and therefore limit the ability to locate small

highly conductive geological layers. Furthermore, the effective (local) borehole resistance is not evaluated, even though it is an important design parameter. Wilke et al. [44] provide a comprehensive review on the historical and technical developments and the current status of distributed (DTRT) and enhanced (ETRT) thermal response tests (TRT).

Aranzabal et al. [45] introduced a novel DTRT method called observer pipe TRT (OP-TRT) and an analysis procedure to determine depth-specific thermal properties of the subsurface. A U-pipe and an auxiliary pipe filled with water are introduced in a borehole while a TRT is conducted in the U-pipe. In this method, the depth-dependent temperature is measured in the auxiliary pipe, known as the observer pipe. The undisturbed temperature, and the temperature profile at 72 h are used as the input to an inverse numerical model with a least-squares parameter estimation solver to determine the effective thermal conductivity of geological layers. The resolution of the calculated depth-specific effective λ is correlated with the spatial resolution of the measured temperature along the observer pipe. To further enhance the accuracy of the latter method, Aranzabal et al. [46] designed and demonstrated the applicability of a novel data logger instrument, called "Geowire", for automatic depth-dependent temperature measurements along vertical BHEs. Furthermore, Aranzabal et al. [47] carried out a comparison study using standard Pt100-sensors, fiber optical thermometers, Geowire, Geoball (an enhanced version of the probe designed by Martos et al. [48]) and GEOsniff®. In this study, qualitative and quantitative differences of the various instruments are evaluated in a 30 m length test borehole. The new instruments (Geowire, Geoball and GEOsniff®) showed several advantages over the standard instruments, such as easier integration in existing BHE and inexpensive, as well as higher spatial and temperature resolution, among others.

The DTRT has proven to be a useful technique to improve the efficiency and cost of GSHP installations. However, more investigations need to be carried out until a method is generalized for its practical use during the design phase. Likewise, more research and developments are necessary until a design software including heterogeneities and a more affordable equipment reaches the market. In this study, the Geoball [48] and the Geowire [46], are tested together with the widespread fiber optical thermometer in a BHE. The new instruments are a potential cost-effective alternative to fiber optics and might also provide some additional advantages. To asses these expected advantages, fiber optical cables are inserted in the same pipes as the novel instruments for results evaluation during the course of an OP-TRT. Fiber optics and the Geoball are installed in the down-flow pipe and fiber optics and the Geoball in the observer pipe, to also compare temperature differences between these two pipes. From the collected data, two TRT interpretation methods are evaluated: the analysis method of Acuña et al. [34] and the numerical procedure introduced by Aranzabal et al. [45]. Both methods are compared using the obtained fiber optics data in the observer pipe however, the method proposed by Aranzabal et al. [45] is evaluated using the collected data from the Geowire with a spatial resolution of 0.5 m. Hence, a method and a device to determine effective thermal conductivity of depth-dependent layers with a spatial resolution of 0.5 m is studied.

2. Methodology

2.1. OP-TRT (Observer pipe thermal response test)

A borehole is used for the implementation of the OP-TRT at a test site in Vallentuna, Sweden. The site geology formation is based on the Bergslagen lithotectonic unit within the Svecofennian orogeny, characterized by clay until a depth of approximately 6 m. A granite and pegmatite bedrock then follow until the end of the borehole, which is naturally filled with groundwater until a depth of 4.3 m. The layout of the borehole for the experiment is presented in Fig. 1. The borehole has a diameter of 115 mm and a length of 50 m, where a single U-pipe collector and an auxiliary pipe (observer pipe) of 40 mm × 2.4 mm are lowered until a depth of 48.5 m. The U-pipe is connected to portable TRT equipment and the auxiliary pipe is used to observe the thermal evolution near the border of the borehole. The test is carried out with an approximate duration of 72 h, with a constant heating power of 1.5 kW and at a constant water mass flow rate of 0.54 l/s. Throughout the test, the heating power, flow rate, pressure, inlet temperature, outlet temperature, and environmental temperature are recorded every minute by a data logger. The distributed temperature along the length of the borehole is measured by fiber optical thermometers and two new instruments: the Geowire and the Geoball.

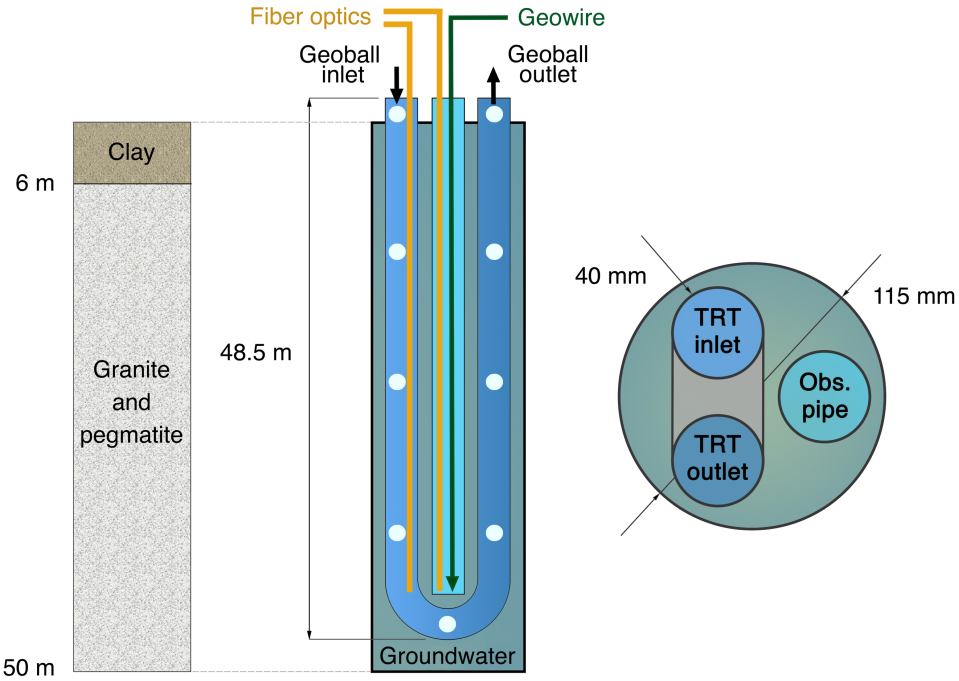

Fig. 1. Bedrock and layout of the borehole in the experiment. The dimensions of the borehole and pipes in the horizontal cross section (right) are in a proportional scale with the experimental set-up.

Fiber optical thermometers are installed inside the down-flow U-pipe until 41 m and inside the observer pipe (filled with water) until 43 m. The working principle of fiber optics to integrate the temperature over time and length sections of fiber, is based on the Raman optical domain reflectometry [34]. There is a trade-off between temperature resolution, spatial resolution, range and speed of measurement (e.g. better temperature resolution is achieved with higher integration times or longer length sections). In this case, the fiber optic equipment Halo-DTS of Sensornet is adjusted to integrate the temperature every 10 min and for fiber sections of 2 m. Fiber optics are connected to the equipment in a single-ended configuration. This means that the temperature is measured through the fiber with a single connection to the instrument.

The Geoball, an improved version (smaller size, less weight and longer autonomy) of the developed device by Martos et al. [48], is circulated through the heated U-pipe at different instances during the test. It is an autonomous probe that flows inside geothermal pipes to store samples of temperature with the corresponding position for each sample. The electronic circuit is embedded in a spherical enclosure of 20 mm diameter, while the temperature sensor remains in direct contact with the fluid to obtain instantaneous samples of temperature. The temperature sensing element is a planar Pt1000 from Heraeus, A-class according to IEC 60751, mounted on a ceramic subtract of size of 2.1 × 2.3 × 0.9 mm. The temperature resolution provided is smaller than 0.05 K. The working principle is based on the probe having the same density as the fluid thereby allowing transport at the same flow rate. The device is able to calculate its exact location along the pipes with the information of the pipe geometry and the flow rate. Moreover, the electronic circuit inside the device can detect the initial and end point of the pipe loop for initiating and stopping the acquisition process. In this experiment, the probe is introduced at the inlet of the U-pipe and extracted at the outlet of the U-pipe by a bypass circuit without interrupting the flow of the TRT. When the probe is recovered after a measurement process, the data is downloaded wirelessly, while the battery is simultaneously charged. The response time of the probe is measured to be faster than 0.5 s. Laboratory tests demonstrated the probe enclosure to hold a pressure of at least 40 bar (e.g. a depth of 400 m) without leaking, although it is expected to be higher. In this study, the Geoball is adjusted to measure the temperature every 0.5 m (every 1.5 s), which is 3 times the response time of the probe.

On the other hand, the Geowire [46] is an electro-mechanical device with a data logger designed to automatically displace a wired temperature sensor down and up along vertical geothermal pipes at pre-configured sequences. In this case, the sensor of the Geowire is introduced in the observer pipe to measure the distributed temperature at different instances during the test. The cable of the sensor is rolled up on a reel, a motor rotates the reel and an encoder measures the released cable length to determine the location of the sensor along the pipes. The instrument is able to measure instantaneous samples of temperature with a maximum resolution of 0.06 K, a spatial minimum resolution of 0.5 mm, an acquisition time of less than 1 s and the thermal response time of the probe is reported to be smaller than 2 s. The user program allows the customization of the acquisition process by configuring parameters such as the time between profiles, spatial resolution of different length intervals and the displacing speed of the sensor. In this experiment, the Geowire is established to displace the sensor with a spatial resolution of 0.5 m and a displacement speed of

1.28 m/min. Thus, the time to measure a temperature profile from 4.5 to 48.5 m is of 49 min. However, this time does not suppose a drawback when applying its particular analysis method (inverse numerical procedure) to measured data. This method only requires two temperature profiles as input, (1) subsurface in equilibrium and (2) at the end of the TRT, where the thermal evolution in 49 min is negligible. In a previous report [46] the minimum time required to achieve a thermal equilibrium after moving the sensor to a new position, and to avoid possible perturbations due to turbulences produced by the displacement of the small sensor, is calculated to be 5 s. Hence, in this case, the sensor remains still for 5 s in each position. After that time, the temperature is measured five times with a sampling interval of 1 s and the average value is stored in the database together with its location.

The Geowire, the Geoball, and the inlet and outlet RTD-sensors of TRT equipment are calibrated in the laboratory with a thermal bath and a thermometer of ±0.01 K accuracy and ±0.005 K resolution. Moreover, the two independent channels of the equipment to read the fiber optical cables are calibrated dynamically in the field using an ice bath and a thermometer of ±0.025 K accuracy and ±0.001 K resolution.

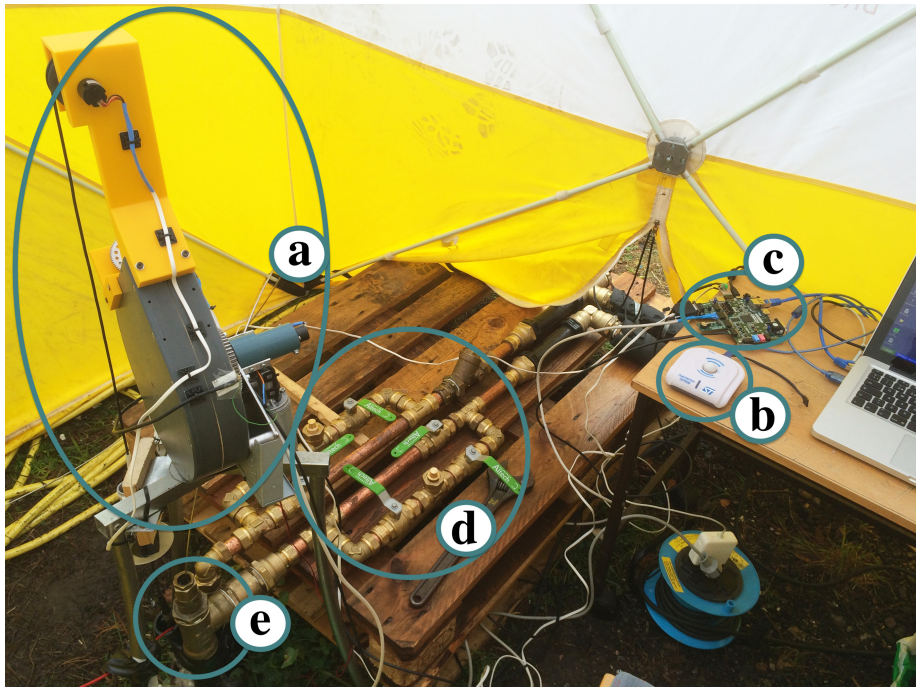

Fig. 2. Field test installation before the beginning of the test. (a) Geowire; (b) Geoball and its data logger reader; (c) Control processing system (d); Geoball insertion and extraction valves; (e) Borehole inlet and outlet pipes.

Fig. 2 shows the field test installation after mounting the instruments and before the beginning of the TRT. From the standard TRT measurements (heating power, fluid flow, inlet, outlet and ambient temperature) based on the infinite line source (ILS) model of Kelvin

[49,50], an effective thermal conductivity of 3.20 W/m-K and an effective borehole resistance of 0.10 m-K/W are calculated analytically for the entire subsurface surrounding the borehole.

2.2. Methods to estimate depth-specific thermal properties

Two methods are carried out to determine the depth-specific effective thermal conductivity from OP-TRT results, namely: an analytical solution and an inverse numerical procedure. Both these methods are evaluated using the recorded temperature profiles from the fiber optical cable installed in the observer pipe. Additionally, the inverse numerical procedure is implemented using the obtained temperature measurements with the Geowire.

The analytical solution is based on the time-superposed ILS approach for parameter estimation in TRT presented by Acuña et al. [34]. A computer program calculates the transitory response of the temperature difference between the undisturbed ground and the borehole wall based on the ILS model [32]. The program superposes the temperature responses for different time intervals of transitory heat power steps. The process is carried out at each borehole section. The heating power for each segment is defined by the measured temperatures at the edges of the section. Further, the sum of squared error (SSE) between the experimental and the calculated data is minimized by adjusting thermal conductivity (and borehole resistance if calculated during heating) of every section.

The second method is implemented based on the inverse numerical procedure suggested by Aranzabal et al. [45] while incorporating some improvements. The distributed temperature in the observer pipe is measured more accurately with specific instrumentation (fiber optics and the Geowire). Moreover, a parameter optimization solver is added to the model instead of applying an iterative algorithm manually to fit experimental results. This allows for an automatic more accurate determination of the depth-specific effective thermal conductivity in one simulation iteration. The method is simplified and divided into two main steps (Fig. 3):

Step (a): model calibration (to follow inlet and outlet thermal evolution of the TRT).

1. Development of a 3D finite element model with the experimental BHE geometry.
2. Configure the model with measured parameters during the TRT such as dynamic heating rate, dynamic flow rate, dynamic ambient air temperature and initial subsurface temperature.
3. Borehole domain: assign thermal properties of the materials in the borehole (e.g. grouting material, groundwater, pipes, fluid in the pipes…).
4. Global subsurface domain:
    - Assign analytically calculated effective thermal conductivity (λ) based on the Kelvin infinite line source approach [49].
    - Assign density and heat capacity of geological materials found during the perforation.

Step (b): parameter estimation (depth-specific thermal conductivity). To carry out this step, it is required to measure the distributed temperature in an observer pipe.

1. Divide the subsurface in layers along the vertical axis. The number of layers is determined by the number of spatial samples measured in the observer pipe. Each layer is bounded between two consecutive samples and shifted up half of the spatial resolution.
2. Assign each measured sample of temperature along the observer pipe at 72 h as the objective function of each individual layer. Thermal conductivity of each layer is assigned as a control variable.
3. Run simulation. Control variables (thermal conductivity of each layer) are fine-tuned by the optimization solver to fit the least-squares multiple objectives function, $f = \sum_{i=1}^{n}(T_{exp,n} - T_{sim,n})^2$, where n is the layer number and T_n the reference temperature for each layer.

As result, numerical and experimental profiles in the observer pipe fit and the model output is the depth-specific effective thermal conductivity profile.

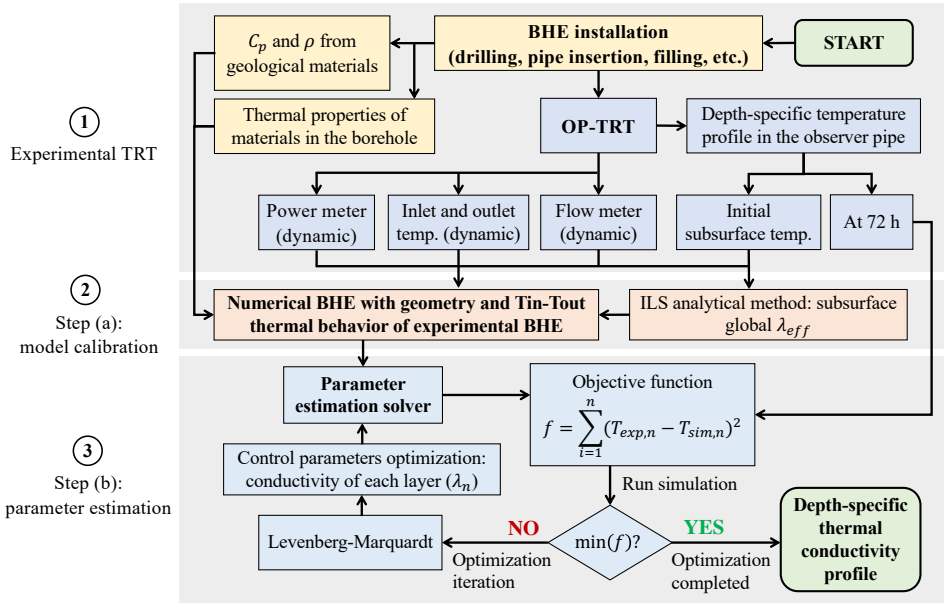

Fig. 3. Layout of the inverse numerical procedure for the OP-TRT.

2.3. Numerical model

To carry out the reported procedure by Aranzabal et al. [45] a 3D finite element model is developed using COMSOL Multiphysics®. From the physics-based modules, the available heat transfer in fluids (HT) and the non-isothermal pipe flow (NIPF) are included to replicate the TRT thermal behavior and the BHE geometry (Table 1). Heat is transferred merely by conduction and the convective effects are neglected. Nevertheless, if convective effects or other effects that may increase/decrease the heat transfer rate of the subsurface are present, the model will take them into account as an increment/decrement of the thermal

conductivity. Additionally, an optimization module is integrated to implement the inverse parameter estimation method. On the other hand, the thermal parameters of groundwater inside the borehole are considered constant.

To simplify computer operations and reduce simulation time, the 3D geometry of the model is divided by a 2D symmetry plane onto the XZ axes and the middle of the U-pipe.

Fig. 4 illustrates the model after applying the symmetry, where the total volume is reduced by half and the two domains are represented as two concentric semi-cylinders. The bigger half-cylinder depicts the subsurface, while the smaller half-cylinder represents the perforation filled with groundwater. The subsurface domain radius and the model meshing configuration are based on an earlier report conducted by Aranzabal et al. [45], in which optimal COMSOL performance is studied for a vertical BHE. The model mesh, formed by generating tetrahedral elements refined for the borehole and the pipes, contained 676,995 elements.

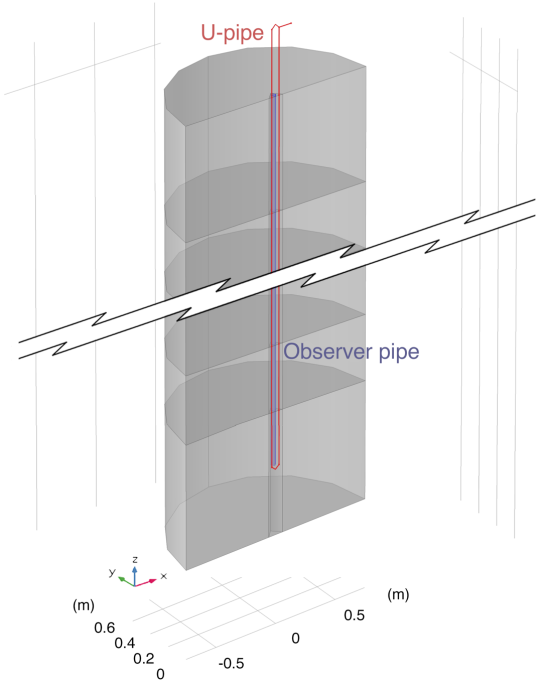

Fig. 4. 3D model of the experimental BHE.

Table 1
Simulation parameters.

Parameter	Value
Borehole depth (m)	50 m
Borehole radius	57.5 mm
Observer pipe depth	48.5 m
Pipes inner radius	17.6 mm
Pipes outer radius	20 mm
U-pipe length	48.5 m
Subsurface radius	0.75 m
Subsurface depth	50 m
Subsurface effective thermal conductivity	3.2 W/m-K
Groundwater effective thermal conductivity	2.9 W/m-K
Groundwater heat capacity	850 J/kg-K
Groundwater density	2600 kg/m^3

A thermal conductivity of 2.9 W/m-K is assigned to the borehole domain. This values is estimated based on the Nusselt number for natural convection in groundwater-filled boreholes [51] by calculating the modified Rayleigh number from [52].

Due to the applied symmetry, the injected heat power and fluid flow are divided by two with respect to the experimental values. The injected heat source is set with a constant power of 0.75 kW and the water pump with the measured dynamic flow rate (average value of

0.27 l/s). With the NIPF module the pipes are represented as a line; then by setting the pipe properties (shape, dimensions and flow resistance), pump configuration (location, fluid flow and direction), fluid properties, pressure, heat source and initial temperatures, COMSOL implements the required calculations to simulate the heat transfer in the pipe surroundings.

The model time dependent solver is configured to simulate a TRT for three days and to record data every 20 min. The initial temperature of the subsurface domain is established as the measured distributed temperature profile before the pre-circulation (undisturbed) and the initial temperature of the borehole domain as the measured distributed temperature profile after the pre-circulation. In addition, the measured transitory outdoors temperature during the experimental TRT is assigned to the top boundary domain of the semi-cylinder.

The model calibration step is conducted by assigning the analytically calculated effective thermal conductivity of 3.2 W/m-K and the volumetric heat capacity of granite-pegmatite to the subsurface. Fig. 5 illustrates the superposition of the obtained numerical (after the calibration) and experimental results at the inlet and the outlet of the TRT.

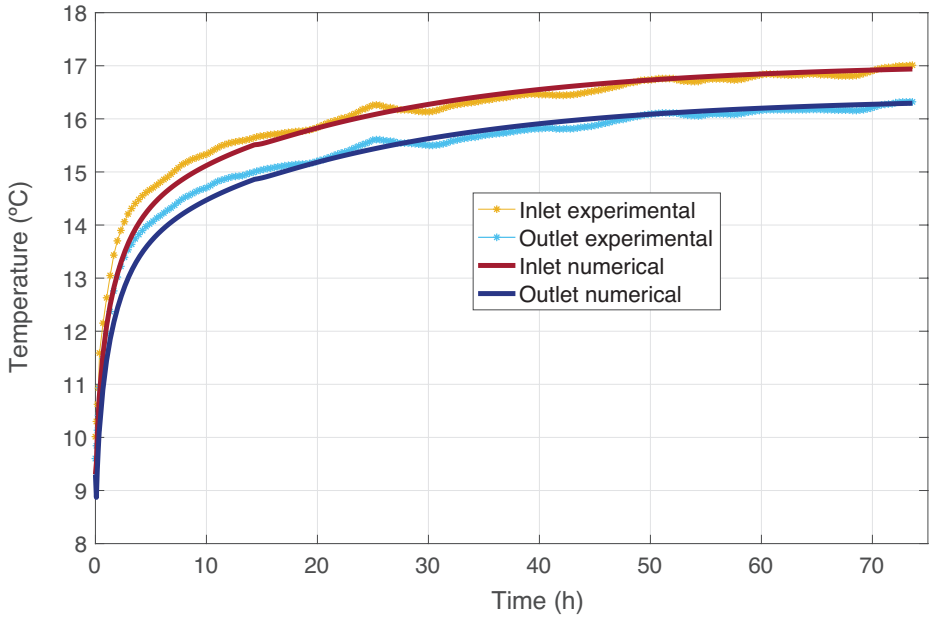

Fig. 5. Superposition of inlet and outlet temperature evolution for the experimental TRT, and numerical model results after the calibration.

To implement the proposed OP-TRT, it is recommended to keep a uniform distance between the geothermal pipes with separators of polyethylene distributed along the depth. Unfortunately, in this experiment it was not possible, hence the uncertainty is reduced by optimizing the position of the observer pipe using a Nelder-Mead derivative-free (gradient-free) method. The distance between the observer pipe and the center of the U-pipe legs is the control variable, and the average value of the measured in-situ distributed temperature profile at 72 h is the objective function. Only a minute difference of 0.0008 K is calculated

between the average value of the experimental measurements and the average value of the numerical results.

The model is calibrated for estimating the depth-specific thermal conductivity by fitting inlet and outlet thermal evolution during the entire TRT, as well as the average value of the distributed temperature profile in the observer pipe between the model and experimental data at 72 h. The domain of the subsurface is divided into as many layers along the depth (Z axis) as the number of the temperature samples acquired throughout the observer pipe.

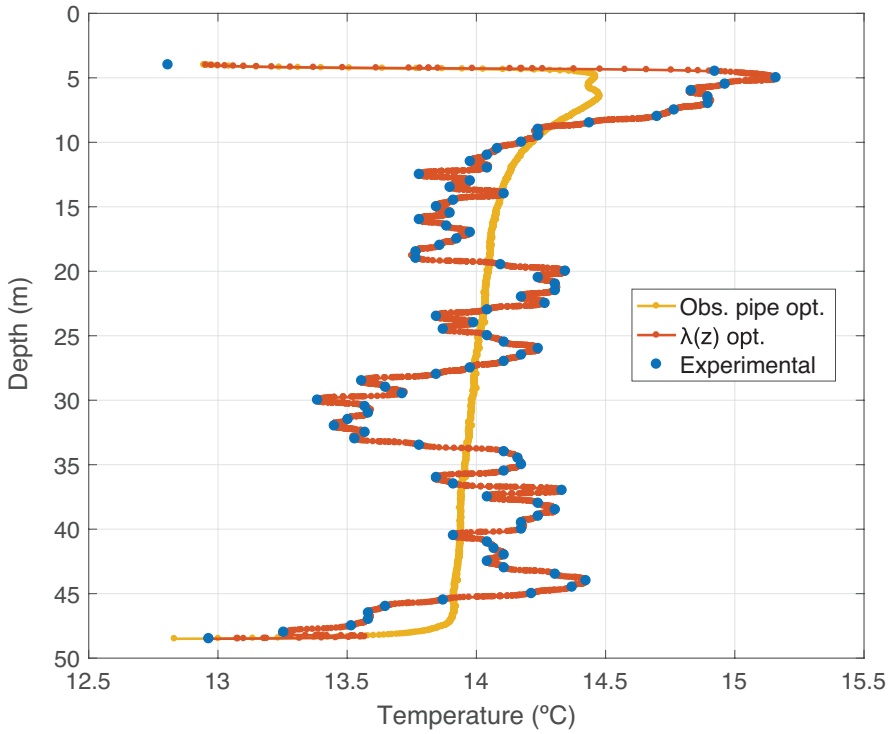

Fig. 6. (1) Yellow curve: represents the results from the model after the optimization of the observer pipe position to fit the average value of the experimental data. (2) Red curve: represents the results from the model after the optimization of $\lambda(z)$ to fit experimental data. (3) Blue points: represent the recorder experimental data by the Geowire in the observer pipe at 72 h.

After the model calibration in order to calculate the depth-specific conductivity, two models are developed using the Levenberg-Marquardt optimization method (minimization type, sum of objectives, optimality tolerance of 0.001 W/m-K and maximum number of objective evaluations of 1000): (1) using the collected data from the fiber optics and (2) using the data from the Geowire. The fiber optics integrates the temperature every 2 m, therefore the subsurface is divided into 20 layers. A line along the center of the observed pipe is added to simulate the fiber optical cable and the average temperature of each 2 m is used as target for the fitting. Then, the thermal conductivity of each layer is assigned as the control variables to fit each layer target temperature with the experimental data. Similarly,

the model using Geowire data as input is divided into 90 layers with 90 points added inside the center of the observer pipe. The temperature in each point is used for the model as the reference to fit the thermal conductivity of each layer with the experimental data. Subsequently, an estimation of the depth-specific effective thermal conductivity for each measured layer is obtained from the results of the model.

As an example, Fig. 6 presents: (1) the superposition of the model results after the optimization to adjust the observer pipe position to fit the average value of the experimental data in the observer pipe by the Geowire, (2) the results of the model optimization to adjust the depth specific thermal conductivity to fit experimental data and, (3) the experimental measurements in the observer pipe by the Geowire at 72 h. Experimental temperature data obtained with the Geowire compared with the temperature profile calculated by the numerical model after optimization of $\boldsymbol{\lambda(z)}$ presented a root mean squared error (RMSE) deviation of only 0.0001 K.

3. Results and discussion

3.1. Experimental results

Fig. 8 shows the temperature depth-profiles using fiber optics throughout the DTRT every 10 min. As expected, the temperature increases faster in the down-flow section of the heated U-pipe than in the observer pipe (around 2 K higher). In the observer pipe, more pronounced temperature fluctuations were measured compared to those in the down-flow pipe, due to the different thermal properties of the geological layers (see also Fig. 9 and Fig. 10). This effect can be explained and calculated by building an equivalent model of the borehole based on a network of thermal resistances and capacitances across the horizontal section [45]. As a simple example, from the simplified thermal resistance circuit in Fig. 7, where T_{df} is the temperature in the TRT down-flow pipe, T_{obs} is the temperature in the observer pipe, T_{fg} is the far ground temperature, R_b is the borehole thermal resistance and R_g is the ground thermal resistance, the heat flow (Q) from the observer pipe until the far ground can be calculated with the following equation:

$$Q = \frac{T_{fg} - T_{obs}}{R_g} \rightarrow T_{obs} = T_{fg} - (Q.R_g) \quad (1)$$

By clearing T_{obs} it is possible to observe the impact of R_g in T_{obs}, which significantly varies for layers with differing thermal resistance. On the other hand, the temperature inside the down-flow pipe corresponds to the temperature of a specific volume of fluid in movement, where the heat flow is highly influenced by the fluid flow rate. In this experiment the heated volume of fluid lost less than 1 K every time it completed a loop in the closed circuit. This means that for intervals of 5 m the temperature changed less than 0.05 K explaining the almost straight line which was observed for the temperature distribution along the down-flow graph presented in Fig. 8. On the contrary, the fluid inside the observer pipe remains static, monitoring progressively how the injected heat along the down-flow pipe is transferred at different rates due to alterations in thermal properties of the ground.

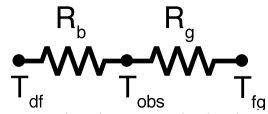

Fig. 7. Simplified thermal resistance circuit across the horizontal section of the borehole.

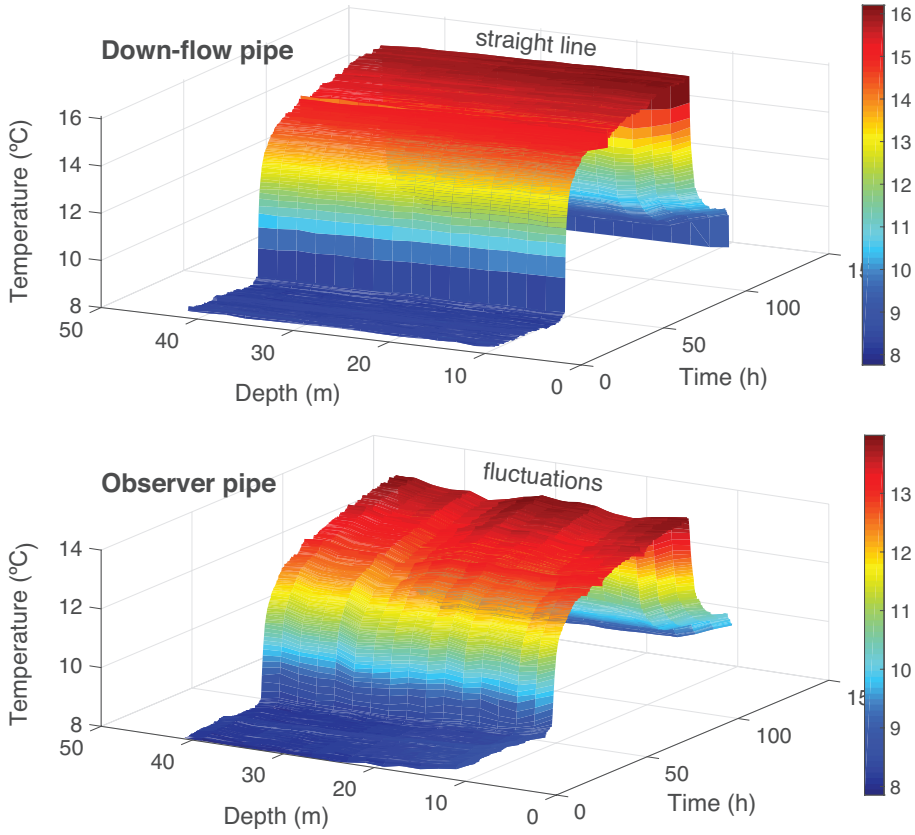

Fig. 8. Obtained distributed temperatures by the fiber optics in the down-flow pipe (top) and observer pipe (bottom) during the DTRT every 10 min.

The measurements at the first 9 m of the fiber optics are removed from the study due to the high influence of outside variable temperature in this layer.

Fig. 9 illustrates the recorded temperature datasets along the heated U-pipe of the TRT by the fiber optics (down-flow) and the Geoball (down-flow and up-flow), as well as the RTD-sensors at the inlet and the outlet of the TRT equipment. The data is presented after 24 h of non-heated fluid circulation (pre-circulation), as well as 3 h, 24 h, 48 h and 72 h from the beginning of the TRT. A strong agreement is found between the first and the last measurements of the Geoball and the RTD-sensors at the inlet-outlet of the installation with an RMSE deviation of 0.0348 K, a SSE of 0.0007 and a coefficient of determination (R^2) of

0.9992. Likewise, there is a strong agreement between the fiber optics and Geoball temperature-depth measurements, with an RMSE difference of 0.0488 K, an SSE of 0.1978 and an R^2 of 0.9997.

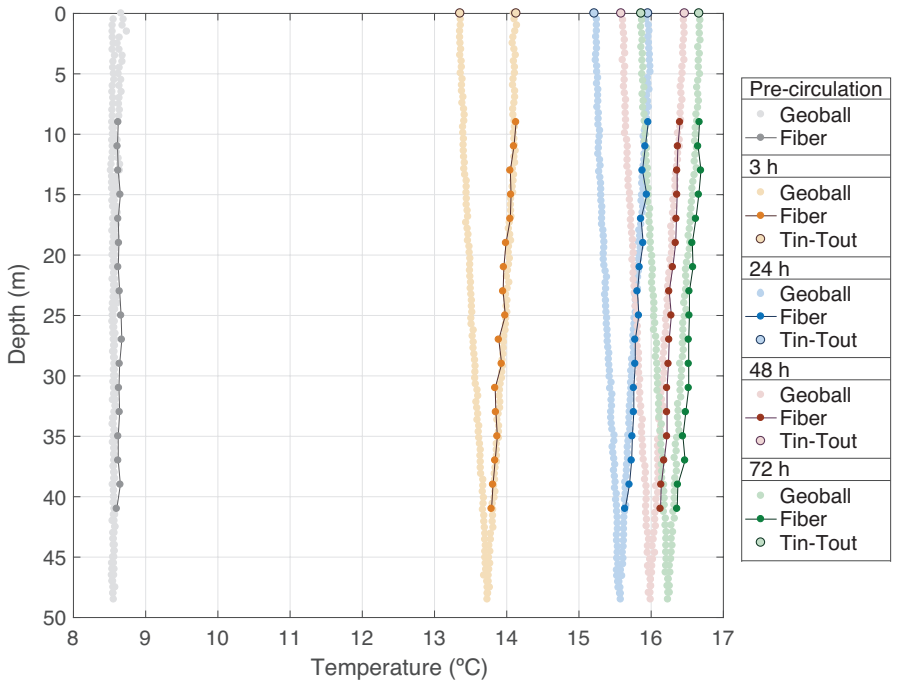

Fig. 9. DTRT thermal evolution for the fiber optics (down-flow) and the Geoball (down-flow and up-flow) inside the heated U-pipe, as well as the inlet and outlet temperature measured by the RTD-sensors in the TRT equipment.

In Fig. 10 the temperature profiles inside the observer pipe obtained using the fiber optics and the Geowire throughout the TRT are presented. The data is depicted for the subsurface in thermal equilibrium (undisturbed); after 24 h of non-heated fluid circulation (pre-circulation); 3, 24, 48 and 72 h from the beginning of the TRT; as well as 2 h after stopping the heat injection (recovery). The temperature variations for the recovery profile correspond with the obtained profiles during the heat injection. Thus, the observed temperature variations must be due to geological layers with different thermal parameters and not caused by displacements of either the observer pipe or the U-pipe inside the BHE. Additionally, the recovery profile also shows a layer between 28 and 33 m with a faster heat transfer rate which might indicate the presence of groundwater flows.

When measuring the nearly stable temperature of the borehole in the observer pipe after the pre-circulation (Fig. 10), the average temperatures obtained using the fiber optics every 2 m are in good agreement with the Geowire measurements at the same depths, having an RMSE deviation of 0.0803 K. However, this deviation increases when a thermal evolution is present in the borehole due to the heat injection of the TRT. At 3 h, 24 h, 48 h and 72 h after the beginning of the TRT, RMSE deviations of 0.2704 K (3 h), 0.2725 K (24 h),

0.2098 K (48 h) and 0.1977 K (72 h) are found respectively. A maximum absolute difference of 0.74 K is observed between the average temperature measurements from the fiber optics and the instantaneous measurements of the Geowire. Similarly, this effect can be better identified in Fig. 11. This figure represents the measured temperature samples by the fiber optics against the Geowire (for the depth locations of the fiber optics) at pre-circulation, 3 h, 24 h, 48 h and 72 h. Plot (a) presents the linear adjustment between the obtained data from both instruments and plot (b) the residual values after removing the temperature offset. With the fiber optics, the equipment that reads the temperature integrated the measured values over cable lengths of 2 m and for time intervals of 10 min, therefore yielding average values. On the other hand, although the Geowire measured each profile in 49 min, it measured the temperature instantaneously (for precise time instants) in each depth-specific position instead. The time interval between displacements of the probe (0.5 m) and a new measurement is of 40 s. This may explain why it can be inferred that the Geowire more accurately detects the temperature fluctuations attributed to the geological layers with different thermal properties. With this, it can be reasoned that the Geowire could have the advantage of detecting thin highly or poorly conductive layers that may be concealed by the implemented distributed temperature sensing (DTS) technic of the fiber optics equipment. It should be noted that a highly conductive layer might be an indication of groundwater flow, which could have a significant impact in the long-term operation of the BHE.

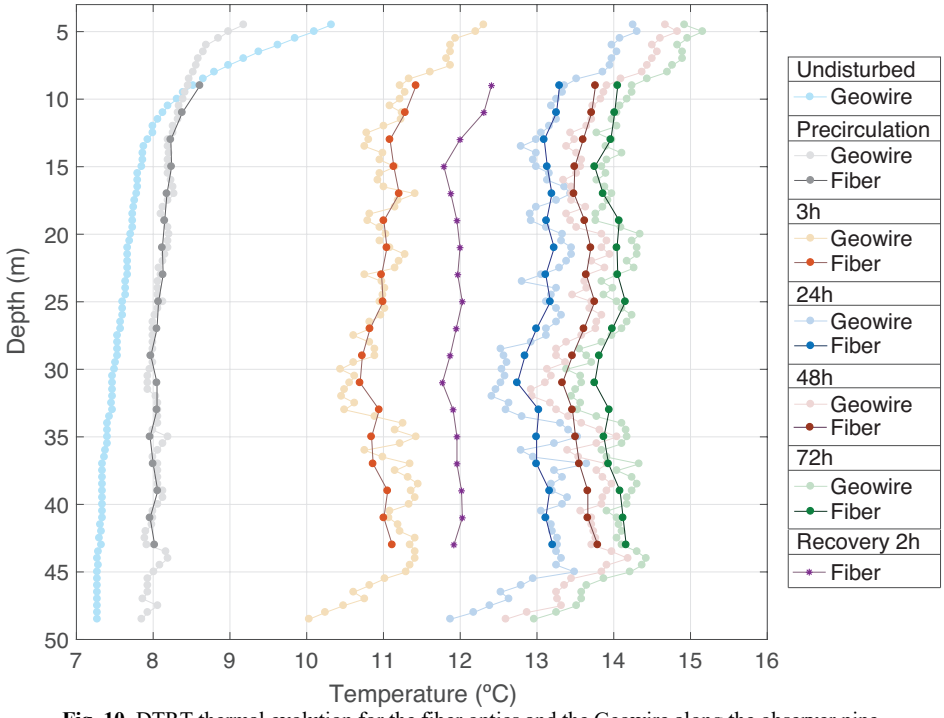

Fig. 10. DTRT thermal evolution for the fiber optics and the Geowire along the observer pipe.

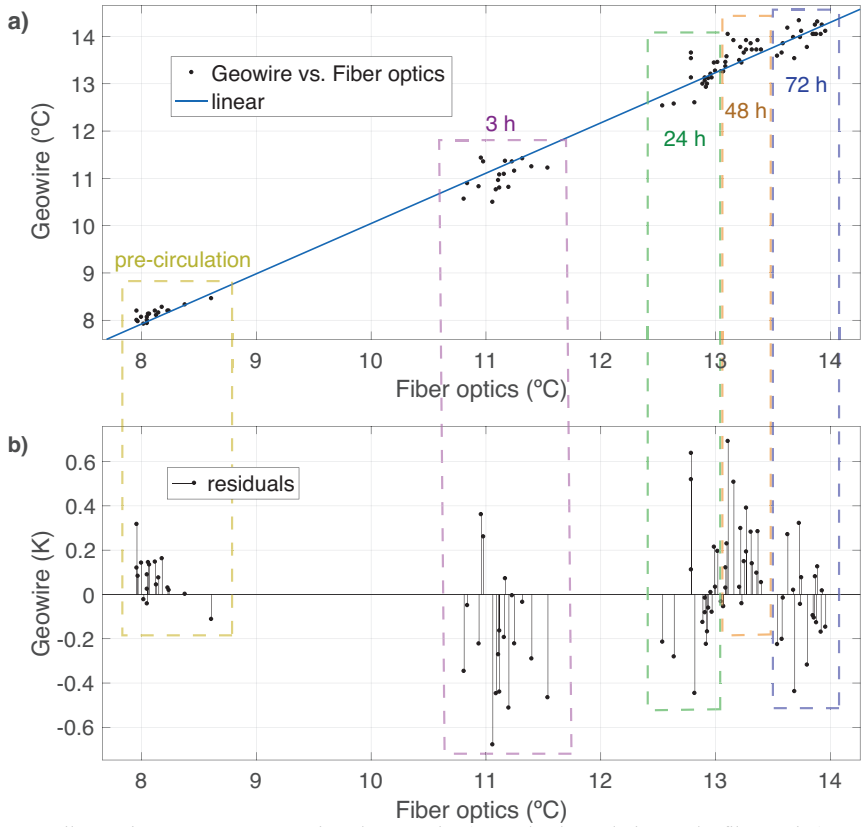

Fig. 11. Fiber optics measurements against the Geowire (same depth resolution as the fiber optics) at pre-circulation, 3 h, 24 h, 48 h and 72 h. (a) linear adjustment between both instruments, (b) residuals after removing the thermal offset.

3.2. Estimated depth-specific thermal conductivity

Fig. 12 shows the calculated depth-specific thermal conductivity profiles (effective values) by the inverse simulation method firstly using the data from the Geowire as input, and secondly using the data from the fiber optics. With the computer program based on ILS model as the basis for calculation, the figure also illustrates the depth-specific effective conductivity using the fiber optics data as input. In addition, the analytically calculated effective thermal conductivity for the global subsurface surrounding the borehole using inlet and outlet temperatures from the TRT is also presented.

Table 2 presents the thermal conductivity estimates for the different methods and its deviation over standard TRT. Global λ_{eff} is calculated by averaging the depth-specific local estimates for the different methods. In addition, the deviation of the global and local estimates is calculated by using the global effective thermal conductivity value from the standard TRT (analytical approach based on ILS). Global thermal conductivity from the

latter models and data inputs are significantly close to that of the standard TRT based on the ILS model.

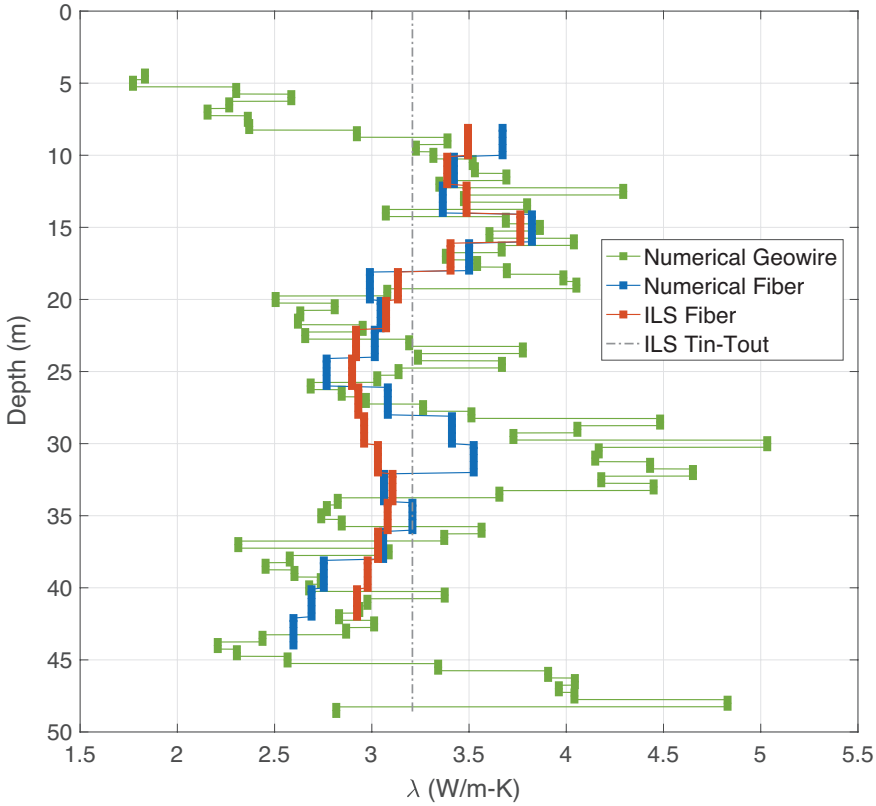

Fig. 12. Estimated depth-specific effective thermal conductivity along the borehole by the inverse numerical simulation (Geowire and fiber optics), by the computer program based on ILS approach (using fiber optics data) and effective thermal conductivity of the global subsurface based on ILS approach (using inlet and outlet temperatures from the TRT).

Local effective thermal conductivity determined with the inverse numerical model at each measured depth with the Geowire are within -44% to +56% of the effective global subsurface conductivity calculated analytically by the ILS approach (standard TRT). The global conductivity by averaging the 90 local estimates is 1.31% above the entire subsurface effective estimate. The local effective conductivity estimated with the inverse numerical model at each measured depth through fiber optics are within -16% to +19% of the effective subsurface conductivity. The global value determined by averaging the 17 local estimates is 0.28% below the effective subsurface conductivity. On the other hand, the local effective conductivity estimated with the computer program based on ILS approach at each measured depth with fiber optics are within -9% to +17% of the effective subsurface conductivity. The global value determined by averaging the 16 local estimates is 1.27% below the effective subsurface conductivity.

Table 2
Thermal conductivity estimates for the different methods and deviation over standard TRT.

Method	Data input	Global λ_{eff} W/m-K	Global estimate	Local estimates
Analytical approach based on ILS	Tin/Tout from TRT	3.20	Standard TRT (reference)	Standard TRT (reference)
Inv. num. model	Geowire (90 layers)	3.25	1.31% above	-44% to +56%
Inv. num. model	Fiber optics (17 layers)	3.19	0.28% below	-16% to +19%
Computer program based on ILS	Fiber optics (17 layers)	3.16	1.27% below	-9% to +17%

The local effective conductivity estimates for the inverse numerical method and the Geowire between 4.5 to 8.5 m are within 1.7 and 2.8 W/m-K. These values do not seem realistic and probably are related to the effect of the outside ambient air temperature. At this depth the subsurface temperature is higher, and the model adjusted to the reference temperature by lowering the conductivity. Likewise, the high conductivity values estimated between 45.5 to 48.5 m might be due to a border effect between the end point of the heat injection and the non-heated ground.

Additionally, the inverse numerical model when using Geowire data as input also shows a highly conductive zone between 28 and 33 m with an average value of 4.33 W/m-K. The conductivity of this layer is 35% above the global subsurface conductivity. The numerical procedure assigns all the heat transfer related processes over thermal conductivity, hence this highly conductive zone could be interpreted as a zone influenced by groundwater flow. However, this highly conductive zone is attenuated when using fiber optics data as input. This is expected since the measured temperature-depth profiles from fiber optics, especially at 72 h, show less temperature fluctuations for subsurface layers with different thermal properties (Fig. 10). In this case, an average value of 3.37 W/m-K is calculated, which is just 5% higher than the global subsurface conductivity. On the other hand, this conductive zone is not detected by the computer program based on ILS model using the fiber optics measurements as input. With the latter method, an average conductivity of 3.02 W/m-K is estimated for this zone which is even 6% lower than the global subsurface conductivity. The yielded lower conductivities for the time-superposed ILS method might be due to the performed calculations over the duration of the TRT, while the inverse numerical model is only optimized for the temperature profile at 72 h. This is especially true if the zone has some groundwater flow, which is indicated towards the end of TRT.

After the optimization of the observer pipe position for the inverse numerical procedure, the observer pipe is positioned in the middle between the two U-pipe legs (inlet, outlet). As the position of the pipes in the experimental borehole might have changed along the depth, two additional simulations were conducted by shifting the observer pipe to the top-left and top-right sides of the borehole. The conductivity profile for these three cases showed the same shape, but with an offset of -0.25 W/m-K for the left and right shifted cases over the observed pipe position after the optimization (middle). Results are presented in Table 3, where after optimizing the observer pipe position, the global estimate, shows the closest

agreement with the global estimate of the analytical ILS method.

Table 3
Results of the change in observer pipe position for the inverse numerical simulation method.

Method	Data input	Obs. pipe position	Global λ_{eff} W/m-K	Global estimate	Local estimates	Local estimates W/m-K
Analytical approach based on ILS	Tin/Tout from TRT	-	3.20	Standard TRT (reference)	Standard TRT (reference)	-
Inv. num. model	Geowire (90 layers)	Optimized (middle)	3.25	1.31% above	-44% to +56%	reference
Inv. num. model	Geowire (90 layers)	Left shifted	2.99	6.46% below	-36% to +44%	-0,66 to +0,02
Inv. num. model	Geowire (90 layers)	Right shifted	2.99	6.37% below	-36% to +43%	-0,67 to +0,01

The main advantage of the approach based on the inverse numerical model is that the depth-specific conductivity is estimated using only two temperature profiles as input: (1) the subsurface in thermal equilibrium and, (2) at the end of the TRT. However, it is important to measure the objective profile (at the end of the TRT) with high accuracy as errors in the measurement might have a considerable impact on the estimation of thermal parameters. For this reason, it is recommended that a few profiles are measured consecutively to verify repeatability, as the temperature at the end of the TRT (72 h) increases at a relatively slow rate. Likewise, an application of an adequate instrument with rigorous repeatability (e.g. Geowire) can avoid uncertainties in the objective profile. The computer program based on the ILS model, requires continuous temperature measurements during the course of a TRT instead. It should be noted however, that the computer program estimates one local conductivity value less than the inverse numerical model for the same amount of input data, plus, axial effects are neglected. The drawback of the inverse numerical approach is that the 3D numerical simulations are cumbersome and time consuming. Nevertheless the model can be simplified by a Borehole-to-Ground (B2G) approach [53–55]. This solution substantially reduces the computational cost and simulation time by an equivalent model based on thermal networks and a vertical discretization of the borehole.

In this test, the combination of the inverse numerical procedure and the use of the Geowire estimated the effective conductivity of the depth-specific layers with a spatial resolution of 0.5 m, which has not yet been achieved with other methods.

4. Conclusion

In this study, thermal properties of a heterogeneous subsurface were investigated in the field using an observer pipe thermal response test (OP-TRT) using fiber optical thermometers and two novel in-borehole temperature instruments: Geoball and Geowire. The obtained data were evaluated by two different procedures to estimate depth-specific

thermal conductivities of the subsurface: (1) an inverse numerical model and (2) a time-superposed computer program based on the infinite line approach (ILS) approach.

Temperature measurements along the observed pipe of the OP-TRT showed amplified temperature differences produced by depth-specific geological layers with different thermal properties in comparison with the heated down-flow pipe of the TRT.

Positive results were obtained highlighting the effective performance of the novel instruments, where the following agreements were observed between:

- The Geowire and the fiber optics when measuring the stable subsurface temperature before the TRT.
- The instantaneous measurements collected with the Geoball and the average temperature measurements of the fiber optics.
- The RTD-sensors of the TRT equipment and the first/last samples of the Geoball.

The investigation also demonstrated that the fiber optics loses information when integrating the temperature over cable lengths and time steps. This is caused by the different rates of thermal evolution along the static fluid in the observer pipe due to heterogeneities in the subsurface. This is not the case for the Geowire, since it measures instantaneous values of temperature in each depth-specific location, providing a more accurate temperature profile of the subsurface. Even though a temperature profile measured by the Geowire is not synchronized in time as it is for the fiber optics, the time difference between a displacement of the probe and a new measurement is small (40 seconds for the Geowire configuration in this study). For the Geoball, the time between consecutive spatial measurements is even smaller with only 1.5 seconds. Likewise, both Geoball and Geowire have proven to measure the temperature with a higher spatial resolution than the widely used distributed temperature sensing (DTS) equipment used in this study.

Meanwhile, the average conductivity of the depth-dependent local effective estimates for both the inverse numerical model and the computer program based on the ILS approach are significantly close to the global subsurface effective conductivity of 3.20 W/m-K based on standard TRT, 0.28% and 1.27% below respectively. Another achievement of this work was the successful improvement of the inverse numerical procedure by incorporating a parameter optimization solver to reach a more accurate solution in one simulation iteration. By adding the optimization solver both the model validation and result estimation processes have become automatic. An advantage of the inverse numerical model is that it only requires two temperature profiles as input, while the method based on ILS approach requires a continous temperature monitoring of the subsurface instead. On the other hand, the local effective conductivity estimates from the inverse numerical procedure using the Geowire data as input showed the highest dispersion with respect to the global effective conductivity of a standard TRT. A highly conductive layer of 5 m long is therefore detected using the novel instrument. This layer might be caused by the presence of groundwater flow, which would essentially improve the heat transfer efficiency of the borehole heat exchanger (BHE). Whereas using the same method with the fiber optics data made this layer less perceivable, indicating another advantage of the Geowire.

The cost of a commercial version of either the Geoball or the Geowire is potentially more affordable than fiber optics equipment. However, these novel instruments are still in a pre-prototype stage and lack to embed a method for calculating the depth-specific

conductivity through some last fully automated validation tests to reach a commercialization stage. Likewise, further development may lead to more advanced computational algorithms for estimating energy savings depending on ground thermal properties, size and power requirements of the installation.

Acknowledgments

This work was supported in part by the European Institute of Innovation and Technology Climate-Knowledge and Innovation Community, a body of the European Union inside the Ph.D. Program of Transforming the Built Environment Platform and in part by Bengt Dahlgren Geoenergi, Avanti Swedish Drillers Association, Stures Brunnsborrningar as well as KTH Royal Institute of Technology. Finally, we also would like to thank both reviewers for the constructive comments, which improved the quality of the manuscript.

List of symbols and abbreviations

BHE	Borehole heat exchanger
B2G	Borehole-to-ground
DTS	Distributed temperature sensing
DTRT	Distributed thermal response test
GSHP	Ground source heat pump
h	Hour
HT	Heat transfer in fluids
IEC	International Electrotechnical Commission
ILS	Infinite line source
J	Joule
K	Kelvin degree
kg	Kilogram
l	Litter
IEC	International electrotechnical commission
m	Meter
mm	Millimeter
min	Minute
NITF	Non-isothermal flow
OP-TRT	Observer pipe thermal response test
Pt1000	Platinum resistance thermometer

Q	Heat flow
RMSE	Root mean square error
s	Second
SSE	Sum of squared errors
R^2	Coefficient of determination
R_b	Borehole thermal resistance
R_g	Ground thermal resistance
RTD	Resistance temperature detector
T_{df}	Temperature in the TRT down-flow pipe
T_{exp}	Experimental temperature
T_{fg}	Far ground temperature
T_{in}	Inlet temperature of TRT
T_{sim}	Temperature from simulation
T_{obs}	Temperature in the observer pipe
T_{out}	Outlet temperature of TRT
TRT	Thermal response test
W	Watt
y	Linear equation
2D	Two dimensional
3D	Three dimensional
λ	Thermal conductivity
λ_{eff}	Effective thermal conductivity
n	Subsurface depth-specific layer number
ºC	Celsius degree

References

[1] P. Cui, H. Yang, Z. Fang, Heat transfer analysis of ground heat exchangers with inclined boreholes, Appl. Therm. Eng. 26 (2006) 1169–1175. https://doi.org/10.1016/j.applthermaleng.2005.10.034.

[2] J.D. Spitler, M. Bernier, Vertical borehole ground heat exchanger design methods, in: Adv. Ground-Source Heat Pump Syst., 2016. https://doi.org/10.1016/B978-0-08-100311-4.00002-9.

[3] J. Luo, J. Rohn, M. Bayer, A. Priess, Thermal performance and economic evaluation

of double U-tube borehole heat exchanger with three different borehole diameters, Energy Build. 67 (2013) 217–224. https://doi.org/10.1016/j.enbuild.2013.08.030.

[4] H. Zeng, N. Diao, Z. Fang, Efficiency of vertical geothermal heat exchangers in the ground source heat pump system, J. Therm. Sci. 12 (2003) 77–81. https://doi.org/10.1007/s11630-003-0012-1.

[5] V. Wagner, P. Blum, M. Kübert, P. Bayer, Analytical approach to groundwater-influenced thermal response tests of grouted borehole heat exchangers, Geothermics. 46 (2013) 22–31. https://doi.org/10.1016/j.geothermics.2012.10.005.

[6] N. Zhang, Z. Wang, Review of soil thermal conductivity and predictive models, 2017. https://doi.org/10.1016/j.ijthermalsci.2017.03.013.

[7] H.M. Abuel-Naga, D.T. Bergado, A. Bouazza, M.J. Pender, Thermal conductivity of soft Bangkok clay from laboratory and field measurements, Eng. Geol. 105 (2009) 211–219. https://doi.org/10.1016/j.enggeo.2009.02.008.

[8] A.-R. Choudhary, An approach to determine the thermal conductivity and diffusivity of a rock in situ, Ph.D. Thesis, Oklahoma State University, 1976. https://www.google.com/url?sa=t&rct=j&q=&esrc=s&source=web&cd=1&ved=2ahUKEwiI4_i22OPgAhUD5uAKHbnmDF4QFjAAegQICRAC&url=https%3A%2F%2Fshareok.org%2Fbitstream%2Fhandle%2F11244%2F32925%2FThesis-1976D-C552a.pdf%3Fsequence%3D1%26isAllowed%3Dy&usg=AOvVaw1FfdHNjJ.

[9] P. Mogensen, Fluid to duct wall heat transfer in duct system heat storages, in: Proc. Int. Conf. Subsurf. Heat Storage Theory Pract., Swedish Council for Building Research, Stockholm, Sweden, 1983: pp. 652–657.

[10] W.A. Austin, Development of an in Situ System for Measuring Ground Thermal Properties, Oklahoma State University, 1998.

[11] S. Gehlin, Thermal response Test – In-situ Measurements of Thermal Properties in Hard Rock, Luleå University of Technology, 1998.

[12] IEA ECES Annex 21 Thermal Response Test, n.d. http://projects.gtk.fi/Annex21/homepage.htm.

[13] B. Sanner, G. Hellström, J. Spitler, S. Gehlin, Thermal response test—current status and world-wide application, in: Proc. World Geotherm. Congr., 2005: pp. 24–29. https://doi.org/LTU-DT-0239-SE.

[14] H.J.L. Witte, TRT: How to get the right number, GeoDrilling Int. 151 (2009) 30–34. http://www.groenholland.nl/download/Geodrilling_2009.pdf.

[15] J.D. Deerman, S.P. Kavanaugh, Simulation of vertical U-tube ground-coupled heat pump systems using the cylindrical heat source solution, ASHRAE Trans. Res. 971 (1991) 287–295.

[16] F. Stauffer, P. Bayer, P. Blum, N. Molina-Giraldo, W. Kinzelbach, Thermal use of shallow groundwater, CRC Press, 2013. https://doi.org/10.1201/b16239.

[17] H.S. (Horatio S. Carslaw, J.C. (John C. Jaeger, Conduction of heat in solids, Clarendon Press, 1959. https://books.google.fr/books/about/Conduction_of_Heat_in_Solids.html?id=y20sAAAAYAAJ&pgis=1&redir_esc=y (accessed September 16, 2018).

[18] P. Eskilson, Superposition Borehole Model, Manual for Computer Code, University

of Lund, Sweden, 1987.

[19] H.-J.G. Diersch, D. Bauer, W. Heidemann, W. Rühaak, P. Schätzl, Finite element modeling of borehole heat exchanger systems, Comput. Geosci. 37 (2011) 1122–1135. https://doi.org/10.1016/j.cageo.2010.08.003.

[20] J. Raymond, R. Therrien, L. Gosselin, R. Lefebvre, Numerical analysis of thermal response tests with a groundwater flow and heat transfer model, Renew. Energy. 36 (2011) 315–324. https://doi.org/10.1016/j.renene.2010.06.044.

[21] V. Wagner, P. Bayer, M. Kübert, P. Blum, Numerical sensitivity study of thermal response tests, Renew. Energy. 41 (2012) 245–253. https://doi.org/10.1016/j.renene.2011.11.001.

[22] D. Marcotte, P. Pasquier, Fast fluid and ground temperature computation for geothermal ground-loop heat exchanger systems, Geothermics. 37 (2008) 651–665. https://doi.org/10.1016/j.geothermics.2008.08.003.

[23] T. V. Bandos, Á. Montero, E. Fernández, J.L.G. Santander, J.M. Isidro, J. Pérez, P.J.F. de Córdoba, J.F. Urchueguía, Finite line-source model for borehole heat exchangers: effect of vertical temperature variations, Geothermics. 38 (2009) 263–270. https://doi.org/10.1016/J.GEOTHERMICS.2009.01.003.

[24] S. Gehlin, G. Hellström, Influence on thermal response test by groundwater flow in vertical fractures in hard rock, Renew. Energy. 28 (2003) 2221–2238. https://doi.org/10.1016/S0960-1481(03)00128-9.

[25] D. Marcotte, P. Pasquier, F. Sheriff, M. Bernier, The importance of axial effects for borehole design of geothermal heat-pump systems, Renew. Energy. 35 (2010) 763–770. https://doi.org/10.1016/j.renene.2009.09.015.

[26] A.D. Chiasson, A. O'Connell, New analytical solution for sizing vertical borehole ground heat exchangers in environments with significant groundwater flow: Parameter estimation from thermal response test data, HVAC&R Res. 17 (2011) 1000–1011. https://doi.org/10.1080/10789669.2011.609926.

[27] E. Rohner, L. Rybach, U. Schärli, A New , Small , Wireless Instrument to Determine Ground Thermal Conductivity In-Situ for Borehole Heat Exchanger Design, Proc. World Geotherm. Congr. 2005. (2005) 3–6. https://pdfs.semanticscholar.org/a20a/91d47ee18a7e978d4d789df3a26678cdca2b.pdf.

[28] N. Aranzabal, J. Martos, Á. Montero, J. Soret, R. García-Olcina, J. Torres, Design and test of an autonomous wireless probe to measure temperature inside pipes, in: ECOS 2015 - 28th Int. Conf. Effic. Cost, Optim. Simul. Environ. Impact Energy Syst., 2015.

[29] J. Raymond, L. Lamarche, M. Malo, Extending thermal response test assessments with inverse numerical modeling of temperature profiles measured in ground heat exchangers, Renew. Energy. 99 (2016) 614–621. https://doi.org/10.1016/j.renene.2016.07.005.

[30] H. Fujii, H. Okubo, K. Nishi, R. Itoi, K. Ohyama, K. Shibata, An improved thermal response test for U-tube ground heat exchanger based on optical fiber thermometers, Geothermics. 38 (2009) 399–406. https://doi.org/10.1016/j.geothermics.2009.06.002.

[31] H. Fujii, H. Okubo, R. Itoi, Thermal response tests using optical fiber thermometers, in: Geotherm. Resour. Counc. Trans., 2006: pp. 545–551.

[32] L.R. Ingersoll, H.J. Plass, Theory of the Ground Pipe Heat Source for the Heat Pump, ASHVE Trans. Vol.54 (1948).

[33] J. Acuña, B. Palm, Distributed thermal response tests on pipe-in-pipe borehole heat exchangers, Appl. Energy. 109 (2013) 312–320. https://doi.org/10.1016/j.apenergy.2013.01.024.

[34] J. Acuña, Improvements of U-pipe Borehole Heat Exchanger, KTH Royal Institute of Technology, 2010.

[35] J. Acuña, Distributed thermal response tests – New insights on U-pipe and Coaxial heat exchangers in groundwater-filled boreholes, 2013. http://kth.diva-portal.org/smash/record.jsf?pid=diva2%3A602905&dswid=-2080.

[36] P. Hakala, A. Martinkauppi, I. Marinkauppi, N. Leppaharaju, K. Korhonen, Evaluation of the Distributed Thermal Response Test (DTRT): Nupurinkartano as a Case Study, 2014. http://tupa.gtk.fi/julkaisu/tutkimusraportti/tr_211.pdf%0A.

[37] V. Soldo, L. Boban, S. Borović, Vertical distribution of shallow ground thermal properties in different geological settings in Croatia, Renew. Energy. 99 (2016) 1202–1212. https://doi.org/10.1016/j.renene.2016.08.022.

[38] J. Luo, J. Rohn, W. Xiang, M. Bayer, A. Priess, L. Wilkmann, H. Steger, R. Zorn, Experimental investigation of a borehole field by enhanced geothermal response test and numerical analysis of performance of the borehole heat exchangers, Energy. 84 (2015) 473–484. https://doi.org/10.1016/j.energy.2015.03.013.

[39] G. Radioti, S. Delvoie, R. Charlier, G. Dumont, F. Nguyen, Heterogeneous bedrock investigation for a closed-loop geothermal system: A case study, Geothermics. 62 (2016) 79–92. https://doi.org/10.1016/j.geothermics.2016.03.001.

[40] P. Monzó, Modelling and monitoring thermal response of the ground in borehole fields, KTH Royal Institute of Technology, 2018. http://kth.diva-portal.org/smash/record.jsf?pid=diva2%3A1178493&dswid=8886.

[41] J. Raymond, L. Lamarche, Development and numerical validation of a novel thermal response test with a low power source, Geothermics. (2014). https://doi.org/10.1016/j.geothermics.2014.02.004.

[42] J. Raymond, L. Lamarche, M. Malo, Field demonstration of a first thermal response test with a low power source, Appl. Energy. 147 (2015) 30–39. https://doi.org/10.1016/j.apenergy.2015.01.117.

[43] G.E.P. Box, W.G. Hunter, J. Stuart Hunter, Statistics for Experimenters: An Introduction to Design, Data Analysis and Model Building., John Wiley & Sons Ltd., New York, 1978.

[44] S. Wilke, M. Menberg, H. Steger, P. Blum, Advanced thermal response tests: A review, Renew. Sustain. Energy Rev. (2020).

[45] N. Aranzabal, J. Martos, Á. Montero, L. Monreal, J. Soret, J. Torres, R. García-Olcina, Extraction of thermal characteristics of surrounding geological layers of a geothermal heat exchanger by 3D numerical simulations, Appl. Therm. Eng. 99 (2016) 92–102. https://doi.org/10.1016/j.applthermaleng.2015.12.109.

[46] N. Aranzabal, J. Martos, H. Steger, P. Blum, J. Soret, Novel Instrument for Temperature Measurements in Borehole Heat Exchangers, IEEE Trans. Instrum. Meas. PP (2018) 1–9. https://doi.org/10.1109/TIM.2018.2860818.

[47] N. Aranzabal, J. Martos, H. Steger, P. Blum, J. Soret, Temperature measurements along a vertical borehole heat exchanger: A method comparison, Renew. Energy. 143 (2019) 1247–1258. https://doi.org/10.1016/J.RENENE.2019.05.092.

[48] J. Martos, Á. Montero, J. Torres, J. Soret, G. Martínez, R. García-Olcina, Novel wireless sensor system for dynamic characterization of borehole heat exchangers, Sensors. 11 (2011) 7082–7094. https://doi.org/10.3390/s110707082.

[49] Á. Montero, J.F. Urchueguía, J. Martos, B. Badenes, Ground temperature recovery time after BHE insertion, Eur. Geotherm. Congr. 2013. (2013) 6.

[50] L. Lamarche, S. Kajl, B. Beauchamp, A review of methods to evaluate borehole thermal resistances in geothermal heat-pump systems, Geothermics. 39 (2010) 187–200. https://doi.org/10.1016/J.GEOTHERMICS.2010.03.003.

[51] H. Holmberg, Transient heat transfer in boreholes with application to non-grouted borehole heat exchangers and closed loop engineered geothermal systems, Norwegian University of Science and Technology, 2016.

[52] J.D. Spitler, S. Javed, R.K. Ramstad, Natural convection in groundwater-filled boreholes used as ground heat exchangers, Appl. Energy. (2016). https://doi.org/10.1016/j.apenergy.2015.11.041.

[53] F. Ruiz-Calvo, M. De Rosa, P. Monzó, C. Montagud, J.M. Corberán, Coupling short-term (B2G model) and long-term (g-function) models for ground source heat exchanger simulation in TRNSYS. Application in a real installation, Appl. Therm. Eng. 102 (2016) 720–732. https://doi.org/10.1016/j.applthermaleng.2016.03.127.

[54] F. Ruiz-Calvo, M. De Rosa, J. Acuña, J.M. Corberán, C. Montagud, Experimental validation of a short-term Borehole-to-Ground (B2G) dynamic model, Appl. Energy. 140 (2015) 210–223. https://doi.org/10.1016/j.apenergy.2014.12.002.

[55] M. De Rosa, F. Ruiz-Calvo, J.M. Corberán, C. Montagud, L.A. Tagliafico, A novel TRNSYS type for short-term borehole heat exchanger simulation: B2G model, Energy Convers. Manag. 100 (2015) 347–357. https://doi.org/10.1016/j.enconman.2015.05.021.

Chapter 8

Conclusion and future work

> *This final chapter presents the general and specific conclusions drawn from this doctoral thesis. In addition, this chapter identifies possible lines of future work that could be derived from this Ph.D. study. At the end, the scientific publications and contributions related to this Ph.D. work are also listed.*

8.1. Conclusion

The TRT method and instruments proposed in this Ph.D. thesis proved to be a useful insight for improving the optimization of ground source heat pump systems in terms of energy efficiency as well as reducing the capital investment. Additionally, this Ph.D. study gives an overview in estimating the depth-specific thermal properties of the ground surrounding a borehole or borehole heat exchanger (BHE).

A new method, called observer pipe TRT (OP-TRT), was proposed to calculate the depth-specific thermal conductivity of the geological layers crossed by the perforation of a borehole. This method is based on an additional measurement that can be implemented in combination with the standard TRT by enhancing its results: A temperature profile along the length of an auxiliary pipe, called observed pipe, filled with water and inserted in parallel to the heated U-pipe legs. Moreover, an inverse simulation procedure was developed to estimate the depth-specific thermal conductivity from the data collected during an OP-TRT. With the intention of evaluating the proposed method, a first experiment was carried out by lowering a wired temperature probe manually into the observer pipe during a TRT. This experiment is presented in Chapter 3, where the following conclusions can be drawn:

- The OP-TRT proved to reflect on a larger temperature scale the thermal fluctuations produced by layers with different thermal properties and, therefore, requiring less accurate sensors for more detailed results.
- The OP-TRT and the inverse numerical procedure were evaluated as a potentially viable method to measure the depth-specific thermal properties of the subsurface surrounding a BHE.
- From the obtained results and by implementing the inverse numerical approach, a highly conductive zone between 24 and 26 m was detected, likely dominated

by groundwater flows.

After the positive results of the OP-TRT and the inverse numerical method, the research efforts associated with this Ph.D. work were oriented towards the development of a specific instrument, called Geowire, to reliably measure temperature profiles along the observer pipe. As described in Chapter 4, the operation of the Geowire was first analyzed in the laboratory, and second in a test BHE using standard Pt100-sensors as reference.

- Measurements between the Geowire and Pt100-sensors were comparable demonstrating its applicability (mean square error of 0.042).
- The Geowire proved to be a valuable device to measure high spatial, temporal and temperature resolution profiles (0.5 mm, 750 ms, 0.06 K).
- Further features of the Geowire were positively validated such as: automatic data recording at pre-defined time intervals; small uncertainty in the measurements (±5 mm in 10 m, ± 0.06 K); acceptable probe thermal response time, user-friendly interface; remote monitoring and control; alarms for detecting anomalies during its operation; and its extensive capacity to store data.

Also, an enhanced version of the flowing probe (Martos et al., 2011), called Geoball, was developed and analyzed in the laboratory (Chapter 5). From this study the following conclusions can be drawn:

- Further improvements over the first version, such as smaller size, less weight and longer operation time.
- Suitable to obtain spatial and temperature measurements inside geothermal pipes along the entire pipe loop (down- and up-flow).
- Suitable for both vertical and horizontal pipe arrangements.

Afterwards, the two instruments developed in this Ph.D. work (Geowire and Geoball) were evaluated with new and standard commercial in-borehole temperature measurement instruments, such as the GEOsniff®, fiber optical thermometers and Pt100-sensors chain. The key features of these instruments were assessed first in the laboratory, and second in a test BHE isolated from external conditions (Chapter 6). This method comparison study suggested that practitioners should carefully evaluate quantitative and qualitative differences of each instrument, calibration procedure and data analysis method prior to the implementation of a distributed thermal response test (DTRT.

- From the laboratory tests, a fast thermal response and a negligible uncertainty was measured with the Geowire (<2.0 s, ± 0.06 K) and Geoball (<0.5 s, ± 0.04 K).
- The new instruments demonstrated to measure the temperature with high spatial and temperature resolutions: Geowire (0.5 mm, 0.06 K) and Geoball (10 mm, 0.05 K).
- The Geowire and Geoball measured the temperature instantaneously, while the accuracy of the measurement is independent among spatial and temporal resolution and sampling time. In comparison to fiber optics, these instruments provide higher spatial resolutions and higher accuracies in environments with transient thermal responses, e.g. during a DTRT.
- They do not require a dynamic calibration for accurate results, are easier to integrate in existing boreholes, and are also a more cost-effective solution.
- Errors in the calibration of multiple sensors can be avoided, as it may be the case with a chain of sensors.

In the last experiment (Chapter 7), an OP-TRT was carried out in a BHE facility. Fiber optical thermometers were introduced inside the down-flow leg of the U-pipe and inside the observed pipe for the evaluation of the Geowire and Geoball. Also, the depth-specific conductivity was assessed using the recorded data along the observed pipe by the suggested inverse simulation method and a computer program based on the infinite line source:

- Temperature measurements along the observed pipe of the OP-TRT showed amplified temperature differences produced by depth-specific geological layers with different thermal properties in comparison with the heated down-flow pipe of the TRT.
- The Geoball and the Geowire once more proved to obtain higher spatial and temperature resolution measurements than the widely used fiber optics.
- The inverse numerical model was effectively improved by incorporating a parameter estimation solver. Both the accuracy of the results and simulation time were significantly enhanced by an automatic process to fit the objective temperature profile (observer pipe) in a single simulation iteration.
- Comparable results were found between the average of the local effective estimates from both data analysis methods and the global subsurface effective conductivity calculated based on standard TRT: 1.27% below for the computer program and 0.28% below for the inverse numerical model.

- The local effective conductivity estimates from the inverse numerical method using the Geowire data as input showed the highest dispersion with respect to the global effective conductivity of a standard TRT. Thus, a highly conductive zone of 5 m long was detected using the proposed instrument and method.
- The inverse numerical method proved the advantage of only requiring two temperature profiles as input: (1) undisturbed ground and (2) at the end of the TRT.

8.2. Future work

This doctoral thesis has presented advances in the extent of estimating the heat transfer efficiency of the geological layer crossed by the perforation of a borehole. However, the method to calculate the thermal properties in the ground still has margin for improvements and the instruments still are in a pre-prototype stage. In this sense, the logical line for continuation of this research work is enumerated as follows:

- Improvements on the inverse numerical model. In the proposed model, convective effects are neglected and only conduction is considered as heat transfer mechanism. The development of an enhanced model including conductive-advective effects is likely to expand the results. In that case, a more detailed information of the axial effects can be inferred, as for instance, an assessment of the location and velocity of groundwater movements.
- Automatic measurements with the Geoball. In this study, the probe was inserted at the inlet of the U-pipe and extracted at the outlet of the U-pipe by a manual bypass circuit without interrupting the flow of the TRT. However, the manual valves can be replaced by electro-valves and the measuring process can become fully automatic. After each measurement along the pipe loop the probe can be stored in the bypass valve, while the data can be wirelessly transmitted, and the battery simultaneously charged. In this manner, the insertion of the ball can be controlled to obtain continuous temperature datasets at pre-defined time intervals. With an automated bypass system, the instrument can implement remote management and visualization functionalities.
- Embed a method to estimate the depth-specific thermal properties. The processing system developed to control the Geowire has enough resources to embed a DTRT analysis method. The simulation of the proposed numerical model is cumbersome and time-consuming. However, the model could be simplified, for example, by a Borehole-to-Ground (B2G) approach (Ruiz-Calvo, 2015; Ruiz-Calvo et al., 2015). In this manner, the instrument can embed a

method to directly plot a depth-specific thermal conductivity after recording the data during an OP-TRT. Similarly, this insight is feasible for the Geoball. The processing system is optimal to control and read the dynamic measurements inside the pipe loop during a DTRT. Another option may be to embed a simplified method to estimate the conductivity after a DTRT. For example, the processing system may have enough resources to integrate a method based on the ILS approach, as the computer program used in the experiment described in Chapter 6.

References

Acuña, J. (2010). *Improvements of U-pipe Borehole Heat Exchanger*. KTH Royal Institute of Technology. Retrieved from http://kth.diva-portal.org/smash/record.jsf?pid=diva2%3A318637&dswid=3979

Acuña, J. (2013). *Distributed thermal response tests – New insights on U-pipe and Coaxial heat exchangers in groundwater-filled boreholes*. *KTH Royal Institute of Technology*. Retrieved from http://kth.diva-portal.org/smash/record.jsf?pid=diva2%3A602905&dswid=-2080

Acuña, J., & Palm, B. (2013). Distributed thermal response tests on pipe-in-pipe borehole heat exchangers. *Applied Energy*, *109*, 312–320. https://doi.org/10.1016/j.apenergy.2013.01.024

Ali Ghoreishi-Madiseh, S., Fahrettin Kuyuk, A., & Antonio Rodrigues de Brito, M. (2019). An analytical model for transient heat transfer in ground-coupled heat exchangers of closed-loop geothermal systems. *Applied Thermal Engineering*. https://doi.org/10.1016/j.applthermaleng.2019.01.020

Alrtimi, A., Rouainia, M., & Manning, D. A. C. (2014). An improved steady-state apparatus for measuring thermal conductivity of soils. *International Journal of Heat and Mass Transfer*, *72*, 630–636. https://doi.org/10.1016/j.ijheatmasstransfer.2014.01.034

Aranzabal, N., Martos, J., Montero, Á., Monreal, L., Soret, J., Torres, J., & García-Olcina, R. (2016). Extraction of thermal characteristics of surrounding geological layers of a geothermal heat exchanger by 3D numerical simulations. *Applied Thermal Engineering*, *99*, 92–102. https://doi.org/10.1016/j.applthermaleng.2015.12.109

ASTM D5334-08. (2008). Standard test method for determination of thermal conductivity of soil and soft rock by thermal needle probe procedure. *ASTM International*. https://doi.org/10.1520/d5334-08

Atam, E., & Helsen, L. (2016). Ground-coupled heat pumps: Part 2—Literature review and research challenges in optimal design. *Renewable and Sustainable Energy Reviews*, *54*, 1668–1684. https://doi.org/10.1016/j.rser.2015.07.009

Austin, W. A., Yavuzturk, C., & Spitler, J. (2000). Development of an in situ system for measuring ground thermal properties. *ASHRAE Transactions*, *106*, 356–379. https://hvac.okstate.edu/sites/default/files/pubs/papers/2000/01a-Austin_Yavuzturk_Spitler_00.pdf

Austin, W.A. (1998). *Development of an in Situ System for Measuring Ground Thermal Properties*. Oklahoma State University. Retrieved from

https://hvac.okstate.edu/sites/default/files/Austin_thesis.pdf

Aydin, M., & Sisman, A. (2015). Experimental and computational investigation of multi U-tube boreholes. *Applied Energy*, *145*, 163–171. https://doi.org/10.1016/j.apenergy.2015.02.036

Bandos, T. V., Montero, Á., Fernández, E., Santander, J. L. G., Isidro, J. M., Pérez, J., … Urchueguía, J. F. (2009). Finite line-source model for borehole heat exchangers: effect of vertical temperature variations. *Geothermics*, *38*(2), 263–270. https://doi.org/10.1016/j.geothermics.2009.01.003

Bandyopadhyay, G., Gosnold, W., & Mann, M. (2008). Analytical and semi-analytical solutions for short-time transient response of ground heat exchangers. *Energy and Buildings*, *40*(10), 1816–1824. https://doi.org/10.1016/j.enbuild.2008.04.005

Bauer, D., Heidemann, W., Müller-Steinhagen, H., & Diersch, H.-J. G. (2011a). Thermal resistance and capacity models for borehole heat exchangers. *International Journal of Energy Research*, *35*(4), 312–320. https://doi.org/10.1002/er.1689

Bauer, D., Heidemann, W., & Diersch, H.-J. G. (2011b). Transient 3D analysis of borehole heat exchanger modeling. *Geothermics*, *40*(4), 250–260. https://doi.org/10.1016/j.geothermics.2011.08.001

Bayer, P., de Paly, M., & Beck, M. (2014). Strategic optimization of borehole heat exchanger field for seasonal geothermal heating and cooling. *Applied Energy*, *136*, 445–453. https://doi.org/10.1016/j.apenergy.2014.09.029

Bayer, P., Rivera, J. A., Schweizer, D., Schärli, U., Blum, P., & Rybach, L. (2016). Extracting past atmospheric warming and urban heating effects from borehole temperature profiles. *Geothermics*, *64*, 289–299. https://doi.org/10.1016/j.geothermics.2016.06.011

Beier, R. A., Acuña, J., Mogensen, P., & Palm, B. (2012). Vertical temperature profiles and borehole resistance in a U-tube borehole heat exchanger. *Geothermics*, *44*, 23–32. https://doi.org/10.1016/j.geothermics.2012.06.001

BniLam, N., Al-Khoury, R., Shiri, A., & Sluys, L. J. (2018). A semi-analytical model for detailed 3D heat flow in shallow geothermal systems. *International Journal of Heat and Mass Transfer*, *123*, 911–927. https://doi.org/10.1016/j.ijheatmasstransfer.2018.03.010

Borinaga-Treviño, R., Pascual-Muñoz, P., Castro-Fresno, D., & Blanco-Fernandez, E. (2013). Borehole thermal response and thermal resistance of four different grouting materials measured with a TRT. *Applied Thermal Engineering*, *53*(1), 13–20. https://doi.org/10.1016/j.applthermaleng.2012.12.036

Bristow, K. L., Kluitenberg, G. J., & Horton, R. (1994). Measurement of Soil Thermal Properties with a Dual-Probe Heat-Pulse Technique. *Soil Science Society of*

America Journal, *58*, 1288–1294. https://doi.org/10.2136/sssaj1994.03615995005800050002x

Carslaw, H. S. & Jaeger, J. C. (1959). *Conduction of heat in solids*. Clarendon Press. Retrieved from

Chen, S., Mao, J., Han, X., Li, C., & Liu, L. (2016). Numerical Analysis of the Factors Influencing a Vertical U-Tube Ground Heat Exchanger. In *Sustainability* (p. 882). https://doi.org/10.3390/su8090882

Chiasson, A. D., & O'Connell, A. (2011). New analytical solution for sizing vertical borehole ground heat exchangers in environments with significant groundwater flow: Parameter estimation from thermal response test data. *HVAC&R Research*, *17*(6), 1000–1011.

Choudhary, A.-R. (1976). *An approach to determine the thermal conductivity and diffusivity of a rock in situ*. Ph.D. Thesis, Oklahoma State University. Retrieved from https://www.google.com/url?sa=t&rct=j&q=&esrc=s&source=web&cd=1&ved=2ahukewii4_i22opgahud5uakhbnmdf4qfjaaegqicrac&url=https%3a%2f%2fshareok.org%2fbitstream%2fhandle%2f11244%2f32925%2fthesis-1976d-c552a.pdf%3fsequence%3d1%26isallowed%3dy&usg=aovvaw1ffdhnjj

Claesson, J., & Javed, S. (2011). An analytical method to calculate borehole fluid temperatures for time-scales from minutes to decades. In *ASHRAE Transactions* (pp. 279–288). Atlanta. Retrieved from https://search.proquest.com/docview/906121053

Colmenar-Santos, A., Folch-Calvo, M., Rosales-Asensio, E., & Borge-Diez, D. (2016). The geothermal potential in Spain. *Renewable and Sustainable Energy Reviews*, *56*, 865–886. https://doi.org/10.1016/j.rser.2015.11.070

Cui, Y., Zhu, J., Twaha, S., & Riffat, S. (2018). A comprehensive review on 2D and 3D models of vertical ground heat exchangers. *Renewable and Sustainable Energy Reviews*, *94*, 84–114. https://doi.org/10.1016/j.rser.2018.05.063

Deerman, J. D., & Kavanaugh, S. P. (1991). Simulation of vertical U-tube ground-coupled heat pump systems using the cylindrical heat source solution. *ASHRAE Transactions: Research*, *971*(1991), 287–295.

Dennis, B., & Harlan, C. (2019, December 16). U.N. climate talks end with hard feelings, few results and new doubts about global unity. *The Washington Post*. Retrieved from https://www.washingtonpost.com/climate-environment/un-climate-talks-end-with-hard-feelings-few-results-and-new-doubts-about-global-unity/2019/12/15/38918278-1ec7-11ea-b4c1-fd0d91b60d9e_story.html

Sanner, B. (2001). Shallow Geothermal Energy. *GHC Bulletin*, *June*(2), 19–25. https://pdfs.semanticscholar.org/b58e/9ce9f89baa27ea06ecf67daa8179dc79e2ad.

pdf

Erol, S., & François, B. (2014). Efficiency of various grouting materials for borehole heat exchangers. *Applied Thermal Engineering*, *70*(1), 788–799. https://doi.org/10.1016/j.applthermaleng.2014.05.034

Eskilson, P. (1987). *Superposition Borehole Model, Manual for Computer Code*. University of Lund, Sweden. Retrieved from https://www.buildingphysics.com/download/Eskilson1987.pdf

Eskilson, P., & Claesson, J. (1988). Simulation Model for Thermally Interacting Heat Extraction Boreholes. *Numerical Heat Transfer*, *13*(2), 149–165. Retrieved from

Fan, R., Jiang, Y., Yao, Y., Shiming, D., & Ma, Z. (2007). A study on the performance of a geothermal heat exchanger under coupled heat conduction and groundwater advection. *Energy*, *32*(11), 2199–2209. https://doi.org/10.1016/j.energy.2007.05.001

Fang, L., Diao, N., Fang, Z., Zhu, K., & Zhang, W. (2017). Study on the efficiency of single and double U-tube heat exchangers. In *Procedia Engineering* (Vol. 205, pp. 4045–4051). https://doi.org/10.1016/j.proeng.2017.09.881

Farouki, O. T. (1986). Thermal properties of soils. Series on rock and soil mechanics series. *Trans Tech*, *11*, 136.

Florides, G., Christodoulides, P., & Pouloupatis, P. (2012). An analysis of heat flow through a borehole heat exchanger validated model. *Applied Energy*, *92*, 523–533. https://doi.org/10.1016/j.apenergy.2011.11.064

Florides, G., & Kalogirou, S. (2007). Ground heat exchangers—A review of systems, models and applications. *Renewable Energy*, *32*(15), 2461–2478. https://doi.org/10.1016/j.renene.2006.12.014

Freifeld, B. M., Finsterle, S., Onstott, T. C., Toole, P., & Pratt, L. M. (2008). Ground surface temperature reconstructions: Using in situ estimates for thermal conductivity acquired with a fiber-optic distributed thermal perturbation sensor. *Geophysical Research Letters*. https://doi.org/10.1029/2008GL034762

Fridleifsson, I. B., Bertani, R., & Huenges, E. (2008). The possible role and contribution of geothermal energy to the mitigation of climate change. In O. Hohmeyer & T. Trittin (Eds.), *IPCC Scoping Meeting on Renewable Energy Sources* (pp. 59–80). Luebeck, Germany.

Fujii, H., Okubo, H., & Itoi, R. (2006). Thermal response tests using optical fiber thermometers. In *Geotherm. Resour. Counc. Trans.* (pp. 545–551).

Fujii, H., Okubo, H., Nishi, K., Itoi, R., Ohyama, K., & Shibata, K. (2009). An improved thermal response test for U-tube ground heat exchanger based on optical fiber thermometers. *Geothermics*, *38*(4), 399–406.

https://doi.org/10.1016/j.geothermics.2009.06.002

Gehlin, S. (1998). *Thermal response Test – In-situ Measurements of Thermal Properties in Hard Rock*. Luleå University of Technology. Retrieved from http://www.diva-portal.org/smash/get/diva2:991135/fulltext01.pdf

Gehlin, S. (2002). *Thermal response test: method development and evaluation*. *Doctoral thesis*. Luleå University of Technology. https://www.diva-portal.org/smash/get/diva2:991442/fulltext01.pdf

Gehlin, S. E. A., Hellström, G., & Nordell, B. (2003). The influence of the thermosiphon effect on the thermal response test. *Renewable Energy*, *28*(14), 2239–2254. https://doi.org/10.1016/S0960-1481(03)00129-0

GSHPA. (2012). *Thermal pile design, installation and materials standards*. https://www.gshp.org.uk/pdf/GSHPA_Thermal_Pile_Standard.pdf

Gupta, S., Tirpak, D. A., Burger, N., Gupta, J., Höhne, N., Boncheva, A. I., … Sari, A. (2007). Policies, Instruments and Co-operative Arrangements. In *Climate Change 2007: Mitigation. Contribution of Working Group III to the Fourth Assessment Report of the Intergovernmental Panel on Climate Change* (pp. 746–807). https://www.ipcc.ch/site/assets/uploads/2018/02/ar4-wg3-chapter13-2.pdf

Gustafsson, A.-M. (2010). *Thermal response test—Influence of convective flow in groundwater filled boreholes*. Luleå University of Technology. Retrieved from https://www.diva-portal.org/smash/get/diva2:990084/fulltext01.pdf

Gustafsson, A.-M., & Westerlund, L. (2011). Heat extraction thermal response test in groundwater-filled borehole heat exchanger – Investigation of the borehole thermal resistance. *Renewable Energy*, *36*(9), 2388–2394. https://doi.org/10.1016/j.renene.2010.12.023

Hakala, P., Martinkauppi, A., Marinkauppi, I., Leppaharaju, N., & Korhonen, K. (2014). *Evaluation of the Distributed Thermal Response Test (DTRT): Nupurinkartano as a Case Study*. *GTK, Report 211, 1-35*. http://tupa.gtk.fi/julkaisu/tutkimusraportti/tr_211.pdf

Hausner, M. B., & Kobs, S. (2016). Identifying and Correcting Step Losses in Single-Ended Fiber-Optic Distributed Temperature Sensing Data. *Journal of Sensors*, (7073619), 10. https://doi.org/10.1155/2016/7073619

Hausner, M. B., Suárez, F., Glander, K. E., van de Giesen, N., Selker, J. S., & Tyler, S. W. (2011). Calibrating single-ended fiber-optic raman spectra distributed temperature sensing data. *Sensors*, *11*(11), 10859–10879. https://doi.org/10.3390/s111110859

Hermans, T., Nguyen, F., Robert, T., & Revil, A. (2014). Geophysical methods for monitoring temperature changes in shallow low enthalpy geothermal systems. *Energies*. https://doi.org/10.3390/en7085083

Ingersoll, L. R., & Plass, H. J. (1948). Theory of the Ground Pipe Heat Source for the Heat Pump. *ASHVE Transactions*, *Vol.54*.

Jahangir, M. H., Sarrafha, H., & Kasaeian, A. (2018). Numerical modeling of energy transfer in underground borehole heat exchanger within unsaturated soil. *Applied Thermal Engineering*, *132*, 697–707. https://doi.org/10.1016/j.applthermaleng.2018.01.020

Javed, S. (2012). *Thermal modelling and evaluation of borehole heat transfer*. Göteborg: Chalmers University of Technology. Retrieved from http://publications.lib.chalmers.se/records/fulltext/149878.pdf

Javed, S., & Spitler, J. (2017). Accuracy of borehole thermal resistance calculation methods for grouted single U-tube ground heat exchangers. *Applied Energy*, *187*, 790–806. https://doi.org/10.1016/j.apenergy.2016.11.079

Lamarche, L., & Beauchamp, B. (2007). A new contribution to the finite line-source model for geothermal boreholes. *Energy and Buildings*, *39*(2), 188–198. https://doi.org/10.1016/j.enbuild.2006.06.003

Lamarche, L., Kajl, S., & Beauchamp, B. (2010). A review of methods to evaluate borehole thermal resistances in geothermal heat-pump systems. *Geothermics*, *39*(2), 187–200. https://doi.org/10.1016/j.geothermics.2010.03.003

Lenhard, R., Gavlas, S., & Malcho, M. (2012). Numerical simulation of borehole model which utilizes low-potential geothermal heat. In *EPJ Web of Conferences*. EDP Sciences. https://doi.org/10.1051/epjconf/20122501048

Low, J. E., Loveridge, F. A., Powrie, W., & Nicholson, D. (2015). A comparison of laboratory and in situ methods to determine soil thermal conductivity for energy foundations and other ground heat exchanger applications. *Acta Geotechnica*, *10*(2), 209–218. https://doi.org/10.1007/s11440-014-0333-0

Lund, J. W., & Boyd, T. L. (2016). Direct utilization of geothermal energy 2015 worldwide review. *Geothermics*, *60*(3), 66–93. https://doi.org/10.1016/j.geothermics.2015.11.004

Lund, J. W., Sanner, B., Rybach, L., & Curtis, R. (2004). Geothermal (ground-source) heat pumps, a world overview. *Geo-Heat Centre Quarterly Bulletin*, *25*(3), 1–10.

Luo, J., Rohn, J., Xiang, W., Bayer, M., Priess, A., Wilkmann, L., … Zorn, R. (2015). Experimental investigation of a borehole field by enhanced geothermal response test and numerical analysis of performance of the borehole heat exchangers. *Energy*, *84*, 473–484. https://doi.org/10.1016/j.energy.2015.03.013

Luo, J., Xiang, W., Blum, P., Bertermann, D., Bertermann, D., & Rohn, J. (2016). A review of ground investigations for ground source heat pump (GSHP) systems. *Energy and Buildings*, *117*, 160–175. https://doi.org/10.1016/j.enbuild.2016.02.038

Marcotte, D., Pasquier, P., Sheriff, F., & Bernier, M. (2010). The importance of axial effects for borehole design of geothermal heat-pump systems. *Renewable Energy*, *35*(4), 763–770. https://doi.org/10.1016/j.renene.2009.09.015

Martos, J., Montero, Á., Torres, J., Soret, J., Martínez, G., & García-Olcina, R. (2011). Novel wireless sensor system for dynamic characterization of borehole heat exchangers. *Sensors*, *11*(7), 7082–7094. https://doi.org/10.3390/s110707082

McDaniel, A., Tinjum, J., Hart, D. J., Lin, Y.-F., Stumpf, A., & Thomas, L. (2018). Distributed thermal response test to analyze thermal properties in heterogeneous lithology. *Geothermics*, *76*, 116–124. https://doi.org/10.1016/j.geothermics.2018.07.003

Mitchel, J. K., & Kao, T. C. (1978). Measurement of soil thermal resistivity. *Journal of Geotechnical and Geoenvironmental Engineering*, *104*(GT10), 1307–1320. Retrieved from https://trid.trb.org/view/80703

Mogensen, P. (1983). Fluid to duct wall heat transfer in duct system heat storages. In *Proc. Int. Conf. On Subsurface Heat Storage in Theory and Practice* (pp. 652–657). Stockholm, Sweden: Swedish Council for Building Research.

Monzó, P. (2018). *Modelling and monitoring thermal response of the ground in borehole fields*. Kungliga Tekniska högskolan. Retrieved from http://kth.diva-portal.org/smash/get/diva2:1178493/fulltext01.pdf

Naldi, C., & Zanchini, E. (2019). A new numerical method to determine isothermal g-functions of borehole heat exchanger fields. *Geothermics*, *77*, 278–287. https://doi.org/10.1016/j.geothermics.2018.10.007

Ozudogru, T. Y., Olgun, C. G., & Senol, A. (2014). 3D numerical modeling of vertical geothermal heat exchangers. *Geothermics*, *51*, 312–324. https://doi.org/10.1016/j.geothermics.2014.02.005

Pasquier, P., & Marcotte, D. (2012). Short-term simulation of ground heat exchanger with an improved TRCM. *Renewable Energy*, *46*, 92–99. https://doi.org/10.1016/j.renene.2012.03.014

Philippe, M., Bernier, M., & Marchio, D. (2009). Validity ranges of three analytical solutions to heat transfer in the vicinity of single boreholes. *Geothermics*, *38*(4), 407–413. https://doi.org/10.1016/j.geothermics.2009.07.002

Radioti, G. (2016). *Shallow geothermal energy: effect of in-situ conditions on borehole heat exchanger design and performance*. University of Liege. Retrieved from https://orbi.uliege.be/handle/2268/204011

Raymond, J., & Lamarche, L. (2014). Development and numerical validation of a novel thermal response test with a low power source. *Geothermics*. https://doi.org/10.1016/j.geothermics.2014.02.004

Raymond, J., Lamarche, L., & Malo, M. (2015). Field demonstration of a first thermal response test with a low power source. *Applied Energy*. https://doi.org/10.1016/j.apenergy.2015.01.117

Raymond, J., Lamarche, L., & Malo, M. (2016). Extending thermal response test assessments with inverse numerical modeling of temperature profiles measured in ground heat exchangers. *Renewable Energy*, *99*(November), 614–621. https://doi.org/10.1016/j.renene.2016.07.005

Raymond, J., Therrien, R., Gosselin, L., & Lefebvre, R. (2011). Numerical analysis of thermal response tests with a groundwater flow and heat transfer model. *Renewable Energy*, *36*(1), 315–324. https://doi.org/10.1016/j.renene.2010.06.044

Rivera, J. A., Blum, P., & Bayer, P. (2016). A finite line source model with Cauchy-type top boundary conditions for simulating near surface effects on borehole heat exchangers. *Energy*, *98*, 50–63. https://doi.org/10.1016/j.energy.2015.12.129

Rohner, E., Rybach, L., & Schärli, U. (2006). *European Patent Office 1600749B1*. Retrieved from https://patents.google.com/patent/EP1600749A1/en

Rohner, E., Rybach, L., & Schärli, U. (2005). A New, Small, Wireless Instrument to Determine Ground Thermal Conductivity In-Situ for Borehole Heat Exchanger Design. *Proceedings World Geothermal Congress 2005*, (April), 3–6. Retrieved from https://pdfs.semanticscholar.org/a20a/91d47ee18a7e978d4d789df3a26678cdca2b.pdf

Ruiz-Calvo, F. (2015). Análisis y modelado de una instalación geotérmica para climatización de un conjunto de oficinas. https://doi.org/10.4995/Thesis/10251/54134

Ruiz-Calvo, F., De Rosa, M., Acuña, J., Corberán, J. M., & Montagud, C. (2015). Experimental validation of a short-term Borehole-to-Ground (B2G) dynamic model. *Applied Energy*, *140*, 210–223. https://doi.org/10.1016/j.apenergy.2014.12.002

Ruiz-Calvo, F., De Rosa, M., Monzó, P., Montagud, C., & Corberán, J. M. (2016). Coupling short-term (B2G model) and long-term (g-function) models for ground source heat exchanger simulation in TRNSYS. Application in a real installation. *Applied Thermal Engineering*, *102*, 720–732. https://doi.org/10.1016/j.applthermaleng.2016.03.127

Sandler, S., Zajaczkowski, B., Bialko, B., & Malecha, Z. M. (2017). Evaluation of the impact of the thermal shunt effect on the U-pipe ground borehole heat exchanger performance. *Geothermics*, *65*, 244–254. https://doi.org/10.1016/j.geothermics.2016.10.003

Sarbu, I., & Sebarchievici, C. (2014). General review of ground-source heat pump

systems for heating and cooling of buildings. *Energy and Buildings*. https://doi.org/10.1016/j.enbuild.2013.11.068

Shortall, R., Davidsdottir, B., & Axelsson, G. (2015). Geothermal energy for sustainable development: A review of sustainability impacts and assessment frameworks. *Renewable and Sustainable Energy Reviews*, *44*, 391–406. https://doi.org/10.1016/j.rser.2014.12.020

Shu, H., Duanmu, L., & Hua, R. (2006). Analysis of selection of single or double U-bend pipes in a ground source heat pump system. *Renewable Energy Resources and a Greener Future V Shenzhen*, 1–3.

Signorelli, S., Bassetti, S., Pahud, D., & Kohl, T. (2007). Numerical evaluation of thermal response tests. *Geothermics*, *36*(2), 141–166. https://doi.org/10.1016/j.geothermics.2006.10.006

Soldo, V., Boban, L., & Borović, S. (2016). Vertical distribution of shallow ground thermal properties in different geological settings in Croatia. *Renewable Energy*, *99*, 1202–1212. https://doi.org/10.1016/j.renene.2016.08.022

Spitler, J., & Gehlin, S. (2015). Thermal response testing for ground source heat pump systems—An historical review. *Renewable and Sustainable Energy Reviews*, *50*, 1125–1137. https://doi.org/10.1016/j.rser.2015.05.061

Stauffer, F., Bayer, P., Blum, P., Molina-Giraldo, N., & Kinzelbach, W. (2013). *Thermal use of shallow groundwater*. *CRC Press* (CRC Press). https://doi.org/10.1201/b16239

Stober, I., & Bucher, K. (2013). History of Geothermal Energy Use. In *Geothermal Energy: From Theoretical Models to Exploration and Development* (pp. 15–24). Berlin, Heidelberg: Springer Berlin Heidelberg. https://doi.org/10.1007/978-3-642-13352-7_2

Sutter, J. D., & Berlinger, J. (2015). Final draft of climate deal formally accepted in Paris.

Teza, G., Galgaro, A., & De Carli, M. (2012). Long-term performance of an irregular shaped borehole heat exchanger system: Analysis of real pattern and regular grid approximation. *Geothermics*, *43*, 45–56. https://doi.org/10.1016/j.geothermics.2012.02.004

Turcotte, D. L., & Schubert, G. (2002). *Geodynamics (second edition)*. New York: Cambridge University Press.

Tyler, S. W., Selker, J. S., Hausner, M. B., Hatch, C. E., Torgersen, T., Thodal, C. E., & Schladow, S. G. (2010). Environmental temperature sensing using Raman spectra DTS fiber-optic methods. *Water Resources Research*. https://doi.org/10.1029/2008WR007052

van de Giesen, N., Steele-Dunne, S. C., Jansen, J., Hoes, O., Hausner, M. B., Tyler, S., & Selker, J. (2012). Double-ended calibration of fiber-optic raman spectra distributed temperature sensing data. *Sensors (Switzerland)*, *12*(5), 5471–5485. https://doi.org/10.3390/s120505471

Wang, H., Qi, C., Du, H., & Gu, J. (2009). Thermal performance of borehole heat exchanger under groundwater flow: A case study from Baoding. *Energy and Buildings*, *41*(12), 1368–1373. https://doi.org/10.1016/j.enbuild.2009.08.001

Wilke, S., Menberg, K., Steger, H., & Blum, P. (2020). Advanced thermal response tests: A review. *Renewable and Sustainable Energy Reviews*, *119*, 109575. https://doi.org/10.1016/j.rser.2019.109575

Witte, H. J. L., van Gelder, G. J. & Spitler, J. (2002). In Situ Measurement of Ground Thermal Conductivity : A Dutch Perspective In Situ Measurement of Ground. *ASHRAE Transactions*, *108*(1), 1–21.

Xamán, J., Lira, L., & Arce, J. (2009). Analysis of the temperature distribution in a guarded hot plate apparatus for measuring thermal conductivity. *Applied Thermal Engineering*, *29*(4), 617–623. https://doi.org/10.1016/j.applthermaleng.2008.03.033

Yavuzturk, C. (1999). *Modelling of vertical ground loop heat exchangers for ground source heat pump systems. Building and Environmental Thermal Systems*. Oklahoma State University.

Yavuzturk, C., & Spitler, J. (1999). A short time step response factor model for vertical ground loop heat exchangers. In *ASHRAE Trans.* (p. 475). United States. Retrieved from http://www.osti.gov/scitech/biblio/20085638

Yavuzturk, C., Spitler, J., & S. Rees. (1999). A transient two-dimensional finite volume model for the simulation of vertical u-tube ground heat exchangers. *ASHRAE Transactions*, *105*(2), 465–474.

Young, T. R. (2004). *Development, Verification, and Design Analysis of the Borehole Fluid Thermal Mass Model for Approximating Short Term Borehole Thermal Response*. Oklahoma State University. Retrieved from https://hdl.handle.net/11244/10095

Yu, X., Zhang, Y., Deng, N., Wang, J., Zhang, D., & Wang, J. (2013). Thermal response test and numerical analysis based on two models for ground-source heat pump system. *Energy and Buildings*, *66*, 657–666. https://doi.org/10.1016/j.enbuild.2013.07.074

Zanchini, E., Lazzari, S., & Priarone, A. (2012). Long-term performance of large borehole heat exchanger fields with unbalanced seasonal loads and groundwater flow. *Energy*, *38*(1), 66–77. https://doi.org/10.1016/j.energy.2011.12.038

Zeng, H., Diao, N., & Fang, Z. (2002). A finite line-source model for boreholes in

geothermal heat exchangers. *Asian Research*, *31*(7), 558–567. https://doi.org/10.1002/htj.10057

Zeng, H., Diao, N., & Fang, Z. (2003a). Efficiency of vertical geothermal heat exchangers in the ground source heat pump system. *Journal of Thermal Science*, *12*(1), 77–81. https://doi.org/10.1007/s11630-003-0012-1

Zeng, H., Diao, N., & Fang, Z. (2003b). Heat transfer analysis of boreholes in vertical ground heat exchangers. *International Journal of Heat and Mass Transfer*, *46*(23), 4467–4481. https://doi.org/10.1016/S0017-9310(03)00270-9

Zhang, W., Yang, H., Lu, L., & Fang, Z. (2012). Investigation on heat transfer around buried coils of pile foundation heat exchangers for ground-coupled heat pump applications. *International Journal of Heat and Mass Transfer*, *55*(21–22), 6023–6031. https://doi.org/10.1016/j.ijheatmasstransfer.2012.06.013

Zhao, J., Li, Y., & Wang, J. (2016). A Review on Heat Transfer Enhancement of Borehole Heat Exchanger. *Energy Procedia*, *104*, 413–418. https://doi.org/10.1016/j.egypro.2016.12.070

Appendix A

Scientific publications and conferences

> *This section includes a list of all the scientific publications and conferences derived from this Ph.D. work in chronological order.*

A.1. Peer-reviewed publications in journals

- Aranzabal, N., Martos, J., Stokuca, M., Hagen, S., Mazzoti, M. P., Acuña, J., Soret, J. & Blum, P. (2020). Novel instruments and methods to estimate depth-specific thermal properties in borehole heat exchangers. *Geothermics*, 86, 101813. https://doi.org/10.1016/j.geothermics.2020.101813
- Aranzabal, N., Martos, J., Hagen, S., Blum, P., & Soret, J. (2019). Temperature measurements along a vertical borehole heat exchanger: A method comparison. *Renewable Energy*, 143, 1247–1258. https://doi.org/10.1016/j.renene.2019.05.092
- Aranzabal, N., Martos, J., Steger, H., Blum, P., & Soret, J. (2018). Novel Instrument for Temperature Measurements in Borehole Heat Exchangers. *IEEE Transactions on Instrumentation and Measurement,* vol. 68 (4), 1062–1070 (2018). https://doi.org/10.1109/tim.2018.2860818
- Aranzabal, N., Martos, J., Montero, Á., Monreal, L., Soret, J., Torres, J., & García-Olcina, R. (2016). Extraction of thermal characteristics of surrounding geological layers of a geothermal heat exchanger by 3D numerical simulations. *Applied Thermal Engineering, 99, 92*–102. https://doi.org/10.1016/j.applthermaleng.2015.12.109

A.2. Peer-reviewed publications in conferences

- Aranzabal, N., Radioti, G., Martos, J., Soret, J., Nguyen, F. & Charlier, R. (2016). Enhanced thermal response test using fiber optics for a double u-pipe borehole heat exchanger analysed by numerical modeling. *In ECOS2016 - 29th International Conference on Efficiency, Cost, Optimization, Simulation and Environmental Impact of Energy Systems*. Portorož, Slovenia. ISBN 978-961-6980-15-9.

- Aranzabal, N., Martos, J., Montero, A., Soret, J., García-Olcina, R. & Torres, J. (2015). Novel method to estimate thermal conductivity of geological layers from experimental data of a TRT by a finite elements 3D model simulation. *In ECOS2015 - 28th International Conference on Efficiency, Cost, Optimization, Simulation and Environmental Impact of Energy Systems*. Pau, France. ISBN 978-2-9555539-0-9.
- Aranzabal, N., Martos, J., Montero, A., Soret, J., García-Olcina, R. & Torres, J. (2015). Design and test of an autonomous wireless probe to measure temperature inside pipes. *In ECOS2015 - 28th International Conference on Efficiency, Cost, Optimization, Simulation and Environmental Impact of Energy Systems*. Pau, France. ISBN 978-2-9555539-0-9.

A.3. Presentations & posters in conferences

- International GSHP Convention, Stockholm, Sweden, September 2016. Poster presentation with tittle “Novel instruments to measure temperature inside geothermal pipes”.
- ECOS2016, Portorož, Slovenia, June 2016. Oral presentation with tittle “Enhanced thermal response test using fiber optics for a double U-pipe borehole heat exchanger analyzed by numerical modeling”.
- ECOS2015, Pau, France, July 2015. Oral presentation with tittle “Novel method to estimate thermal conductivity of geological layers from experimental data of a TRT by a finite elements 3D model simulation”.
- ECOS2015, Pau, France, July 2015. Poster presentation with tittle "Design and Test of an Autonomous Wireless Probe to Measure Temperature Inside Pipes”.
- COMSOL Conference Cambridge 2014, England. Poster presentation with tittle “Extraction of thermal characteristics of surrounding geological layers of a geothermal heat exchanger using COMSOL simulations”.

A.4. Book chapter

- Aranzabal, N., Suarez, A., Torres, J., García-Olcina, R., Martos, J., Soret, J., Menéndez, A. & Martínez, P. A. (2017). Design of digital advanced systems based on programmable system on chip. In G. Dekoulis (Ed.), *Field - Programmable Gate Array* (pp. 124–157). InTech.
  http://dx.doi.org/10.5772/66579